Numerical and Experimental Study of Forced Heave of Two-Dimensional Section in Ice

TMR4900 - Master Thesis

by

Tommy Olsen

June 14, 2010

Supervisor:

Prof. Odd M. Faltinsen

Norwegian University of Science and Technology

Faculty of Engineering Science and Technology

Departement of Marine Technology

Master thesis in Marine Hydrodynamics
Stud. Techn. Tommy Olsen
”Numerical and experimental study of forced heave of two-dimensional section in ice”

Background

Development of offshore fields in arctic waters may include the use of moored structures. These structures may then have to operate year round and thus interact with sea ice features. The interaction of sea ice on the vessel is dynamic and will cause a dynamic response of the vessel. Estimation or measurements of the dynamic ice loads acting on the vessel is difficult. The vessel response is however easier to observe and is usually reported. It is then possible to back-calculate the ice actions on the vessel. However it is then needed to asses properly the hydrodynamic loads applying on the vessel. The moored vessel in ice is a body experiencing forced oscillations. The hydrodynamic loads applying on the body are probably affected by the presence of sea ice around the vessel. The sea ice will affect the added mass and damping. The study in the master thesis is a step in the understanding of the hydrodynamic ship ice problem.

Scope and main activities

The candidate should presumably cover the following,

- The candidate should do experimental 2D tests with a cross-section of a ship model that is forced to oscillate in heave. The tests should be performed in an open water condition, a set-up with ice on one side of the section and ice on both sides of the section. The ship model is to be tested at a range of frequencies determined by the student and the distance from the ice to the ship model is to be varied. The ice should be made of a synthetic material and the dimensions of the ship and ice models is to be determined by the student.

- Comparison should be made with the linear BEM, developed in Dr. Trygve Kristiansens PhD. Discrepancies between numerical and experimental results are to be discussed. An analysis and discussion of error sources in the experiments are also to be discussed.

- Calculation routines to find added mass and damping from experimental and numerical simulations are to be developed in Matlab. The calculation routines should be verified to check its validity.

The report shall be written in English and edited as a research report including literature survey, description of numerical models, discussion and conclusion including a proposal for further work. Source code in Matlab shall be provided on a CD. It is supposed that Department of Marine Technology, NTNU, can use the results freely in its research work by referring to the students work.
The thesis should be submitted in two copies within the 14th of June 2010.

Professor Odd M. Faltinsen
Supervisor

Abstract

A two-dimensional study of a ship section forced to heave in open water and surrounded by plates representing ice have been performed. The setting is a ship moored in ice infested waters. The ice is modeled as a stiff rigid body and is not allowed to move or bend in any degrees of freedom nor modes. The distance between the ship section and ice have been varied and added mass and damping have been calculated in a frequency range including resonance. The investigation is carried out by means of model tests as well by a linear wave tank based on the boundary element method.

In the study it was found that around resonance with ice present an abrupt and steep change in added mass occurs. In the numerical results for the case with two ice-floes the maximum values for added mass it is seen that it becomes larger from $b = 0.01$ m before it becomes smaller after $b = 0.02$ m. For the experiments with the same geometric set up the maximum values show a similar trend. The maximum values for added mass shows a growing trend from $b = 0.01$ m and peaks at $b = 0.08$ m and get a smaller value for $b = 0.10$ m. For the case with one ice-floe the same maximum values decrease a the ship section gets further away from the ice. The model tests show an discrepancy of when resonance occurs compared to the numerical simulation and difference in the maximum and minimum values. In general the numerical program predicts a higher added mass and damping compared to the model tests when ice is present. For the tests without ice present the numerical and experimental results correlate well.

Preface

This work for this thesis has been carried out during the spring of 2010 as part of my Master degree in Marine Technology, with specialization within marine Marine Hydrodynamics at the Norwegian University of Science and Technology.

The research have been carried out under supervision of Professor Odd M. Faltinsen. I am grateful for his excellent guidance. With weekly meetings he has made sure I was on the right track with guidance and critical questions and in that way increasing the quality of my work.

The work in this master thesis includes numerical calculations and model tests, in both Dr. Trygve Kristiansen have been very helpful. I would like to thank him for the help provided during the model tests and making his numerical wave tank available and modifying it for multi-body problems.

Also during the spring Arnt Fredriksen have been a great support in the work through help with the experiments and the development of calculation routines and valuable discussions.

The background for the work done in this thesis came through discussions with Arnor Jensen and Basile Bonnemaire from Barlindhaug Consult during the summer of 2009. I would like to thank them for financing the model tests.

The tasks to complete this assignment have been very challenging at times but also very rewarding when these challenges were overcome. The model tests was planned to take about three weeks to complete but it turned out that five weeks was required to complete all the tests in a sufficient manner.

The work of moving the ice-floes was a cumbersome and time consuming task as the results relied on precision with respect to the distance between the ice and ship section and that the ice was level. This work turned out to be a task more suitable for two persons.

Through the study I have had the opportunity to take theory from courses given within hydrodynamics and put them into practice and learned how to use results published in journals. However it have been hard to find relevant literature on the subject at hand, which made the theoretical part very challenging.

Due to time pressure before the deadline of the thesis I unfortunately did not find the time to make a list of symbols, however all symbols used in the thesis is explained where they have been introduced and applied.

The material treated in the work to complete the report relates to Arctic technology with respect to a vessel in ice with an emphasis on the hydrodynamic coefficients.

Trondheim, 14 June 2010

Tommy Olsen.

Summary

As oil and gas exploration seems to be moving towards Arctic regions, research is taking place to outline possible solutions on how this can be done in a safe and efficient manner. Development of offshore fields in the Arctic may include the use of moored structures. The interaction of sea-ice on a vessel is dynamic and will cause a dynamic response. Such behavior have been devoted a lot of research with emphasis on a structural point of view but not so much with respect to the hydrodynamics involved. The hydrodynamic loads applied on the vessel are affected by the presence of sea-ice surrounding the vessel.

To investigate how the hydrodynamic coefficients are affected by the sea-ice presence a two-dimensional study have been performed. The hydrodynamic coefficients are added mass and damping. The two-dimensional problem consists of a ship section in forced heave motions in three cases. In the first case the ship section is oscillating in open water with no ice present, in the second there is a long ice-floe in close proximity to the oscillating section and in the last the section is surrounded by ice of two sides. This have been investigated both by numerical simulations and model tests.

A model test series of scale *1:100* have been performed in a wave flume with a length of 13 *m*, breadth 0.6 *m* and a depth of 1 *m*. The ship-section have a breadth/depth, B/D ratio of 2.67 where $B = 0.32$ *m* and $D = 0.12$ *m*. The ship section is forced to heave by an actuator and prohibited to move an any other degree of freedom. The forcing amplitudes tested are 2.5 *mm* and 5 *mm*. The ice is modeled by 3.60 *m* long divinycell plates with a draught of 0.04 *m*. The ice is not allowed to move or bend in any degree of freedom nor mode. The tests have been done with the distance between the oscillating ship section and the ice as a variable. This distance varies from 1 *cm* to 10 *cm*.

The results from the experiments have been compared to a linear time domain boundary element method code. Different limitations of both models are discussed and results are presented for an oscillation period range from 0.4 *s* to 2.0 *s*.

In the numerical results for the case with two ice-floes the maximum values for added mass it is seen that it becomes larger from $b = 0.01$ *m* before it becomes smaller after $b = 0.02$ *m*. For the experiments with the same geometric set up the maximum values show a similar trend. The

maximum values for added mass shows a growing trend from $b = 0.01$ m and peaks at $b = 0.08$ m and get a smaller value for $b = 0.10$ m. For the case with one ice-floe the same maximum values decrease a the ship section gets further away from the ice. The model tests show an discrepancy of when resonance occurs compared to the numerical simulation and difference in the maximum and minimum values. In general the numerical program predicts a higher added mass and damping compared to the model tests when ice is present. For the tests without ice present the numerical and experimental results correlate well.

Contents

Chapter 1

Introduction

Development of offshore fields in arctic waters may include the use of moored structures. These structures may have to operate year round and thus interact with sea ice features. Experience with moored structures in ice infected seas is limited. The main full scale experience is from the operation of the conical drilling vessel Kulluk in the Beaufort Sea, see [23]. In addition, some ice basin model test studies have been performed studying challenges linked to the operation of moored vessels in ice are reported e.g. [15] and [3].

The interaction of sea ice on the vessel is dynamic and will cause a dynamic response of the vessel. Estimation or measurements of the dynamic ice loads acting on the vessel is difficult. The vessel response is however easier to observe and is usually reported. It is then possible to back-calculate the ice actions on the vessel as reported by e.g. [19]. However it is then needed to assess properly the hydrodynamic loads applying on the vessel.

The moored vessel in ice is a body experiencing forced oscillations. The hydrodynamic loads applying on the body are probably affected by the presence of sea ice around the vessel. The sea ice will affect the fluid boundary conditions and the added mass or hydrodynamic potential damping in the different DOF will differ from the open water case.

For a case where a ship is found in frozen sea-ice one can imagine that the ship is surrounded by infinite ice. In the present work this is not been investigated due to physical limitations. Instead the ice will be considered big compared to the ship.

The goal of the work in the thesis is to investigate the hydrodynamic coefficients by performing a two-dimensional study with a ship-section. In the work the two-dimensional ship-section is forced to heave in open water and between one and two plates representing ice.

1.1 Present situation

Due to expectations that large reserves of undiscovered oil and gas might be found in Arctic areas and waning opportunities for exploration elsewhere makes this region interesting. As technology and solutions are improving the challenges related to Arctic petroleum exploration might be overcome in the near future. Also the melting of sea-ice is making the Arctic a more attractive option. Some examples already exists of activity in harsh Arctic climate like the developments in the sea of Okhotsk and on the Sakhalin Shelf. However there is yet more research to be done to explore such regions in an efficient and safe manner.

There are several examples related to the development of solutions for Arctic operation. Some of these presents e.g. a tandem offloading terminal with mooring lines see [4] and the subsurface interaction under a moored offloading icebreaker, [5]. Also another system with an Arctic shuttle barge system for loading of oil in ice can be seen in [18].

1.2 Previous work

For the case of a vessel in ice many publications have been released, but mainly concerned with structural loads for various ice conditions and dynamic behavior, like e.g. [7], [6] and [14]. Also for waves propagating through a Marginal Ice Zone (MIZ) many publications can be found like e.g. [12]. But the hydrodynamic problem with a vessel operating in sea-ice features or model tests of such vessels to study the hydrodynamic coefficients have not as far as the author's knowledge been published.

However when considering a vessel in motion close to level sea-ice it may be broken down to something that resembles a gap problem. Such gap problems that is referred to are two-

dimensional studies related to moonpools as found in the publication of B. Molin in [21] and Odd M. Faltinen in [9]. The gap problem can also be related to studies performed for ships and fixed terminals as Kristiansen have done in [17] and further discussed in his Phd. thesis. Other studies that are interesting in relation to the problem is another publication from B. Molin where he looks into wave propagation and decay in a channel through a rigid ice-sheet and McIver's study of complex resonances in the water-wave problem for a floating structure.

Common for all the above publications are the coupled motion of a structure and fluid in a confined space. By studying the theory provided in these papers it is possible to relate it to the ship-ice system, which is described in chapter 2.

1.3 Outline

The work in this thesis is outlined in the different chapters as the following:

- **Chapter 2** gives a description of the physical problem that is to be investigated and physical effects to be expected.
- **Chapter 3** presents the Numerical wave tank with the theoretical principles behind it and the parameters related to the numerical model.
- **Chapter 4** provides a discussion related to the hydrodynamic coefficients and how they can be calculated.
- **Chapter 5** presents a description of the experimental test set-up, routines , measuring equipment and an uncertainty analysis.
- **Chapter 6** presents the results from the experiments and numerical simulations.
- **Chapter 7** provides a discussion of the the results and the main differences between the numerical calculation scheme and the physical model.
- **Chapter 8** concludes this work and suggests future work.

Chapter 2

The physical problem

This work is concerned with the two-dimensional motion of a structure in an incompressible and inviscid fluid with the objective of studying the fluid interaction with a two dimensional ship section forced to heave in open water and between one and two ice-floes with a specified gap. The work is done in order to try and further understand the how the hydrodynamic coefficients behaves.

The work is conducted with the assumption that theory related to piston-mode problems is valid and hence it will be treated thereafter. As a consequence literature related to such problems have been consulted to understand the physics involved.

The problem with a two-dimensional ship-section in ice resembles the principles in [11] chapter *3.7 Sloshing in external flow*. The problem is also analogous to Dr. Trygve Kristiansens work in his PhD. [16], who's thesis is used as the main source for the following description in the present work. The theory has been adapted to fit the ship-ice system.

2.1 Formulation of the basic two-dimensional problem

Throughout the study the ship and ice floes have been considered to be of simple rectangular shape with sharp corners. A rectangle with sharp corners will resemble a simplified version of a vessel. In this case the vessel is meant to be operating in ice infested waters. In the study the

effect of round corners or bilge keels have not been investigated i.e. only a ship section with 90°corner is considered. The details of the separated flow around the different bilge geometries mentioned will be different. The imagined flow pattern that would occur round the three different geometries are illustrated in figure 2.1. For more details regarding bilge keels the reader can consult e.g. [10].

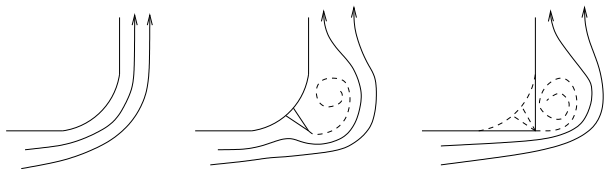

Figure 2.1: Instantaneous scenarios of flow around bilges. The flow will always separate around a sharp corner. Left: No bilge keel. The flow will still separate at sufficiently large *KC*-numbers, but not in the illustrated case. Middle: Bilge keel. Right: Sharp corner with bilge keel superimposed for illustration purposes.

The ship beam is defined by B_{ship} and and the draft by D_{ship} as seen in figure 2.2. Ice floes are defined by B_{ice} and D_{ice}. In the figure both ship and ice floes are represented with the ship in the middle. The distance between the ship and the ice floe is denoted *b* and will throughout the work also be referred to as gap, ice gap or ship ice gap. Due to symmetry only *b* is needed to describe the gap distance. The still water depth is denoted *h*.

The ice is modeled as a stiff rigid structure that is restricted to move in any degrees of freedom and bending modes. This means that the ice can be considered as a horizontal wall with a draft D_{ice} in the mean free-surface of the water in the tank. The ice is modeled with a more significant draught compared to real level sea-ice and equally large freeboard. This have been done in order to as a large as possible way create comparable environments for comparing numerical an experimental results. This is due to that the numerical calculation scheme is based on linear theory and effects like e.g. green water is not included nor dry spots under the due to the oscillating water column.

The amount of parameters to consider in the problem are many. The beam-to-draft ratio *B/D* is the main parameter for the ship section itself. In this case this parameter is *B/D=2.67*. The reason to the somewhat odd ratio number is due to an error in the fabrication of the model for the experiments. The ratio between the beam and the water depth B/h is a relevant parameter when considering finite water depth effects on ship section motion. When considering the ship

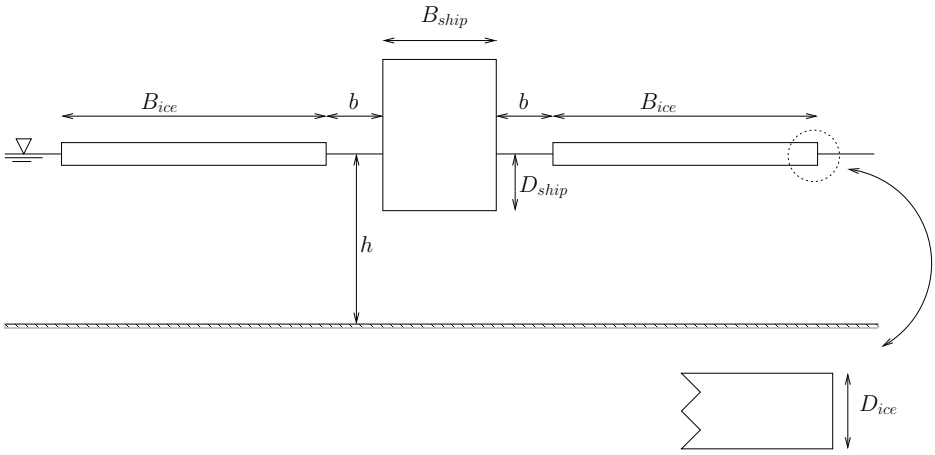

Figure 2.2: Dimensions in the problem of a ship section by two ice-floes: Water depth h, ship section beam or breadth B_{ship}, ice floe beam B_{ice}, ship section draft D_{ship}, ice floe draft D_{ice} and the gap between the ship and ice floe b

ice system, the ratios between the gap width and the ship section beam and ice floe draft, *b/B* and *b/D*, are relevant. These parameters describe the ship sections ability to to disturb the fluid in the ice gap when the section is forced to oscillate in heave.

The main parameter mostly used to define the problem is the ship beam, B_{ship}, because it defines the relative extent of the gap and an important variable related to added mass.
Most of the analysis will be done with the previous mentions *B/D* ratio of *2.67* which have been used during the experiments. However a variation in the B/D ratio will be tested numerically in addition to a few variations of the beam of the ice floe. The ship section will be forced to oscillate in a sinusoidal motion in heave. In the experiments with also a varying heave amplitude. The results will in general be presented as a function of non dimensional frequency $\omega\sqrt{B/2g}$.

2.2 Resonant behavior

The basic principle in the present work can be related to a gap resonance problem. In theory there is an infinite number of resonance frequencies in the gap. Most of these are associated with modes of the free surface localized in the gap between the ice and the ship. These localized modes are referred to as sloshing modes. Note that there is a distinction between the sloshing modes and the piston mode, which is of a more global character.

The approach used in the study is to solve the linear problem by means of the Boundary Element Method (BEM) and not of a modal method. Hence modes are not separated and only the full problem is solved.

It should be noted that there will also be other disturbances in the gap, they are evanescent-like disturbances.

In addition to the sloshing modes, there is a zeroth mode which is usually referred to as the piston mode. The piston mode is characterized by that the fluid entrained in the ship-ice gap undergoes near uniform vertical oscillatory motion with a flat, horizontal free surface. The piston mode has an amplitude which is called the piston-mode amplitude and is denoted by Ag. The amplitude is defined $A_g = H_g/2$ where H_g is the trough-to-crest height of the free surface averaged over the gap. Associated with the piston-mode is a resonance frequency which is denoted the piston-mode resonance frequency. This frequency is typically lower than those of the sloshing modes. This means that if the excitation frequency is in the vicinity of the piston mode-mode resonance frequency, the dominating part of the fluid motion is that of the piston-mode. This is called piston-like behavior. The piston-like behavior is illustrated in figure 2.3.

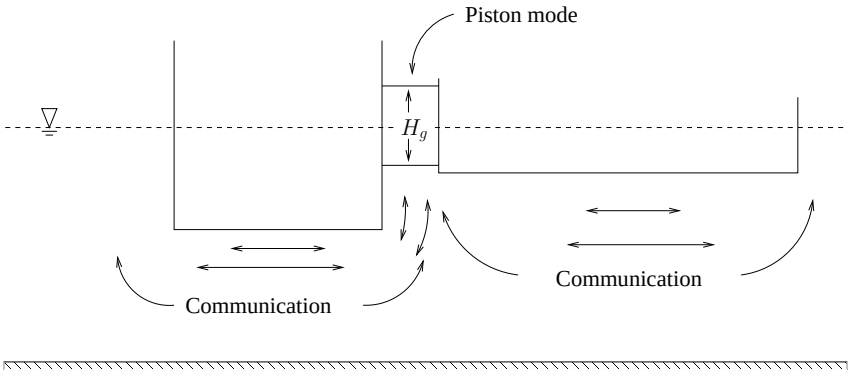

Figure 2.3: Illustration of the piston-mode motion. Piston-mode motion is $H_g/2$ where H_g is the crest-to-trough height of the free-surface elevation averaged over the gap. Due to continuity of mass the piston mode must communicate with the outer flow.

Associated with the piston mode is a resonance frequency which is denoted the piston-mode resonance frequency.

It is the piston-like behavior that will be treated in the study, no sloshing behavior that might include run-up and wave breaking is going to be treated. The geometrical set-up with the ship forced to oscillate in close proximity to the ice-floes represent an external problem, which means the following. In the the external problem there exists a piston mode as previously discussed. As a consequence of mass conservation this does not exist in the internal problem. By internal problem it is meant that of a tank partially filled with fluid. Under forced heave of such a tank, linear theory predict zero sloshing. Another difference between the internal and external problem is that in the external problem energy may escape via radiated waves. The radiated waves generated by the fluid motion in the ice-gap introduces damping, and by that keeping the motion at a finite level.

The damping effect due to the radiated waves in the external problem applies in principle to all modes in the ice-gap, although most pronounced for the piston mode, since the basic nature of the piston mode is such that it communicates with the external flow outside of the ice floe due to continuity of mass. This is illustrated as communication in figure 2.4 and 2.3.

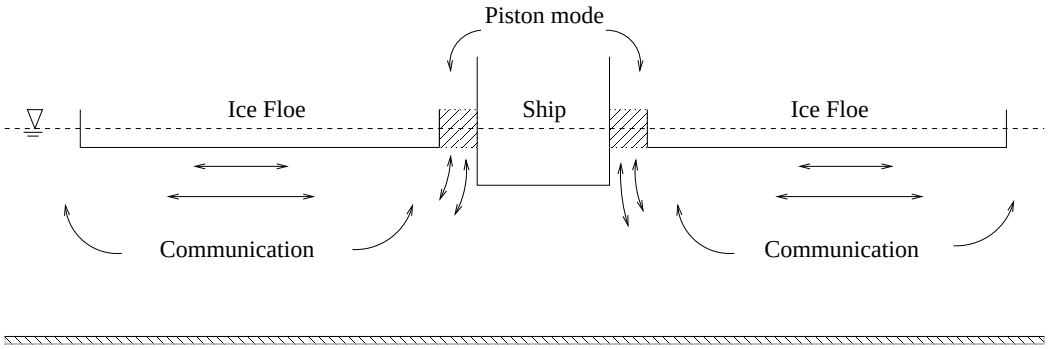

Figure 2.4: Illustration of the piston-mode motion but with two ice-floes.

As previously mentioned the ship section is forced to oscillate, which means it is a part of the usual diffraction and radiation sub-problems, see e.g. [8]. One can also imagine that the ship could be moving freely and then oscillate and hence the resonant piston-like motion will be triggered whether excited by waves entering the system or by forced ship section motions. So disregarding which sub-problem, there is one single frequency of the piston-mode motion, which is denoted ω_p. This resonance frequency have also been referred to as the piston-mode resonance frequency, and terms like ice-gap resonance and piston-mode resonance will be used interchangeably.

In the following chapter a description on how to obtain the piston-mode resonance frequency, ω_p. A discussion on the dependence of the geometric parameters as well as the overall behavior of the system is included. In addition throughout the report the term resonance period will be used, $T_p = 2\pi/\omega_p$.

2.3 Piston-mode resonance

An approximate method to estimate natural periods in gaps similar to the situation under consideration was derived within linear theory by [21] for the case of infinite water depth. The problem for finite water depth was treated by [9]. In the mentioned references a frequency domain approach have been utilized, but in this work a time domain approach have been used.

The resonance frequency of the piston mode ω_p is found by performing forced motion of the ship section for a range of frequencies using the linear time-domain numerical wave tank which will be described in a later chapter. The simulations are run until they reach steady state. However it it was discovered that not all cases was solvable with the present code, this is discussed in chapter 6. The resonance frequency of the piston mode , ω_p, is taken as the frequency for which the averaged amplitude of the free surface in the gap between the ship and the ice-floe attains a local maximum when plotted versus frequency.

Piston body reasoning

The existence of a natural period of the piston mode is a consequence of the mass-spring type behavior of the piston mode. This can be illustrated by a simplified linear analysis. The problem is similar to that of a moonpool see e.g. [8] page 99 and the procedure is translated to fit the current problem. The fluid motion in the ice gap is assumed to be uniform, e.g. the fluid in the shaded area in figure 2.4. The flat free surface is denoted $\eta(t)$ as illustrated in figure 2.5. This means that all the fluid in the shaded area denoted Ω_p in the figure oscillates vertically with velocity η_t. Under the assumption of uniform fluid motion within Ω_p, the fluid in Ω_p will act as a rigid body on the surrounding fluid. The equation of motion in heave of the piston body Ω_p

can then be written as,

$$(\rho Db + A_p)\,\eta_{tt} + B_p\eta_t + \rho gb\eta = F_D \tag{2.1}$$

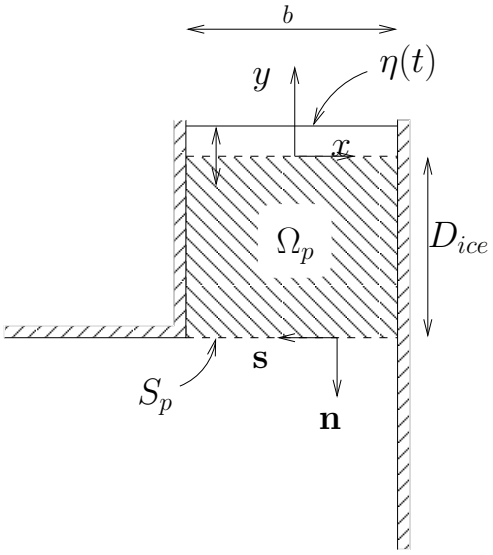

Figure 2.5: Simplified, linear hydrodynamical problem of piston-mode motion. The fluid motion within Ω_p is assumed uniform, so the shaded mass acts like a rigid body. S_p is the dashed (horizontal) line only.

where $A_p(\omega)$ and $B_p(\omega)$ are the added mass and damping coefficients of the piston body, respectively, and F_D is the excitation force. The draft D is the draft of the ice-floe, D_{ice}, but just denoted D here for simplicity. If the motion in equation 2.1 is assumed to be harmonic, $\eta = \eta_a e^{i\omega t}$, the homogeneous problem can be solved to find the body's natural period $\tilde{T}_p$. The homogeneous equation is $\omega^2\left(\rho Db + \tilde{A}(\omega)\right) + i\omega\tilde{B}(\omega) + gb = 0$. The undamped natural period is found to be,

$$\tilde{T}_p = \frac{1}{2\pi}\sqrt{\frac{\rho Db + \tilde{A}_p}{\rho gb}} \tag{2.2}$$

where $\tilde{A}_p$ is the added mass at the natural period. From equation 2.2 it is observed that the natural period increases with the square root of the draft D. However as the ship is the driver in the system the draught would be more correct if the mean value of the ship and ice draught is used. It further depends on the added mass term $\tilde{A}_p$. The added mass term depends on all geometric variables B for ice and ship, D for ice and ship and h. The behavior of the added mass $\tilde{A}$ is a

variable that is not easy to quantify as it varies appreciably in gap problems. It should also be noted that the fluid flow along the lower parts of Ω_p will not behave as the assumed uniform flow. An in depth study of the simplified problem have not been performed in this work but this example illustrates that the piston mode can be, to a certain extent, be thought of as a rigid body. In the present work the ship-ice system is the main focus. An explicit approximate formula for T_p is given by Molin [21] for the case of deep water and small b/B ratio. In the following chapter a study of the relative importance of the calculation paramters is presented. It is observed that the resonance frequency change significantly with the ship-beam ratio. This implies that b/B ratio mentioned above is not always small and hence the Molin approximation is strictly not valid for the ship-ice problem.

2.3.1 Relative importance of calculation parameters

As previously mentioned the added mass varies appreciably in gap problems. To aid in the understanding of the relative importance of the variables in the problem, a set of numerical simulations were done to establish this. The simulations were done in the numerical wave tank that is explained in 3. The calculations were done with the symmetrical set-up of the ship-section in the middle of two ice-floes, as seen in figure 2.4. In these simulations the *beam-draft* ratios,B/D, of the ship section and and ice-floes were tested and the importance of the tank depth h.

For the simulation to test the importance of the B/D for the ship all other parameters were kept the same as used in the experimental and numerical calculations. For the other parameter tests the procedure were similar, only the parameter that were to be tested were changed. The results can be seen in figures 2.6 to 2.11.From the results it is observed that the most significant change in the resonance frequency and added mass is related to the B/D ratio of the ship. This also indirectly indicate that for the gap problem the b/B is the dominating parameter in the system. When the B/D ratio for the ship is small e.g. 1 as seen in figure 2.6 and 2.7 it also means that the b/B ratio is bigger because the gap width, b have been kept constant while the ship-section beam, B has become smaller. Thus the most important parameter in the ship-ice system is the gap width and ship beam ratio b/B.

For the results related to the ship section parameters it is seen that the water elevation amplitude in the gap A_g is linearly dependent on the ships beam B. It is also observed in the plots for

the beam-draught ratios for the ice that the resonance frequency is dependent on the beam of the ice-floe and there is a peak at a frequency corresponding to approximately the width of the ice.

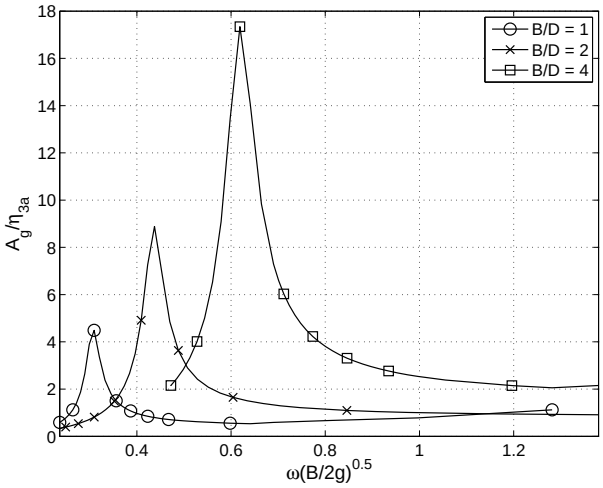

Figure 2.6: A_g/η_{3a} for $B/D = 1$, $B/D = 2$ and $B/D = 4$ for ship-section

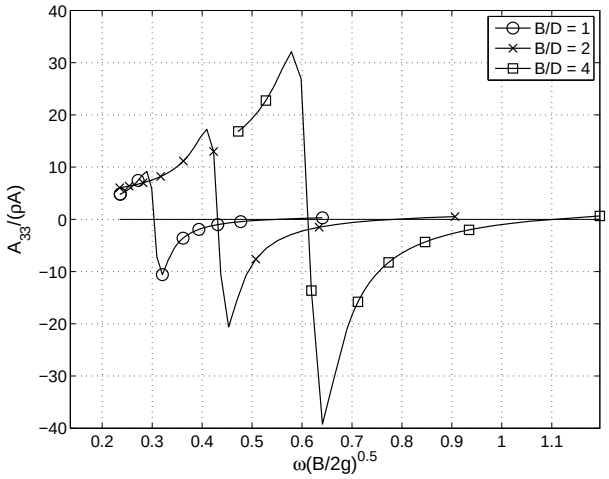

Figure 2.7: $A_{33}/\rho A$ for $B/D = 1$, $B/D = 2$ and $B/D = 4$ for ship-section

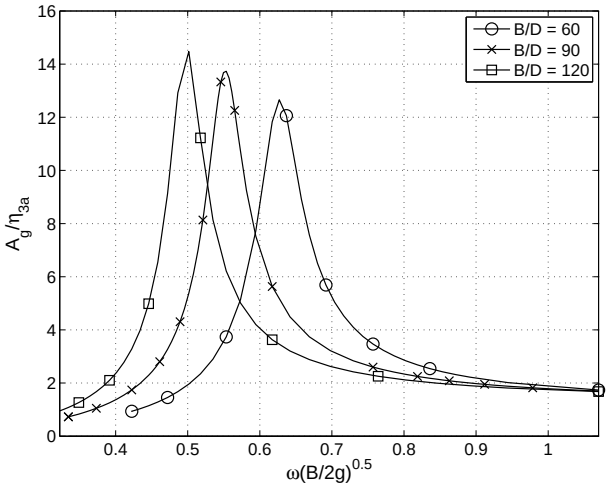

Figure 2.8: A_g/η_{3a} for $B/D = 60$, $B/D = 90$ and $B/D = 120$ for ice-floe

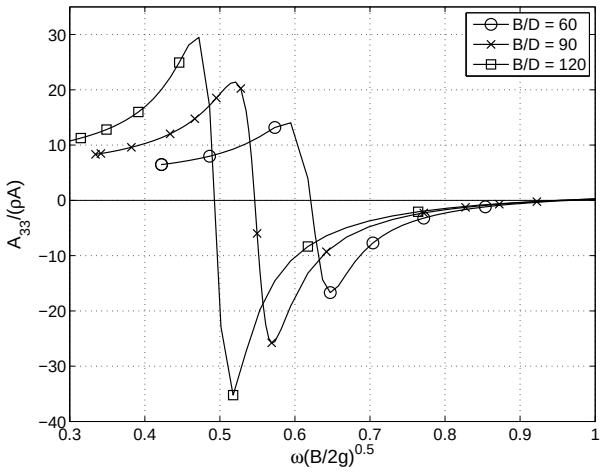

Figure 2.9: $A_{33}/\rho A$ for $B/D = 60$, $B/D = 90$ and $B/D = 120$ for ice-floe

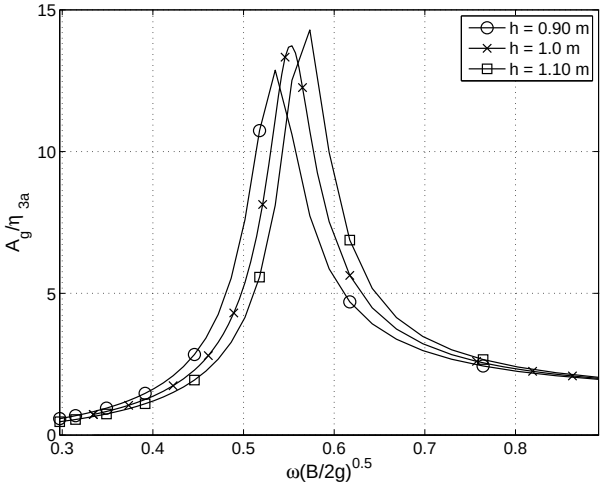

Figure 2.10: A_g/η_{3a} for depths of $h = 0.90\ m$, $h = 1.00\ m$ and $h = 1.10\ m$

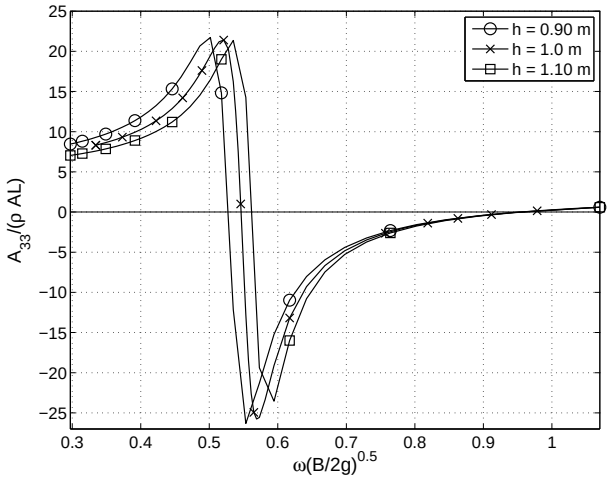

Figure 2.11: $A_{33}/\rho A$ for depths of $h = 0.90\ m$, $h = 1.00\ m$ and $h = 1.10\ m$

2.3.2 Coupled ship and piston-mode resonance

The presence of ice, as used in this study, introduces coupling between the flow of the fluid and the rigid body motions of the ship section. The couplings are in sway, heave and roll. If an open water problem is considered, no ice presence in proximity of the ship, there is only a coupling between sway and roll, for a symmetric shaped ship. In this study only heave is considered. With the ship set up, the coupling between the motion of the ship and the piston-mode is an essential feature.

In the paper written by McIver [20] he investigates the gap problem for both the radiation, diffraction and freely oscillating problem by a linear potential flow analysis. In his study of the homogeneous solution of the equations of motion (added mass, damping and exciting forces included) he finds that for a freely floating body that ω_p do not exist. An exception exists if the ship section is fixed in one or two degrees of freedom. The system may then retain piston-mode, ω_p, resonance. He also shows that in general that the piston-mode resonance is different from the system resonance, $\omega_p \neq \omega_n$. He describes this as a shift in resonance frequency, from ω_p to ω_n. This means that the coupled ship and piston-mode resonance, when the ship is free to oscillate in all degrees of freedom, will be significant around ω_n only. There is in particular no pure heave resonant-motion, only that of the coupled ship section and fluid motion.

In the same paper from McIver he also discuss the occurrence of negative added mass. When sloshing is considered or as in this study a special case of sloshing, previously referred to as the zeroth mode denoted piston-mode, resonances are found. In the gap problem with the ship forced to oscillate in heave characteristic rapid changes are observed in the added mass and damping coefficients near resonance frequency. This means that in the present case with the ship-ice system the phenomenon of negative added mass is observed.

When no moorings are assumed in the set-up there is one resonant frequency for each variation of the gap b in heave. If the heave motion is coupled with sway, two resonant frequencies exist for the asymmetric set-up with onc ice-floe with the ship section oscillating next to it, see figure 2.3.

In the present work, the required added mass and damping coefficients is found from forced heave oscillations of the ship section in ice by a numerical wave tank and from experiments. The

numerical wave tank is explained in chapter 3 and the model tests are explained in chapter 5. The simulations are run to steady-state and the hydrodynamic coefficients extracted from steady parts of the time-series.

The main driving mechanism for the piston-mode motion is the forced heave oscillation of the ship-section and the communication with the external domain. The external domain means the fluid outside of the ice-floes.

The system that determines the level of response in in the ship-ice gap, i.e. the achieved steady-state piston-mode amplitude A_g is the amount of fluid needed, hence the gap width b is of importance. When the gap is small i.e. $b = 0.01m$ resonance appear at a high oscillating period which means longer wave lengths then when the gap is bigger, $b = 0.10m$ the resonance effect happens at lower periods i.e. shorter wavelengths. Thus more fluid must be accelerated beneath the ice-floe and into the gap.

At resonance, the amplitude of the ship motion is proportional to the net force and also inversely proportional to the damping. Waves radiated as a consequence of the ship section motion and the piston-mode motion contribute to the potential damping.

2.4 Effect of flow separation

In the chapter is the piston-mode behavior in the ship-ice gap described like a damped, linear harmonic oscillator. Therefore, the response level relative to the level of excitation is at resonance directly dependent on the level of damping, where linearly, damping is manifested through wave radiation only. This is the potential flow damping. In reality the flow separates at the sharp corners of the ship and ice-floe. This means that vorticity is shed into the bulk of the fluid with the main consequence that circulation is introduced, illustrated in figure 2.12. The circulation is in such a phase relative to the ambient flow, such that that the phase creates a back-flow acting as a damping factor. This is further conceptually illustrated in figure 2.13. Kristiansen, [16], found that the damping effect of flow separation on the piston-mode amplitude due to forced heave of the ship is significant.

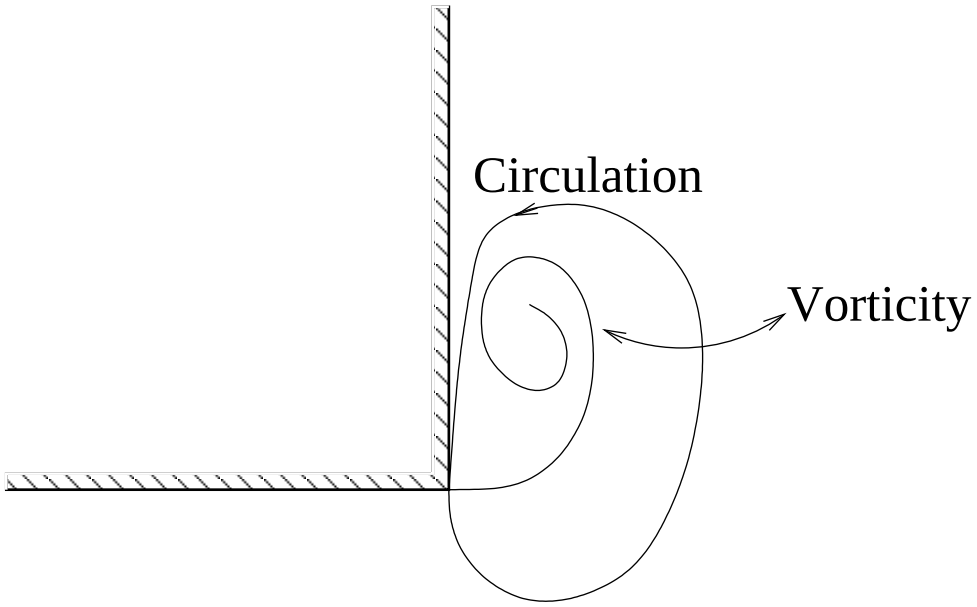

Figure 2.12: Illustration of the circulation introduced by the shed vorticity.

As only linear theory is considered in the numerical calculations it do not predict well the resonant behavior in the ship-ice gap system. This is most likely related to non-linear effects from flow separation.

2.5 Three-dimensional effects and hydroelasticity

In the study of the ship-section in forced heave with the ice-floes present, only the two-dimensional problem is considered. All realistic situations are in three dimensions, meaning that the fluid will have the opportunity to flow in all directions. Also green water on the top of the ice is expected. Also for the case of a ship in open water, waves will be scattered in all directions around the ship and in particular radiate from the fore- and aft ends of the structure, see e.g. [8] page 196. When real ice is considered it will show elastic properties. If ice is floating in close proximity to a floating structure that is oscillating one can imagine that because of the acceleration of the fluid will induce a vertical motion in the flexible ice. In figure 2.14 this effects is illustrated. When the structure is moving upwards there is an immediate deformation of the ice downwards and opposite when the structure has a motion downwards.

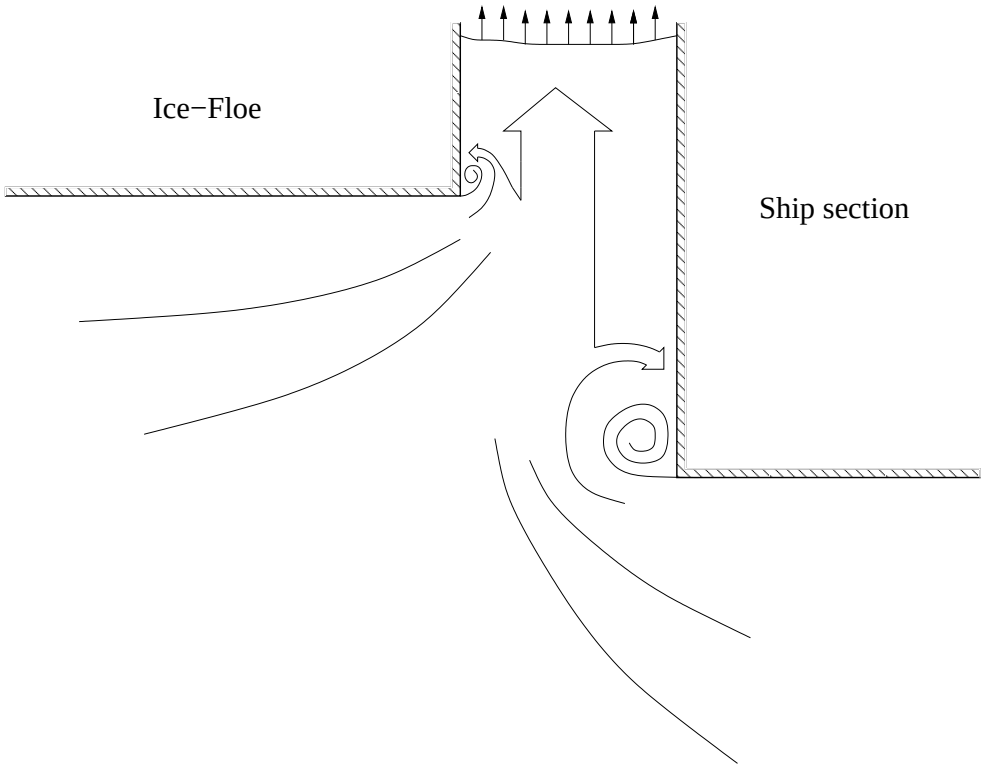

Figure 2.13: Schematic of the effect of circulation.

In hydroelastic problems the hydrodynamic forces are influenced by the elastic deformation of the structure. This deformation is governed by inertia forces and elastic forces in the structure. The modeling of the elastic properties of structures will therefore give several additional problems compared to the modeling of wave induced dynamic response of rigid structures. Requirements to an elastic model can be summarized as follows:

- Correctly scaled global structure stiffness
- Structural damping must be similar to full scale values
- The mass distribution must be similar

Geometrical similarity between model and full scale for an elastic structure will require that the elastic deformation is similar, [1].

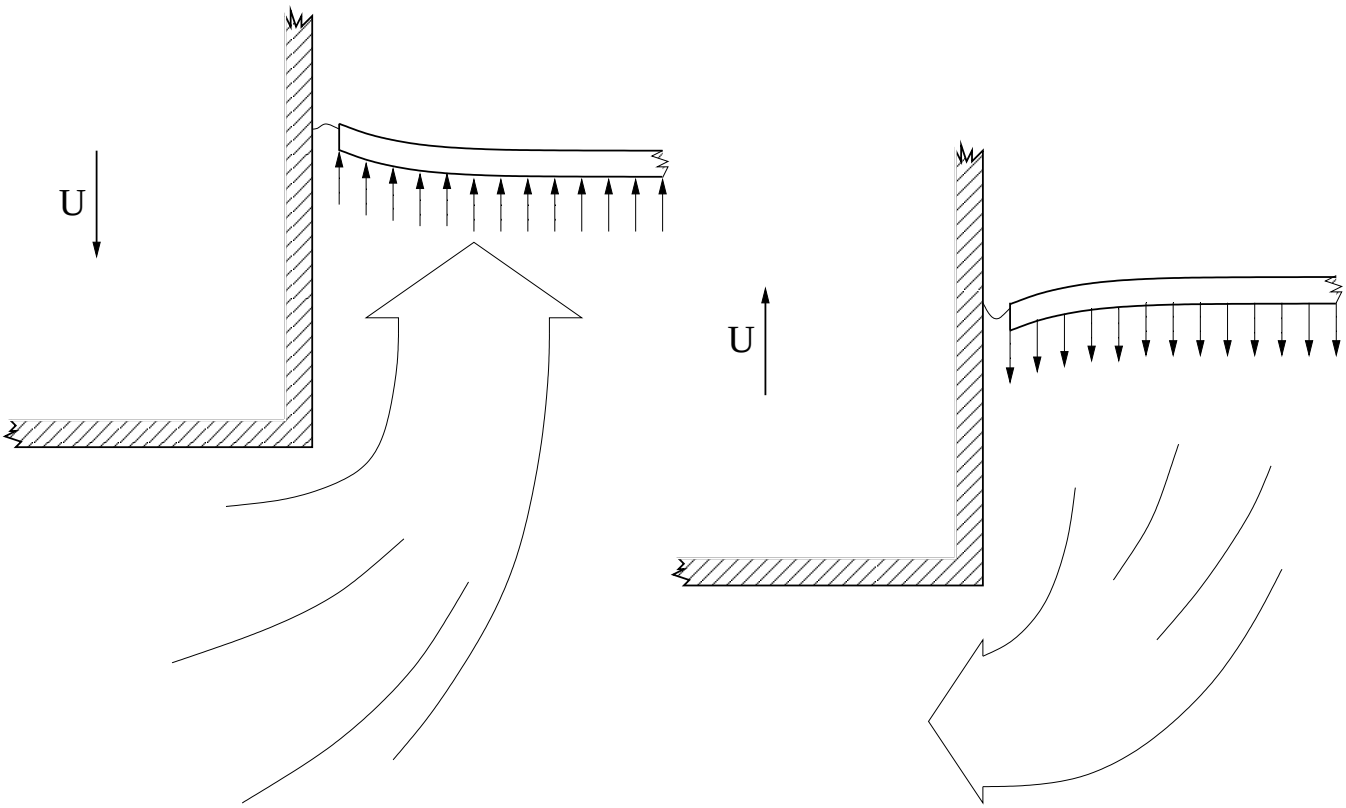

(a) Ship moving downwards. (b) Ship moving upwards.

Figure 2.14: Illustration of flexible level ice showing hydroelastic behavior.

2.6 Boundary layer

The boundary layer is of importance of the ship-ice problem in this study. When the ship section is oscillating close to the thickness of the boundary layer is important to determine how close the ice floe can be allowed to be and not provoke unphysical behavior. Note that the numerical calculations are performed according to linear theory and hence no boundary layer is found in them, i.e. the boundary layer is relevant for the model tests.

When flow around corners are considered, some turbulence is to be expected. The level of turbulence can be quantified with the Reynolds number and can be written as,

$$Rn = \frac{2\omega a^2}{\nu} \tag{2.3}$$

Now, the flow around a ship section corner will behave similar to that around one corner rectan-

gle in infinite fluid. This applies at least if the vortical structures confined to the vicinity of the corner such that the bottom, ice-floe corner and free surface are considered to be in the far-field. In all the investigated cases a steady state have been reached and the observed piston-mode motion of the fluid are quite sinusoidal. This means that the piston-mode amplitude can be used as a relevant measure of the ambient flow amplitude a in 2.3, [16].

According to Kristiansen [16] a measure of the boundary layer thickness can be found by saying the distance δ from a wall, i.e. Ship side, where the actual flow differs from the outer flow by 1%. For a laminar boundary layer this is $\delta \simeq 4.6\sqrt{2\nu/\omega}$. For the open water where the ship section is oscillating without any ice-floes this is valid. For the cases with ice-floes located close to the oscillating ship the flow might be considered turbulent. At resonance the Reynold's number is in the order of $o(10^5)$. In an oscillatory flow over a smooth surface, the critical Reynold's number for transition between laminar and turbulent boundary layer flow is actually $o(10^5)$. This means that the boundary layer must be estimated in a different manner. For a turbulent boundary layer the thickness can be estimated by $\delta = 0.093aRn^{-0.11}$,[16]. The latter estimation yields a boundary layer of about 2.3 *mm*, assuming the boundary layer has the same thickness at the ice-floe the total boundary layer is in the order of 5 *mm*. With this in mind the ice-floes were not placed closer to the oscillating ship section than 1 *cm*, the effect of surface tension is also considered in this choice as such effects are not relevant for full scale vessels.

2.6.1 Scaling

In the study a model with sharp corners i.e. 90°have been used. This creates vortex shedding, due to this no significant scaling effects is expected. The beam of the model is 0.32 *m* and the draught is 0.12 *m*. A real ship might have a beam of 32 *m* and a draught of 12 *m*, this means that the scaling can be said to be *1:100*. Further the ice is modeled with a beam of 3.6 *m*, which gives a full scale beam of 360 *m* and is considered large compared to the ship, the ratio between the ship beam and ice beam is then 11.25.

Chapter 3

Numerical calculation method

In the work of obtaining values for the hydrodynamic coefficients by numerical calculations the method, commonly known as the Boundary Element Method (BEM), have been used.

The code is developed by Dr. Trygve Kristiansen as part of his PhD and recently modified for multibody problems. The following text is based on Kristiansens thesis [16], and is included here for easy reference to the theory and numerical method which has been utilized.

The boundary element method, also sometimes referred to as panel method, is a very economical method used for two-dimensional potential flow problems. The calculations have been carried out within a closed tank as illustrated in figure 3.1. The domain of the tank is denoted by Ω and its boundary S. In this S is defined to consist of the solid surfaces S_0+S_B as well as the free surface S_F such that S=S_F+S_W+S_0+S_B.

An Earth-fixed right-handed coordinate system is defined with Cartesian coordinates (x,y) where y is positive upwards, and the horizontal axis defined by $y = 0$ in the mean water line. The surface S_B represents a ship section, while S_0 typically represents the tank wall and bottom and S_W is the surface of a flap type wave maker. In the current setting the wave maker is inactive and is considered as a wall, like S_0. The domain Ω bounded by the closed surface S is hereafter usually referred to as the numerical wave tank.

The numerical wave tank is created after linear theory which means that the domain and its boundary are fixed in time. The free-surface elevation is denoted $\zeta(x,t)$.

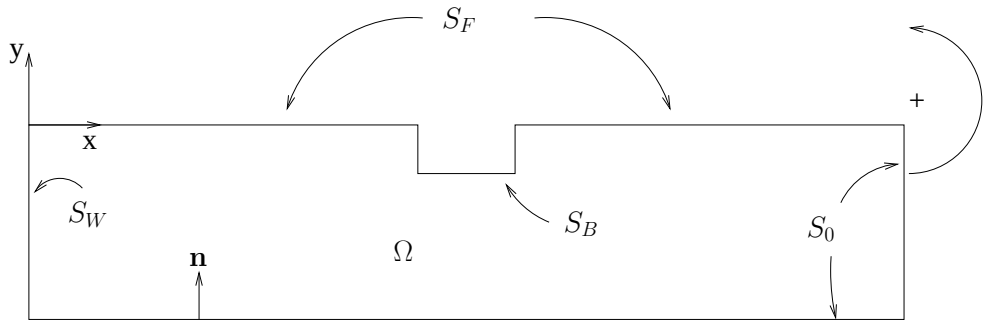

Figure 3.1: Illustration of the closed linear tank considered in the work. The domain is denoted Ω and its boundary S=S_F+S_W+S_0+S_B. The cartesian coordinate system denoted (x,y) is defined so that $y = 0$ is in the mean water line. The unit normal vector **n** is defined positive into the water.

3.1 Governing equation

The fluid is assumed incompressible and inviscid. The governing equation for the fluid motion is the Laplace equation.

$$\nabla^2 \varphi = 0 \text{ in } \Omega \tag{3.1}$$

Because the fluid is assumed inviscid the velocity may be represented by the gradient of a velocitypotential φ, such that $u = \nabla\varphi$.

Conservation of mass is described by the divergence of the velocity $\nabla u = 0$, where u is the fluid velocity at any point and at any time, and $\nabla = (\partial/\partial x, \partial/\partial y)$.

The unknown φ is solved over the domain Ω defined by the closed surface $S = S_F \cup S_W \cup S_0 \cup S_B$. The Laplace equation implies that this is an elliptic problem. The consequence of this is that at any point in the domain the solution depends the solution everywhere else in the domain. Hence boundary conditions along the boundary S are needed.

3.2 Representation of a solution by surface singularity

The use of a surface singularity as outlined by [13] and [8]. A source in two dimensions can be written as

$$\varphi = q \log r \tag{3.2}$$

In higher dimensions it can be written as

$$\varphi = q r^{n-2} \tag{3.3}$$

Where r is the radial distance from the source point given as $r = \sqrt{\sum_i^n x_i^2}$, and q is the source strength and n is the dimension of the space. If $q < 0$, the source is negative, then the previous equations 3.2 and3.3 are referred to as sinks.

Potential flow problems can be solved by distributing sources along the boundaries of the fluid and solving for the source strengths q by applying proper boundary conditions. By assuming a continuous representation of sources over the boundary the velocity potential can be written as

$$\varphi(x,y) = \int_S q(s) \ln \left((x - \xi(s))^2 + (y - \eta(s))^2 \right)^{\frac{1}{2}} ds \tag{3.4}$$

Where $(\xi(s), \eta(s))$are the coordinates along the boundary and s is an integration variable over the boundary. To make a numerical approximation the boundary can be divided into N straight lines and it is assumed a constant source density over each segment.

$$\begin{aligned} \varphi(x,y) &= q_1 \int_S (s) \ln \left((x - \xi(s))^2 + (y - \eta(s))^2 \right)^{\frac{1}{2}} ds \\ &= + \dots \\ &= q_N \int_S (s) \ln \left((x - \xi(s))^2 + (y - \eta(s))^2 \right)^{\frac{1}{2}} ds \end{aligned} \tag{3.5}$$

3.2.1 Boundary conditions

When boundary conditions are introduced a matrix system for solving the unknown source strengths can be established.

Along S_F the boundary conditions comprise the dynamic and kinematic free-surface conditions, while along $S_0 + S_B$ there is the zero-penetration boundary condition.
For the free surface S_F

$$\frac{\partial \varphi}{\partial t} = -g\zeta \text{ on } y = 0 \tag{3.6}$$

$$\frac{\partial \varphi}{\partial t} = -\frac{\partial \varphi}{\partial n} \text{ on } y = 0 \tag{3.7}$$

Where by $y = 0$ is the mean waterline outside the body and n is the normal vector pointing in to the fluid.

On the solid boundaries of the wave tank the zero penetration is imposed

$$\frac{\partial \varphi}{\partial n} = 0 \text{ on } S_0 \tag{3.8}$$

And for the boundary of the ship section and ice floes, when they are applied;

$$\frac{\partial \varphi}{\partial n} = \mathbf{U_B n} \text{ on } S_B \tag{3.9}$$

Here $\mathbf{U_B}$ is the velocity along the ship and ice floe.

3.2.2 Boundary integral equation

In the program sources and dipoles are distributed all along the boundary. Them BEM is based on Greens second identity. For any point x in the fluid domain including its boundaries, we have

$$\theta(\mathbf{x})\,\varphi(\mathbf{x}) = -\int_S \varphi(\xi)\frac{\partial\psi(\xi,\mathbf{x})}{\partial n_\zeta}ds - \int_S \psi(\xi,\mathbf{x})\frac{\partial\varphi(\xi)}{\partial n_\xi}ds \tag{3.10}$$

Where the first integral is defined as a principal value integral, is analytic everywhere, and the source term is

$$\psi(\xi,\mathbf{x}) = \ln r \tag{3.11}$$

$$r = \left((x-\xi)^2 + (y-\eta)^2\right)^{1/2} \tag{3.12}$$

The positive direction of integration is counterclockwise, and n is the unit normal to vector pointing into the fluid, see figure 3.1. The internal angle $\theta(\mathbf{x})$is measured counterclockwise and is, e.g.,$-\pi$ when $\mathbf{x}$ is on a flat part of the boundary. The field point is $\mathbf{x} = (x,y)$, and $\xi = (\xi,\eta)$ is the integration parameter. Furthermore $\partial/\partial n_\xi = n_1\partial/\partial\xi + n_2\partial/\partial\eta$ is the normal derivative with respect to the integration parameter ξ.

3.2.3 Boundary element method

The Boundary Element Method (BEM) is the discretized version of the boundary integral equation. The boundary of the fluid domain, S, is divided into elements of some prescribed shape, and the variation of the unknowns over each element assumed to be of a certain order. The program used in the work use a linear variation of the unknowns over each element.

The boundary element program works by dividing the full boundary S into a total of N (free surface) $+M$ (solid boundaries) straight elements and assume that φ and φ_n vary linearly over each element. It is chosen $N+M$ collocation points to be the end points of the elements. The integral equation then reduces to a set of $N+M$ linear equations in the same number of unknowns. The resulting linear system of equations is dense and is solved by a direct solver. With the boundary conditions for φ on the free surface and φ_n on the solid boundary, the $M-2$ unknowns φ on the solid boundaries and the $N+2$ unknowns on the free surface are calculated.

3.2.4 Numerical beach

A numerical damping zone is used to damp out waves in the far-field. The damping is introduced by artificial dissipation terms that are added in the free surface conditions which are chosen to be proportional to the vertical coordinate of the free surface y and the potential φ in the kinematic free-surface conditions, respectively,

$$\frac{Dx}{Dt} = \nabla\varphi - \nu\zeta \text{ on } S_F \tag{3.13}$$

$$\frac{D\varphi}{Dt} = \frac{1}{2}\left(\frac{\partial\varphi}{\partial x} + \frac{\partial\varphi}{\partial y}\right) - g\zeta - \nu\varphi \text{ on } S_F \tag{3.14}$$

here $\nu = \nu(x)$ is typically a smooth function, which is nonzero in the damping zone, and zero elsewhere. See figure 3.2. It is taken such it is smoothly increasing up to ν_{max}. The interval over which $\nu = \nu(x)$ is nonzero is denoted L_d. Because the function is smooth to minimize reflections it varies with x.

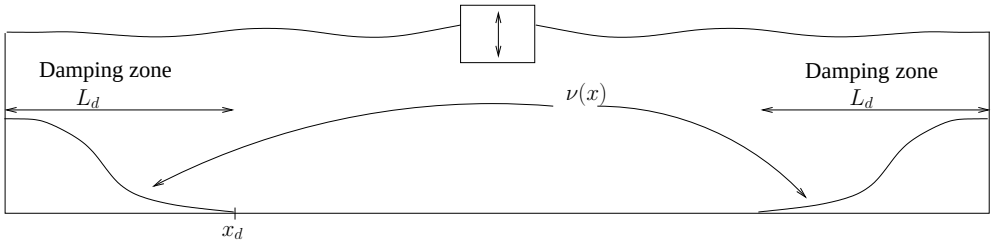

Figure 3.2: Illustration of numerical damping zone parameter $\nu(x)$ with the scenario of a body in forced heave motion.

3.3 Formulation of forces

When the velocity potential is known at every location of the wave tank the pressure along a body can be found, and by integration of the pressure along the bodys boundary gives the forces acting on it.

$$\mathbf{F} = -\int_{S_B} p\mathbf{n}ds \tag{3.15}$$

where the normal vector ($\mathbf{n} = (n_x, n_y, n_\theta)$) points into the fluid, where $n_\theta = x_a n_y - y_a n_x$ and x_a and y_a are the distance from the center of gravity in x- and y-direction. The pressure p for any point in the fluid is found using the *Bernoulli* equation

$$\frac{p}{\rho} + \frac{\partial \varphi}{\partial t} + \frac{1}{2}\left(\frac{\partial \varphi}{\partial x}\right)^2 + \frac{1}{2}\left(\frac{\partial \varphi}{\partial y}\right)^2 + gy = c \tag{3.16}$$

Where c is a constant and is set to zero. Inserting the Bernoulli equation in equation 3.15 for the pressure yields

$$\mathbf{F} = \rho \int_{S_B} \frac{\partial \varphi}{\partial t}\mathbf{n}ds + \rho \int_{S_B} \frac{1}{2}|\nabla\varphi|\,\mathbf{n}ds + \rho g \int_{S_B} y\mathbf{n}ds \tag{3.17}$$

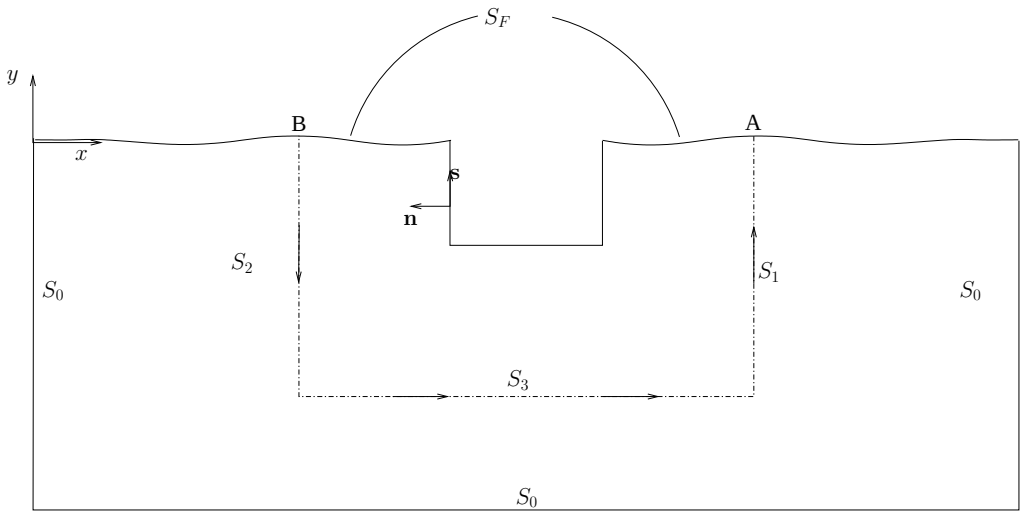

Figure 3.3: Path of integration, point A and B are to be taken to be a ship breadth from the ship ends. Note that S_F is now the free surface between point A and B.

The equation can be rewritten to eliminate the φ_t terms and a control surface is introduced as shown in figure 3.3. The expression for the force can now be written as

$$\mathbf{F} = -\int_{S_B} p\mathbf{n}ds = -\int_{S} p\mathbf{n}ds + \int_{S_B+S_C} p\mathbf{n}ds \tag{3.18}$$

Where the integrals on the free surface S_F is zero, as the pressure is zero and S_C is defined as equal to $S_1 + S_2 + S_3$. Similar equation 3.17 can be rewritten as

$$\mathbf{F} = \rho \int_S p\mathbf{n}ds + \rho \int_{S_B+S_F} \frac{1}{2}|\nabla\varphi|^2\mathbf{n}ds + \rho g \int_{S_B+S_F} y\mathbf{n}ds - \rho \int_{S_C} p\mathbf{n}ds \tag{3.19}$$

The integration of φ_t over the surface S is not trivial and has been completely removed from the calculation scheme. This is achieved by first using *Gauss* theorem

$$I_1 = -\frac{\partial\varphi}{\partial t}\mathbf{n}ds = -\int_\Omega \nabla\varphi_t d\Omega \tag{3.20}$$

and next using the Transport theorem is utilized

$$I_1 = -\frac{d}{dt}\int_\Omega \nabla\varphi_t d\Omega - \int_S \nabla\varphi U_n ds \tag{3.21}$$

Where U_n is the normal velocity of the boundary. And again using *Gauss* theorem and that and that $U_n = 0$ on S_C and $U_n = \varphi_n$ on $S_B + S_F$

$$I_1 = \frac{d}{dt}\int_S \varphi\mathbf{n}ds - \int_{S_B+S_F} \nabla\varphi\varphi_n ds \tag{3.22}$$

inserted into equation 3.19 gives the following expression

$$\mathbf{F} = \rho\frac{d}{dt}\int_S \varphi\mathbf{n}ds + \rho \int_{S_B+S_F} \left(\frac{1}{2}|\nabla\varphi|^2\mathbf{n} - \nabla\varphi\varphi_n\right) ds + \rho g \int_{S_B+S_F} y\mathbf{n}ds - \rho\int_{S_C}\frac{\partial\varphi}{\partial t}\mathbf{n}ds \tag{3.23}$$

The expression in the second integral can be rewritten, and the partial derivative with respect to time in the last integral can be eliminated using the non-dimensional equivalent of the Transport theorem. See [16] for the complete derivation of the force terms.
The resulting equation for the force terms can be written as

$$\mathbf{F} = \rho\frac{d}{dt}\int_{S_B+S_F} \varphi\mathbf{n}ds + \rho\int_{S_B+S_F}\left(\frac{1}{2}\left(\varphi_s^2 - \varphi_n^2\right)\mathbf{n} - \varphi\varphi_n\mathbf{s}\right)ds + \rho g\int_{S_B+S_F} y\mathbf{n}ds + \rho[u\varphi\mathbf{s}]_a + \rho[u\varphi\mathbf{s}]_b \tag{3.24}$$

Here the first integral (only considering integral overS B) represents added mass and damping, and the third integral is the restoring force.

3.4 Limitations

During calculations with an asymmetric geometric layout with one ice floe on one side of the oscillating ship it was shown that it was not possible to retrieve good results for all cases to be evaluated numerically. For all situations where the ice-floe is located closer than 4 *cm* for the asymmetric configuration the calculations either broke down or the solution go towards infinity and also some times heavily influenced by beating. A short description of beating is given below. It should also be noted that as the numerical wave tank is based on linear theory effects like vortex shedding are hence not included in the solution. One consequence of this is that it will in general over predict the hydrodynamic forces the ship section is experiencing.

Beating was observed in the vicinity of the resonance frequency when the ice-floes was included in the calculations. Beating is provoked due to transient behavior when starting from initially calm conditions. This is a result from small damping. Therefore, steady state may in general not be reached within the time of simulation.

3.5 Parameters and numerical model

Because the numerical calculations are performed in two dimensions all quantities are taken per length in the xy-plane. All parameters from the experiments are therefore scaled in such a way that they are comparable to the two dimensional values from the numerical calculations.

To model the setups that were to be evaluated, three models was used in the numerical code presented. The three geometrical discretized setups used are shown in figure 7.1b, the models are a open water setup, the ship and one ice floe and the ship in the middle of two ice floes

The length of the tank was set by $L = 12ambda + B_{ship}$ for the open water case. For the geometrical set up with one and two ice-floes the length was set, respectively, by $L = 12\lambda + B_{ship} + b + B_{ice}$ and $L = 12\lambda + B_{ship} + 2b + 2B_{ice}$. A sinusoidal signal with linear initial ramp of ten periods was used to, as a large extent as possible, avoid beating. The simulations were run for 60 to 100 oscillation periods to achieve steady state and the number of time steps N_p per period is set to 80.

3.6 Convergency and accuracy

A convergence test was performed to test the effect of the number of elements per wavelength on the free surface and the number of elements used on the oscillating ship. The result of the convergency test at resonance is seen in figure fig:konvagl. The results from the test with the highest density of elements to the lowest is about 0.2 %, hence the number of elements used in most of the calculated cases are $15/\lambda$.

Free surface (external + gap left + gap right)	$N_F = 180 + 8 = 188$
Ship section (side + bottom + side)	$N_{B,ship} = 12 + 32 + 12 = 56$
Ice-floe (side + bottom + side), min. value	$N_{B,ice} = 3 + 15/\lambda + 3$
Bottom of wave tank	$N_{BOT} = 80$
Far end of damping zone	$N_{WM} = 8/\lambda$
Tank length, open water	$L = 12\lambda + B_{ship}$
Tank length, one ice-floe	$L = 12\lambda + B_{ship} + b + B_{ice}$
Tank length, two ice-floes	$L = 12\lambda + B_{ship} + 2b + 2B_{ice}$
Numerical beach length	3λ
Dissipation parameter	$\nu_{max} = 0.4$
No. of time steps per period	$N_p = 80$
No. of oscillation periods	$N_T = 60, 80$ and 100
Forcing amplitude (steep)	$\eta_{3a} = 0.01\ m$

Table 3.1: Numerical parameters in the simulations.

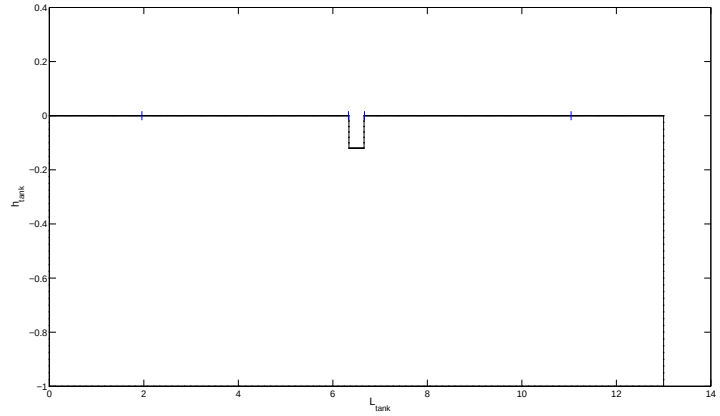

(a) Only ship

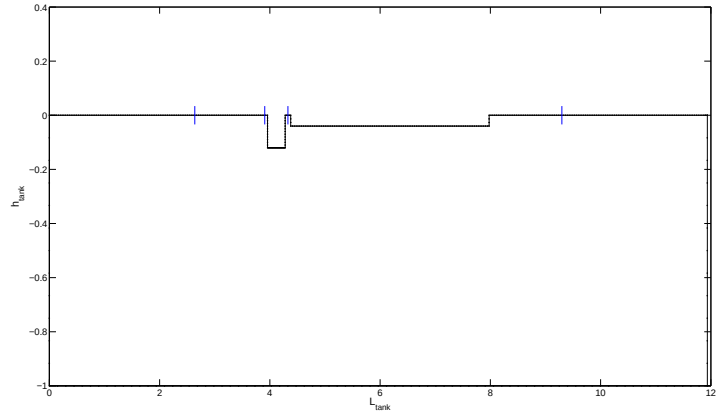

(b) Ship with one ice-floe

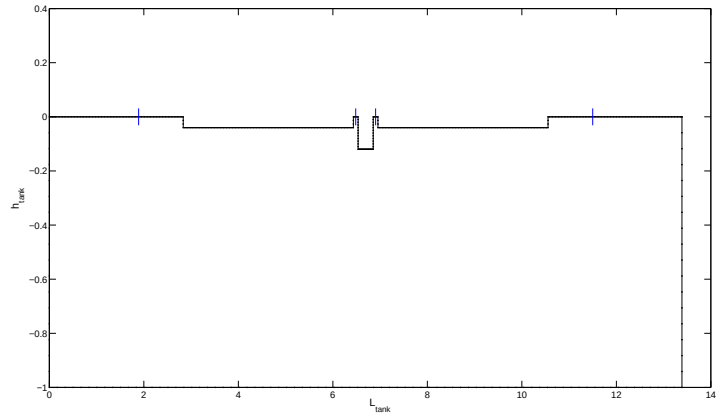

(c) Ship with two ice-floes

Figure 3.4: Overview of the numerical models used in the work with grid. Note that the axis are not equally scaled.

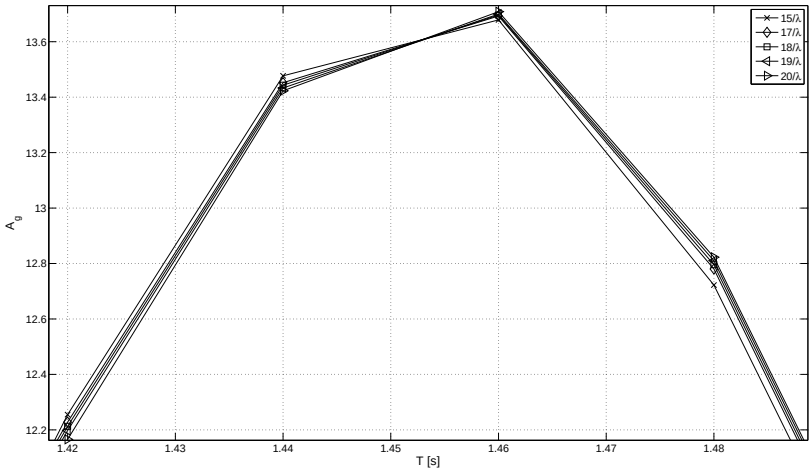

Figure 3.5: Results from a convergency test done in the numerical wave tank with from 15 to 20 elements per wave length λ. The results differ with only 0.2% from the simulations with $15/\lambda$ to the simulations with $20/\lambda$.

Chapter 4

Hydrodynamic coefficients

The present work is concerned with the two-dimensional motion of a structure in an incompressible and inviscid fluid with the main objective of studying the fluid interaction with a ship section that is oscillating in close proximity of one and two ice-floes.

In the study linear theory is used for the theoretical considerations. A steady state condition is assumed, which means that no no transient effects are present due to initial conditions. This condition implies that the linear dynamic motions and loads on the ship are harmonically oscillating with the same frequency as the wave loads that excites the ship, or in this case the opposite as the ship section is operating in forced oscillations. This is the second of the usual two sub-problems as described in [8] and [11].

In the second sub-problem the forces and moments are found on the body when the structure is forced to oscillate in calm water with the wave excitation frequency in any rigid-body motion mode. Incident waves are not present, but the oscillating body causes causes radiating waves. The hydrodynamic loads are identified as *added mass, damping* and *restoring* forces, and moments. This subproblem is often denoted the *radiation problem*. With this in mind the equations of motion will be looked into.

4.0.1 Equations of motion

For a steady state sinusoidal motion the equations of rigid-body motions may be can be written as

$$\sum_{k=1}^{6} \left[\left(M_{jk} + A_{jk} \right) \ddot{\eta}_k + B_{jk} \dot{\eta}_k + C_{jk} \eta_k \right] = F_j e^{i\omega t} \ \ (j = 1, ..., 6) \tag{4.1}$$

where M_{jk}, A_{jk}, B_{jk} and C_{jk} are, respectively, the components of the generalized mass, added mass, damping and restoring for the ship. F_j are the complex amplitudes of the exciting force and moment components. The subscripts in e.g. $A_{jk}\ddot{\eta}_k$ refer to force (moment) component in the j-direction because of motion in the k-direction. As only heave is considered j and k is equal to 3.

The added mass and damping loads are considered to be to be steady-state hydrodynamic forces and moments due to forced harmonic rigid-body motions, as discussed in relation to the second sub-problem. No incident waves are present but the forced motion generates outgoing waves. The forced motion results in oscillating fluid pressure on the exterior wetted hull surface. As the ship has no forward speed the dynamic pressure is written as $P_D = -\rho {}^{\partial \phi}/_{\partial t}$, which is to be considered in the equation of added mass and damping loads. The velocty potential φ is linearly dependent on the forced motion amplitude and harmonically oscillates with the forcing frequency. Integration of these pressure loads over the mean position of the ship's wetted surface gives the resulting forces and moments on the ship. In general the hydrodynamic added mass and damping loads due to an harmonic motion mode η_k can be written as

$$F_j = -A_{jk}\ddot{\eta}_k - B_{jk}\dot{\eta}_k \tag{4.2}$$

where F_j is the total hydrodynamic force in the direction of the motion. With this it is implicitly said that added mass has nothing to do with a finite mass of water that is oscillating. In this problem when resonant response is considered the main sources of damping are from wave radiation and viscous damping. Where the most important effect in viscous damping is associated with vortex shedding from the sharp bilges and the resulting influence on the pressure distribution on the hull. Eddy making damping could also be a significant factor due to the rectangular cross-section.

The restoring force can be found by integration of the hydrostatic pressure loads on the ship

hull (i.e. the term $-\rho gz$). It is necessary to integrate over the instantaneous position of the ship. The linear restoring force may in general be written as

$$F_j = -C_{jk}\eta_k \tag{4.3}$$

And for the heave motion the coefficient C_{jk} is $C_{33} = \rho g A_w$m where A_w is the waterplane area. However, to demonstrate how equation 4.2 behaves in the current gap problem numerical time-series of the hydrodynamic, added mass and damping forces are plotted in figures 4.1 to 4.4 for $b = 0.10\ m$. Because the numerical wave tank is based on linear theory the plots show results for inviscid fluid. Because heave motion is considered equation 4.2 is written as

$$F_3 = -A_{33}\ddot{\eta}_3 - B_{33}\dot{\eta}_3 \tag{4.4}$$

The plots are from different oscillating frequencies for the ship-section. In figure 4.1 the oscillating frequency is far from the non-dimensional resonance frequency and the added mass and damping forces are not very different. In the next figure, 4.2, the plot shows the forces just before the resonance frequency and it is observed that the damping forces is starting to become the dominant force. In figure 4.3 the results are in the immediate proximity of the non-dimensional resonance frequency and because of the nature of the gap problem the added mass is getting smaller, hence a lot of the hydrodynamic force is damping. In the last plot, figure 4.4 the added mass has become negative as the non-dimensional resonance frequency have been passed.

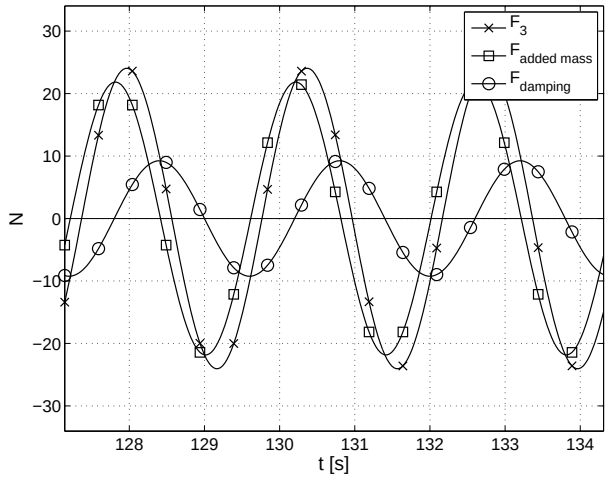

Figure 4.1: F_3, $-A_{33}\ddot{\eta}_3$ and $-B_{33}\dot{\eta}_3$ far from resonance

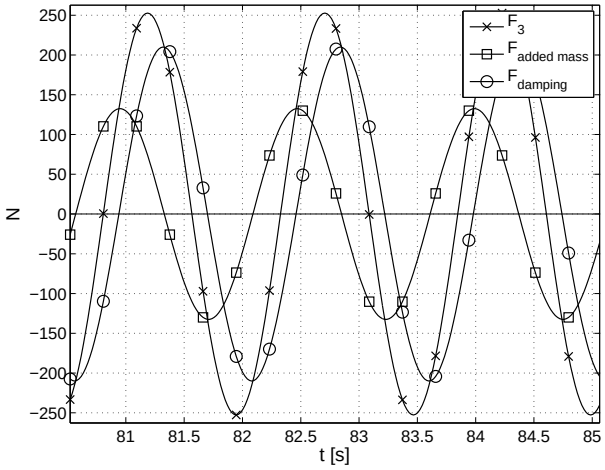

Figure 4.2: F_3, $-A_{33}\ddot{\eta}_3$ and $-B_{33}\dot{\eta}_3$ before resonance

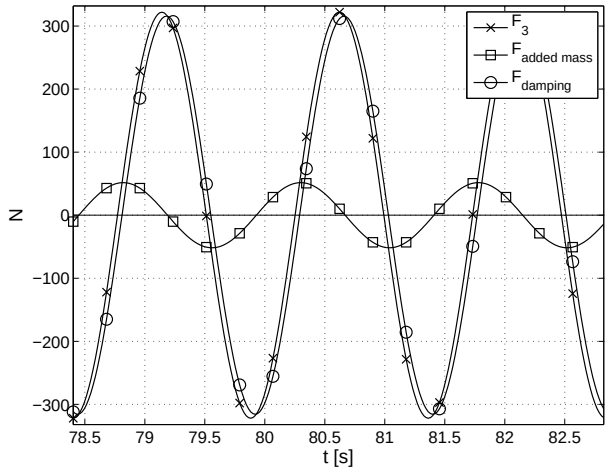

Figure 4.3: F_3, $-A_{33}\ddot{\eta}_3$ and $-B_{33}\dot{\eta}_3$ in close vicinity from resonance

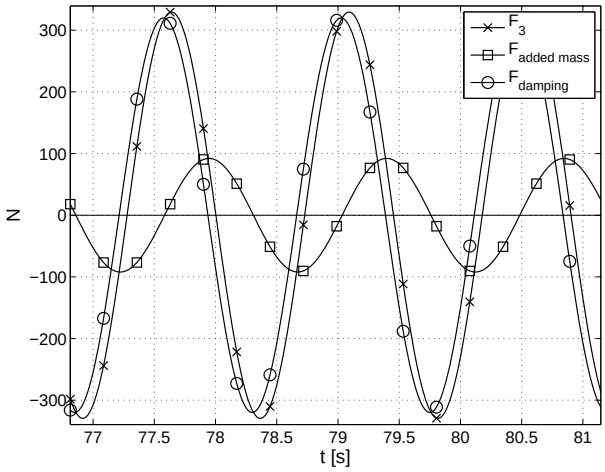

Figure 4.4: F_3, $-A_{33}\ddot{\eta}_3$ and $-B_{33}\dot{\eta}_3$ after resonance

4.0.2 Calculation of the hydrodynamic coefficients

To find values for the added mass and damping from forced oscillations of the ship section the starting point is from equation 4.2. By first multiplying the entire equation with the acceleration term $\ddot{\eta}_k$ and then integrate over an integer amount of periods equation 4.5 is found.

$$\int_0^{nT} F_j \ddot{\eta}_k dt = -\int_0^{nT} A_{jk} \ddot{\eta}_k^2 dt - \int_0^{nT} B_{jk} \ddot{\eta}_k \dot{\eta}_k dt \tag{4.5}$$

By now using the orthogonality properties of *cosine* and *sine* an expression without the damping term is found

$$\int_0^{nT} F_j \ddot{\eta}_k dt = -\int_0^{nT} A_{jk} \ddot{\eta}_k^2 dt \tag{4.6}$$

Because the integration is performed in the time domain and the added mass is a function of frequency an expression for added mass can be written as in equation 4.7

$$A_{jk} = -\frac{\int_0^{nT} F_j \ddot{\eta}_k dt}{\int_0^{nT} \ddot{\eta}_k^2 dt} \tag{4.7}$$

The same procedure is applied to get an expression for the damping, but in this case equation 4.2 is multiplied by the velocity $\dot{\eta}_k$

$$\int_0^{nT} F_j \ddot{\eta}_k dt = -\int_0^{nT} A_{jk} \ddot{\eta}_k \dot{\eta}_k dt - \int_0^{nT} B_{jk} \dot{\eta}_k^2 dt = -\int_0^{nT} B_{jk} \dot{\eta}_k^2 dt \tag{4.8}$$

an expression for the damping is found as seen in equation 4.9

$$B_{jk} = -\frac{\int_0^{nT} F_j \dot{\eta}_k dt}{\int_0^{nT} \dot{\eta}_k^2 dt} \tag{4.9}$$

Calculation of the coefficients from the numerical wave tank

In the numerical wave tank the force is found as $F_j = \rho \int_{S_B} \varphi_t n_k ds$, where the force is due to the unsteady term in the Bernoulli equation, φ_t, in the k'th direction due to a forced motion in the j'th degree of freedom and n_k is the corresponding component of the normal vector. Here, S_B is the fixed mean boundary of the ship section. φ_t is estimated by numerical differentiation of φ, in the present taken as $\left(\varphi^{n+1} - \varphi^n\right)/\Delta t$, where n is main time-step number. The added mass and damping are calculated by equation 4.7 and 4.9. The velocity and acceleration is found by numerical differentiation of the displacement of the ship. The restoring force is not included in the calculated result from the wave tank, but if it was it would be have to subtracted to be left with only the hydrodynamic force.

The added mass and damping are made non-dimensional in the following way

$$\begin{aligned} b_{33} &= \frac{B_{33}}{\rho A}\sqrt{\frac{B}{2g}} \\ a_{33} &= \frac{A_{33}}{\rho A} \end{aligned} \tag{4.10}$$

where A is the area of the wetted cross-section.

Calculation of the coefficients from model tests

In the model-tests the hydrodynamic force is not directly found from the measurements. The measured force includes hydrostatic forces from the restoring term as well as inertia forces from the mass of the rig itself, which means that

$$\begin{aligned} F_{measured} &= F_{hydrodynamic} + F_{hydrostatic} + F_{inertia} \\ &= F_3 - \rho g A_w \eta_3 - M_{rig}\ddot{\eta}_3 \end{aligned} \tag{4.11}$$

hence the hydrodynamic force is found by

$$F_3 = \rho g A_w \eta_3 + M_{rig}\ddot{\eta}_3 - F_{measured} \tag{4.12}$$

The velocity and acceleration is found by differentiation of the forced displacement of the model.

The added mass and damping are made non-dimensional in the following way

$$b_{33} = \frac{B_{33}}{\rho A L}\sqrt{\frac{B}{2g}}$$
$$a_{33} = \frac{A_{33}}{\rho A L} \tag{4.13}$$

where A is the area of the wetted cross-section and L is the length of the model, as the model is a three dimensional volume.

Damping from the radiation problem

As the oscillating ship generates waves there is also damping related to far-field wave generation. There are waves outside the ice-floes, when present, and wave generation when the ship is forced to oscillate in open water. Due to the propagating waves energy transported away from the system and causes damping. By considering energy transport the damping can also be calculated by using the wave amplitudes far away from the oscillating ship-section with equation 4.14, see [8] page 47. The reason far-field waves is used to calculate the damping caused by radiating waves is because of the fluid close to the ship is accelerated in a much higher degree, hence close to the ship added mass is dominating. The water rise-up is higher in the immediate vicinity of the ship is thus higher then the wave height itself, this effect decrease exponentially as the water travels away from the ship until the actual wave height is achieved.

$$B_{33} = \rho \left(\frac{A_3}{|\eta_{3a}|} \right)^2 \frac{g^2}{\omega^3} \tag{4.14}$$

where A_3 is the wav amplitude far away and η_{3a} is the heave amplitude of the ship section. Again the damping is made non-dimensional as

$$b_{33} = \frac{B_{33}}{\rho A}\sqrt{\frac{B}{2g}} \tag{4.15}$$

4.0.3 Viscous damping

In chapter 2.4 the effect of flow separation is discussed in a qualitative way. As the ship section is oscillating it produces vortices that add to the damping in addition to potential damping.
The contribution from the drag force experienced in heave caused by vortices being shed at the corners may be written as,

$$F_D = \frac{\rho}{2} A C_D \dot{\eta}_3 \left| \dot{\eta}_3 \right| \tag{4.16}$$

where A is the projected area, C_D is the drag coefficient, ρ the density of water and $\dot{\eta}_3$ the heave velocity.
In [8] there is a presentation on how to calculate the drag coefficient from experiments, an expression for the drag coefficient can be written as,

$$C_D = \frac{3}{8} \frac{1}{\frac{1}{2}\rho U_A^2 A} \int_0^{2\pi} F_y \sin(\theta)\, d\theta \tag{4.17}$$

where θ is

$$\theta = \frac{2\pi t}{T} \tag{4.18}$$

For an oscillating flow U is found by

$$U = U_A \sin\left(\frac{2\pi t}{T}\right) \tag{4.19}$$

From model tests the measured hydrodynamic force will include damping contributions from both potential and viscous forces. If equation 4.17 is rewritten as an intgral in the time domain and the potential damping force is subtracted equation 4.20 is the result.

$$C_D = \frac{3}{8} \frac{1}{\frac{1}{2}\rho U_A^2 D} \frac{2\pi}{nT} \int_0^{nT} (F_y - B_{33}\dot{\eta}_3) \sin(\omega t)\, dt \tag{4.20}$$

and

$$U = U_A \sin(\omega t) \tag{4.21}$$

where B_{33} is potential damping calculated by linear theory, F_y is the measured vertical hydrodynamic force and ω is the oscillation frequency of the ship section and $U_A = \dot{\eta}_{3a}\omega$.
When evaluating the drag coefficient it should be done in connection with the *KC* number. The *KC* number is defined as follows,

$$KC = \frac{U_A T}{D} \tag{4.22}$$

where D is the ship draught and used as a characteristic length in the *KC* number. The *KC* number says something on how much the respective structure moves in a fluid relative to itself , which is of importance when looking into the effect of vortex shedding. Berthelsen has shown in [2] that for low *KC* numbers high values for the drag coefficient,C_D, is to be expected. For the open water situation with the ship section forced to oscillate with 2.5 *mm* and at resonance, which is at a period of about $T = 1.1$ *s* the *KC* number is 0.13 which is considered to be very small. Hence large values for C_D is expected to be found. Note in practice with the ship in forced oscillations the parameters in the *KC* number is the forcing amplitude η_{3a} and ship draught D see equation 4.23.

$$KC = \frac{\eta_{3a} 2\pi}{D} \tag{4.23}$$

Chapter 5

Model tests

The model tests were performed in the Ladertank at Marine Technology Center, NTNU Trondheim during week 9, 10, 11, 12 and 13. The first week was spent arranging the set-up and calibrating measurement equipment. The rest of the time was devoted to doing test runs.

5.1 Set-up and instrumentation

An overview of the model test set up is presented in figure 5.1 . The model of the ship section and ice-floes used in the model tests have the same geometry as the model used in the numerical calculations. This means that the draught of the ship section is 12 *cm* and the beam is 32 cm, the draught of the ice-floes are 4 *cm* and the beam is 3.6 *m*. The total height of the ship-section model is 36 *cm* and the height of the ice-floes are 8 *cm*. The length of the ship model is 59.5 *cm*, 5 *mm* shorter than the breadth of the tank, this is to avoid friction from the tank glass walls. The ship-model and ice can be seen in figure 5.2.

Both the ship section and the ice-floes were made from divinycell, a hard foam material. The ship model was also painted to make it more robust. The model is connected to the actuator and force-gauge through an aluminum frame. The set-up do not allow the model to move freely in any degrees of freedom, the actuator impose a forced heave motion. The force gauge measures the force in shear, meaning that it only registers force in vertical direction. The force gauge was produced by MARINTEK and of high quality. The actuator with the force gauge mounted can

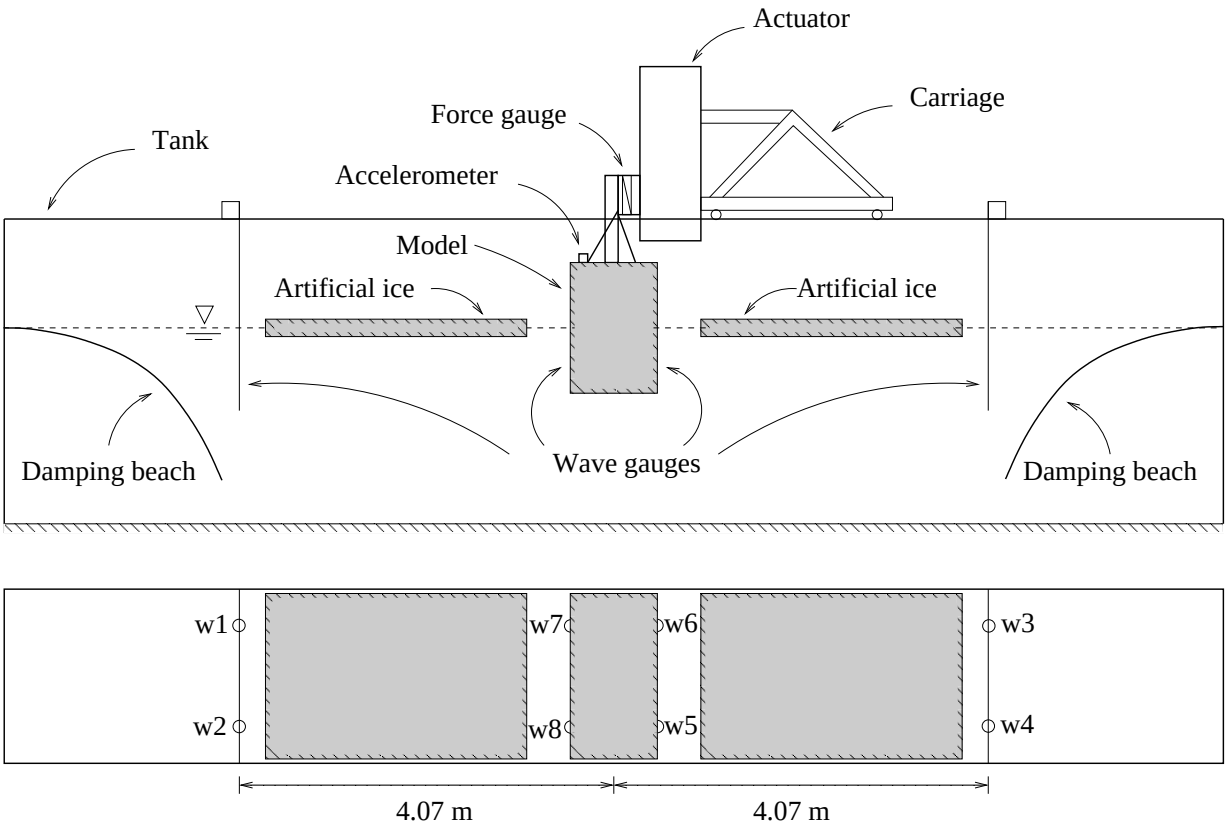

Figure 5.1: Illustration of the general model test set-up. Upper: the test set up seen from the side. Lower: The location of the wave gauges denoted w1 to w8.

be seen in figure 5.4. In addition there is a displacement monitor on the actuator to register the actual actuator displacement.

The actuator is automated in the way that it is possible to load a test program in to the actuator control unit. With this it is possible to define a test program in such a way that for a geometric set up the actuator can continually run tests with a given amplitude and frequency on its own. It was found that a test run of 60 *seconds* and a pause of 60 *seconds* to let the water calm down was sufficient. In all test-runs two forcing amplitudes were tested, 2.5 *mm* and 5 *mm*.

The ice was to be modeled as a rigid body, meaning that it is not allowed to move or bend in any degrees of freedom. To achieve this the ice-floes was hold in place by wooden frames and wedges, seen in figure 5.3. The frames were fastened to the tank by clamps.

Both the ice and ship model was constructed by workers at MARINTEK.

There are in total eight wave gauges in the tank located at four different locations in the tank to measure the free-surface elevation. The wave gauges are placed in pairs so it is possible to average the water elevation in the width of the tank. There is a pair of wave gauges outside the ice-floes on both sides of the tank as indicated in figure 5.1and on the ship model. The wave gauges used to measure the far field wave elevation were of standard capacitance type with two metal bars. The wave gauges located on the ship model are also of a capacitance type but different in the way that they are made up of copper tape. In total there were 8 wave gauges, and an amplifier shown in figure 5.4 were used to generate the signals.

On top of the ship model an accelerometer capable of measuring acceleration in 3 degrees of freedom was mounted. The accelerometer measures the rigid body acceleration in the x, y and z direction, analogue to a ordinary coordinate system. The accelerometer was used as an indication to whether the model were feeling any friction from the glass walls, and also calculate the velocity of the model to find damping and use the measured acceleration to find added mass. Later during the analysis it was found that the approach with the accelerometer did not give good values for velocity and acceleration so only the measured displacement from the actuator was used.

In total, with all the measurement gauges there were 12 channels to be logged in each run. To sum it up; 8 *wave gauges, one for the displacement of the actuator, one for the force gauge and three for the accelerometer*.

An amplifier of type Hottinger MGCplus received all the signals in the end, the amplifier can be seen in figure 5.4. The signal from all of the channels were acquired at a sampling frequency of $F_s = 200\ Hz$.

At each end of the tank a parabolic beach was placed to prevent reflection of generated waves from the oscillating ship model, the beach is illustrated in figure 5.1.

In addition to the measurement equipment mentioned a control PC for the actuator and a logging PC was used. The logging program used to log the measured data was MARINTEKs version of Catman. All the equipment was provided by MARINTEK.

5.2 Calibration

All of the output signals from the sensors are in volt. The sensors are linear, meaning e.g. A higher load gives a bigger output that is linearly proportional to the loading. This means that the calibration factors found are in the form of m/V, N/V and $m/s^2/V$. For the calibration of the wave gauges and the force gauge a calibration program provided by MARINTEK was used. The calibration factors are found by a MARINTEK program and then fed into the MGC amplifier. The program calculates the linear slope number, which is the calibration factor.

5.2.1 Force transducer

The force can be registered as either Kg/V or N/V, for the use in this study the latter was chosen. The calibration factor was found by placing known weights on the aluminum frame, without the model mounted, and measure the signal from the force gauge. The procedure is to start with no load, log the result and then put on a load and do another measurement, when done with the last weight another zero-load case is measured and the averaged zero level is used. In total 5 measurement points was found in a range from 0 to 58.84 N. It was not possible to calibrate the the gauge after the initial calibration but it was frequently inspected by placing known weights on the model and check the offset in the measured force. This procedure revealed any discrepancies between the extra load and the measured load.

5.2.2 Wave gauges

At the first week the model was not available but the aluminum frame was, hence an easy way to do the calibration of the far field wave gauges to mount them to the actuator and do the calibration. This was done by imposing a displacement on the actuator, thus lowering the gauges a known distance and then log the output. When the ship model was mounted to the actuator the procedure was repeated for the copper tape wave gauges placed on . The procedure to calibrate the wave gauges are similar to that of the force gauge. Start with a zero level, impose a known displacement for a wanted number of times and then do the zero level measurement again, the average zero-level measurement is then used.

The wave gauges on the model was calibrated every morning, but the far field gauges were not due to practical reasons and available time. To keep the gauges drifting they were cleaned every morning in their positions to keep the oxidation level as constant as possible. They could have been calibrated by tapping and filling the tank by known quantities but to achieve a steady water temperature throughout the entire tank takes about one night and hence not practical.

5.2.3 Accelerometer

The accelerometer mounted on the model measures the acceleration in three directions, and registers a positive or negative acceleration depending on the motion and defined positive direction. The accelerometer was calibrated in the following manner, the zero level is found by placing the accelerometer on a still surface with the measuring direction pointing upwards, for one of its degrees of freedom and measure the output. The calibration factor is then found by turning the accelerometer in such a way that the measuring direction is in horizontal direction. The difference between the two cases is then the gravity constant $g = 9.81\ m/s^2$. This was done in all the three degrees of freedom of the accelerometer.

5.2.4 Documentation

All the measured data is stored as *.bin* files and the time-series analyzed by the help of Matlab routines. Several photos were taken to document the set up and a high speed camera was used to be able to study the fluid behavior in the gap between the model and ice-floe. The spread sheets with the calibration data were stored on a hard drive with the measurement data and also printed.

5.3 Routines

The test runs were done in the following manner.

Open water test

For the set up with only the ship model in the tank,

1. Calibration of the wave gauges on the model (not before every single run)
2. Check that the model is clear of the tank glass wall
3. Define a frequency range and wanted oscillating amplitude and feed it into the actuator control unit, the input for the control unit is $f = 1/T$
4. Check that the water in the tank is calm i.e. still water surface
5. Set the length of the test in Catman
6. Take zero settings of the sensors and store them
7. Start the actuator and check the live feed from Catman to see if the measured data oscillates symmetrically around zero level
8. Start logging of data
9. When a series of automated tests was done Catman automatically stops the login
10. Save timeseries
11. Run an analysis to check the results to see if re-runs is needed

Ship and one ice-floe

For the set up with one ice-floe in the tank the routine is similar but the model have to be placed at a wanted distance away from the divinycell plate representing the ice. The ice-flow was placed to the right of the model, when seen from the front side as seen in figure 5.3. For practical reasons the model was moved instead of the ice floe. Once the ice-floe is placed in the tank the following procedure is done,

1. Move the carriage to place the model in the wanted position relative to the ice-floe
2. Check that the draught of the ice is correct and that it is level

3. Double check the distance along the ship side has an even distance to the ice-floe
4. Check that the model is clear of the tank glass wall
5. Calibration of the wave gauges on the model (not before every single run)
6. Define a frequency range and wanted oscillating amplitude and feed it into the actuator control unit, the input for the control unit is $f = 1/T$
7. Check that the water in the tank is calm i.e. still water surface
8. Set the length of the test in Catman
9. Take zero settings of the sensors and store them
10. Start the actuator and check the live feed from Catman to see if the measured data oscillates symmetrically around zero level
11. Start logging of data
12. When a series of automated tests was done Catman automatically stops the loging
13. Save time-series
14. Run an analysis to check the results to see if re-runs is needed

Ship and two ice-floes

For the tests with two ice-floes in the tank the ice-floe that was in the tank for the above configuration was held permanently in the same position while the model and the new ice-floe, located on the left side of the model was moved to regulate the gap distance. For the case with two ice-floes the following routine was followed,

1. Move the left ice-floe to next position
2. Move the carriage to place the model in the wanted position relative to the two ice-floes
3. Check that the draught of the ice is correct and that it is level
4. Double check the distance along the ship side has an even distance to the ice-floes

5. Check that the model is clear of the tank glass wall
6. Calibration of the wave gauges on the model (not before every single run)
7. Define a frequency range and wanted oscillating amplitude and feed it into the actuator control unit, the input for the control unit is $f = 1/T$
8. Check that the water in the tank is calm i.e. still water surface
9. Set the length of the test in Catman
10. Take zero settings of the sensors and store them
11. Start the actuator and check the live feed from Catman to see if the measured data oscillates symmetrically around zero level
12. Start logging of data
13. When a series of automated tests was done Catman automatically stops the loging
14. Save time-series
15. Run an analysis to check the results to see if re-runs is needed

5.4 Error sources

To be able to evaluate the quality of the results from the experiments an identification of possible error sources have been done. Also an attempt to quantify them have been performed. Basically there are two kinds of error; random error and bias error. The random errors may be quantified by repetition tests. Other means of investigation methods are needed to identify potential bias errors. The process of identifying possible sources for bias errors includes actions such as quantifying limitations of the equipment and utilizing the experience of others, as the authors experience with model testing is very limited, as well as careful observation during the model testing.

During the model testing, continues efforts were made to observe and identify artifacts of potential significance to the results.

A parabolic beach , or any shaped beach, will not in general be a perfect wave absorber. The strategy of the beach is to induce wave breaking. It is not possible to remove all the energy in a wave with this damper, in particular for shallow water waves, [16]. In figure 5.6 is a plot indicating when the waves are to be considered as shallow water waves, this happens at an oscillating period of the ship model of approximately $T = 1.6\ s$. A wave is to be considered a shallow water wave when $\lambda/4 > h$, i.e. the tank depth. In total the tests performed cover a periodic range of $T = 0.4\ s$ to $T = 2.15\ s$. Hence reflections are to be expected but, however no reflections of significance were found to hit the oscillating ship model.

Capacitance type wave gauges consists in general of two parallel steel wires penetrating the free surface. Bias error may be introduced through nonlinearity in the voltage created. This might be caused by that the water climb on the steel wires, this is also known as the meniscus effect or by drifting over time. A semi-quantitative estimate of the error introduced by the latter effect is said to be in the order of the diameter of the steel wires, [16], which were about 3 *mm* in diameter. However experience have shown that this type of error source can be neglected. In addition to steel wire wave gauges, copper tape were used as a capacitance type wave gauge on the ship model, a meniscus effect is not believed to have a significant effect but water film on top of the tape might yield a higher output then what it suppose to give. A quantified value for this was not achieved. Drifting of the far-field wave gauges might have occurred, but not to a big extent as it was not possible to do recalibration of them.

A slight motion of the ship was observed during the tests with the ship model and one ice-floe in the tank. The aluminum frame that was originally constructed to mount the model to the actuator was found to be to weak with respect to horizontal forces applied on the model. This was seen as an horizontal rigid body motion in combination with a small rotation of the model. There was also another source for the horizontal motion, this was found to originate from the actuator mounting as it was mounting with about one degree off relative to a vertical axis. The aluminum frame was modified until it was considered strong enough for the purpose. However a small horizontal motion was still observed, and measured to be of an amplitude of approximately 2 *mm*.

Seiching is a low-frequncy oscillation of the fluid corresponding to the first longitudinal eigen-period of the basin, meaning a standing shallow water wave. This is in theory always triggered in any flume or basin. Typically the standing wave has a very low amplitude but

might result in a significant horizontal motion of the fluid, [16]. From close observations it was found that a stop of about 60 *seconds* was enough time to adequately damp out this effect, hence it is not believed to influence the results in a significant way.

Transverse sloshing is the corresponding transverse standing wave of the first eigenperiod in the transverse direction of the wave flume, [16]. The breadth of the flume is about 0.60 *m*, this gives a resonant period of about 0.88 *s*, assuming the deep water dispersion relation. Transverse sloshing was observed in the tests around this period of oscillation. The trigger for this is believed to be caused by small three dimensional effects from the model and perturbations when the ice was present in the tank.

Glass wall gap. To avoid friction from the tank glass wall on the model the ship section was constructed with a 5 *mm* margin with respect to the tank width, hereby denoted the glass wall gap. The gap was a necessity in connection with force measurements. The ship section had to be denied any mechanical contact except through the force gauge. This gave room for a standing wave between the model and the glass wall on both sides of the model.

Slight tilt. When the model was observed from above, birds eye view, it was found that is was not mounted completely orthogonal with respect to the tank wall. This means that the glass wall gap was not constant on both sides. In the runs with the ice it was possible to observe a slight transverse variation of the distance *b* between the ice and ship of about 1 *mm* on the right side and approximately 2 *mm* on the left side A picture of the ship-model and ice as seen from above is found in figure 5.7. In the test runs when the gap was small i.e. 1 *cm* this becomes important. It was observed that the wave elevation in the gap was sensitive to this tilt as the elevation was not constant throughout the width of the tank. When analyzing the time series the amplitude at the location where the gap was relatively bigger the elevation was bigger.

Presence of ice. The rigging of the divinycell plates representing the ice was a cumbersome process that required high precession fitting to achieve the correct draught, location relative to the ship model and to get it level over its entire length. Similar to the ship model, it was for the ice a glass wall gap, though slightly smaller it gave room for a standing wave along the side of the plate. It was found that the results with respect to the resonance period was sensitive to this water elevation. To mitigate this a rubber list was taped to the tank glass wall to prevent the water from flowing freely up and down, later thin plastic bags were forced down in addition to the rubber lists, see figure 5.8 and5.9. These actions prevented

the water to run up the side of the ice-floe to a certain extent but it did not stop this from happening completely. In addition the ice-floes experienced some flexing but this was small and the exact effect of it is not known.

Slight flexing if the ice, could sometimes be observed in the tests. Even if this was not always possible to see in such an extent that it was possible to measure an amplitude it is expected to give a damping effect on the piston mode motion in the ship-ice gap and perhaps a slightly smaller hydrodynamic force.

Force measurements. The graph from the calibration of the force gauge is seen in figure 5.5 . The graph shows that the calibrated range is from zero to approximately 60 N and the measured force during the experiments range from approximately 3 N to about 80 N. The accuracy of the of the force measurements is questionable when the oscillating period is high. This means that the dominating force is the restoring term, measurements from the open water tests show a spring like result for low frequencies. The ship model was meant to have space milled out to fit weights so it would float with the wanted draught, but the milling machine was not available and this was not done. As a consequence of this the force gauge had to operate with e pre tension and this could possbile have affected the sensitivity of the measurements.

The actuator forcing amplitude was not able to keep up with the correct displacement for oscillating periods below approximately $T = 0.6\ s$, for these frequencies the actual amplitude is lover than it was meant to be, this does not effect non dimensional values in a very significant extent as the actual forcing amplitude is used in the analysis and calculations.

Accelerometer. The accelerometer have not been thoroughly analyzed as the measured signal from it was not used.

5.5 Analysis of the experimental data

The raw data was analyzed using Matlab where time series from the tests were plotted as well as reduced data. The time seres that were plotted was the wave elevation inside the gap and the far field wave elevation, the actuator displacement and the measured force. The reduced data comprise the non dimensional wave elevation inside the gap and far field plotted against oscillating period in addition non dimensional added mass and damping is calculated and plotted against a

Object	*Mass*
Outer plate of force gauge	3367g
Model and aluminum frame	12113g
Accelerometer	56g
Nuts and screws	177g
Total	*15713g*

Table 5.1: List of structural masses felt by the force gague.

non dimensional frequency.

To find the hydrodynamic force the hydrostatic force was subtracted and the inertia force from the force gauge. The analytic procedure on how this is done is discussed in chapter 4.0.2. The masses that is used when determining the inertia force is listed in table 5.1.

5.5.1 Filtering

To be able to do an analysis of the measurements the raw data had to be filtered. This was done in Matlab using a bandpass filter on the logged force signal and the wave gauges. The upper and lower frequency set for the band pass filter were $f_{low} = 0.2\ Hz$ and $f_{high} = 2.5\ Hz$. The displacement data for the actuator did not need filtering.

5.5.2 Uncertainty

During the model tests repetition tests was performed to check the repeatability of the measured results. Every repetition showed good that the results was nearly the same, the standard deviation and mean value for such tests for the open water, one ice-floe and two ice-floe configurations are showed in figure 5.10, 5.11 and 5.12. The plots show results for the measured force and wave elevation to the right of the ship, denoted A_g.

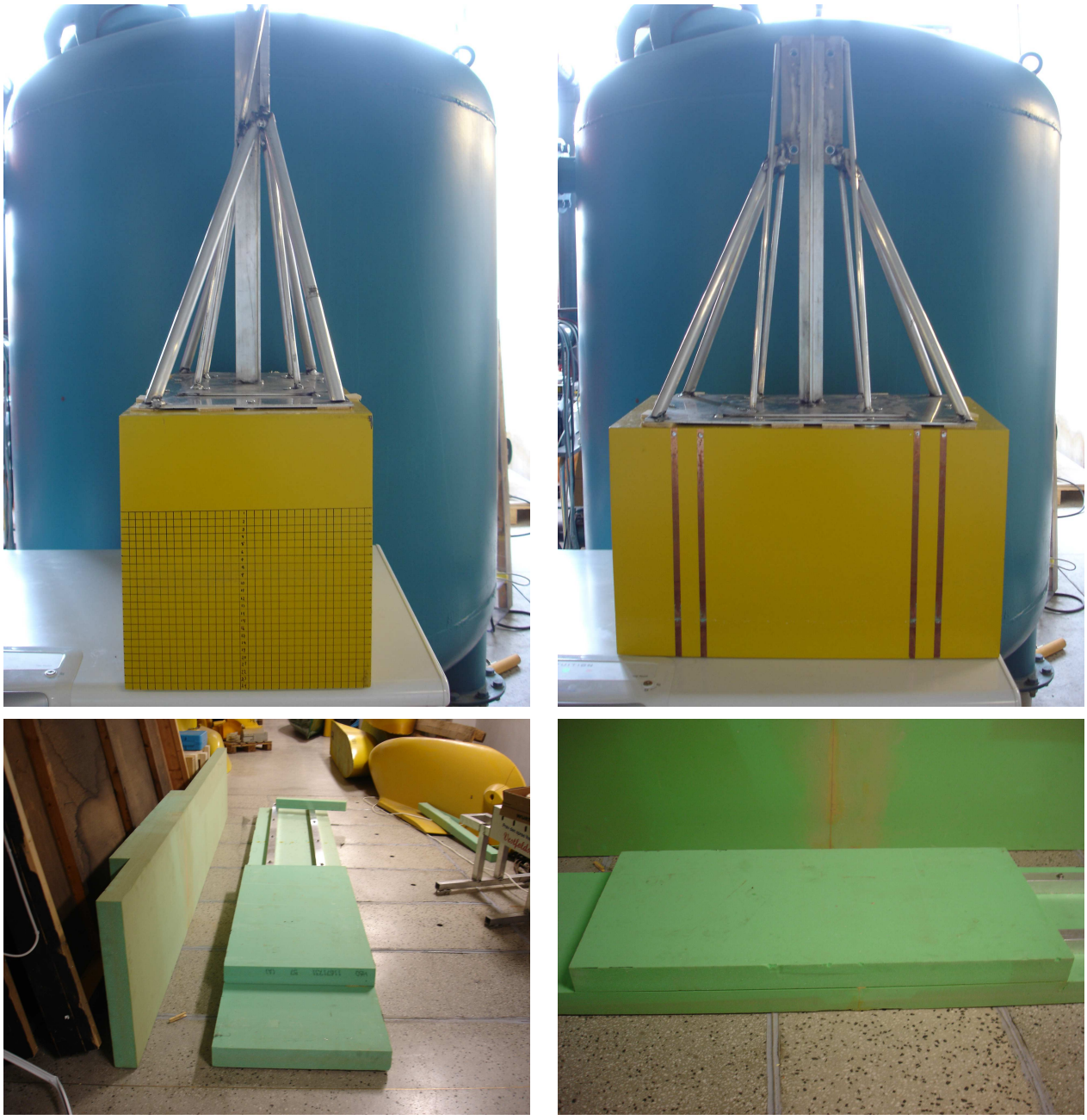

Figure 5.2: Upper: Ship-section model, on the left it is seen from the front and the right from the side, the copper tape makes a wave-gauge in two pairs i.e. two wave-gauges. Lower: the two divinycell plates that makes the artificial ice.

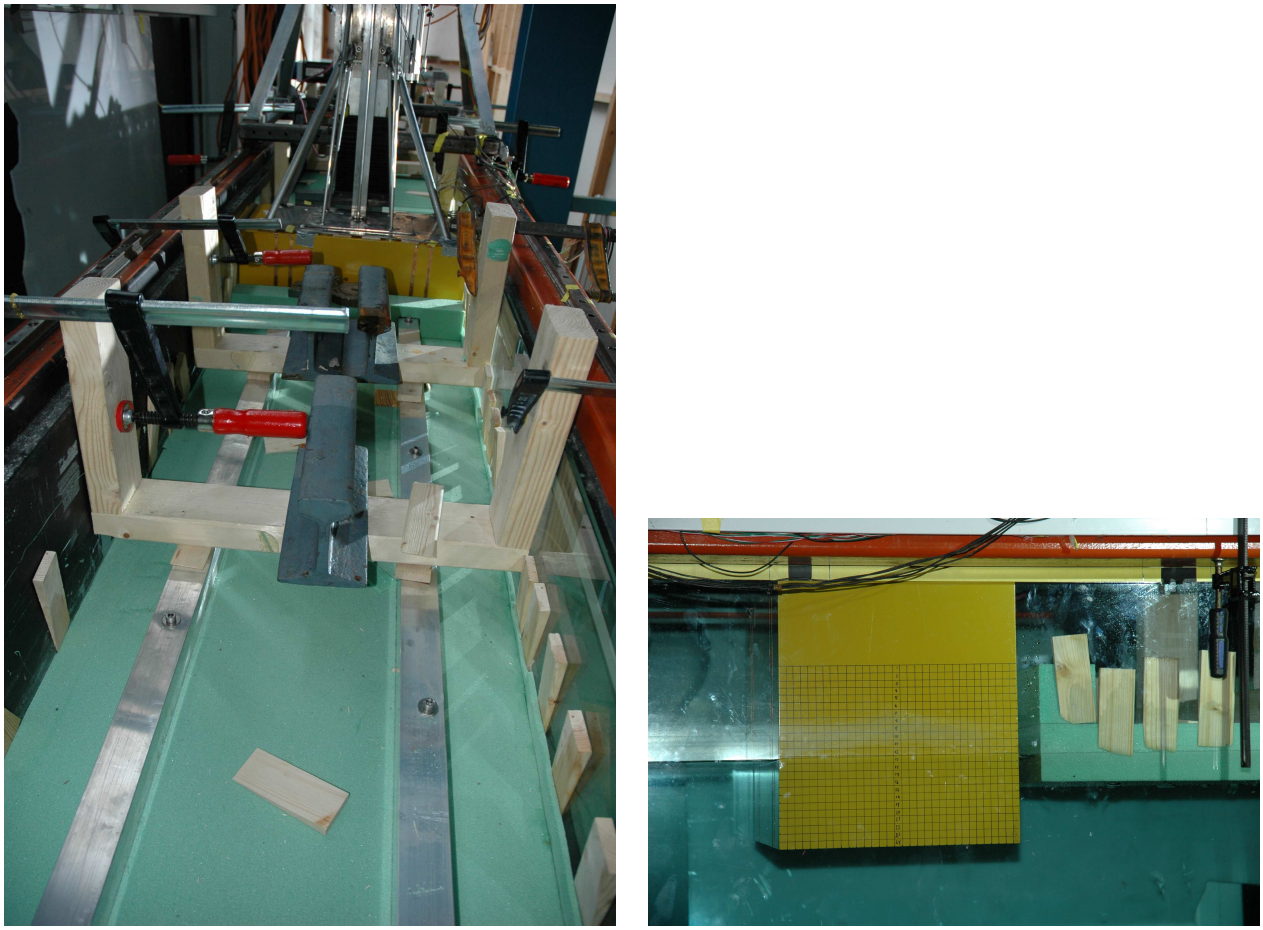

Figure 5.3: Left: the ice seen in the tank from above, fixed with wooden frames and wedges. Right: The model and ice-floe seen from the side through the tank glass wall.

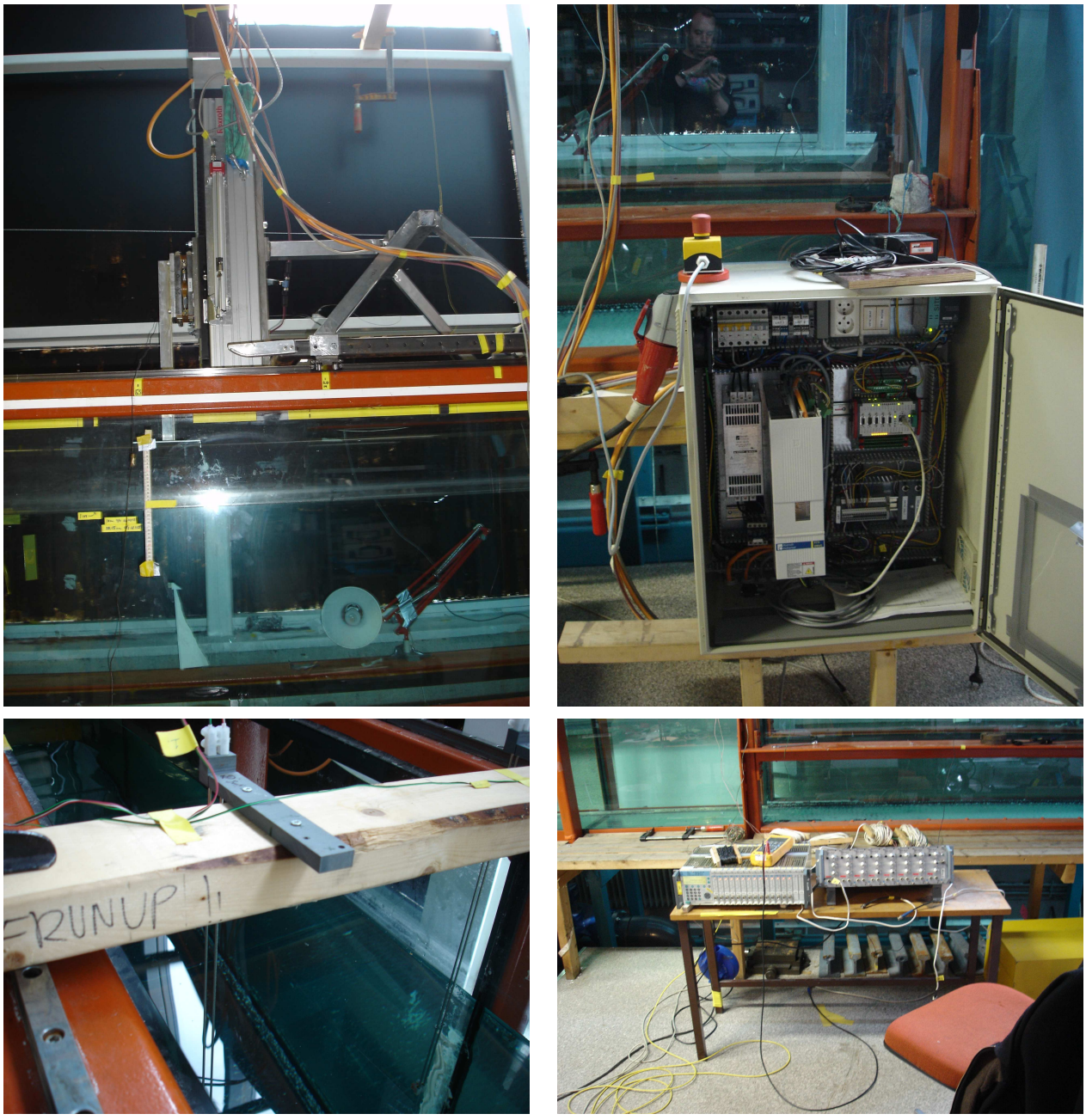

Figure 5.4: Upper: To the left the actuator with the force gauge mounted and a aluminum frame to hold a model. To the right the actuator control unit with emergency stop button on top. Lower: on the left wave-gauge for far-field wave elevation registration and in the lower right wave gauge amplifier (right) and signal amplifier for all measurement devices.

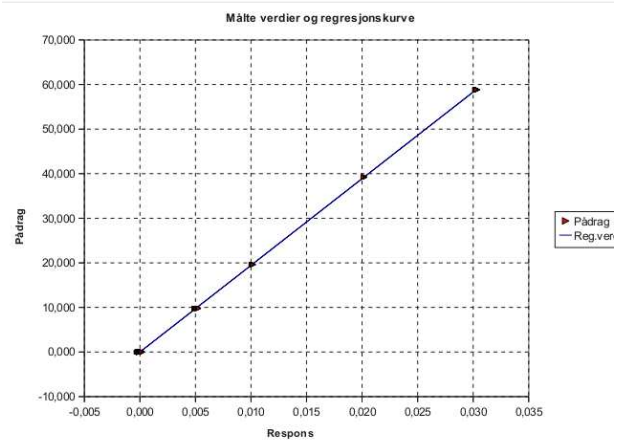

Figure 5.5: Calibration curve for the force gauge.

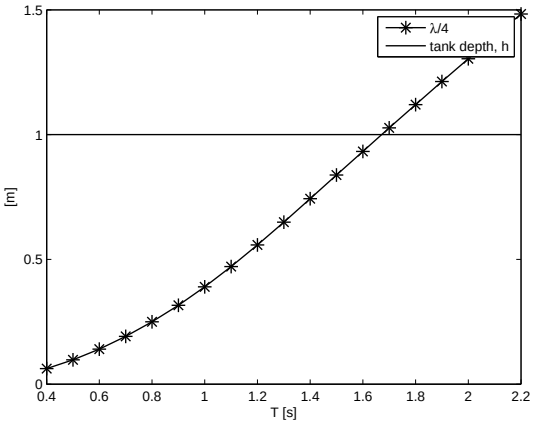

Figure 5.6: The graph displays when a wave is to be considered as a shallow water wave in the tank, the curved line is $\lambda/4$ and the straight line is the depth of the tank $h = 1\ m$, the waves at an oscillation period of $T = 1.6\ s$ is to be considered as shallow water waves.

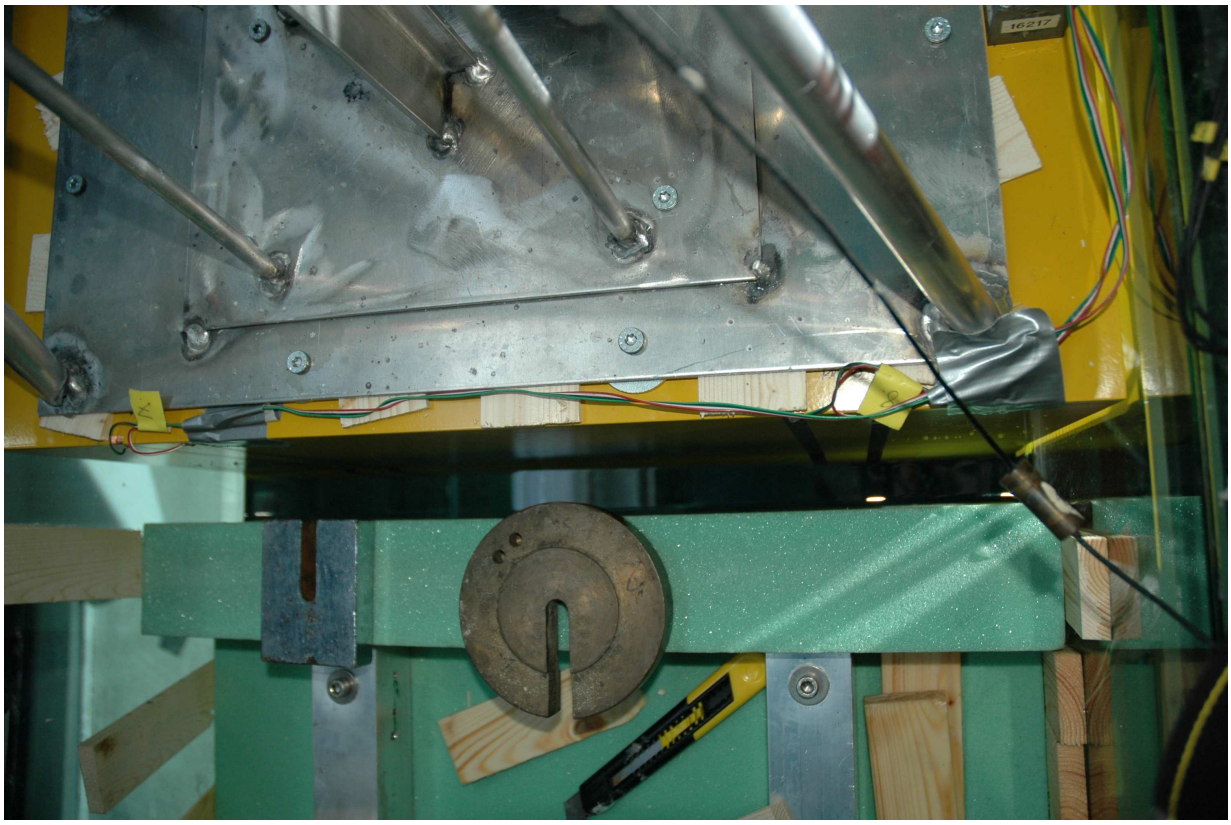

Figure 5.7: A view of the gap between the ship and ice seen from above.

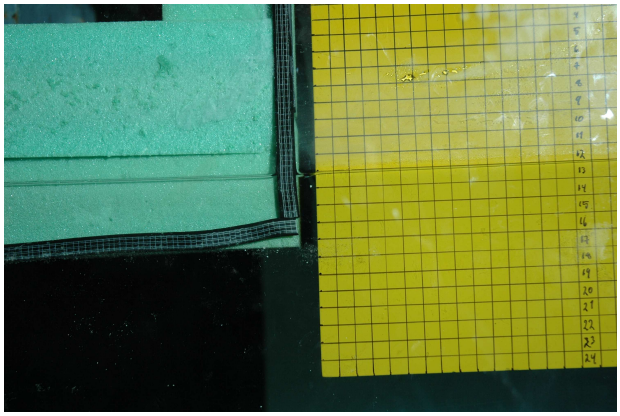

Figure 5.8: Rubber list taped on the tank wall with ice-floe and ship model.

Figure 5.9: Rubber list and plastic bags forced between the ice and glass wall.

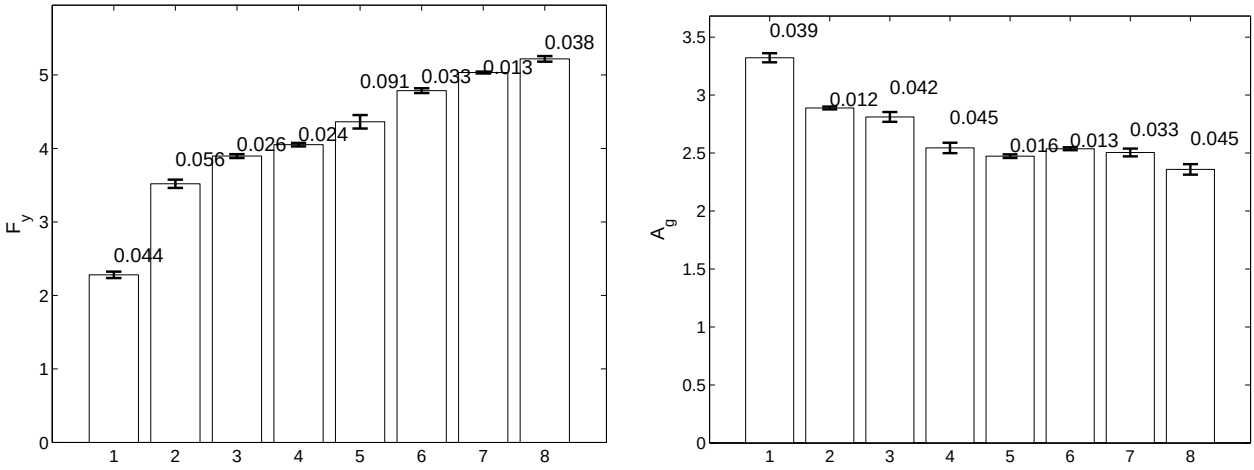

Figure 5.10: Repetition tests for the open water configuration where the horizontal axis ticks 1-8 correspond to tests 20090, 20130, 20160, 20190, 20230, 20260, 20290 and 20330 and their respective two respitions. Bars represents mean values and the error bar on top represent 2 times the standard deviation, the numbers is one time the standard deviation

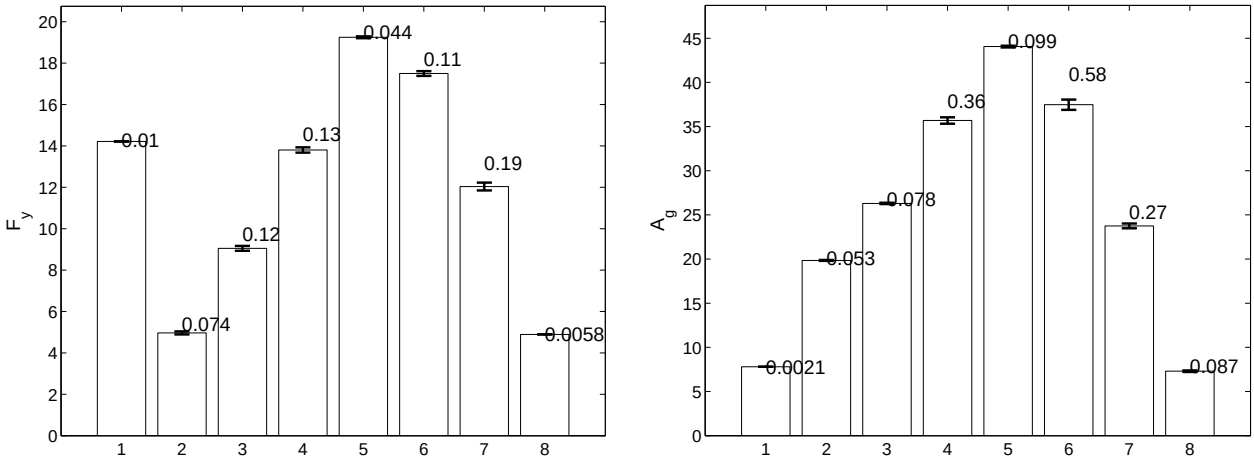

Figure 5.11: Repetition tests for the one ice-floe configuration where the horizontal axis ticks 1-8 correspond to tests 8030, 8060, 8090, 8130, 8160, 8190, 8230 and 8260 and their respective two respitions. Bars represents mean values and the error bar on top represent 2 times the standard deviation, the numbers is one time the standard deviation

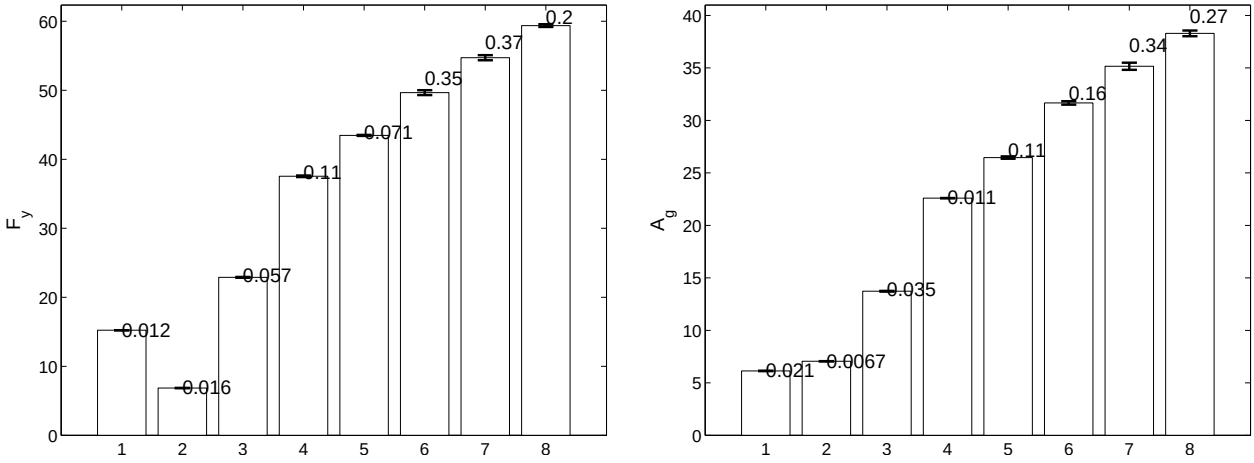

Figure 5.12: Repetition tests for the two ice-floe configuration where the horizontal axis ticks 1-8 correspond to tests 10030, 10060, 10090, 10130, 10160, 10190, 10230 and 10260 and their respective two respitions. Bars represents mean values and the error bar on top represent 2 times the standard deviation, the numbers is one time the standard deviation

Chapter 6

Results from experiments and numerical calculations

In this chapter condensed data retrieved from the numerical simulations and model tests are presented in the same plots. In the plots the experimental results are from a forcing amplitude of 2.5 *mm*. This is done for easy comparisment of the results for added mass, damping and the gap amplitudes. First the open water results are presented where the two-dimensional ship section is in forced heave oscillations without any ice present. Next the results for the tests where there is two ice-floes in addition to the ship. The last results are from the tests done with one ice-floe is placed next to the oscillating ship.

In appendix A and B separated plots of experimental and numerical, respectively, results are plotted. In the plots for the experimental results in appendix A the graphs show the results for a forcing amplitude of 2.5 *mm* and 5 *mm*.

Unless specified the added mass and damping have been calculated according to equation 4.7 and 4.9 as shown in chapter 4.0.2. Where it is specified the damping have been calculated by the principle of damping from radiating waves as shown in chapter 4.0.2.
For the geometrical set-ups where there is ice present, results for the non-dimensional waater elevation in the gap between the ship-section and the ice is also presented and refered to as A_g. Also the non-dimensional far-field wave elevation amplitudes, A_f, are included in those results.
As previously shown the added mass and damping have been made non-dimensional the following way for the numerical results

$$b_{33} = \frac{B_{33}}{\rho A}\sqrt{\frac{B}{2g}}$$
$$a_{33} = \frac{A_{33}}{\rho A} \tag{6.1}$$

the results from the modeltests are made non-dimensional in the following manner

$$b_{33} = \frac{B_{33}}{\rho AL}\sqrt{\frac{B}{2g}}$$
$$a_{33} = \frac{A_{33}}{\rho AL} \tag{6.2}$$

6.1 Open water test

Numerical and experimental results for the case when the ship is forced to oscillate in heave without any ice-floes present in the wave flume and numerical wave tank are found in figure 6.3. The first results shows the results for the drag coefficient C_D.

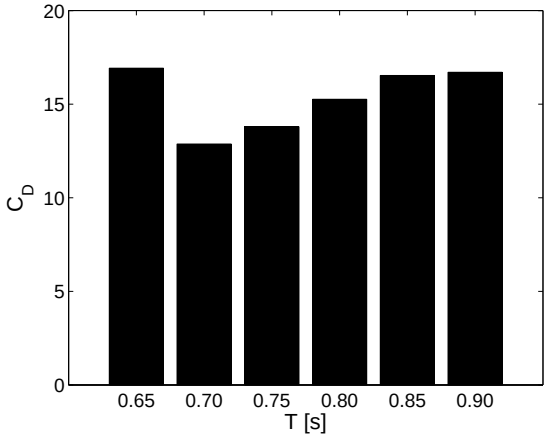

Figure 6.1: Drag coefficient C_D, forcing amplitude 2.5 *mm*.

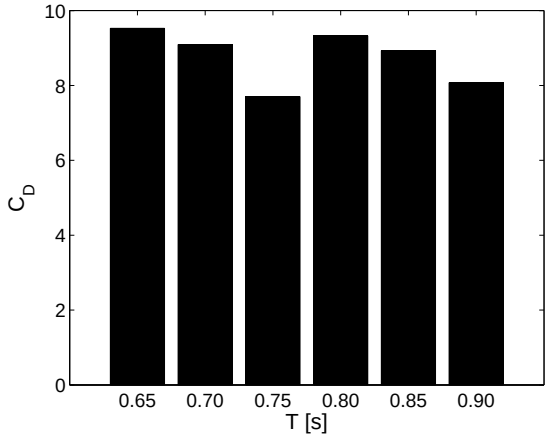

Figure 6.2: Drag coefficient C_D, forcing amplitude 5 *mm*.

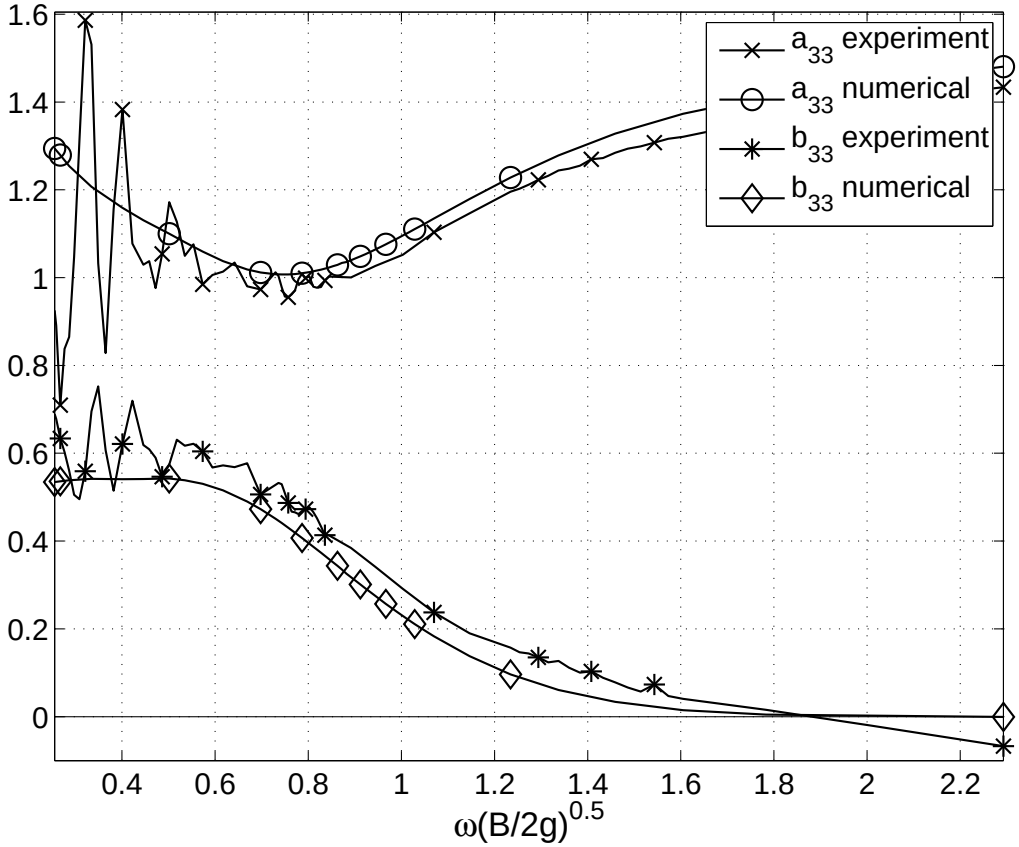

(a) a_{33} and b_{33}.

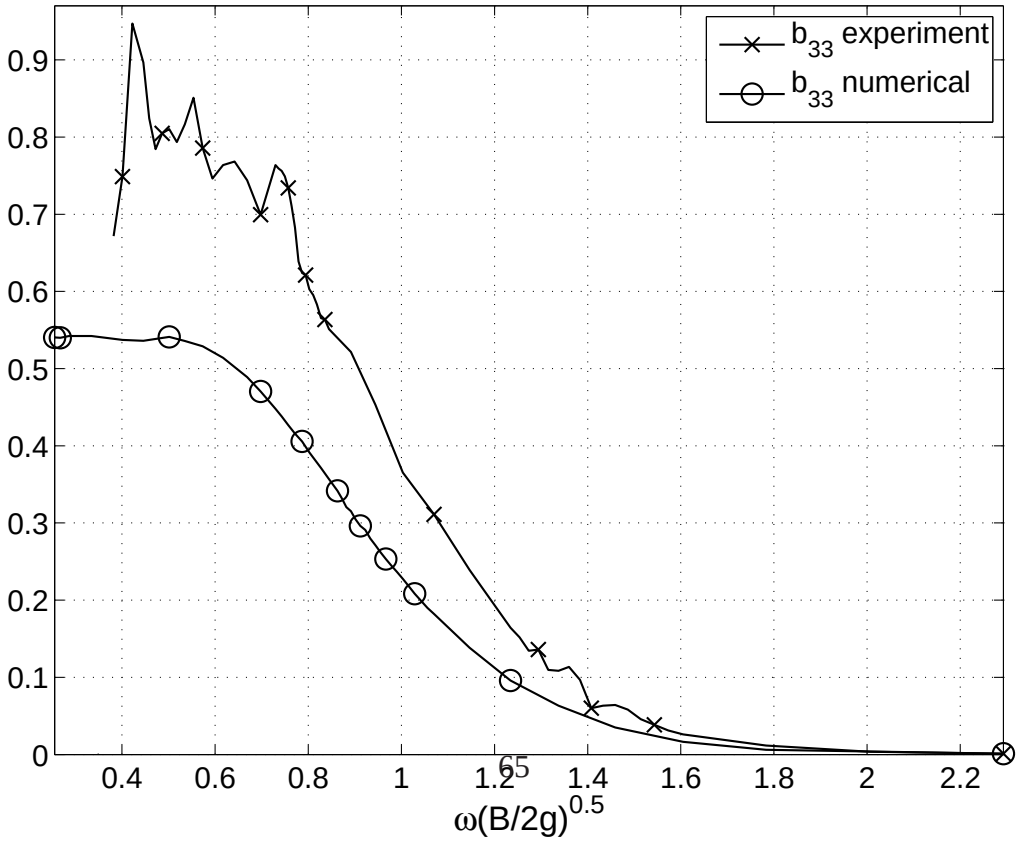

(b) b_{33} from radiating waves.

Figure 6.3: Ship-section in open water.

6.2 Ship in middle of two ice-floes

Numerical and experimental results for the case when the ship is forced to oscillate in heave with two ice-floes present in the wave flume and numerical wave tank. The ship and the two ice-floes makes a symmetrical set-up where the *gap* varies from 0.1 *m* to 0.10 *m*. The condensed results for the non-dimensional added mass b_{33}, damping a_{33} and non-dimensional gap amplitude A_g are presented in the following figures.

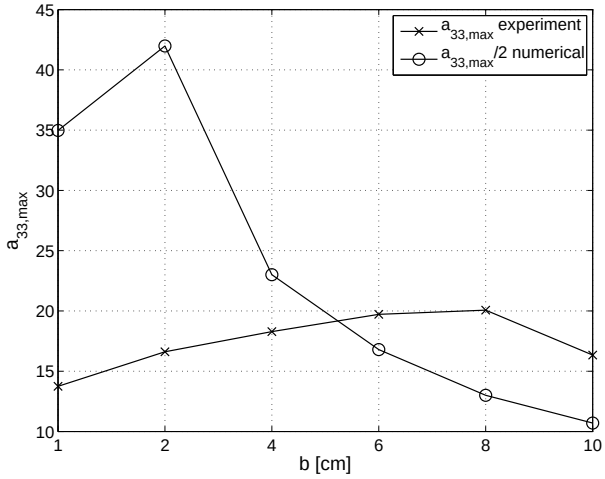

Figure 6.4: Maximum values of a_{33}.

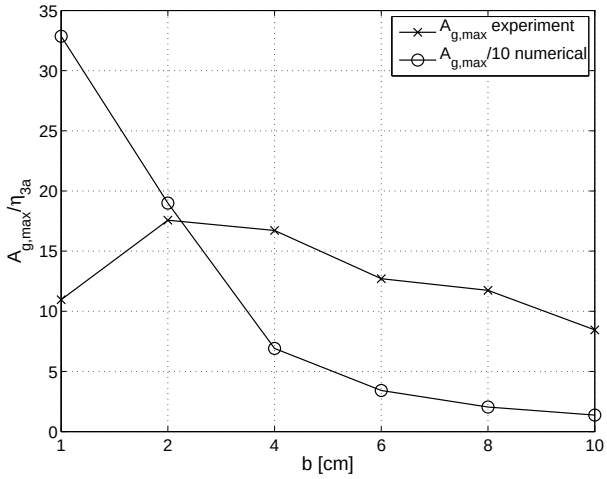

Figure 6.5: Max. values A_g.

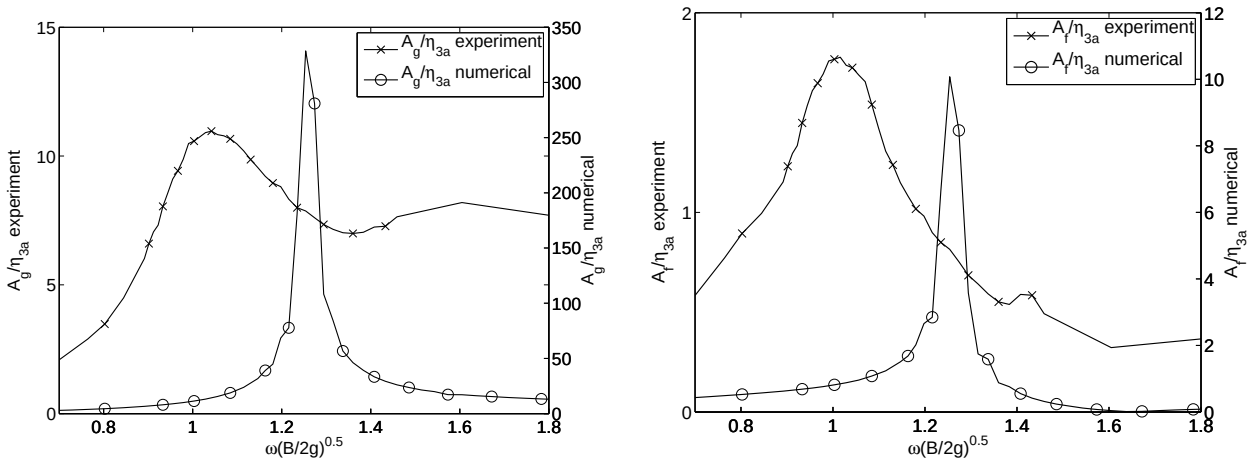

Figure 6.6: A_g and A_f. $b = 0.01\ m$.

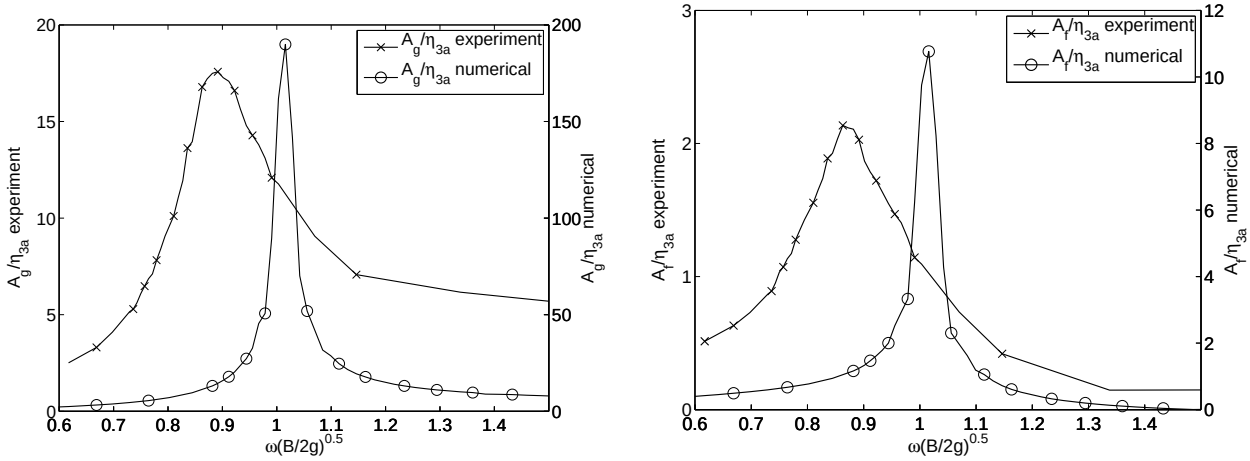

Figure 6.7: A_g and A_f. $b = 0.02\ m$.

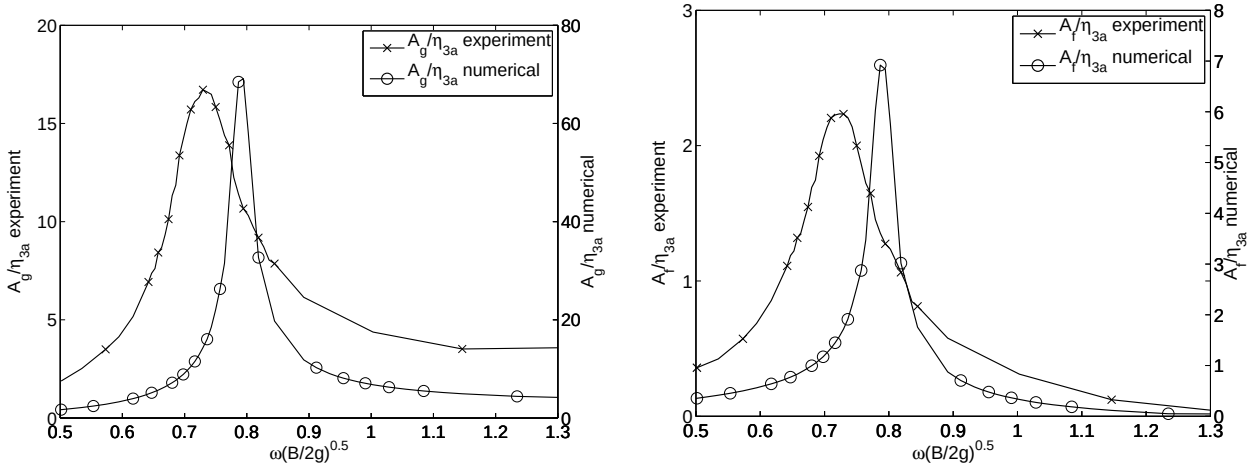

Figure 6.8: A_g and A_f. $b = 0.04\ m$.

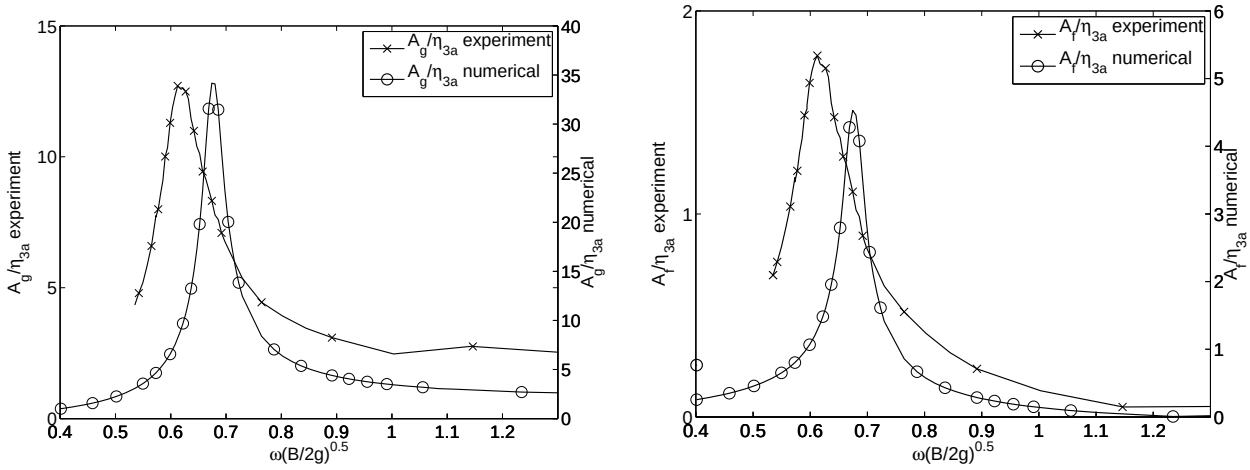

Figure 6.9: A_g and A_f. $b = 0.06\ m$.

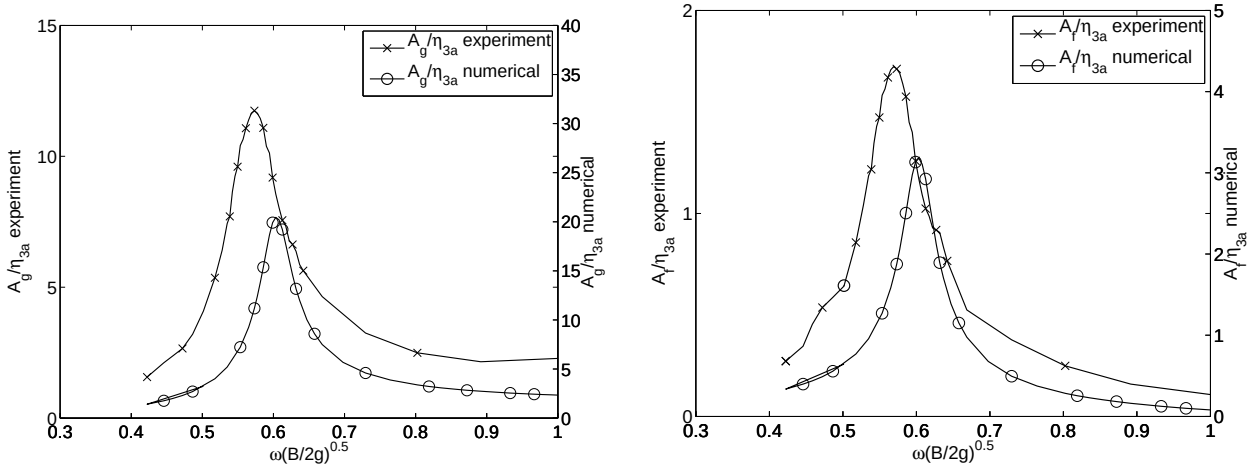

Figure 6.10: A_g and A_f. $b = 0.08\ m$.

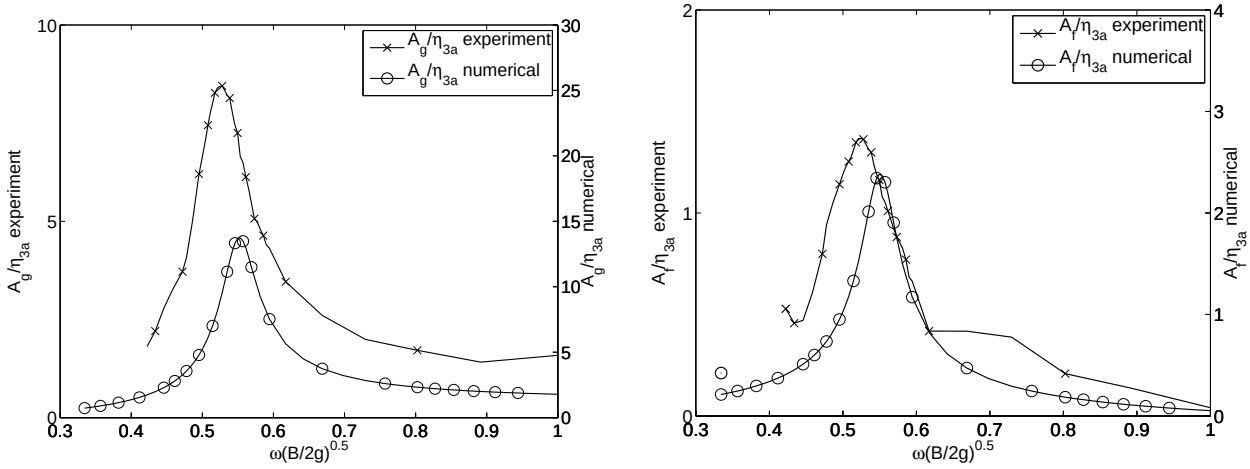

Figure 6.11: A_g and A_f. $b = 0.10\ m$.

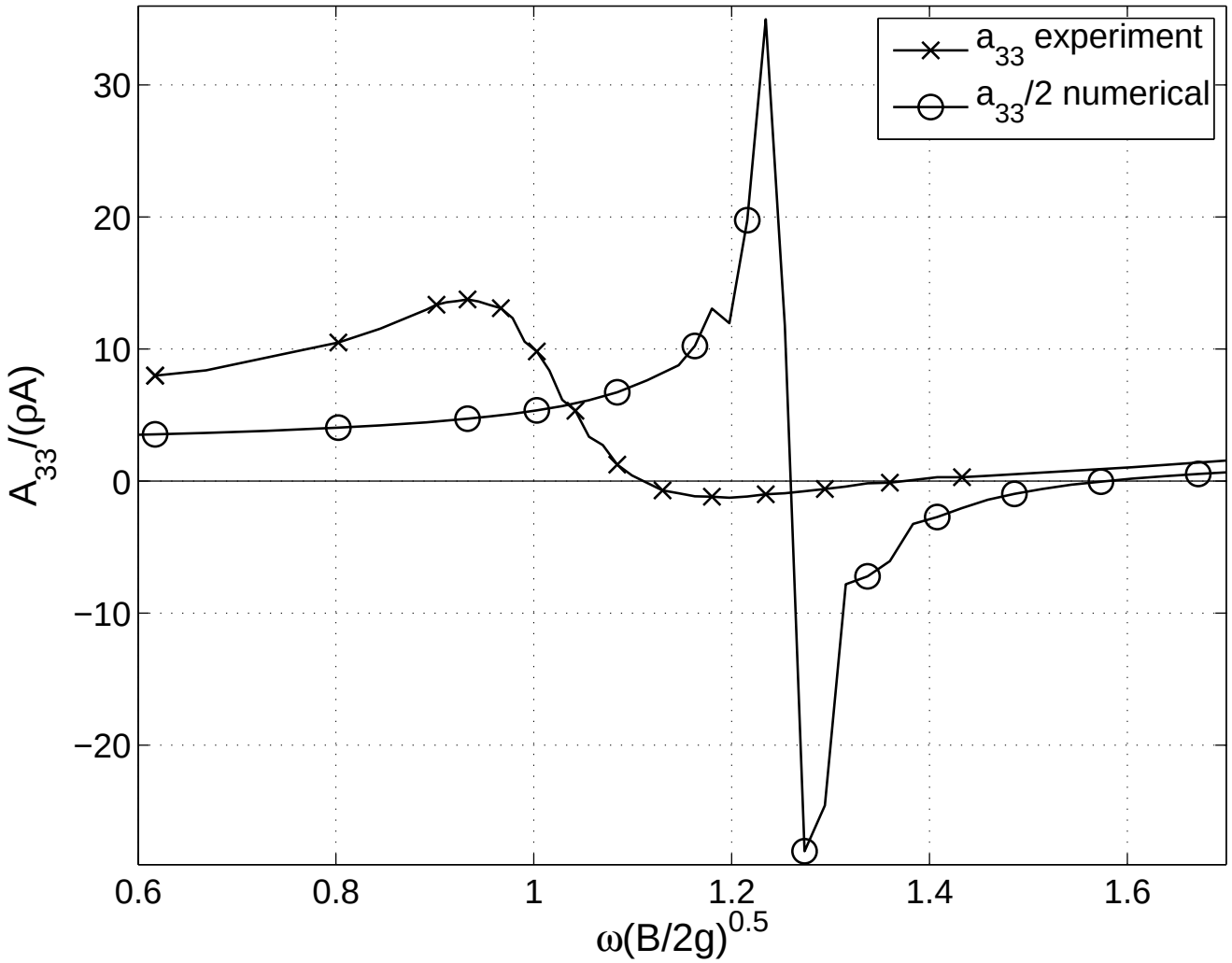

Figure 6.12: a_{33}, $b = 0.01$ m.

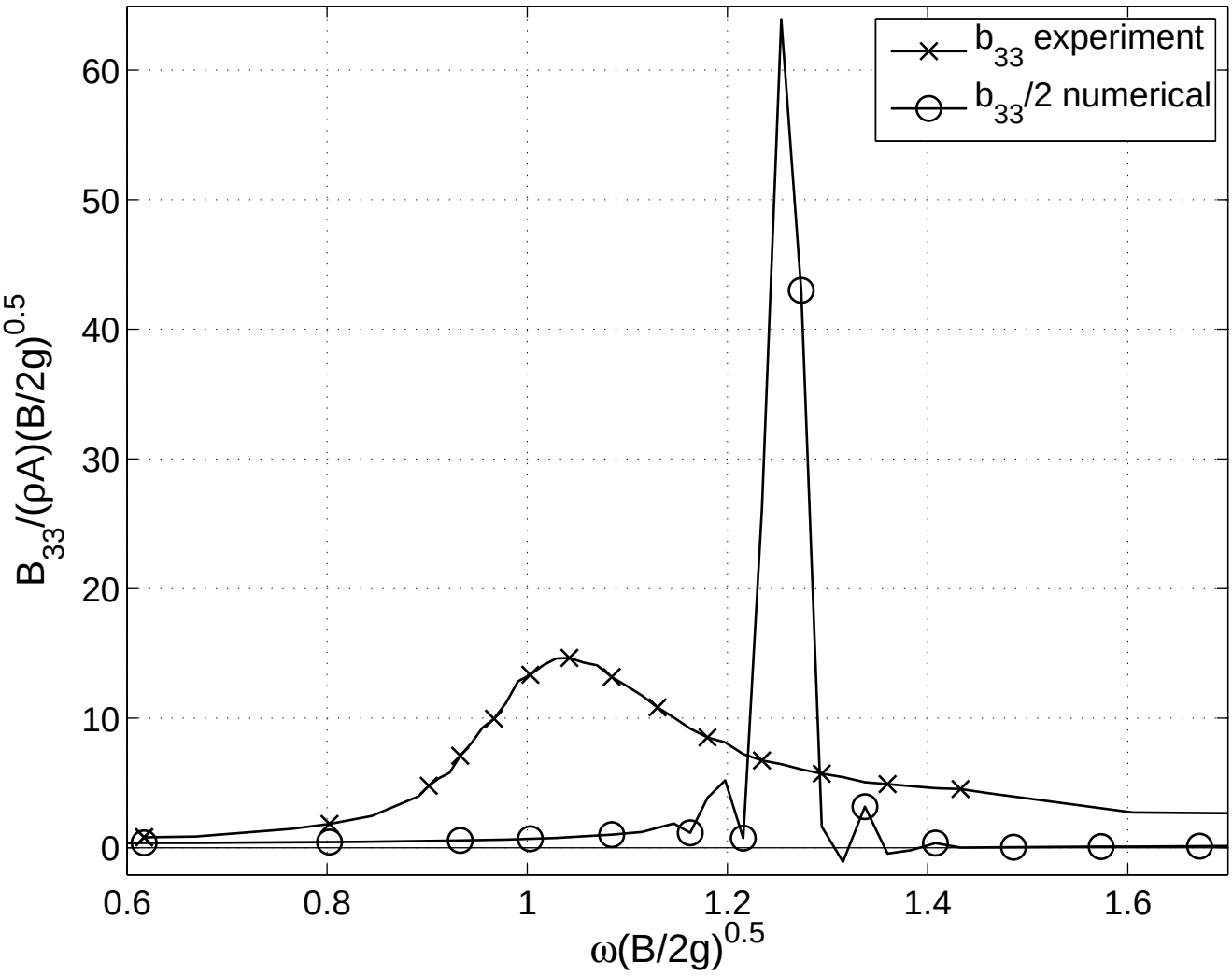

Figure 6.13: b_{33}, $b = 0.01\ m$.

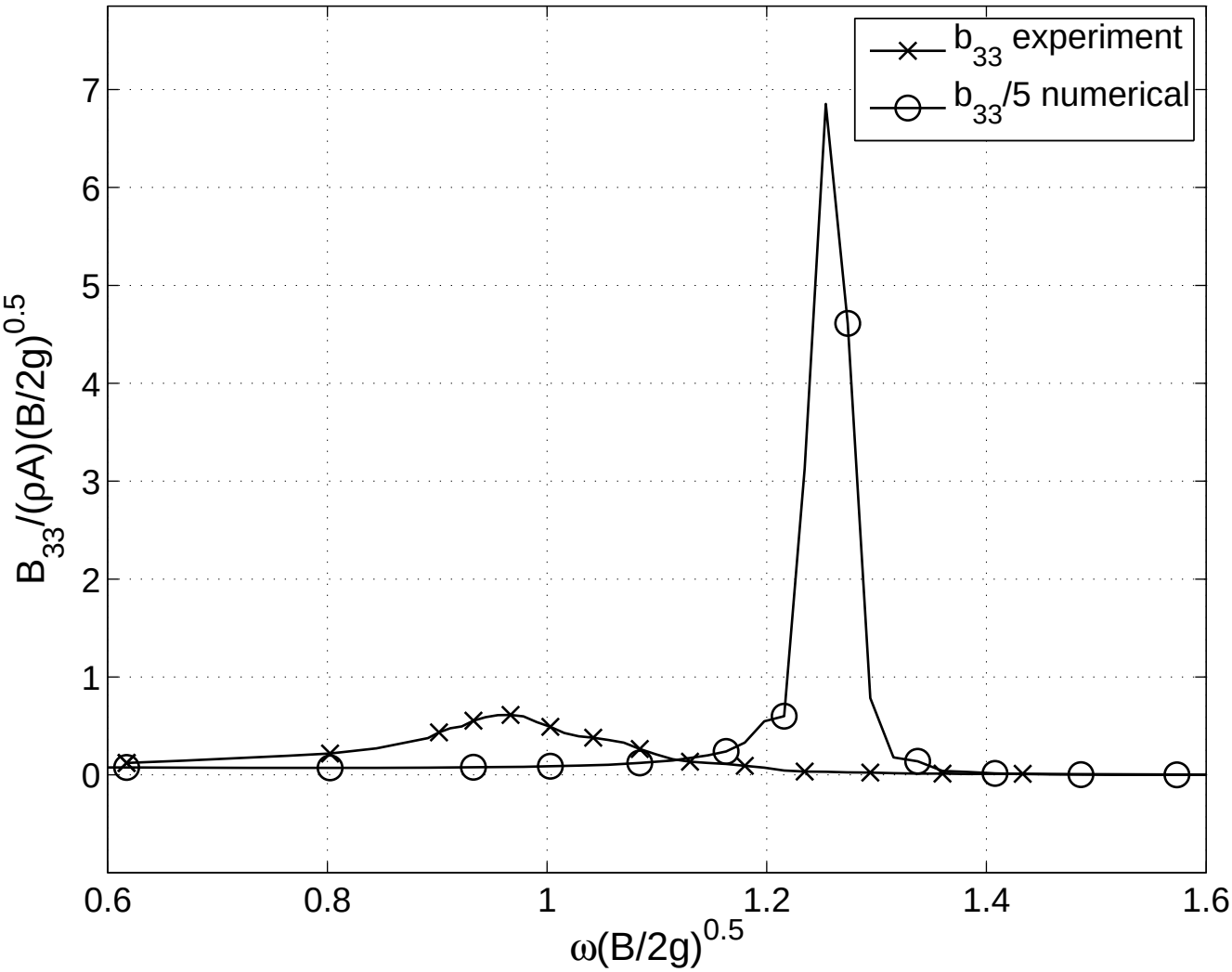

Figure 6.14: b_{33} from radiating waves. $b = 0.01\ m$.

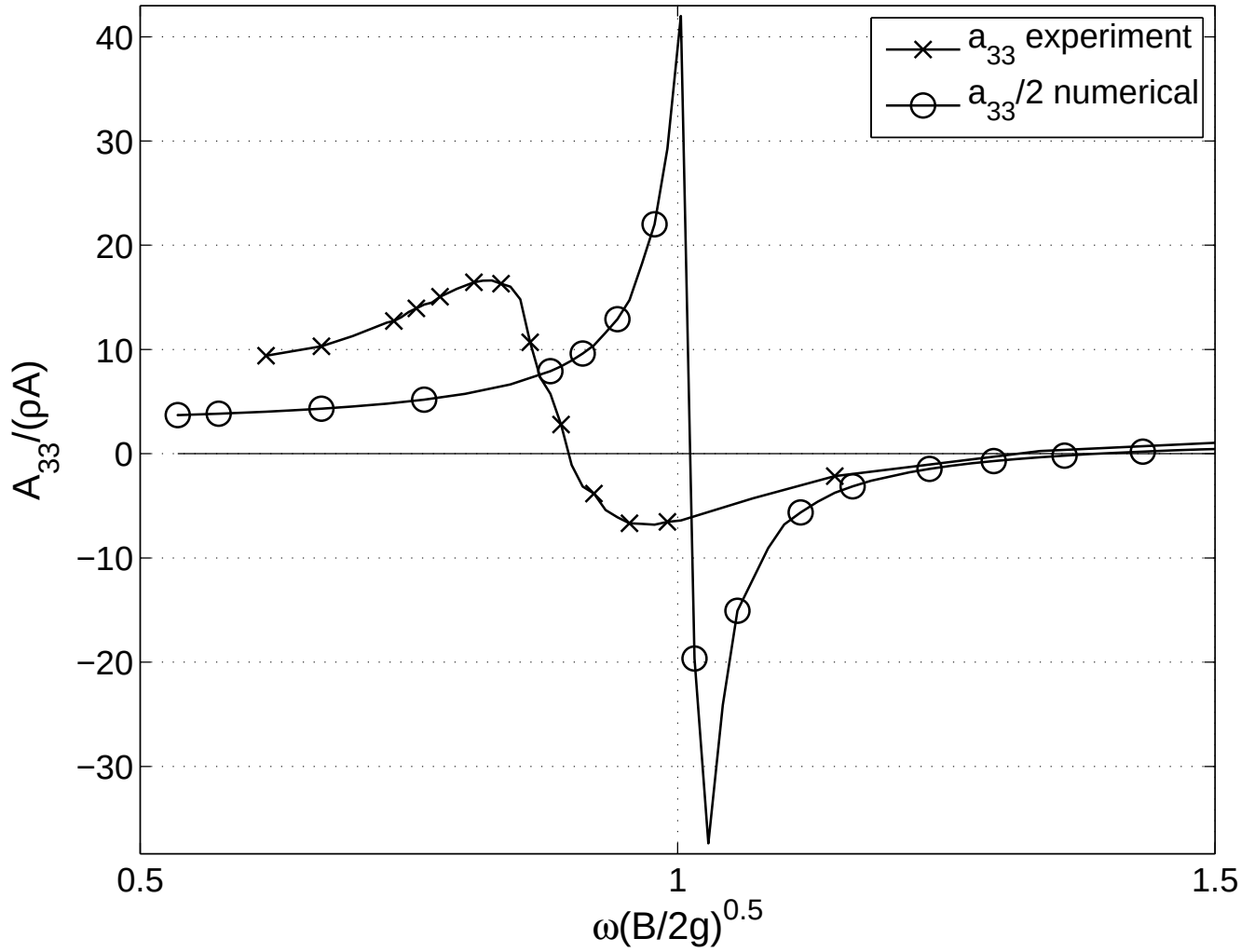

Figure 6.15: a_{33}, $b = 0.02\ m$.

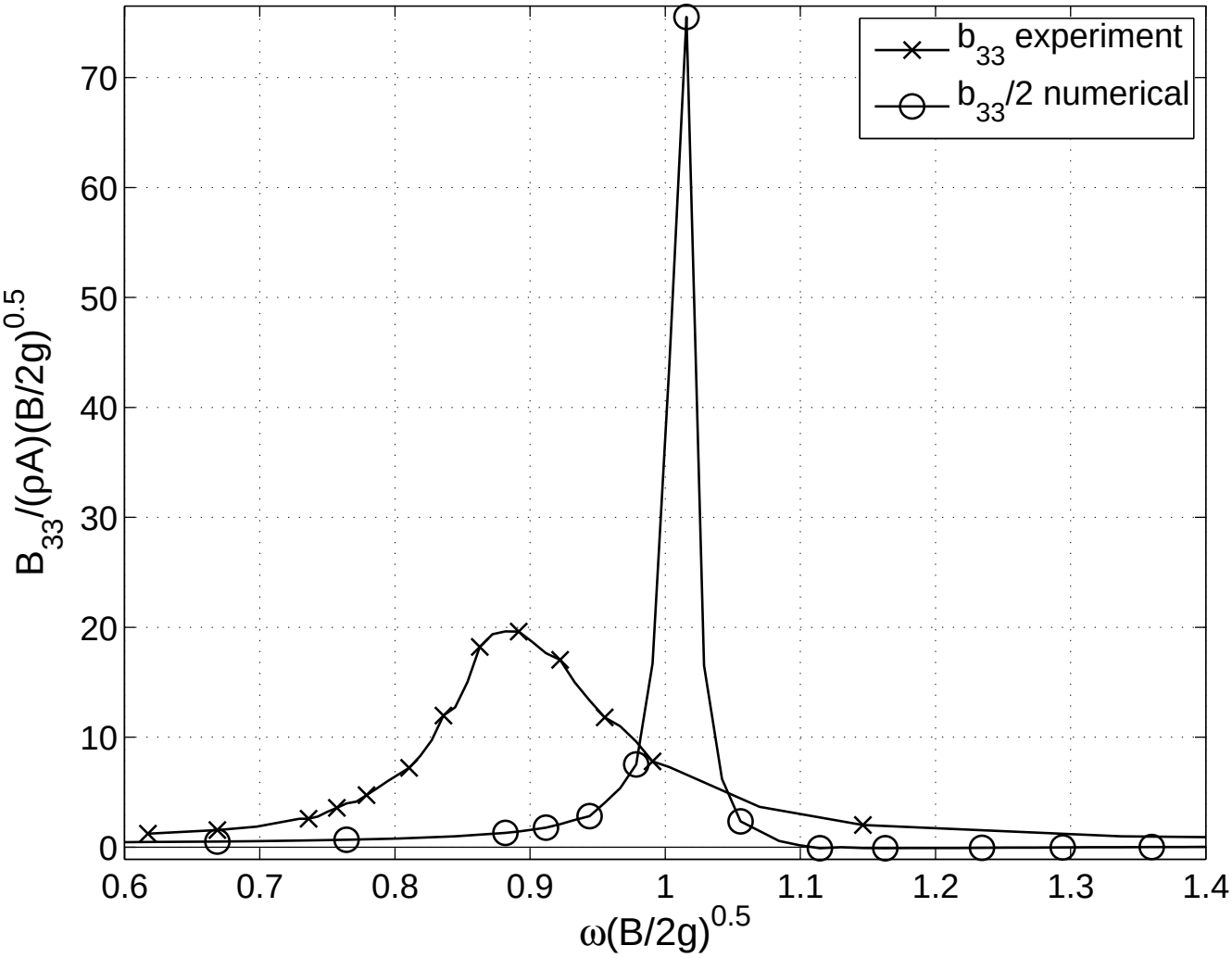

Figure 6.16: b_{33}, $b = 0.02\ m$.

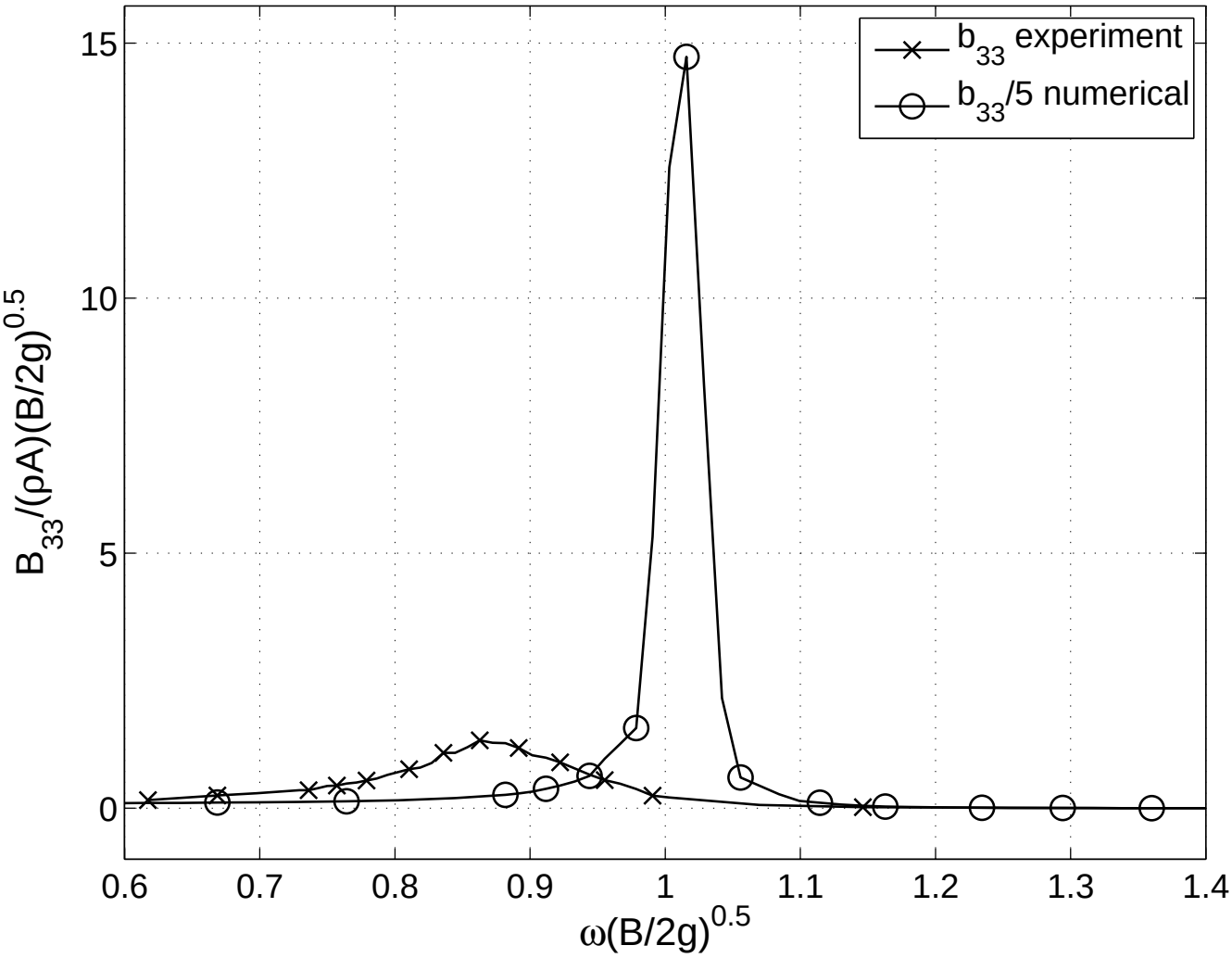

Figure 6.17: b_{33} from radiating waves. $b = 0.02$ *m*.

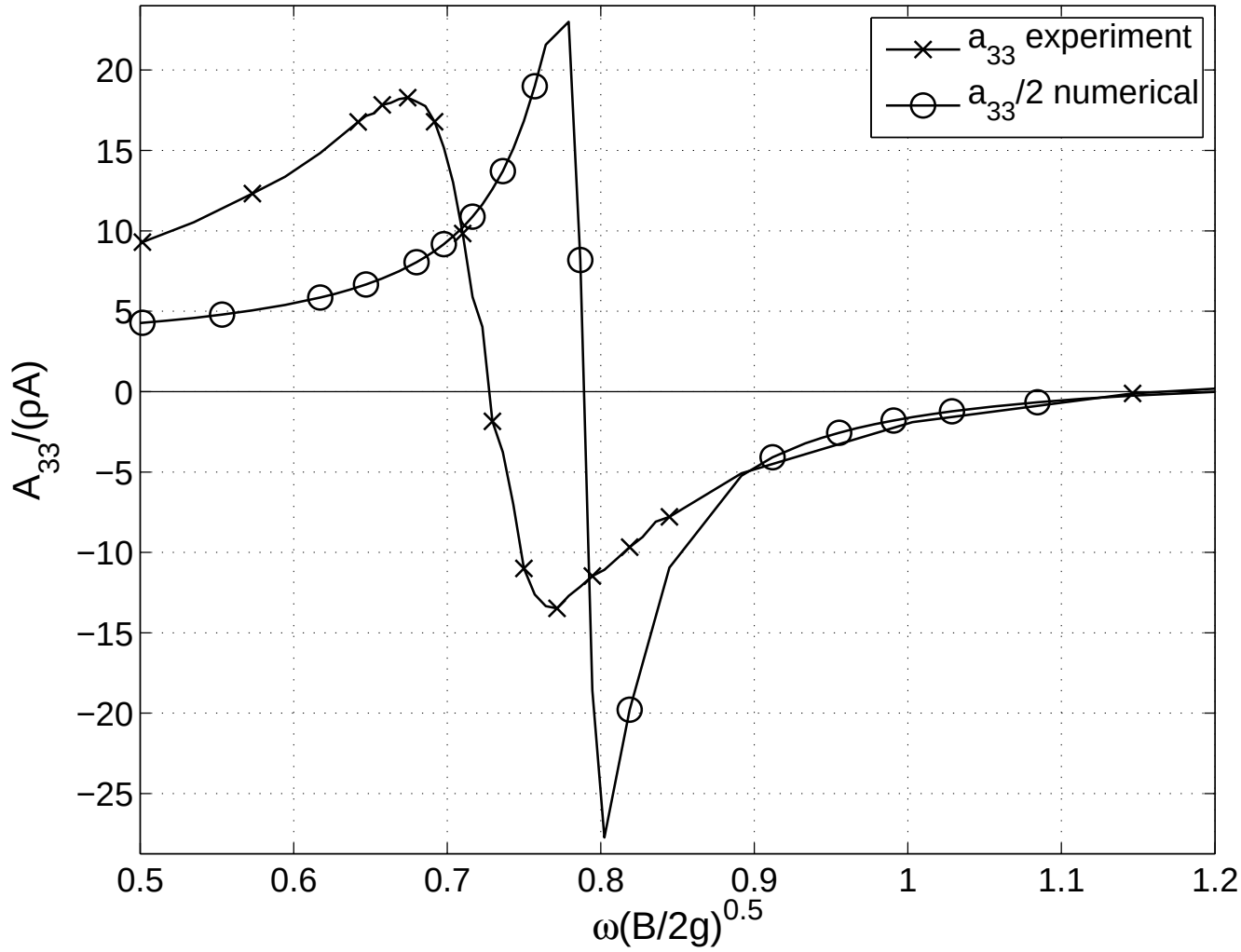

Figure 6.18: a_{33}, $b = 0.04\ m$.

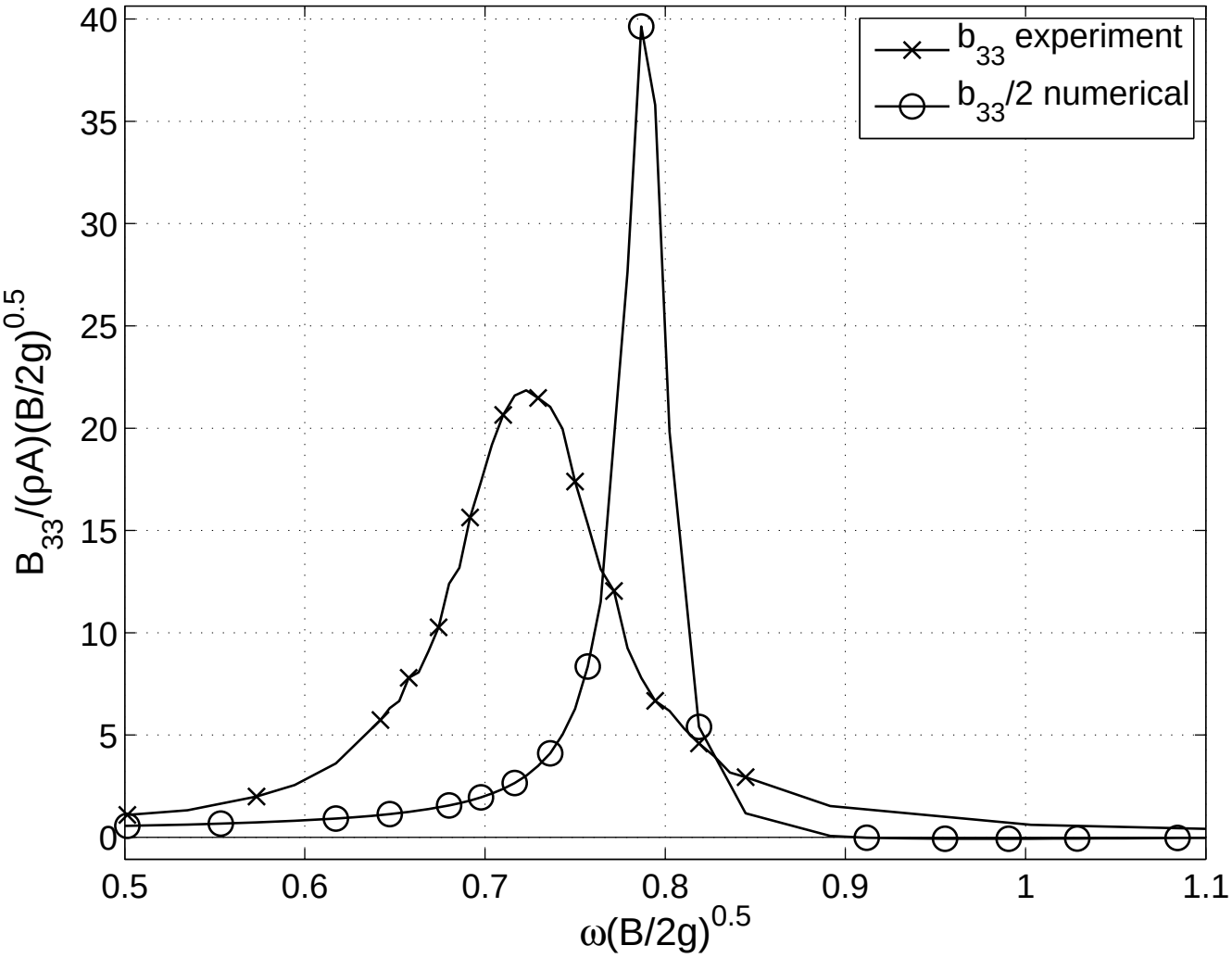

Figure 6.19: b_{33}, $b = 0.04\ m$.

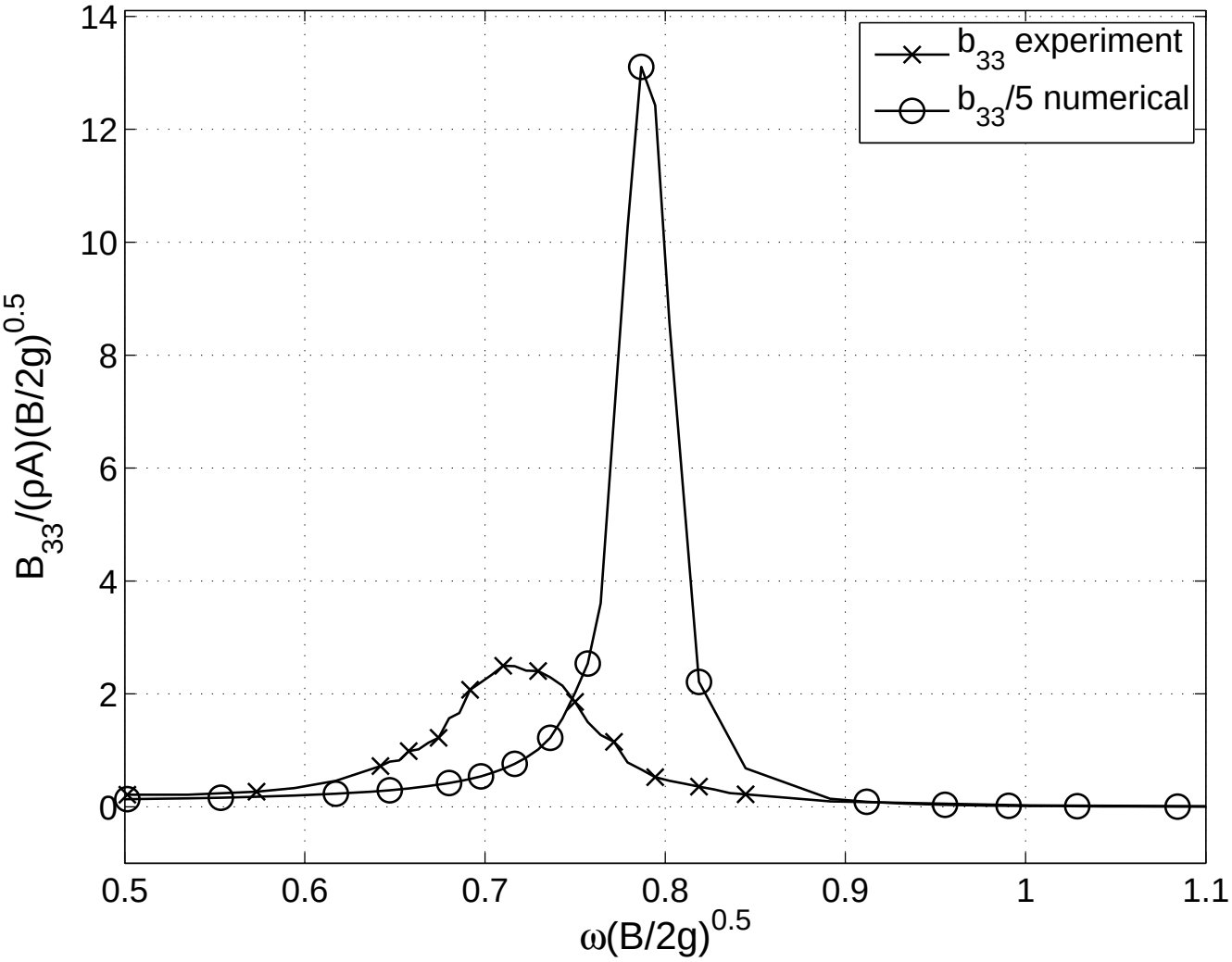

Figure 6.20: b_{33} from radiating waves. $b = 0.04\ m$.

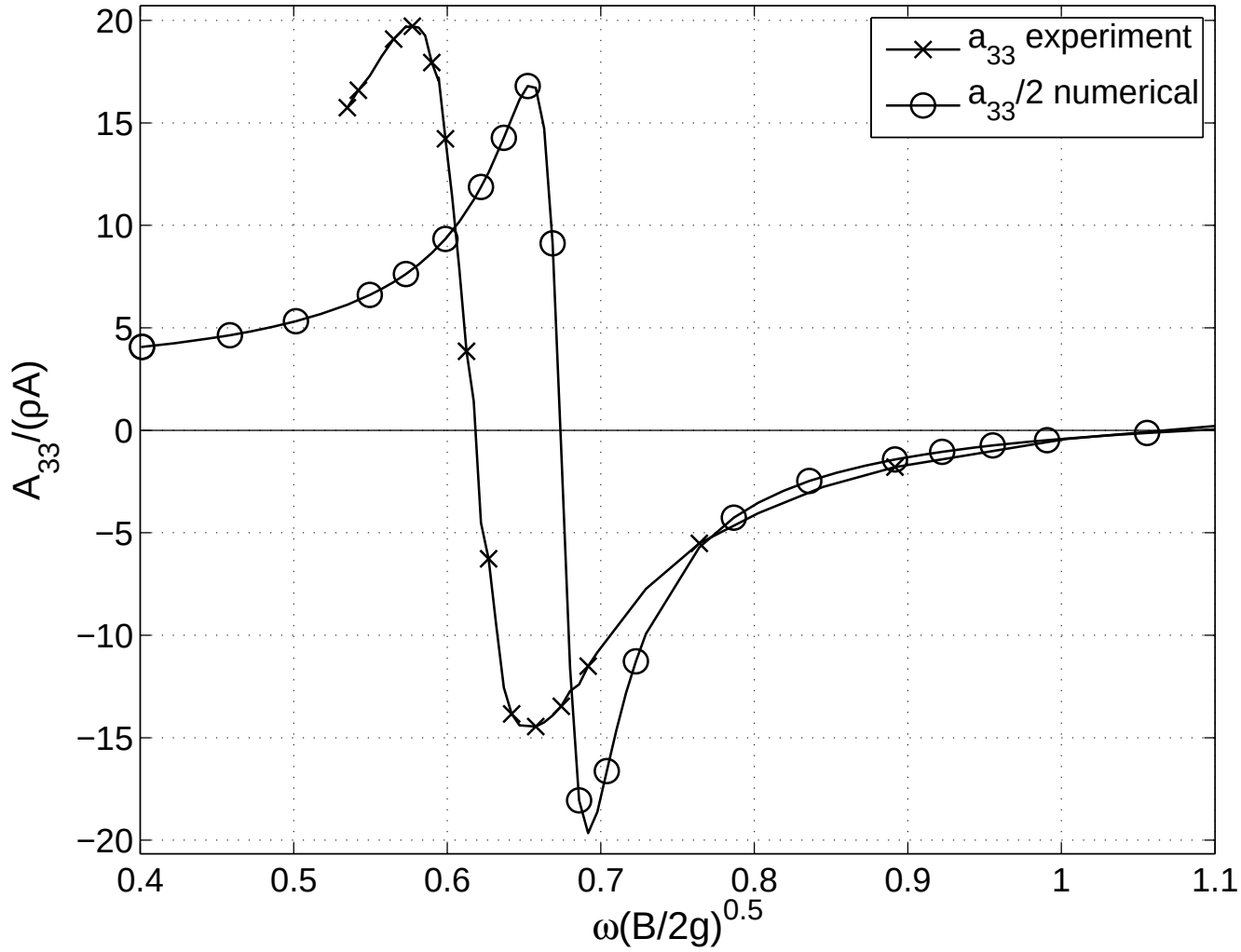

Figure 6.21: a_{33}, $b = 0.06\ m$.

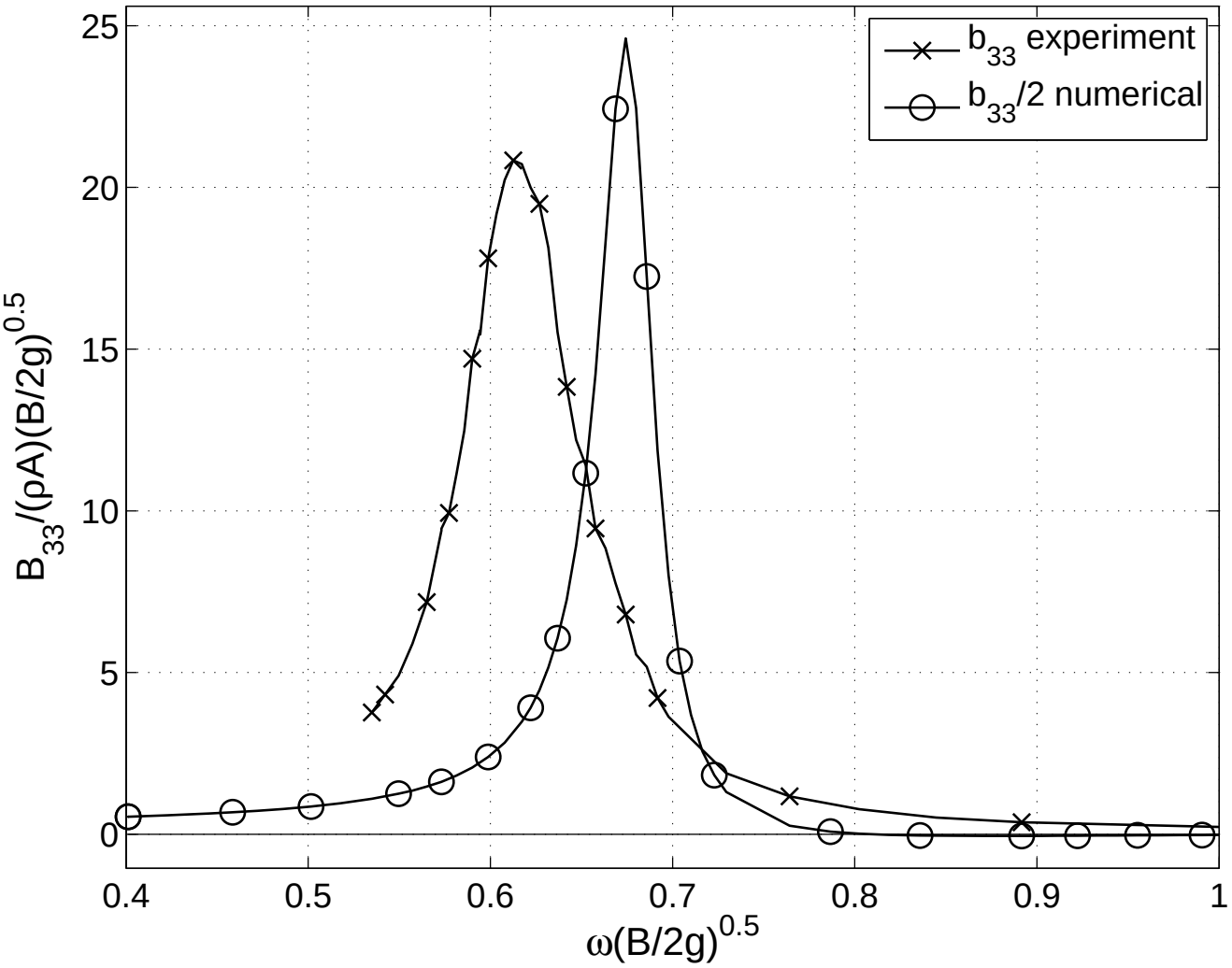

Figure 6.22: b_{33}, $b = 0.06\ m$.

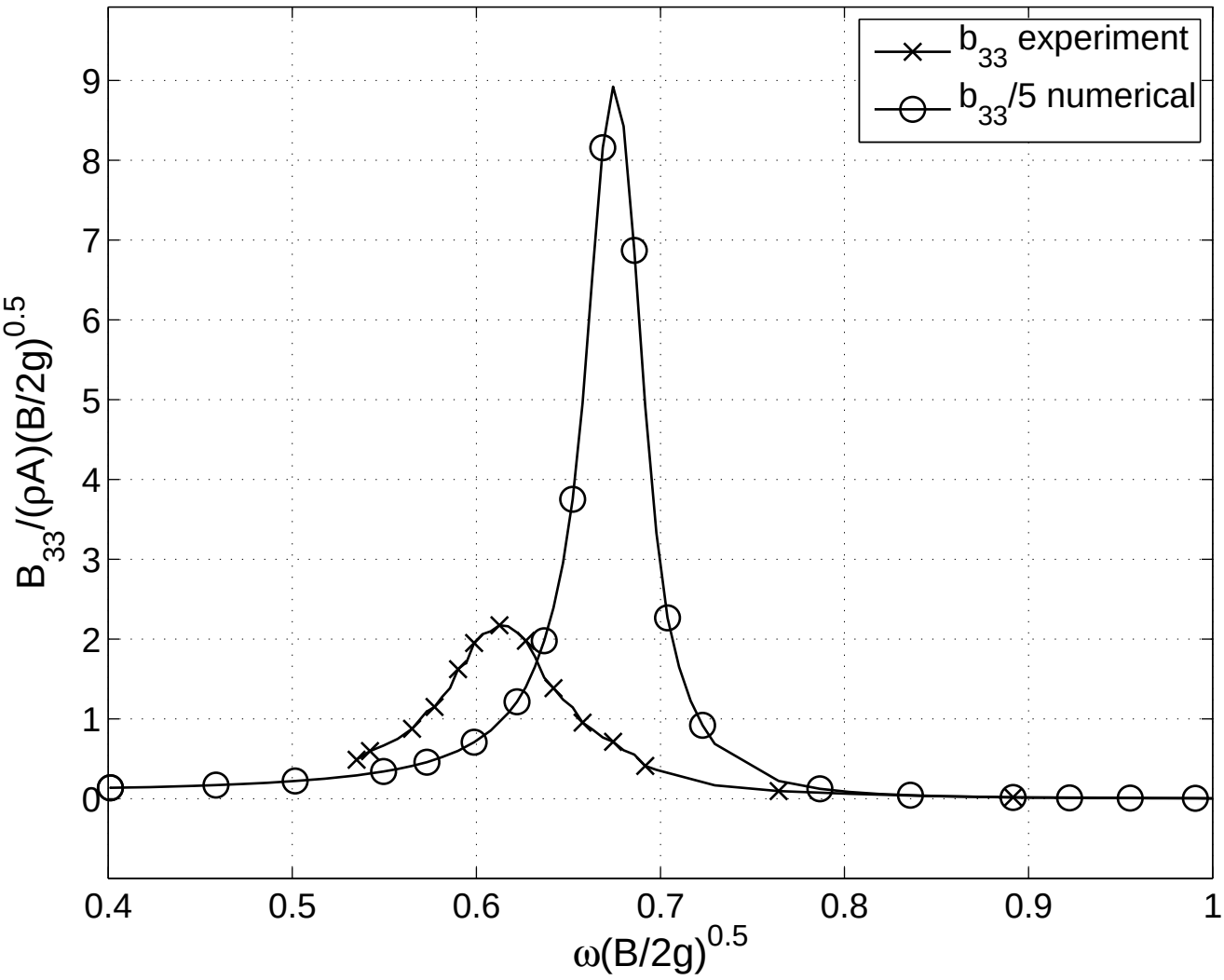

Figure 6.23: b_{33} from radiating waves. $b = 0.06\ m$.

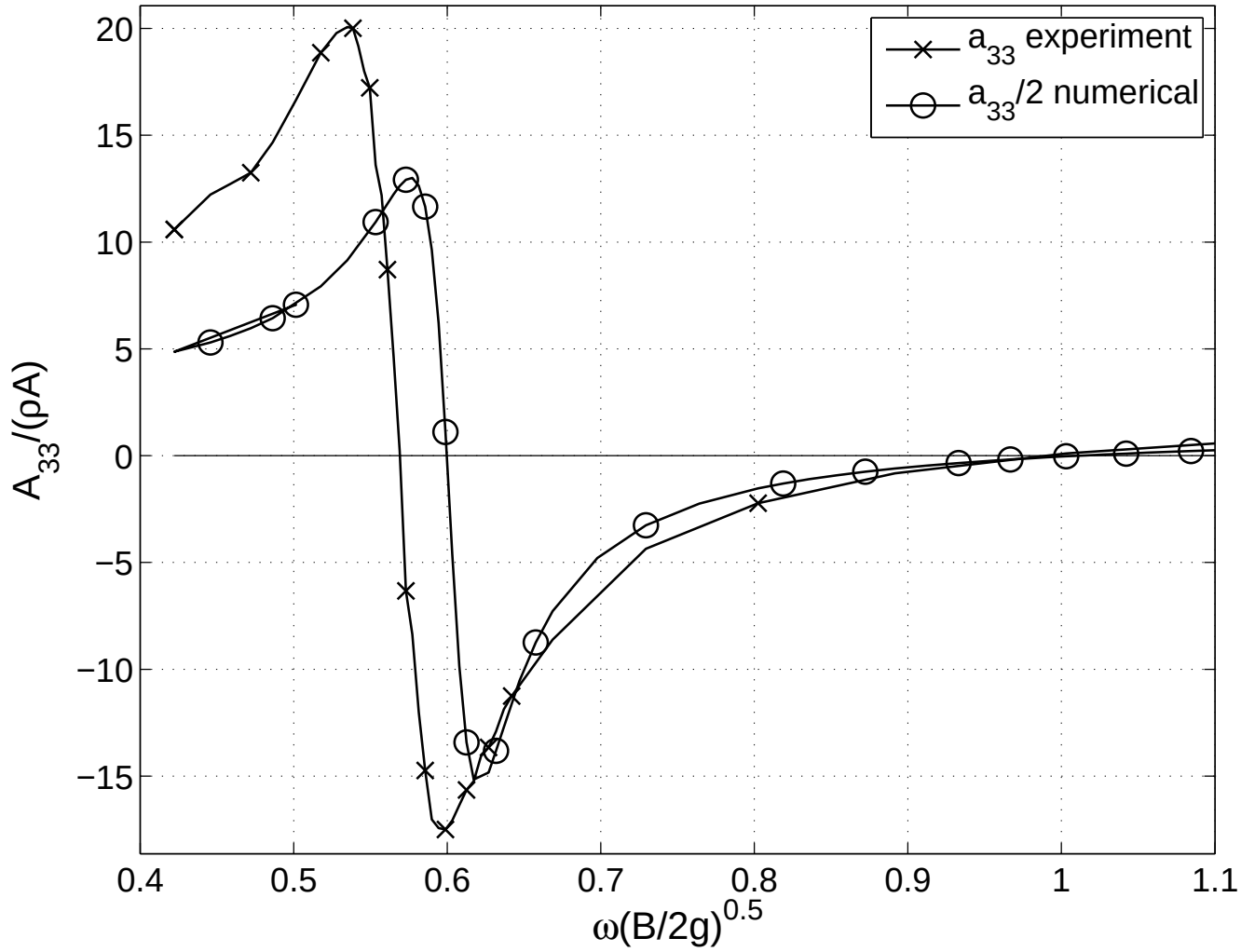

Figure 6.24: a_{33}, $b = 0.08\ m$.

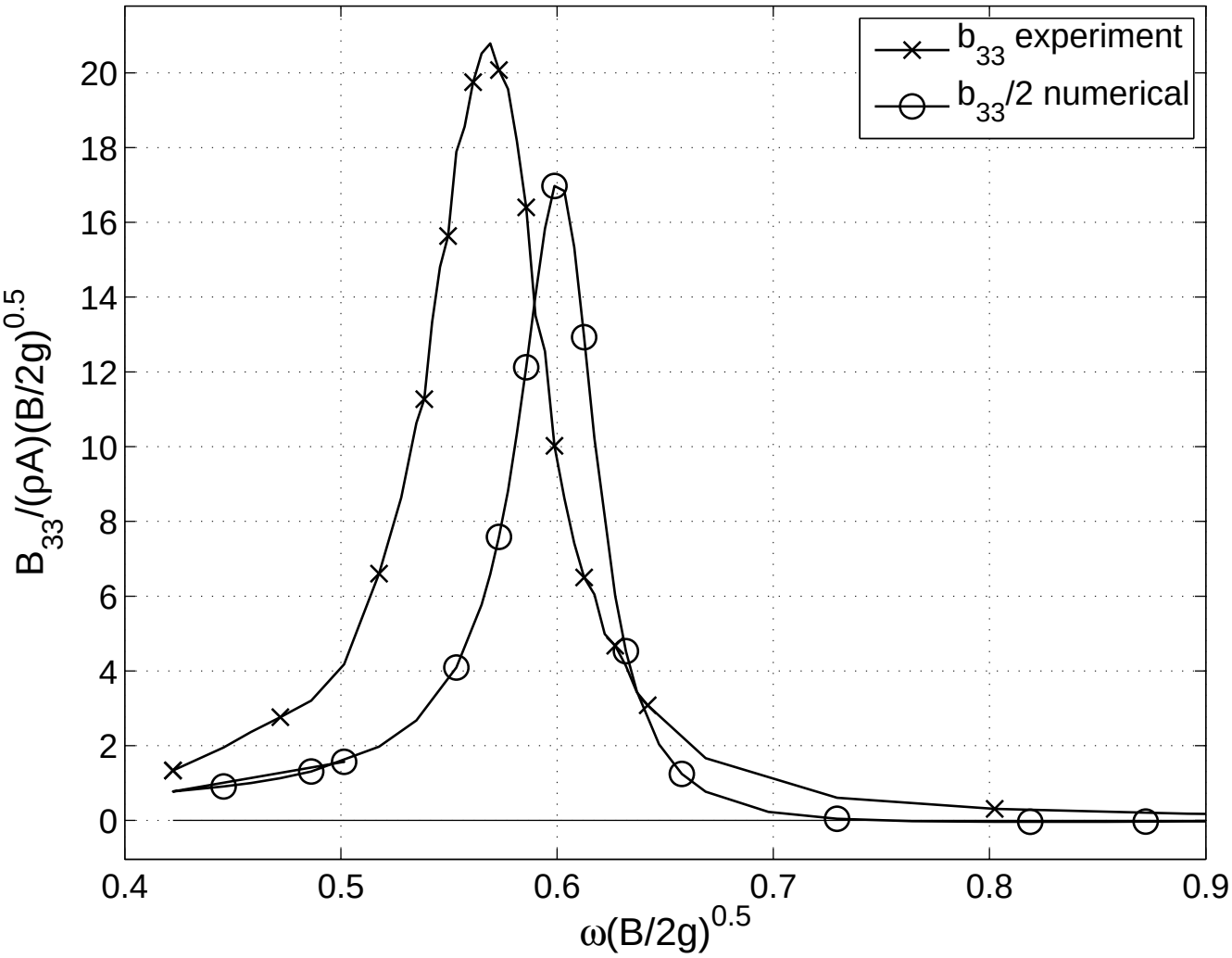

Figure 6.25: b_{33}, $b = 0.08\ m$.

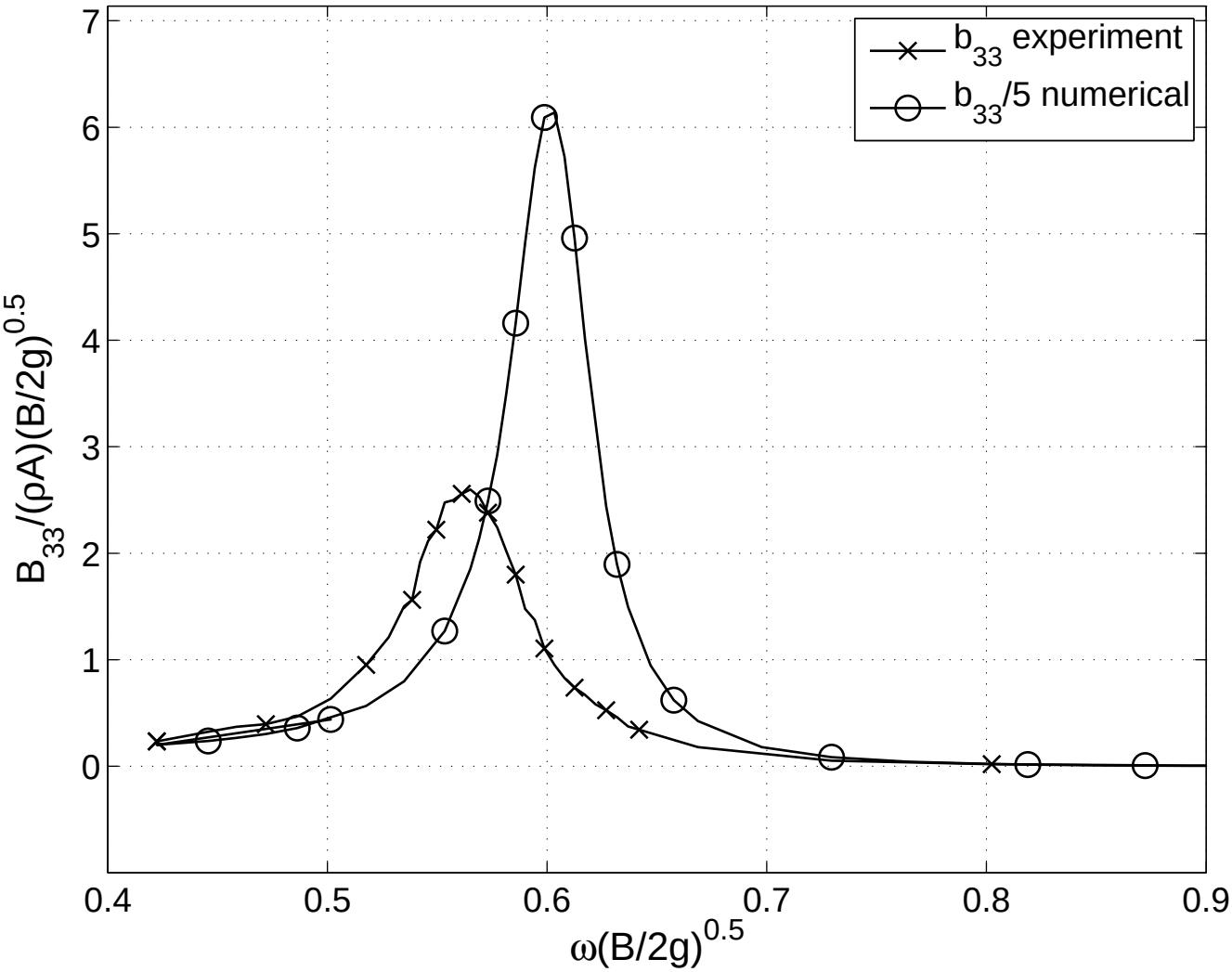

Figure 6.26: b_{33} from radiating waves. $b = 0.08\ m$.

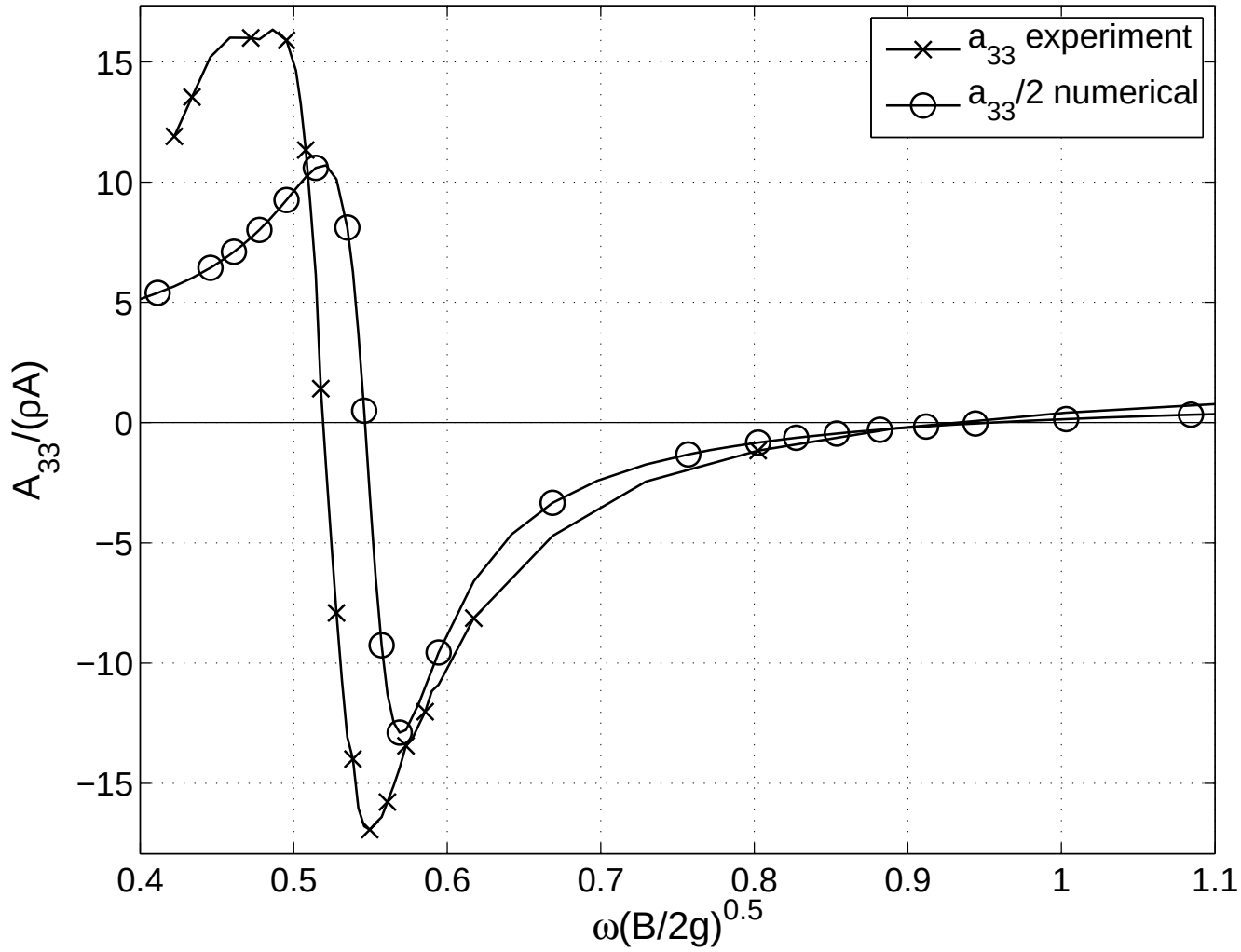

Figure 6.27: a_{33}, $b = 0.10\ m$.

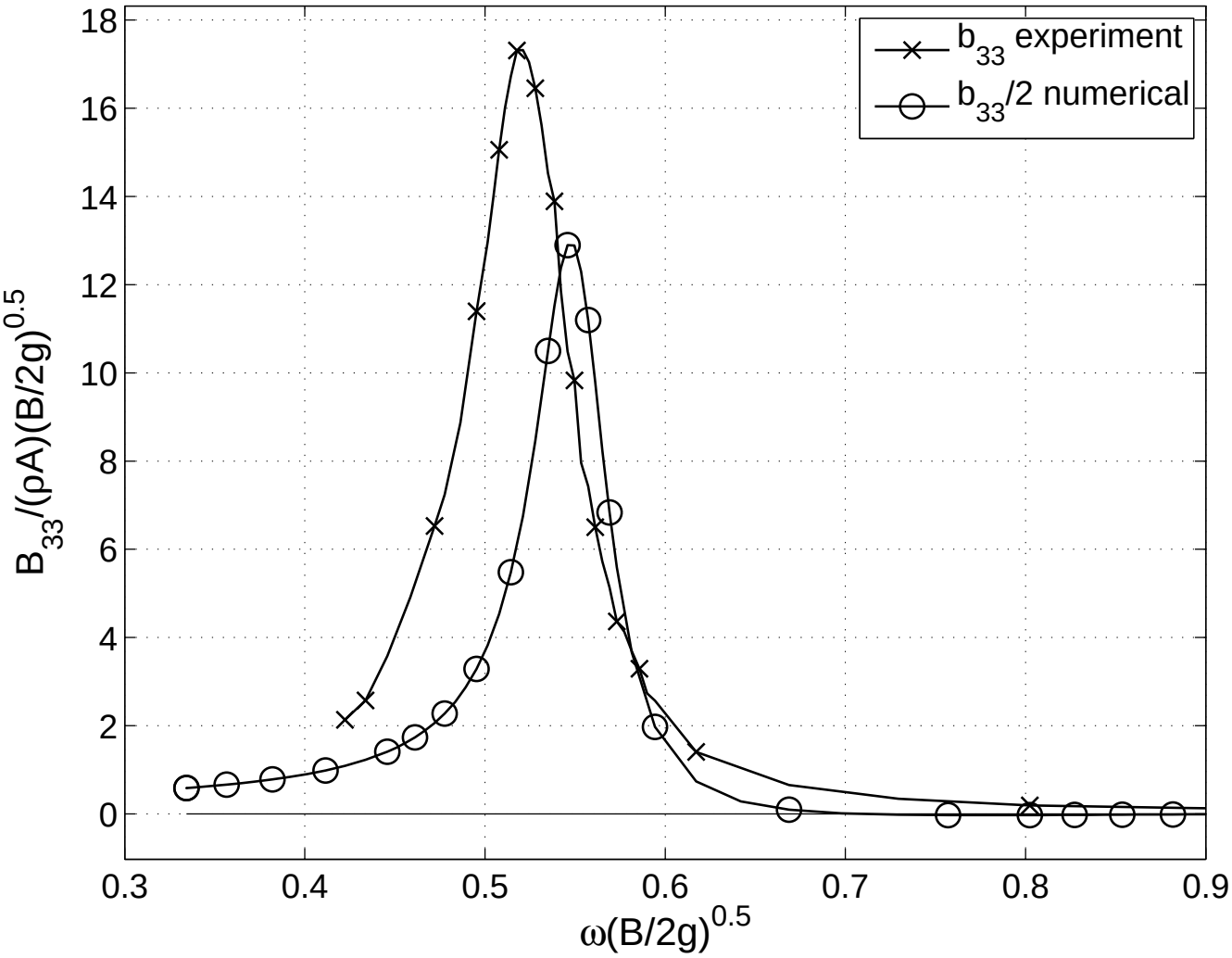

Figure 6.28: b_{33}, $b = 0.10\ m$.

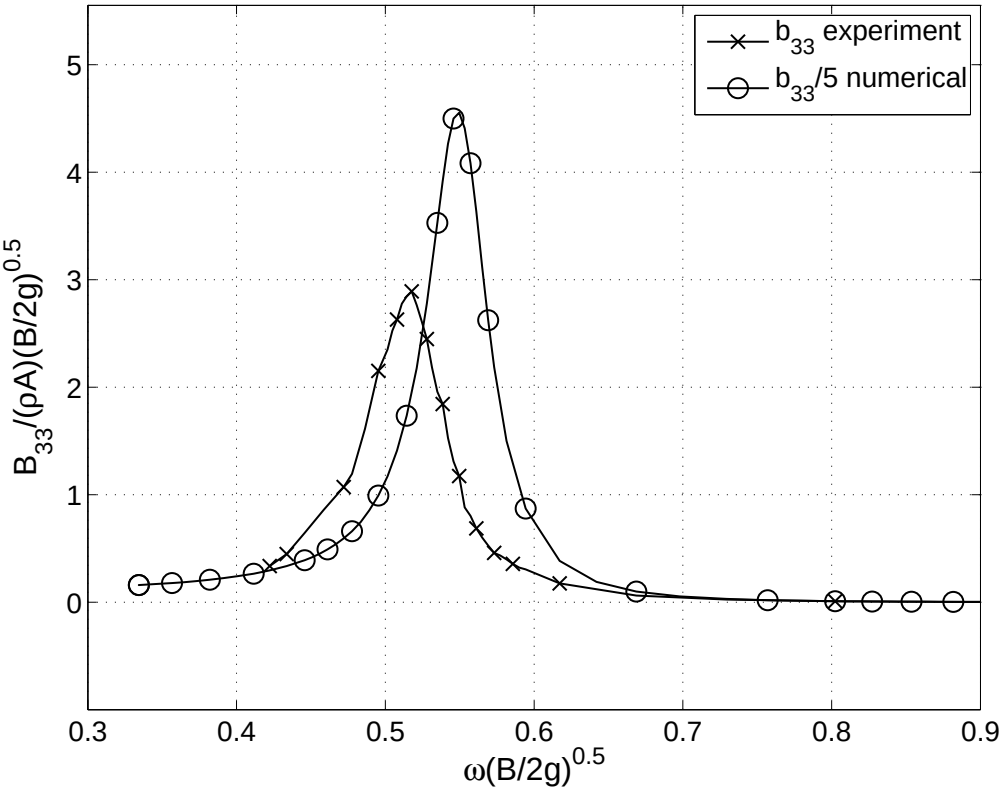

Figure 6.29: b_{33} from radiating waves. $b = 0.10$ *m*.

6.3 Ship and one ice-floe

Numerical and experimental results for the case when the ship is forced to oscillate in heave with one ice-floe present in the wave flume and the numerical wave tank. The ship and the two ice-floes makes an anti-symmetrical set-up where the *gap* varies from 1 *cm* to 10 *cm*. The condensed results presented here range from $b = 0.04$ *m* to $b = 0.10$ *m*. And again the results given are the non-dimensional added mass b_{33}, damping a_{33} and non-dimensional gap amplitude A_g presented in the following figures.

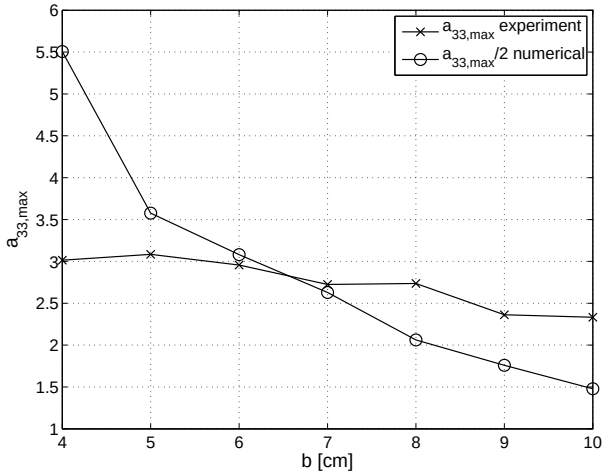

Figure 6.30: Maximum values of a_{33}.

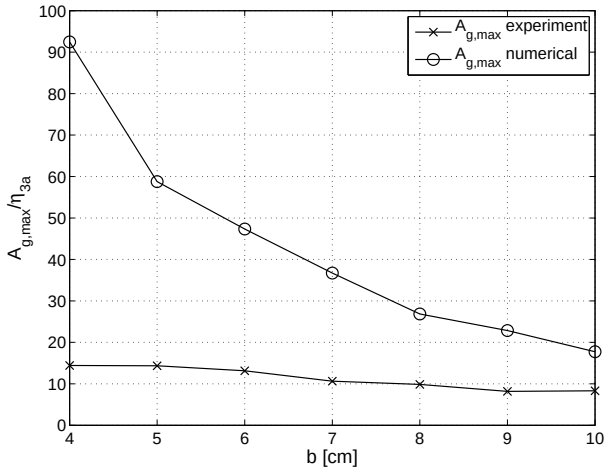

Figure 6.31: Max. values A_g.

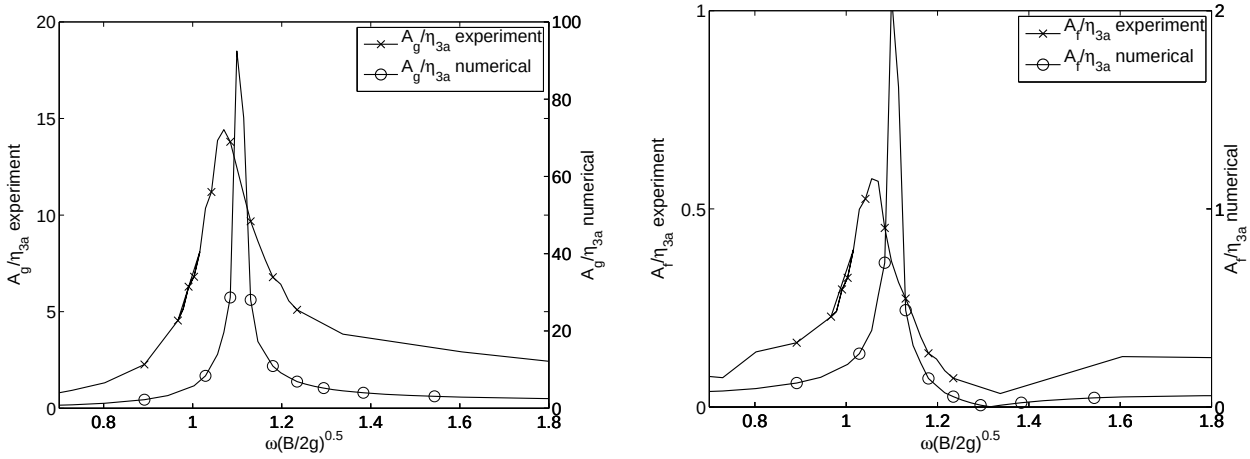

Figure 6.32: A_g and A_f. $b = 0.04\ m$.

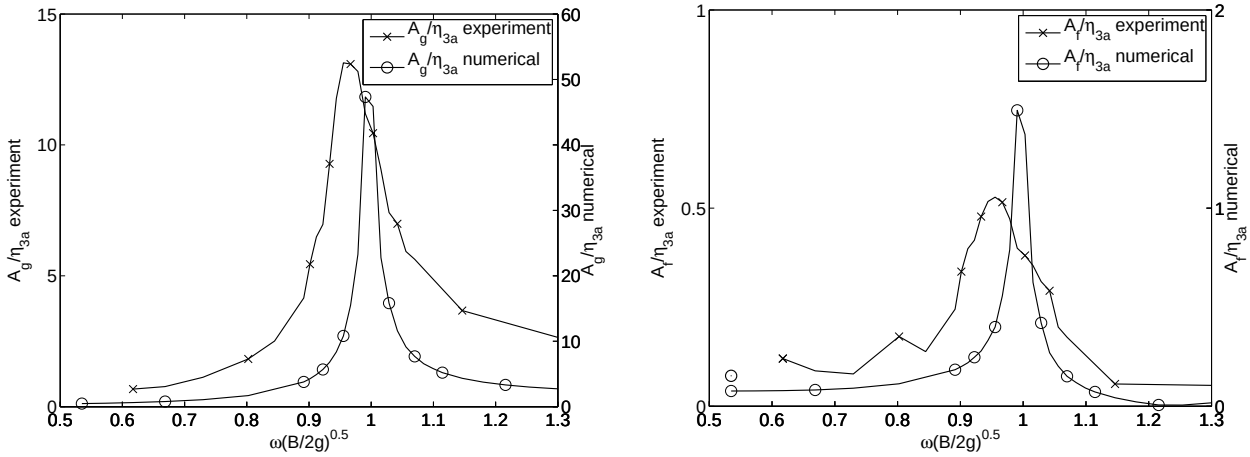

Figure 6.33: A_g and A_f. $b = 0.06\ m$.

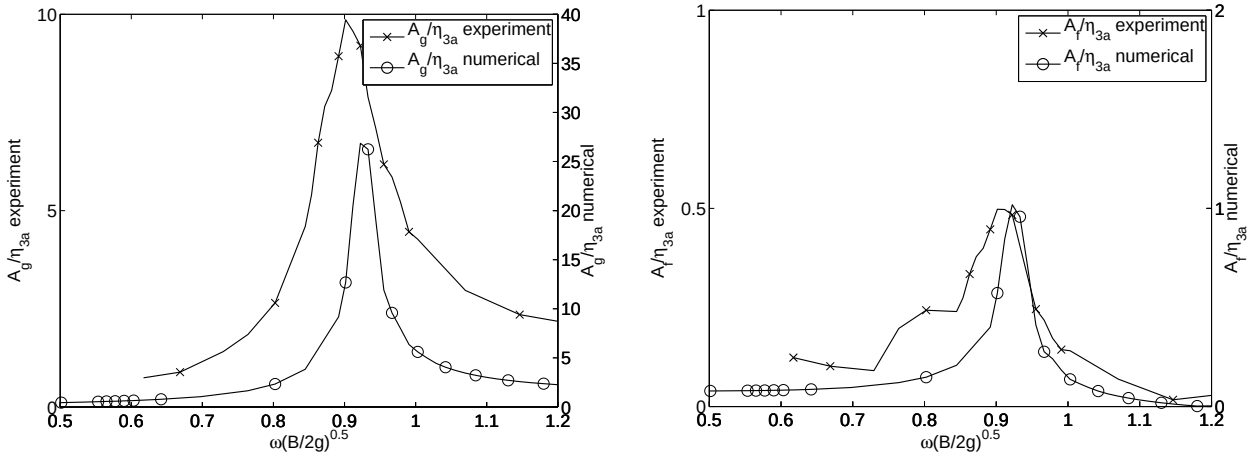

Figure 6.34: A_g and A_f. $b = 0.08\ m$.

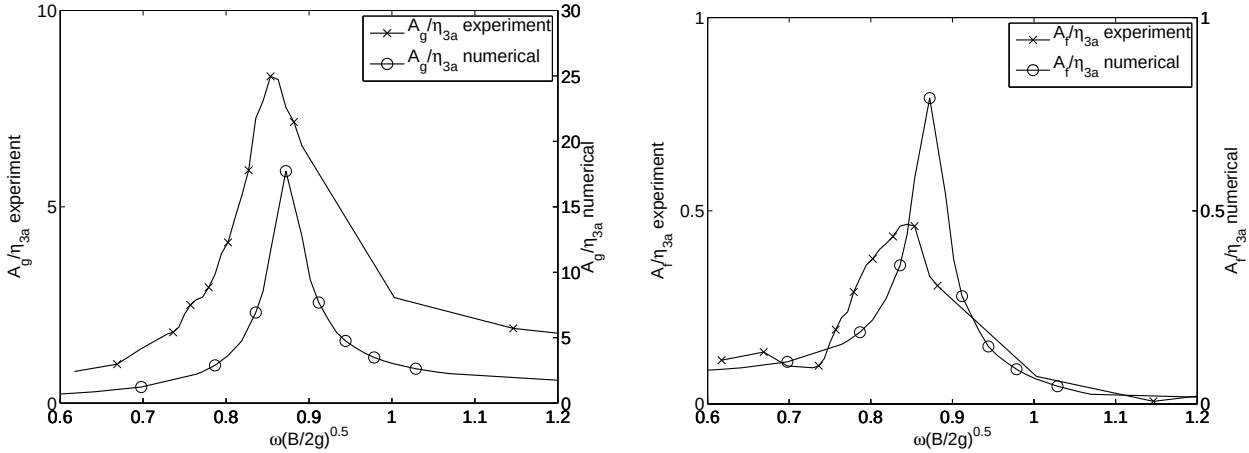

Figure 6.35: A_g and A_f. $b = 0.10\ m$.

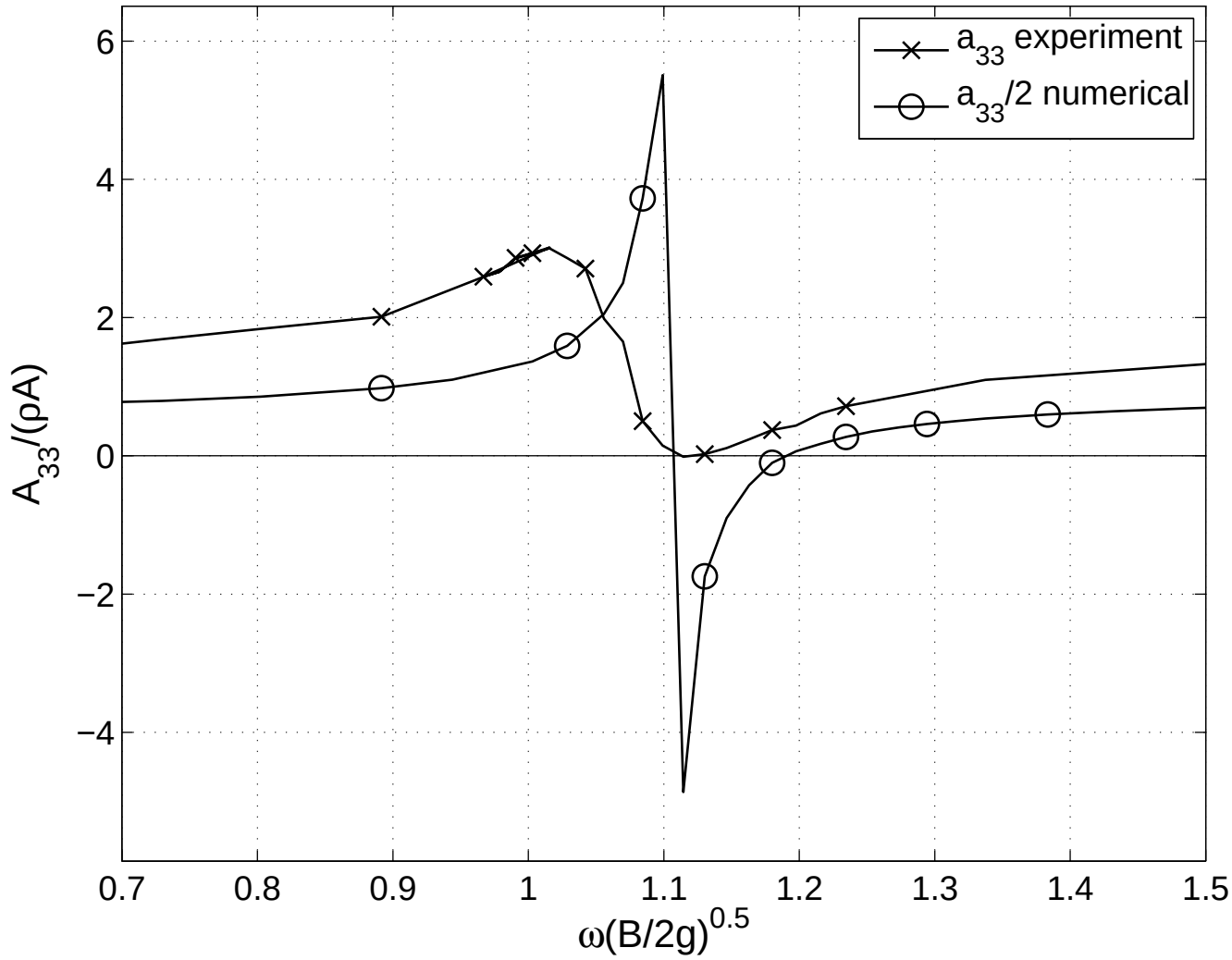

Figure 6.36: a_{33}, $b = 0.04\ m$.

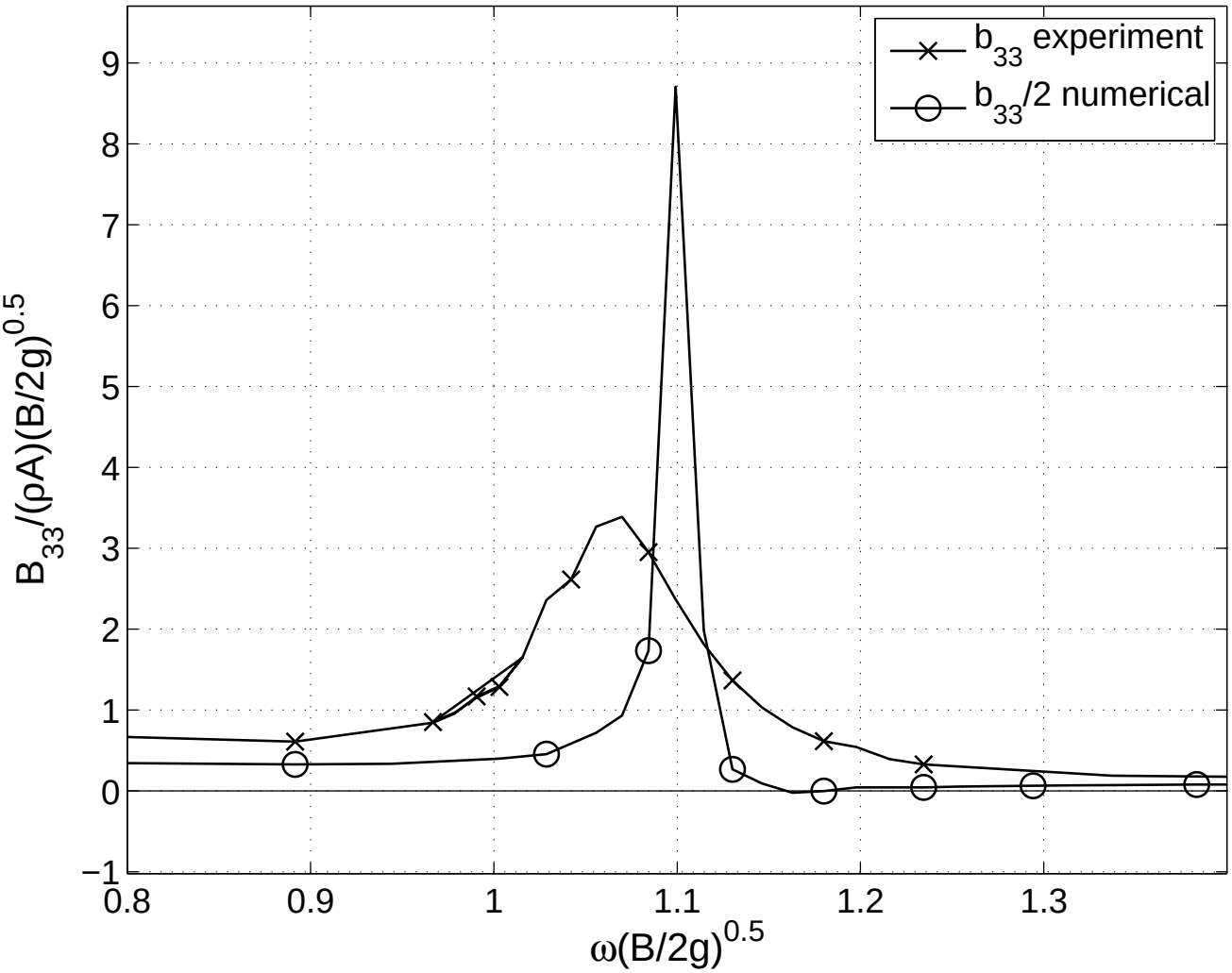

Figure 6.37: b_{33}, $b = 0.04\ m$.

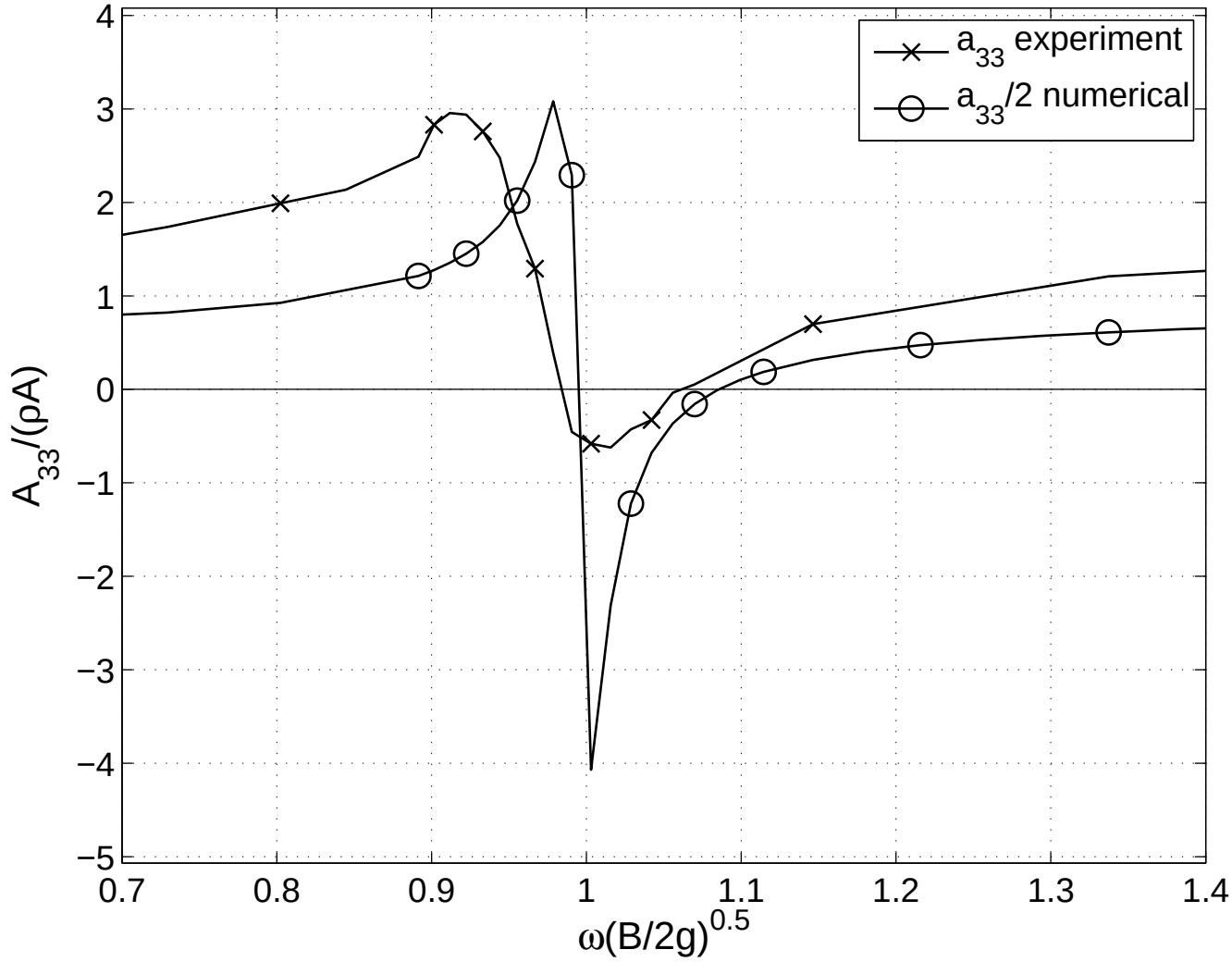

Figure 6.38: a_{33}, $b = 0.06\ m$.

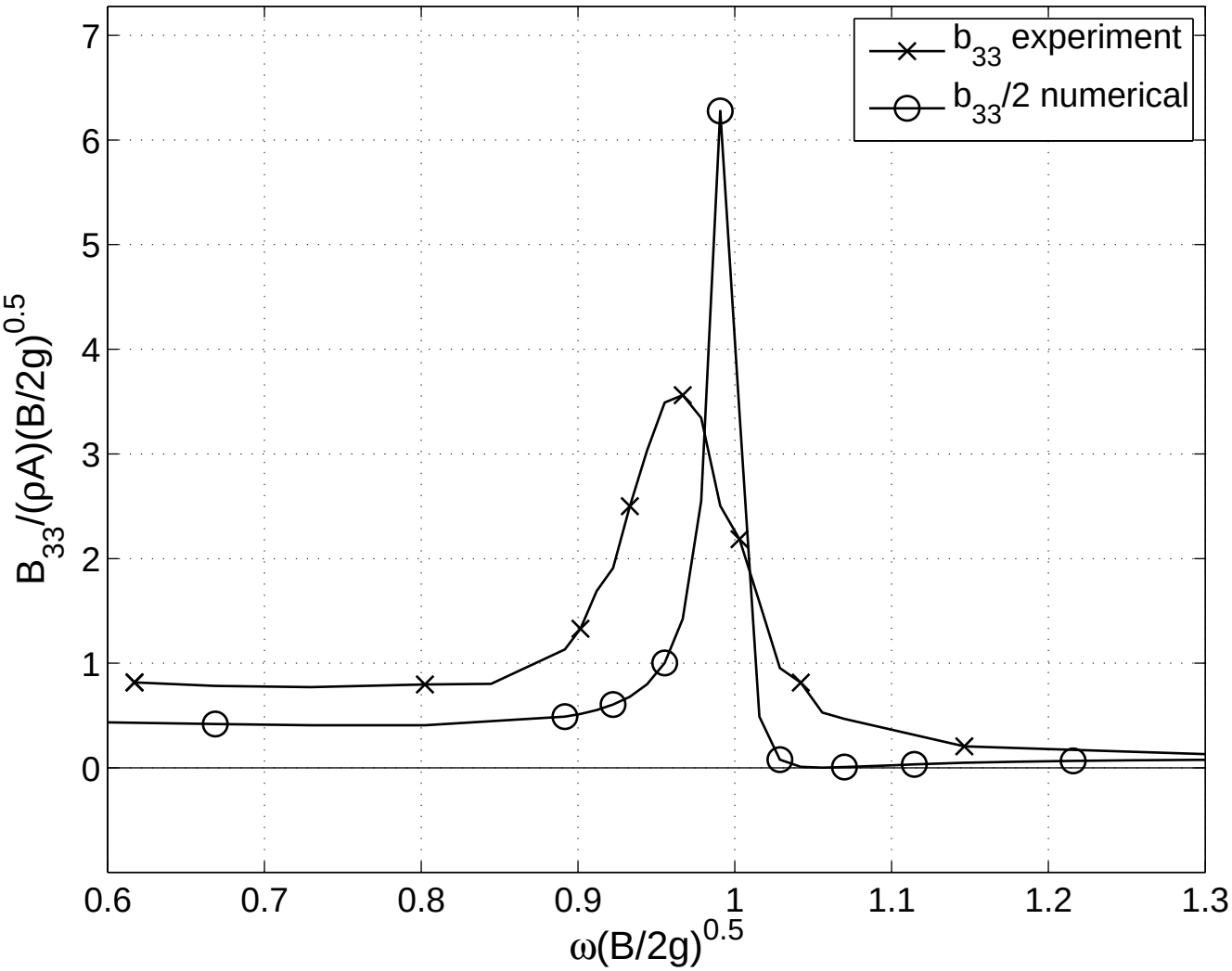

Figure 6.39: b_{33}, $b = 0.06\ m$.

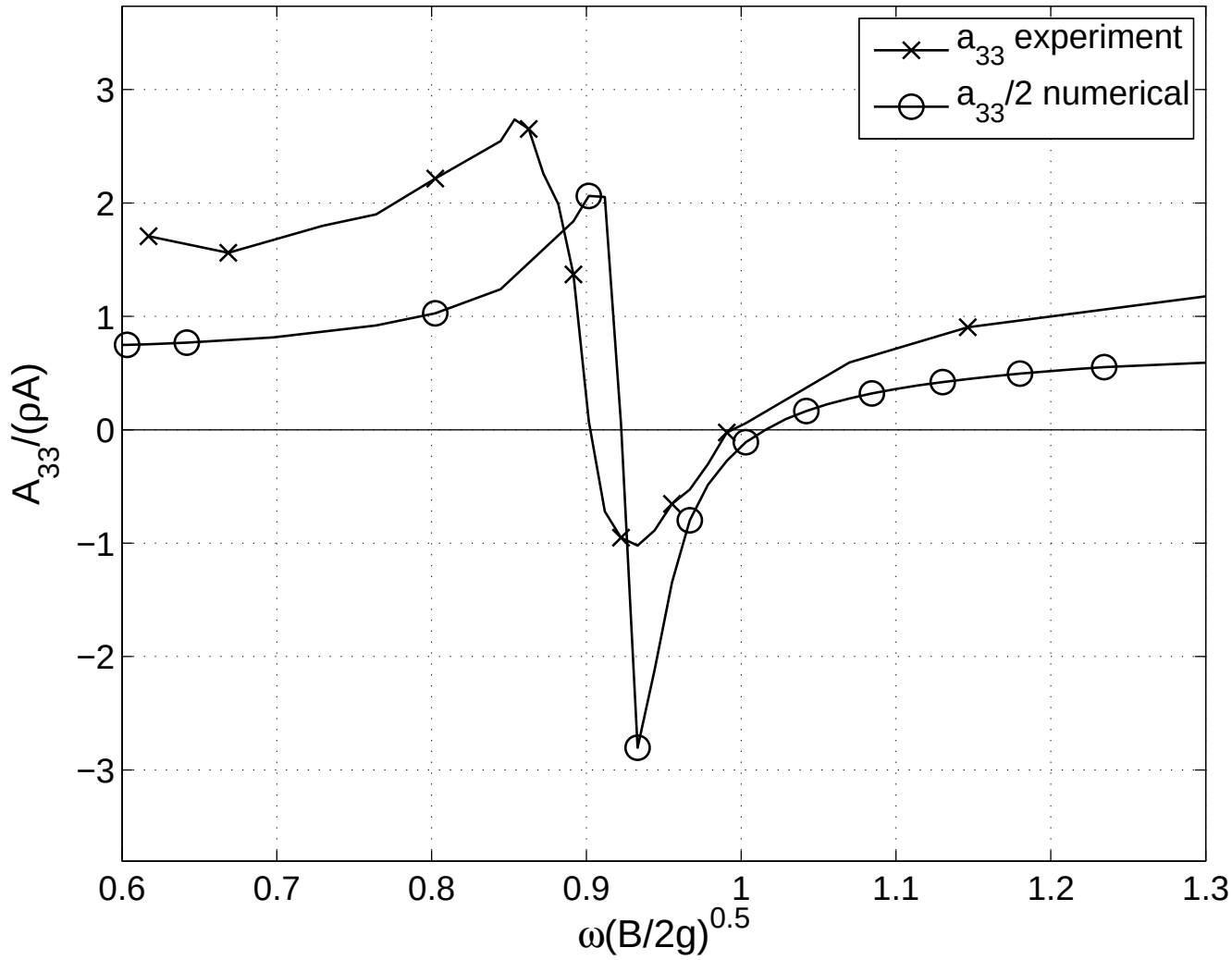

Figure 6.40: a_{33}, $b = 0.08\ m$.

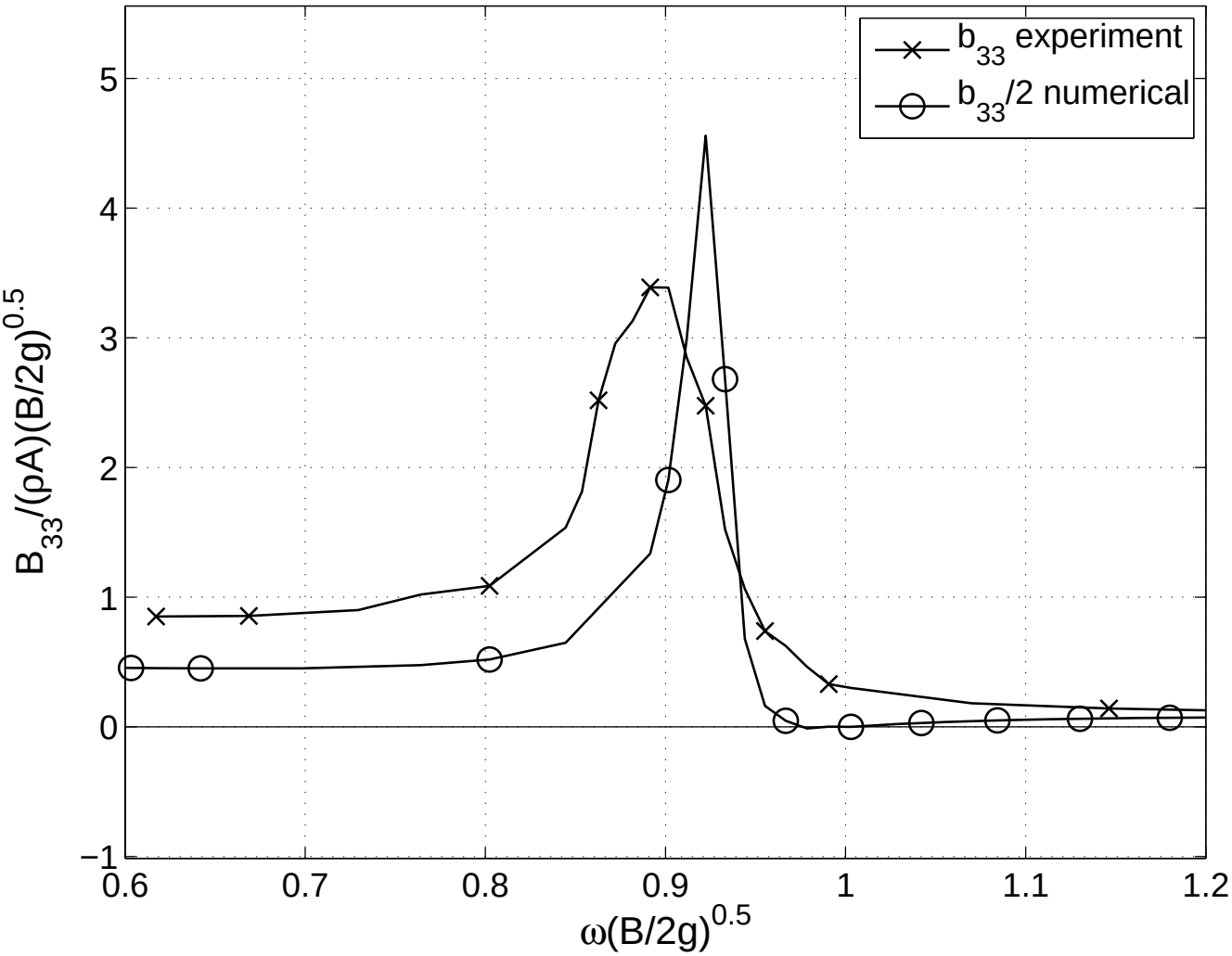

Figure 6.41: b_{33}, $b = 0.08\ m$.

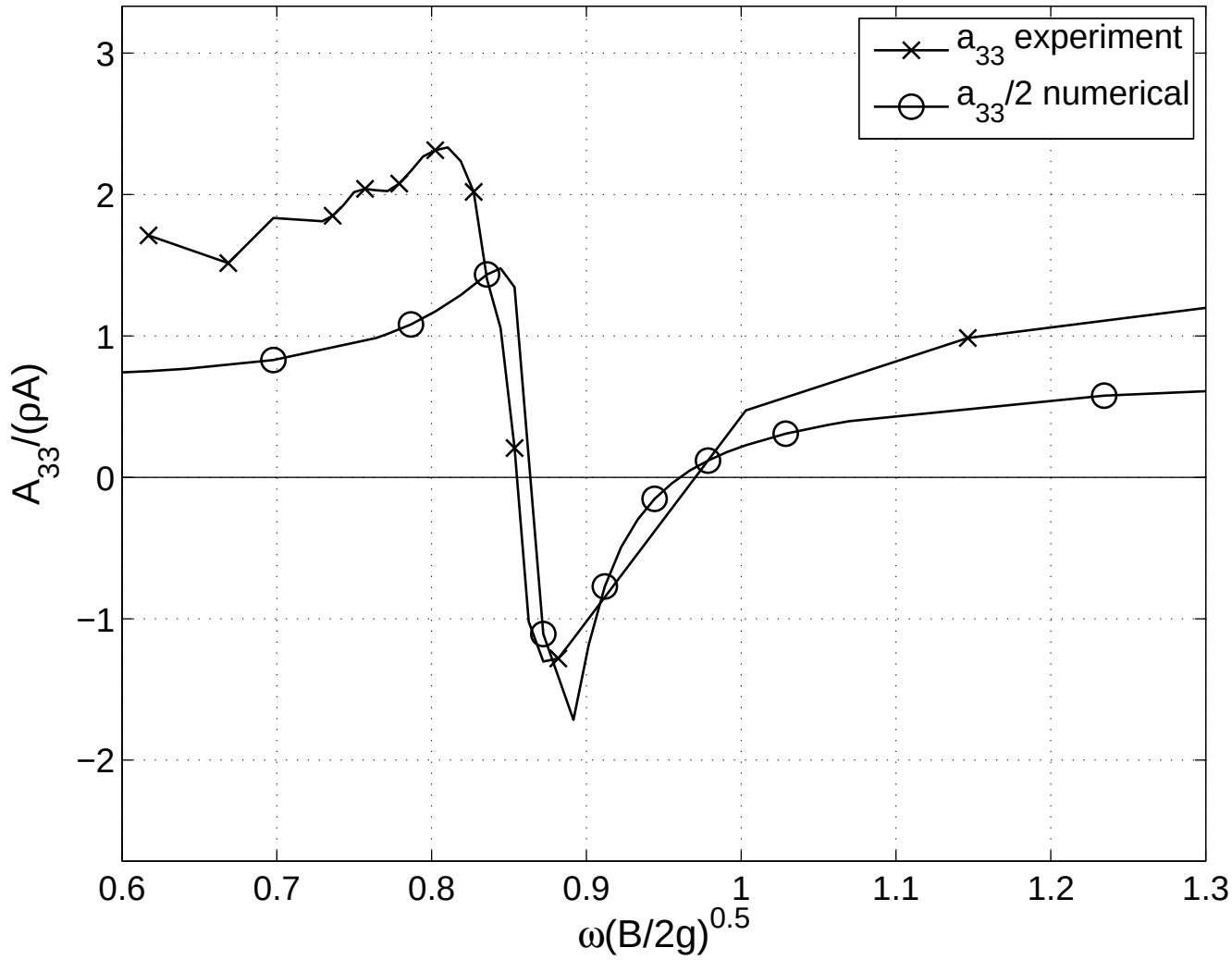

Figure 6.42: a_{33}, $b = 0.10\ m$.

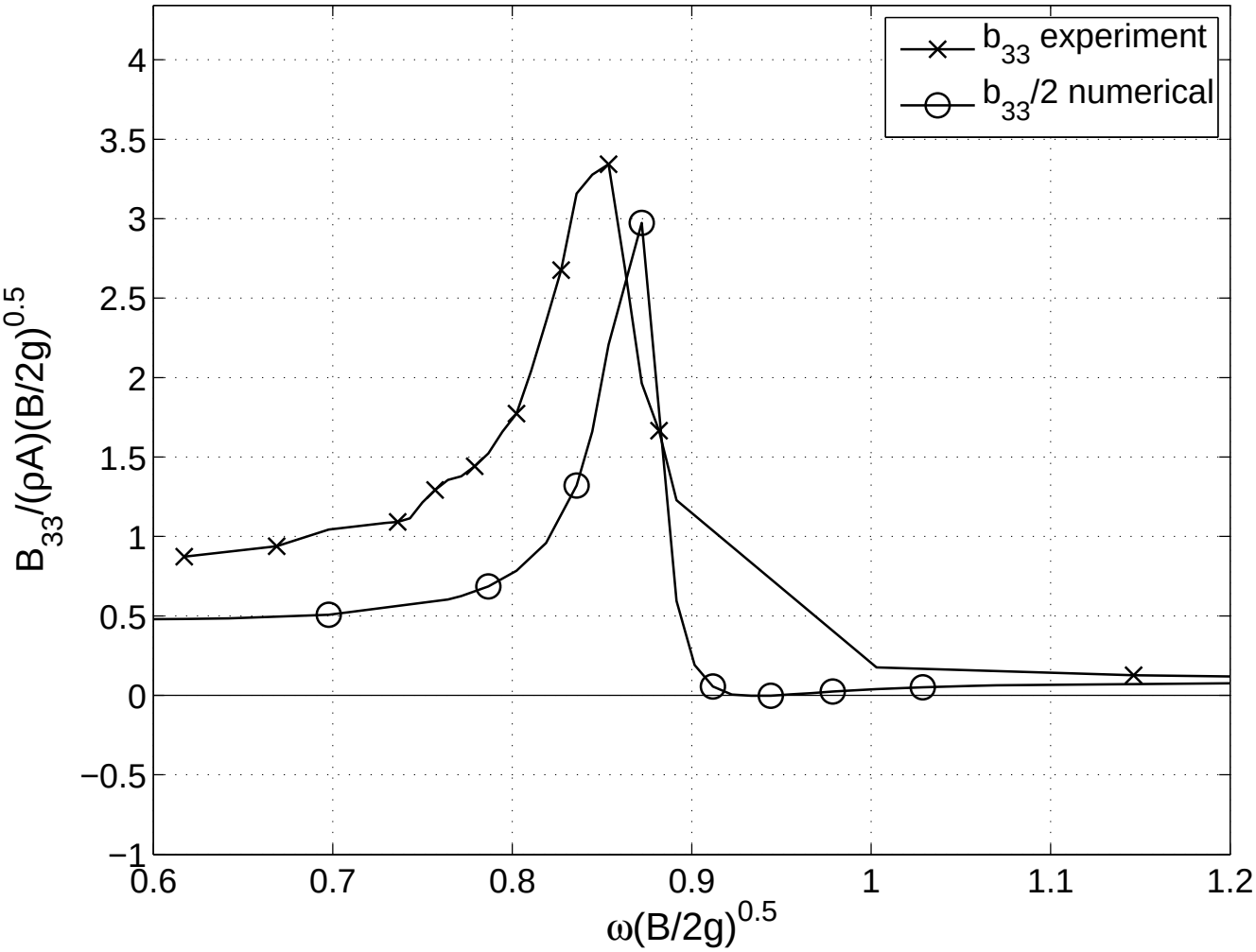

Figure 6.43: b_{33}, $b = 0.10\ m$.

Chapter 7

Experiments versus numerical modeling

In the results presented in chapter 6 it is observed discrepancies between the numerical and experimental results for the cases where ice is present. For the open water case the numerical and experimental results correlate well. The latter shows that the calculation routines to find added mass and damping are valid. In addition results from Ir. Vugts, [22], report on on hydrodynamic coefficients for swaying, heaving and rolling cylinders in a free surface was consulted for this purpose.

The drag coefficient have also been estimated for the open water case. The results shows large values for this coefficient. This is to be expected for small values of the *KC* number, this is shown in [2]. From the results it is seen that for the forcing amplitude of 5 *mm* the values for the drag coefficient gets smaller, this can be seen in connection with that the *KC* number is larger as the oscillation amplitude is larger.

The discrepancies that can be seen in the comparison plots in chapter 6 are at what frequency resonance occur in the experiments and numerical calculations and the hydrodynamic force i.e. the values of added mass and damping and the non-dimensional gap amplitudes. For the one ice-floe set up the difference of when the resonance frequency occurs is about 5% for $b = 0.04\ m$ and approximately 3% for $b = 0.10\ m$. For the symmetric set up with two ice-floes the difference is about 20% for $b = 0.01\ m$ and 6% for $b = 0.10\ m$.

Even though there are differences in the results both the numerical and experimental show the same trend. The results for when one and two ice-floes are present show an abrupt and steep

change in the added mass occur close to and at resonance frequency where added mass change sign. As the ice-floes are moved away from the ship section it was found that the resonance occur at a lower frequency. The added mass shows a tendency to show smaller maximum value as the ship-ice gap gets wider.

This is an interesting observation. If one think intuitively of how the added mass would be from the ships pint of view it is to be expected to find that it would be at its highest when the ship-ice gap b is smallest. The latter would be expected because the ship would have to accelerate more mass to communicate with the outer flow i.e. more water is needed to be pushed by the ship to make a wave outside the ice-floes. From this reasoning, a further investigation to check if this is correct would be favorable. If the result do not come from experimental and numerical artefacts it might be triggered by that the piston-mode motion introduce an increased communication with the external flow.

Another importent comment is that in the results there is a significant difference in the damping from radiated waves. They should have been more equal, this discrepancy might caused by a mistake from the author when performing the calculations or from wrong measurements during the experiments.

In appendix A the experimental results are presented. From those results it is observed that the smallest forcing amplitudes gives the largest added mass and largest damping. This is believed to be caused by viscous effects.

7.1 Physics versus linear theory

To be able to achieve results that are somewhat comparable between the linear numerical simulations and the model tests the ice-floes were modeled as stiff rigid bodies with a significant draught and freeboard. This provides an environment that is expected to provoke less non-linearities for the water to oscillate in. The intention with giving the draught and freeboard. In linear theory effects of green water (water on deck) nor dry spots under the ice is taken into account. For this reason the height of the ice flow at the gap had to be built up to twice the total height as the rise of the water column was found to move above the ice freeboard of 4 cm. The modified ice can

be seen in figure 7.1c.

While doing the model tests non-linearities was observed, especially near and at resonance frequency of the ship-ice system. A series of snapshots from the high speed camera is shown in figure 7.1, the snapshots are from resonance frequency with two ice-floes with a gap of $b = 0.04$ *m* and a forcing amplitude of 5 *mm*. From this a series of non-linearities are revealed. The most dramatic is that the water level actually becomes so low that a part of the ice becomes clear of the water column. As the water is rising again, air is trapped and as the water is rising beyond the bottom of the ice, air bubbles is escaping and disturbs the free surface. When the water has a vertical velocity upwards and hits the ice flow it also gets an horizontal velocity towards the ship model where it is then ricochet back towards the ice and crashes. The latter gives an appearance of a sloshing mode. In addition when the water column is moving upwards it is disturbed by vortex shedding from the ship model itself but especially the sharp corner of the ice-floe. The effect of flow separation is also discussed in chapter 2.4.

An illustration of the difference between the physical model and the linear numerical model is seen in figure 7.1a and 7.1c. In linear theory inviscid fluid is assumed, meaning that there is no effect of vorticity, trapped air, boundary layers and there is of course no water oscillating between the model and the tank wall and the gap between the ice and the wall, hence it is more simplified and ideal. All these effects increase the damping in the physical system. From the results it can be seen that the frequency where resonance occur change significantly the closer the ice floes are to the ship section.

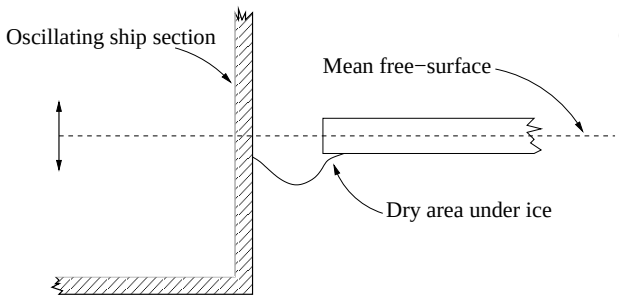

(a) Illustration of physical model.

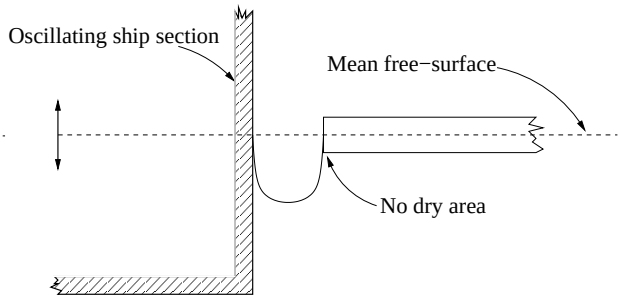

(b) Illustration of numerical model.

(c) Picture of the divinycell plate with doubled height.

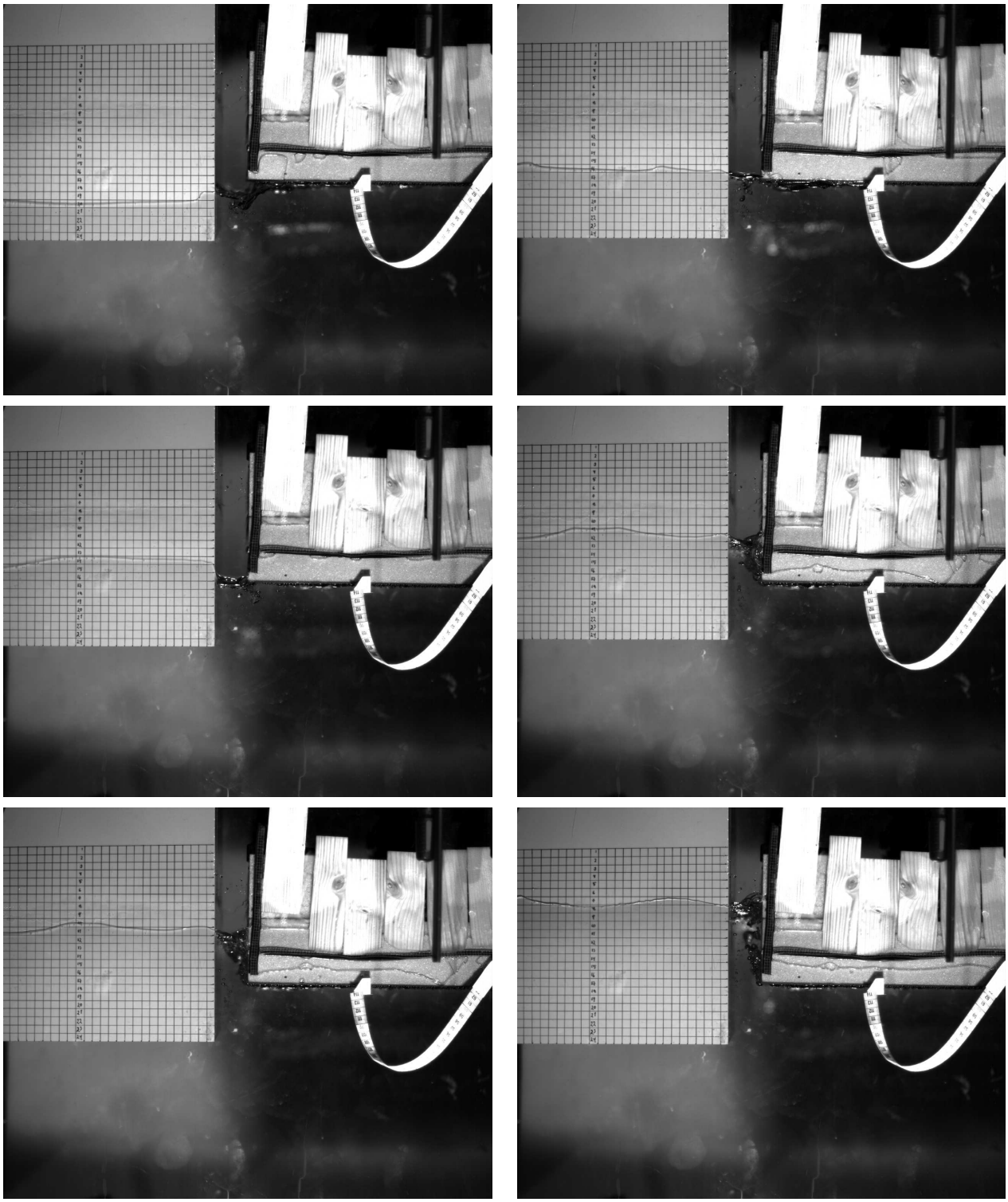

Figure 7.1: Resonance with two ice-floes and $b = 0.04\ m$. Top: (left) Water at lowest point, (right) water level is rising and air trapped under ice . Middle: (left) Water level with ice again, (right) water risen above ice bottom and ricochet off the ship model while air bubbles escape. Bottom: (left) The free surface is disturbed by air bubbles and vortices, (right) water hits the wall of the ice again with disturbed free surface.

Chapter 8

Conclusion

In the study performed in this master thesis the hydrodynamic interaction between an oscillating two dimensional ship section and ice have been investigated with emphasis on the hydrodynamic coefficients. The study includes numerical calculations and model tests where added mass and damping in heave have been calculated using Matlab and compared.

The work have been conducted with the assumption that theory related to piston-mode problems is valid and hence been treated thereafter. As a consequence literature related to such problems have been consulted to understand the physics.

Numerical tests of the geometric parameters have been performed to establish what relationships that will be dominating. It was found that the gap breadth b and ship beam B ratio, b/B, is the dominating factor with respect to change in resonance period and added mass.

The calculation routines to find added mass and damping based on measured force have been validated with open water tests and qualitative comparison from Ir. Vugts' results published in [22]. The open water experiments correlate well with the numerical calculations.

In both the experimental and numerical study of the ship-ice problem the results showed same tendencies but discrepancies were discovered. The discrepancies are believed to be mainly due to linear theory being applied in the numerical wave tank. The nonlinearities considered to give a significant effect being mainly vortex shedding and the effect of air being trapped beneath the ice floe. In addition the physical modeling of the ice-floes gave room for water elevation between

the ice-floe and the glass wall in the tank. The tests showed that the measured force was sensitive for this behavior.

In the numerical results for the case with two ice-floes the maximum values for added mass it is seen that it becomes larger from $b = 0.01\ m$ before it becomes smaller after $b = 0.02\ m$. For the experiments with the same geometric set up the maximum values show a similar trend. The maximum values for added mass shows a growing trend from $b = 0.01\ m$ and peaks at $b = 0.08\ m$ and get a smaller value for $b = 0.10\ m$. For the case with one ice-floe the same maximum values decrease a the ship section gets further away from the ice. In general the numerical program predicts a higher added mass and damping compared to the model tests when ice is present.

8.1 Suggestions for further work

Due to the discrepancies discovered between the model tests and the linear numerical simulations another approach can possible be taken to include nonlinearities. And also a study to further investigate if it is correct that the maximum values of the added mass should rise as the ice-floes gets further away from the ship section. In addition the damping from radiating waves should be checked for mistakes in the calculations and experiments.

The force gauge used in the experiments might be considered to be to robust and stiff relative to the measure forces. Another model of the ship section where it is hollow so it is possible to place weights inside can be constructed. A model with room for weights is possible to be floating at the correct draught instead of applying a pretension on the force gauge. In this case a softer force gauge can be used and that will be more sensitive and be able to measure the forces more correctly at lover oscillation frequencies. With a model floating freely with the correct draught it is possible to do free decay tests to estimate the sections natural frequency and estimate added mass at resonance.

During the model tests a water elevation between the ice-floes and the tank glass wall was observed. It was found that this effect influenced the measured hydrodynamic force and the frequency at when resonance occurred. Instead of using divynicell for the modeling of the ice-floes they could be constructed by stiffened aluminum plates with a rubber gasket on the sides to

prevent water elevation between the tank wall and ice structure. Also the effect of the ice darught can be further investigated. In connection with the water elevation on the side 3D effects in the model scale tests can be looked into.

Different ways of modeling the ice can be undertaken. In the present study the ice-floes have been modeled as stiff rigid bodies which are not allowed to move or bend in any degrees of freedom. Similar model tests could be performed in a wave flume with real model ice or use a backbone model with the correct scaled stiffness to achieve a more correct hydroelastic behavior. The ice can be anchored with springs or another adequate solution to keep it from drifting.

A less complicated way of modeling an elastic ice-floe could be to design it as an Euler beam. This could be done by clamping the end furthest away from the ship section and let the other end, close to the ship be free.

When considering what would be possible to model numerically the latter is possibly the most feasible to include in a code. With the beam approximation different bending modes can be allowed to contribute in the solution and in that way include various effects of hydroelaticity. The use of flexible modes in the free surface can also be a way to approach the problem.

List of Figures

List of Tables

Bibliography

[1] Jan V. Aarsnes and Sverre Steen. *Experimental Methods in Marine Technology*. Department of Marine Technology, 2008.

[2] Petter A. Berthelsen and Odd M. Faltinsen. A local directional ghost cell approach for incompressible viscous flow problems with irregular boundaries. *Journal of computational physics*, 227:4354–4397, 2008.

[3] Basile Bonnemaire, Trine Lundamo, Karl-U. Evers, Sveinung Løset, and Arnor Jensen. Model testing of the arctic tandem offloading terminal mooring ice ridge loads. In *19th IAHR International Symposium on Ice*. IAHR, July 2008.

[4] Basile Bonnemaire, Trine Lundamo, Karl-U. Evers, Sveinung Løset, and Arnor Jensen. Model testing of the arctic tandem offloading terminal mooring ice ridge loads. In *19th IAHR International Symposium on Ice*. IAHR, July 2008.

[5] Basile Bonnemaire, Trine Lundamo, Arnor Jensen, and Karl-H. Rupp. Subsurface ice interactions under a moored offloading icebreaker. In *19th IAHR International Symposium on Ice*. IAHR, July 2008.

[6] Oddgeir Dalane, Vegard Aksnes, Sveinung Løset, and Jan V. Aarsnes. A moored arctic floater in first-year sea ice ridges. In *Proceedings of the ASME 28th International Conference on Ocean, Offshore and Arctic Enginering*. OMAE, June 2009.

[7] Oddgeir Dalane, Ove T. Gudmestad, Sveinung Løset, Jørgen Amdahl, Tor E. Hilden, and Knut H. Fjell. Ice tank testing of a surface buoy for arctic conditions. In *Proceedings of the ASME 27th International Conference on Offshore Mechanics and Arctic Enginering*. OMAE, June 2008.

[8] Odd M. Faltinsen. *Sea Loads on Ships and Offshore Structures*. Cambridge University Press, 1990.

[9] Odd M. Faltinsen, Olav F. Rognebakke, and Alexander N. Timokha. Two-dimensional resonant piston-like sloshing in a moonpool. *Journal of Fluid Mechanics*, 575:359–397, 2007.

[10] Odd M. Faltinsen and Bjørn Sortland. Slow drift eddy making damping of a ship. *Applied Ocean Research*, 9:37–46, 1987.

[11] Odd M. Faltinsen and Alexander N. Timokha. *Sloshing*. Cambridge University Press, 2009.

[12] Susan Frankenstein, Sveinung Løset, and Hayley H. Shen. Wave-ice interactions in barents sea marginal ice zone. *Journal of cold regions engineering*, 15:91–102, 2001.

[13] Arnt G. Fredriksen. Ship motion in exposed harbors. Master's thesis, Norwegian University of Science and Technology, 2008.

[14] Edmond H. Hansen and Sveinung Løset. Modelling floating offshore units moored in broken ice: comparing simulations with ice tank tests. *Cold Regions Science and Technology*, 29:107–119, 1999.

[15] Arnor Jensen, Sveinung Løset, Ove T. Gudmestad, Ola Ravndal, and Svein Inge Eide. Model testing of an arctic shuttle barge system for loading of oil in ice, March 2001.

[16] Trygve Kristiansen. *Two-Dimensional Numerical and Experimental Studies of Piston-mode Resonance*. PhD thesis, Norwegian University of Science and Technology, April 2009.

[17] Trygve Kristiansen and Odd M. Faltinsen. Studies on resonant water motion between a ship and a fixed terminal in shallow water. *Journal of Offshore Mechanics and Arctic Enginnering*, 131:11 pages, 2009.

[18] Sveinung Løset, Arnor Jensen, Ove T. Gudmestad, Ola Ravndal, and Svein I. Eide. Model testing of an arctic shuttle barge system for loading of oil in ice. In *11^{th} International Offshore and Polar Engineering Conference*. ISOPE, June 2008.

[19] Trine Lundamo, Basile Bonnemaire, Arnor Jensen, and Ove T. Gudmestad. Back-calculation of the ice load applying on a moored vessel. In *19^{th} IAHR International Symposium on Ice*. IAHR, 2008.

[20] P. McIver. Complex resonances in the water-wave problem for a floating structure. *Journal of Fluid Mechanics*, 536:423–443, 2005.

[21] B. Molin. On the piston and sloshing modes in moonpools. *Journal of Fluid Mechanics*, 430:27–50, 2001.

[22] J. M. Vugts. The hydrodynamic coefficients for swaying, heaving and rolling cylinders in a free surface, March 1968.

[23] B. Wright and Associates. Evaluation of full scale data for moored vessel stationkeeping in pack ice, March 1999.

Appendices

Appendix A

Experimental results

Open water tests

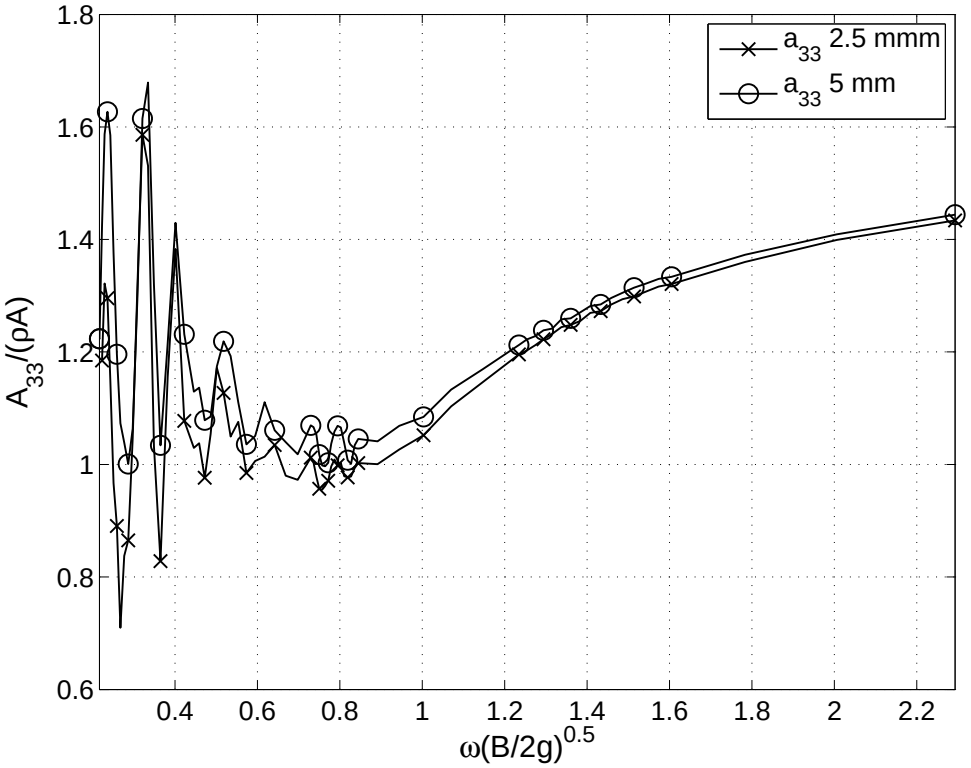

(a) Added mass a_{33}, forcing amplitude 2.5 and 5 *mm*.

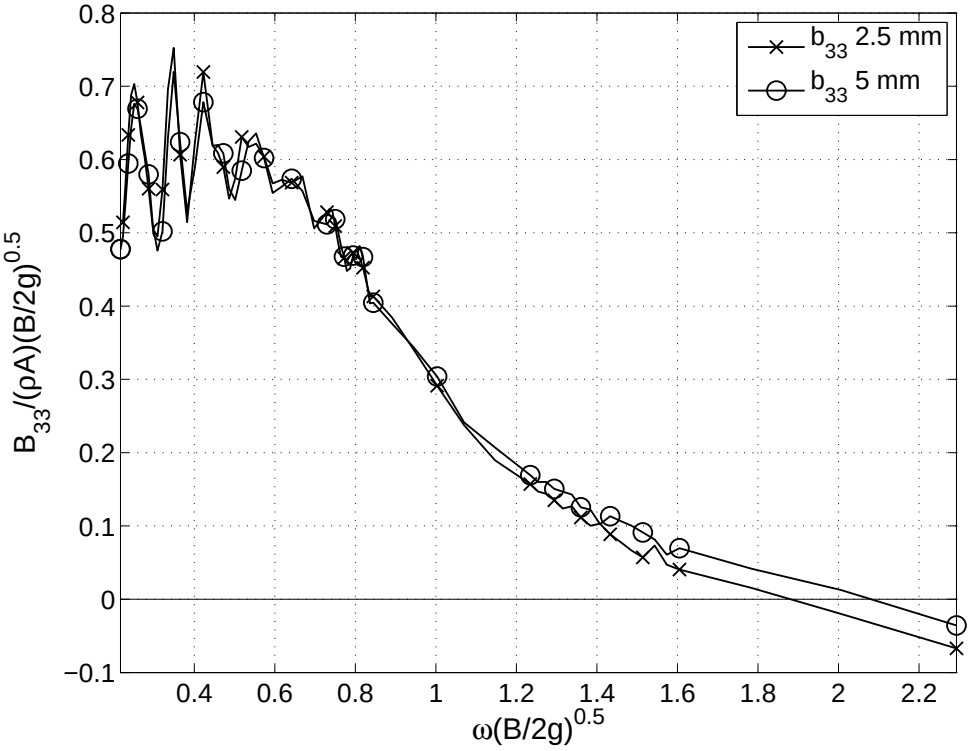

(b) Damping b_{33}, forcing amplitude 2.5 and 5 *mm*.

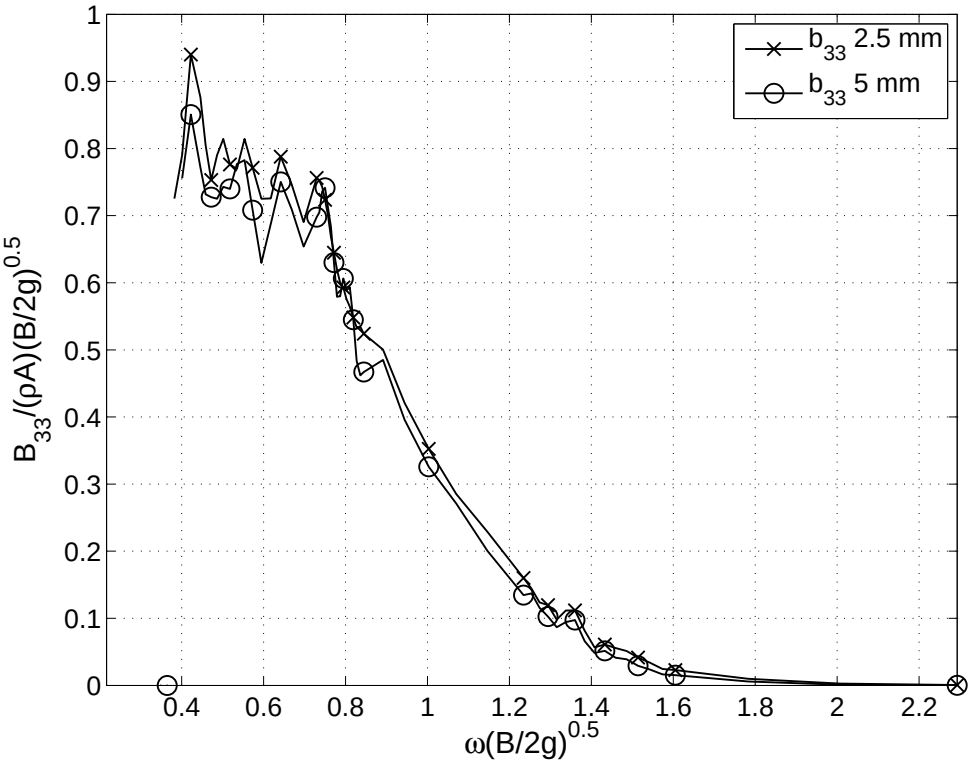

Figure A.1: Damping b_{33} from radiating waves.

Ship in the middle of two ice-floes

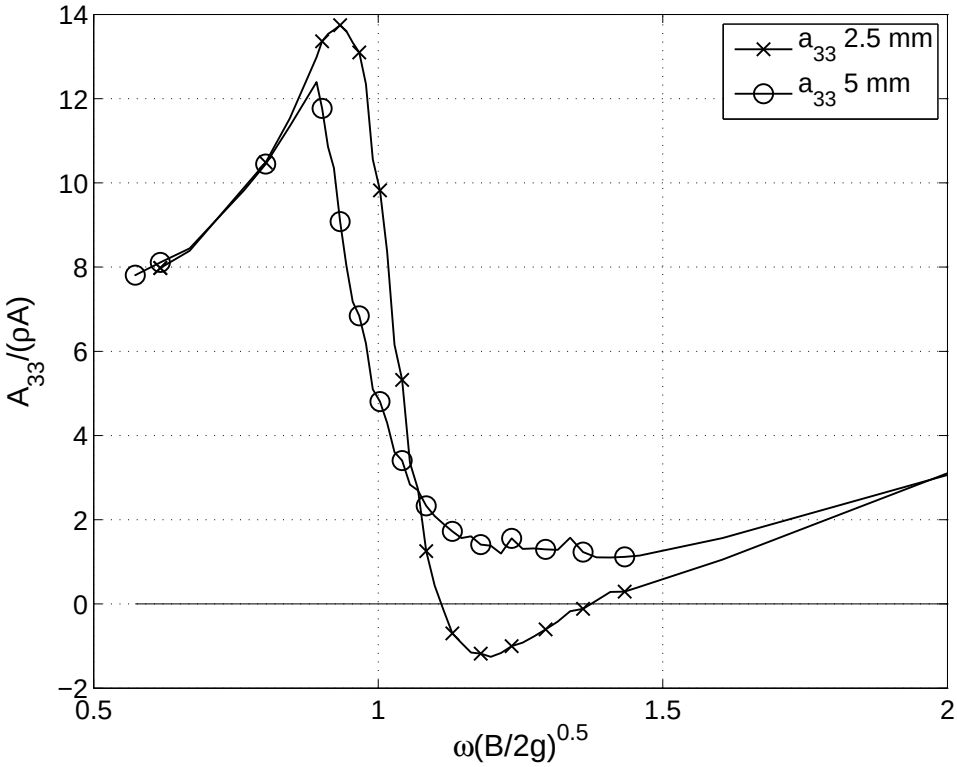

(a) Added mass a_{33}, $b = 0.01m$ forcing amplitude 2.5 and 5 *mm*.

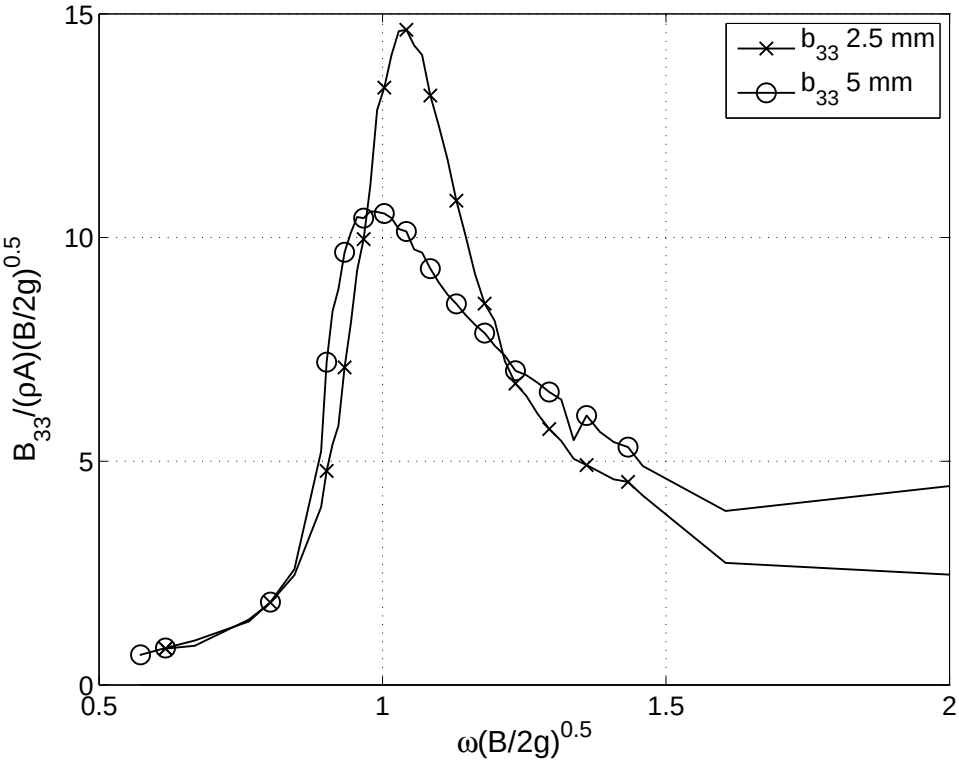

(b) Damping b_{33}, $b = 0.01$ forcing amplitude 2.5 and 5 *mm*.

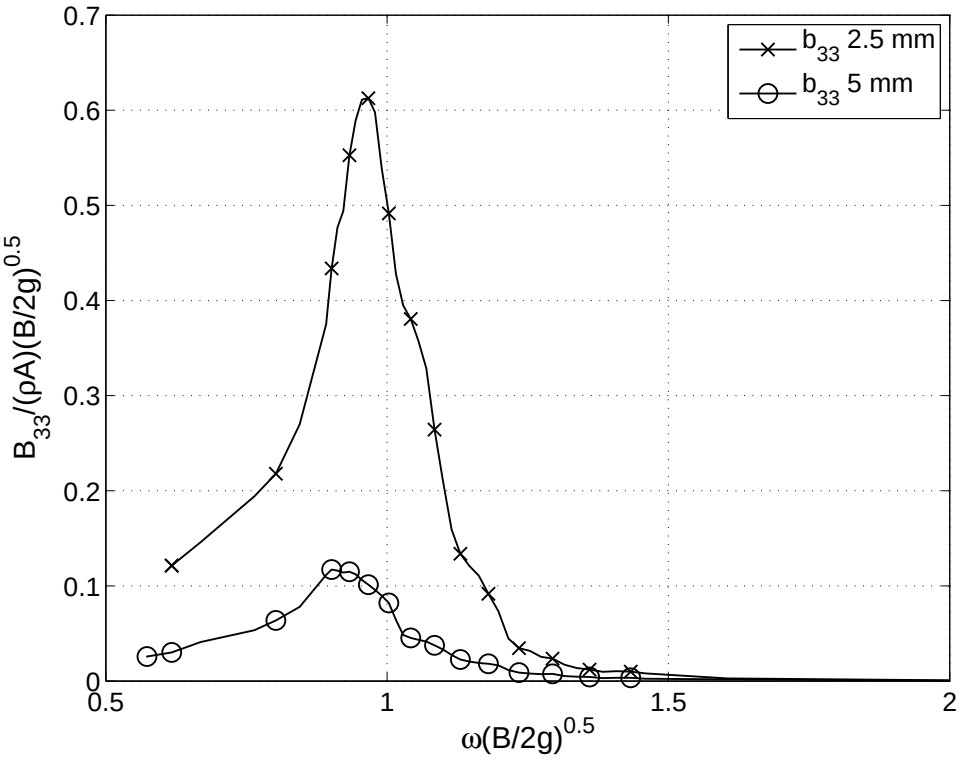

Figure A.2: Damping b_{33},radiating waves, $b = 0.01\ m$.

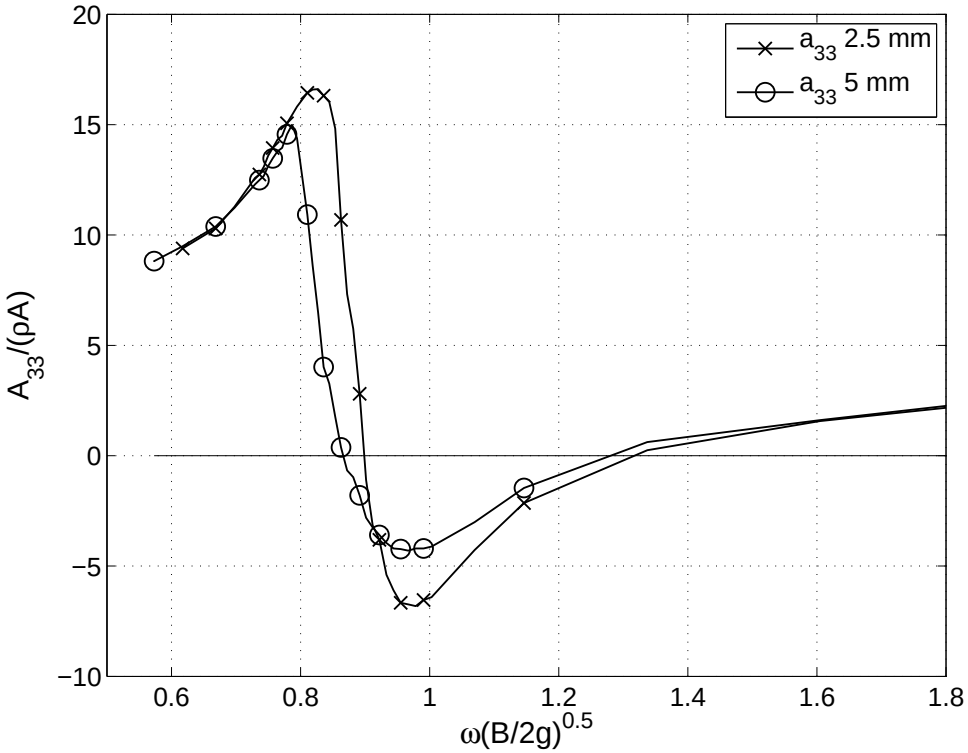

(a) Added mass a_{33}, $b = 0.02m$ forcing amplitude 2.5 and 5 *mm*.

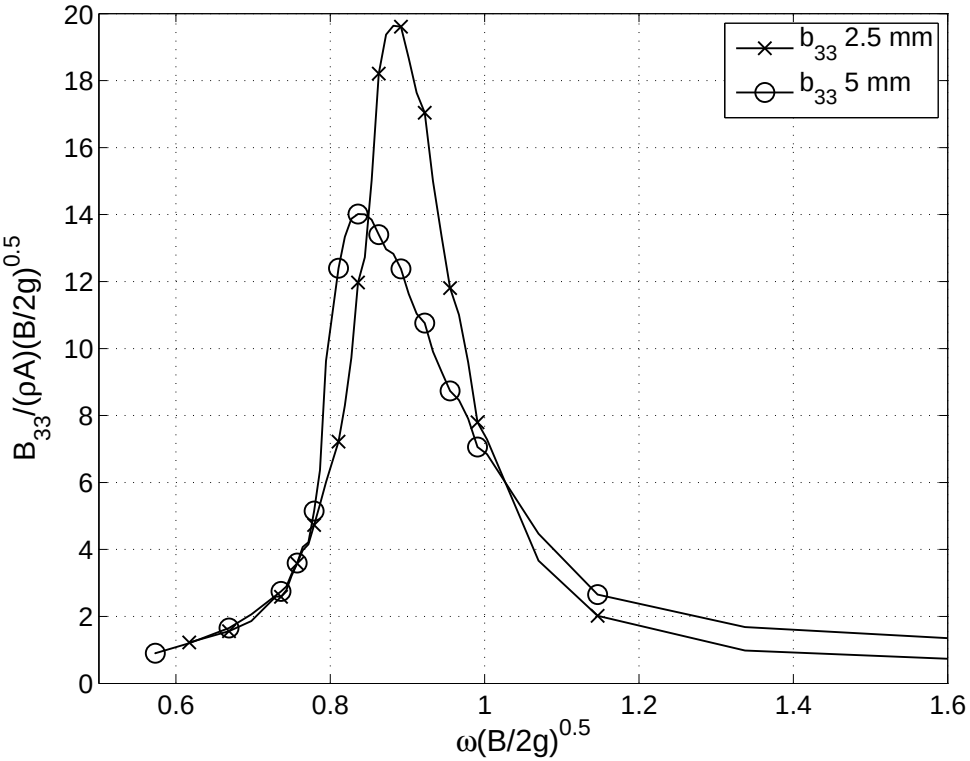

(b) Damping b_{33}, $b = 0.02$ forcing amplitude 2.5 and 5 *mm*.

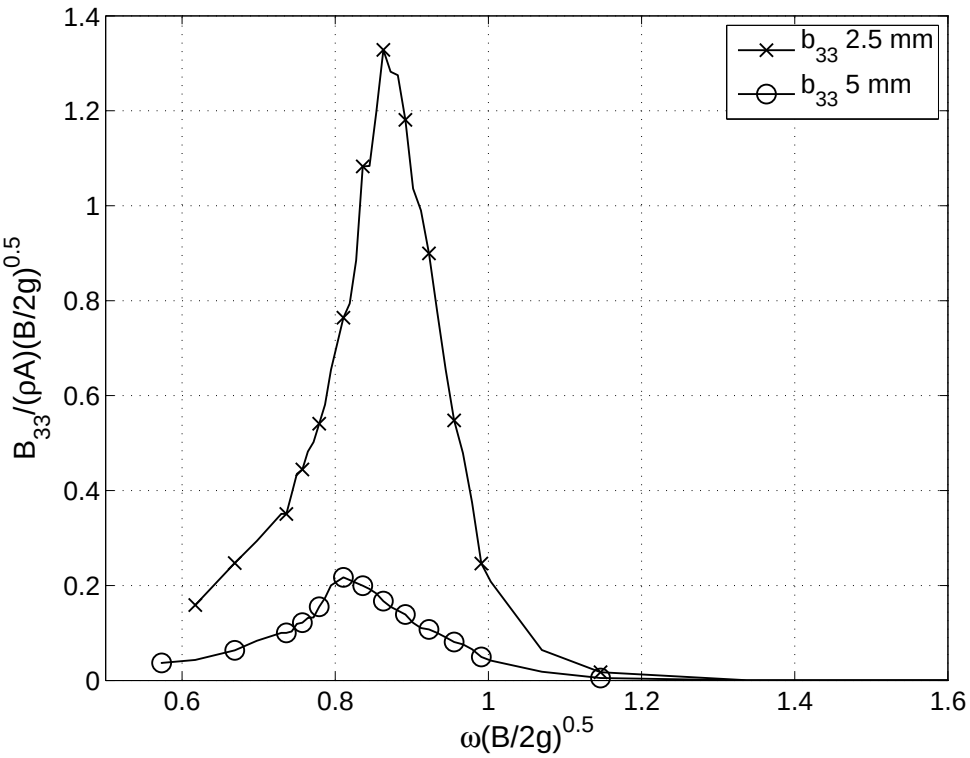

Figure A.3: Damping b_{33},radiating waves, $b = 0.02\ m$.

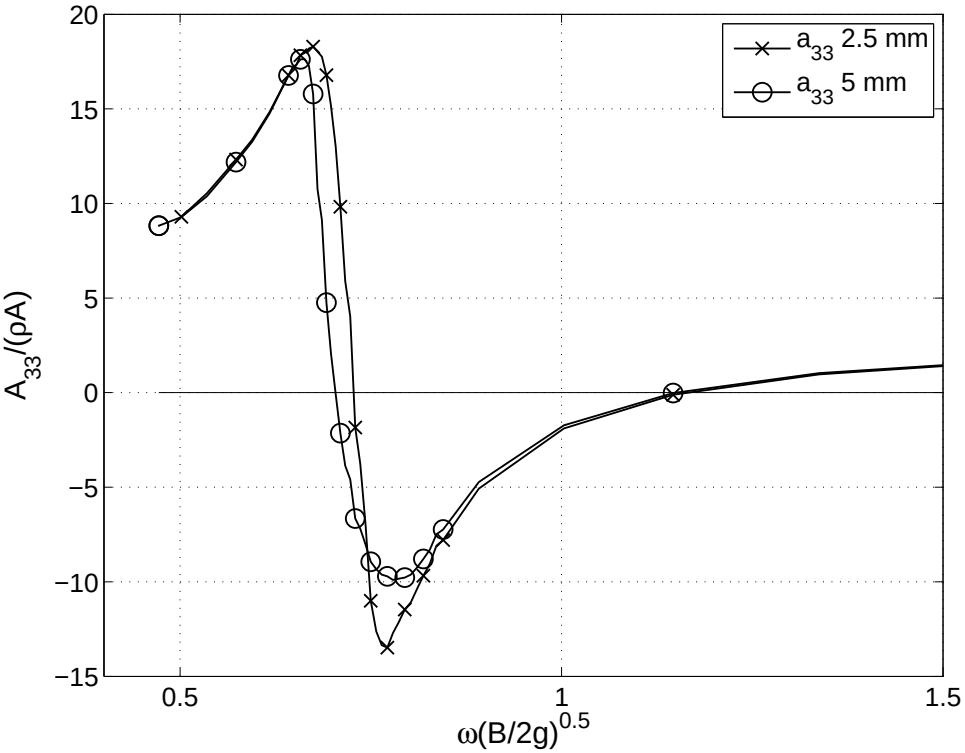

(a) Added mass a_{33}, $b = 0.04m$ forcing amplitude 2.5 and 5 *mm*.

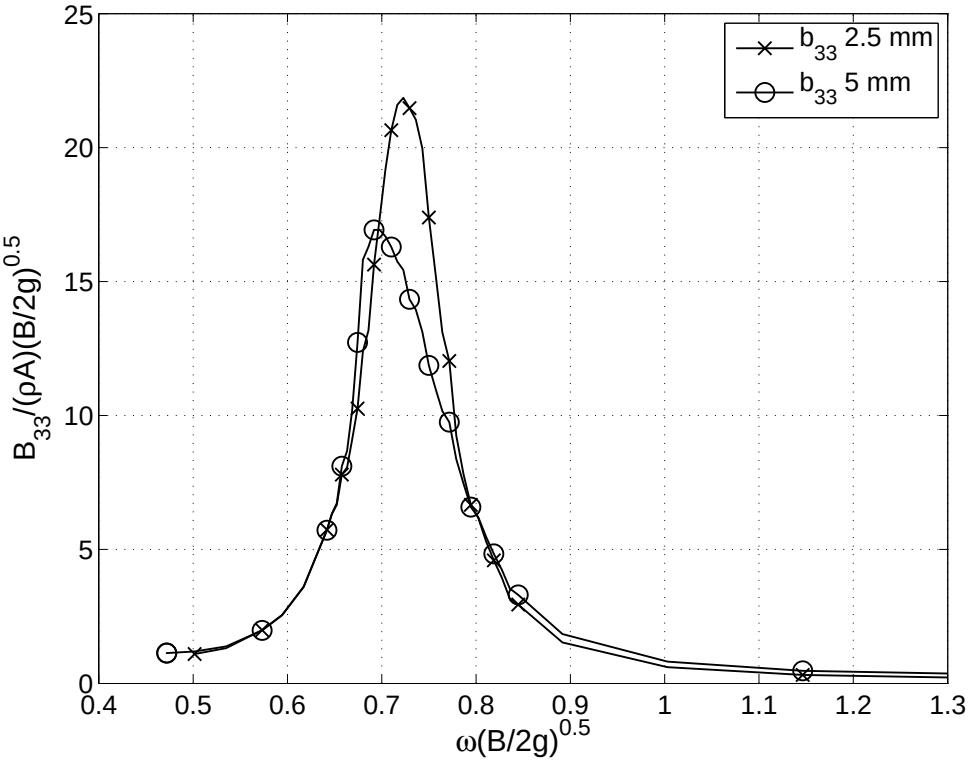

(b) Damping b_{33}, $b = 0.04$ forcing amplitude 2.5 and 5 *mm*.

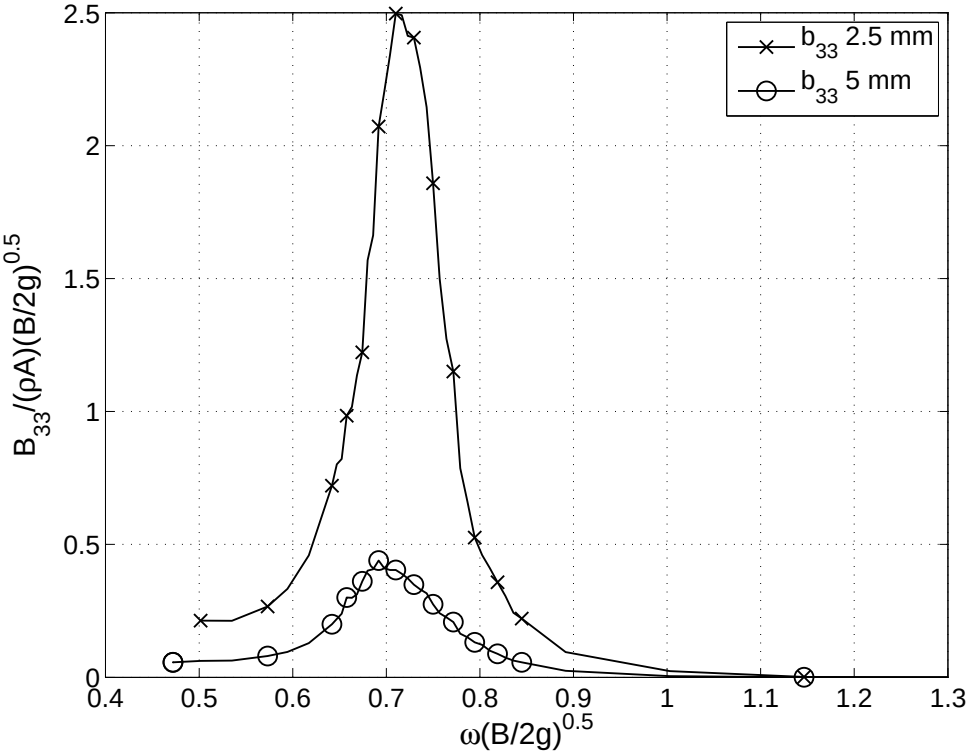

Figure A.4: Damping b_{33},radiating waves, $b = 0.04\ m$.

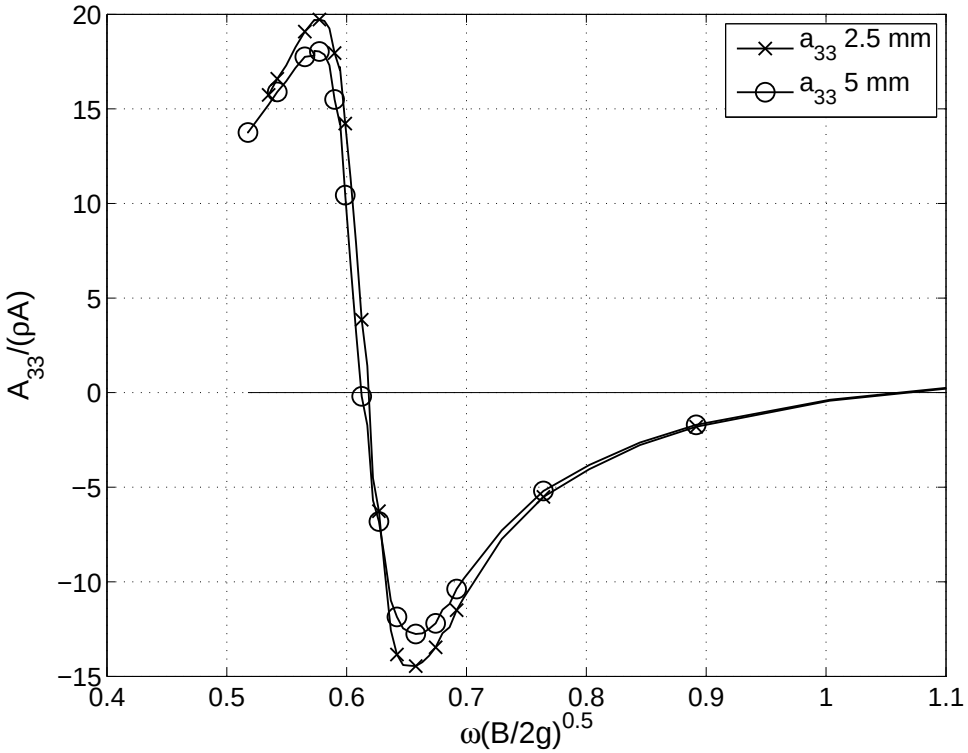

(a) Added mass a_{33}, $b = 0.06m$ forcing amplitude 2.5 and 5 *mm*.

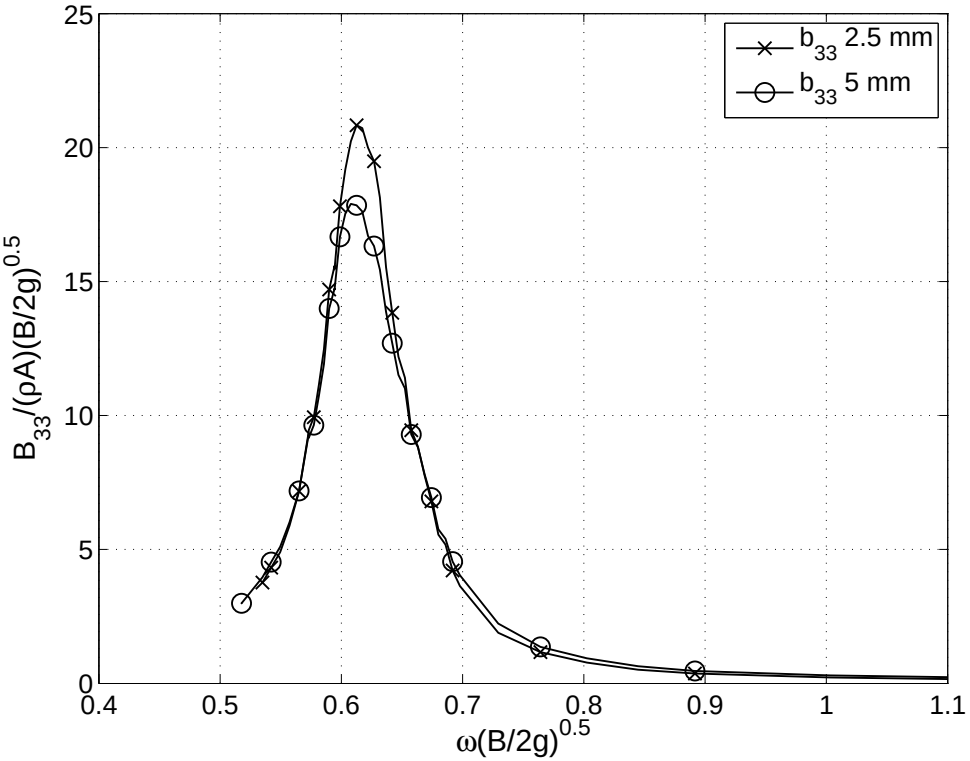

(b) Damping b_{33}, $b = 0.06$ forcing amplitude 2.5 and 5 *mm*.

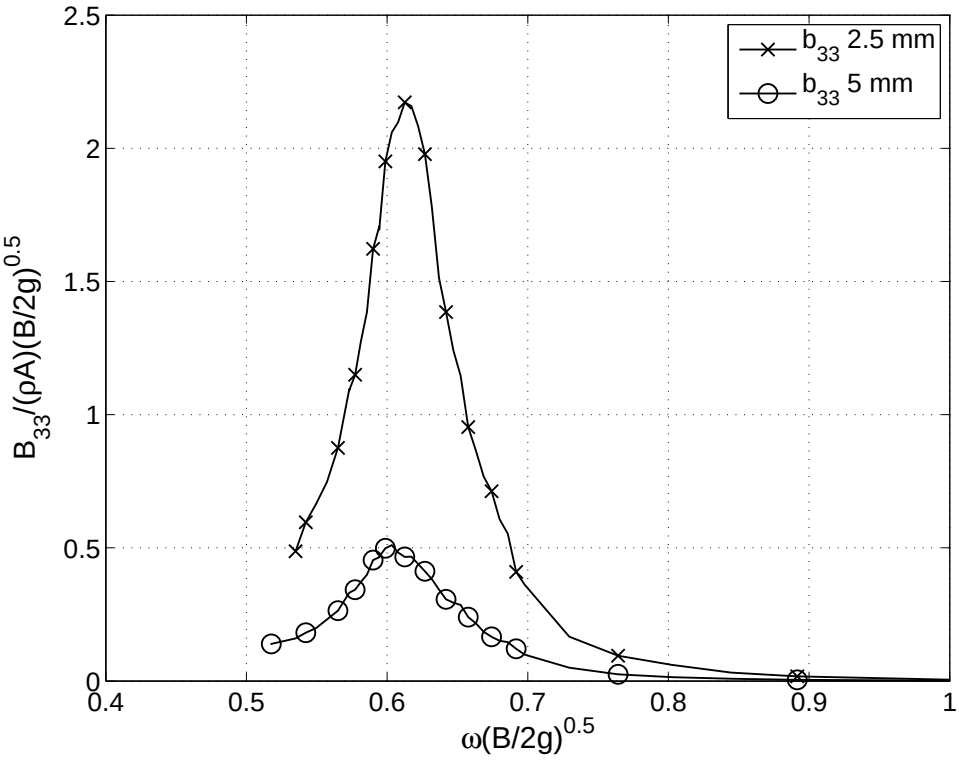

Figure A.5: Damping b_{33},radiating waves, $b = 0.06\ m$.

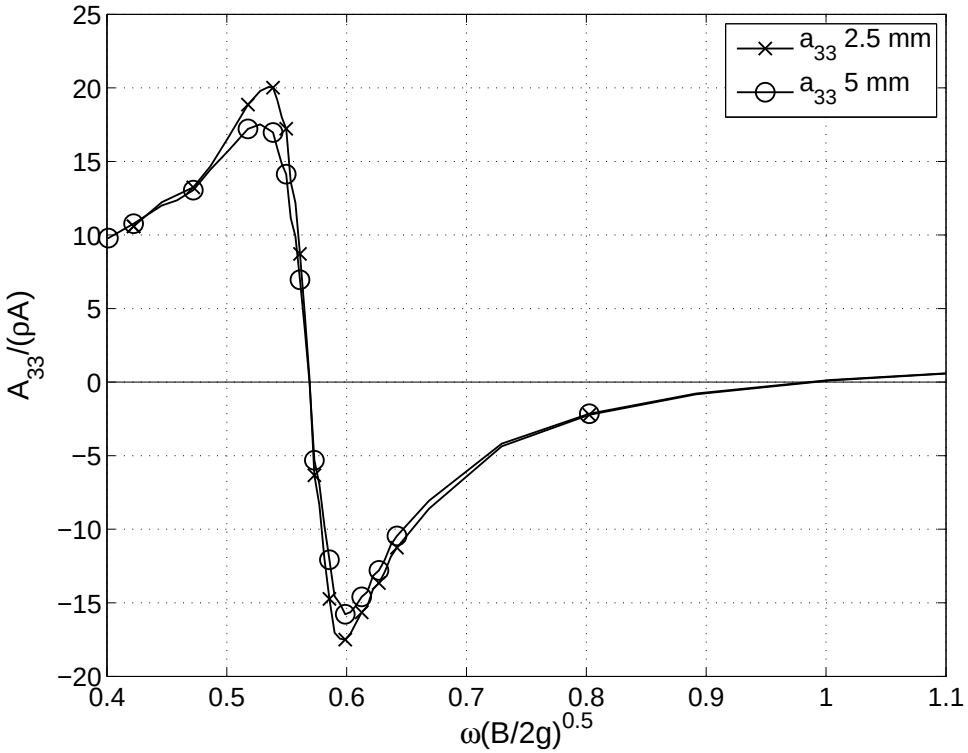

(a) Added mass a_{33}, $b = 0.08m$ forcing amplitude 2.5 and 5 *mm*.

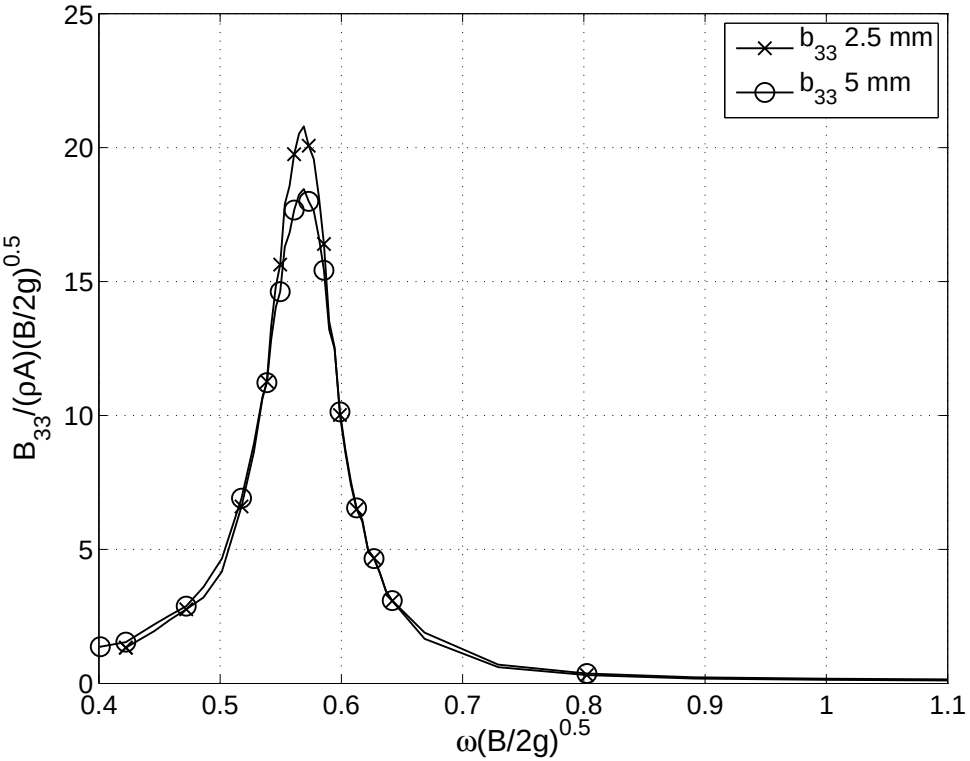

(b) Damping b_{33}, $b = 0.08$ forcing amplitude 2.5 and 5 *mm*.

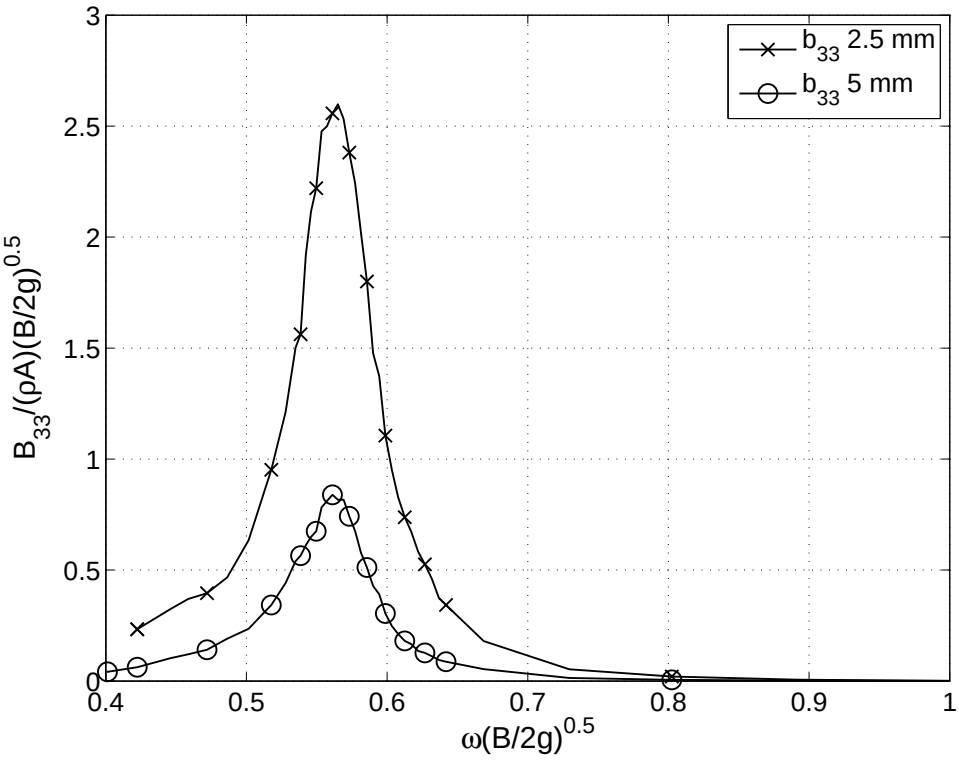

Figure A.6: Damping b_{33},radiating waves, $b = 0.08\ m$.

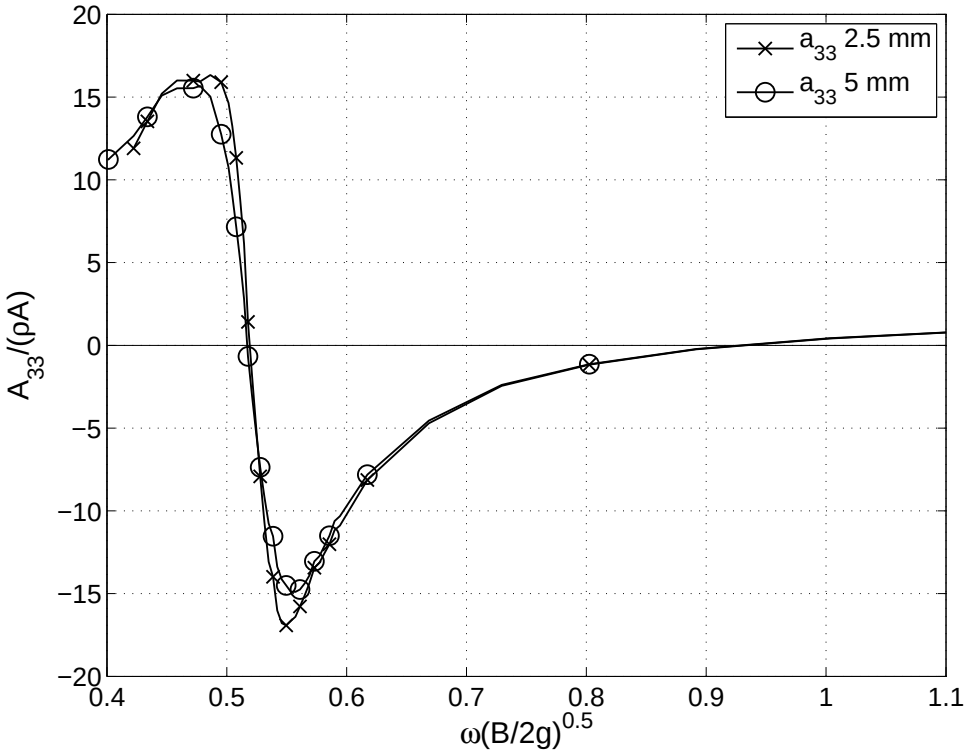

(a) Added mass a_{33}, $b = 0.10m$ forcing amplitude 2.5 and 5 *mm*.

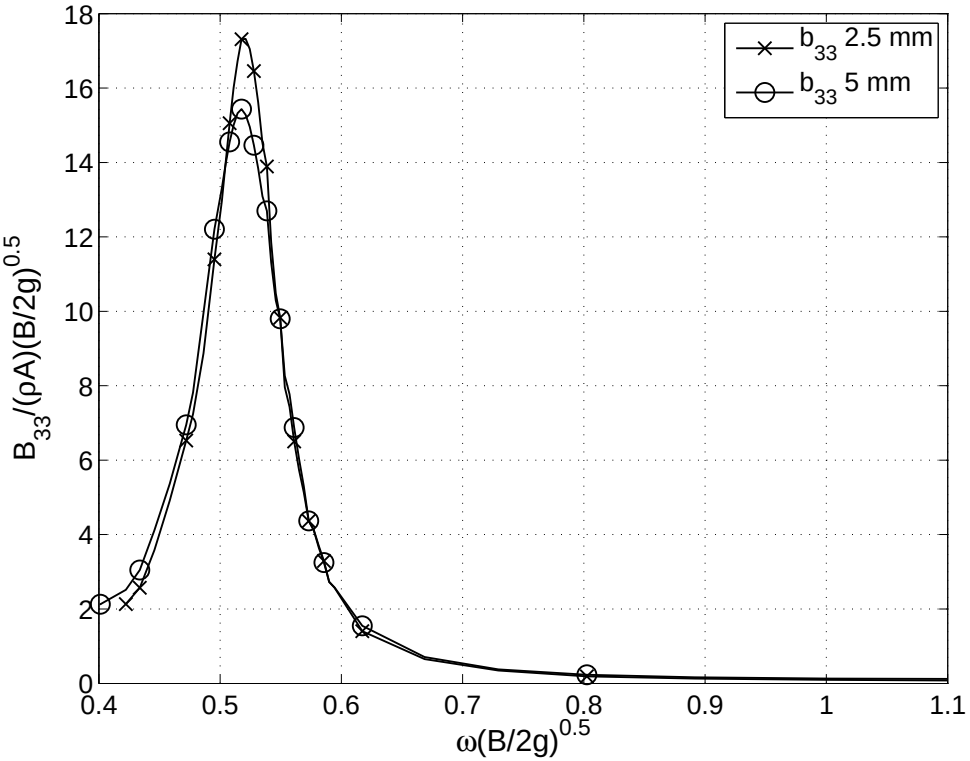

(b) Damping b_{33}, $b = 0.10$ forcing amplitude 2.5 and 5 *mm*.

Tests with one ice-floe

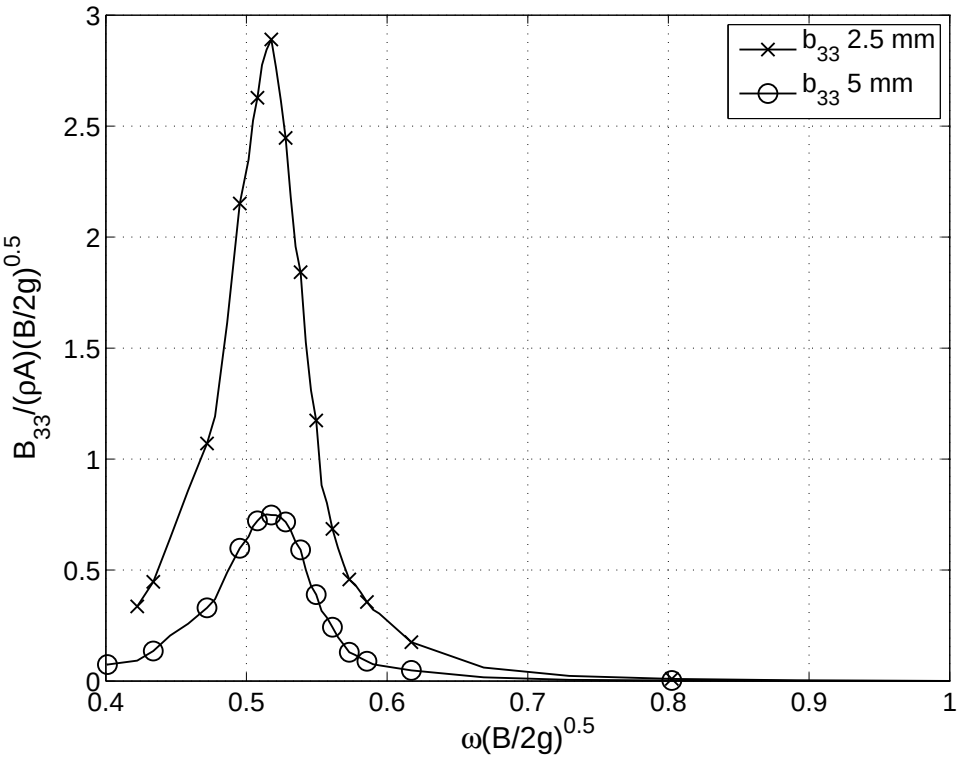

Figure A.7: Damping b_{33},radiating waves, $b = 0.10\ m$.

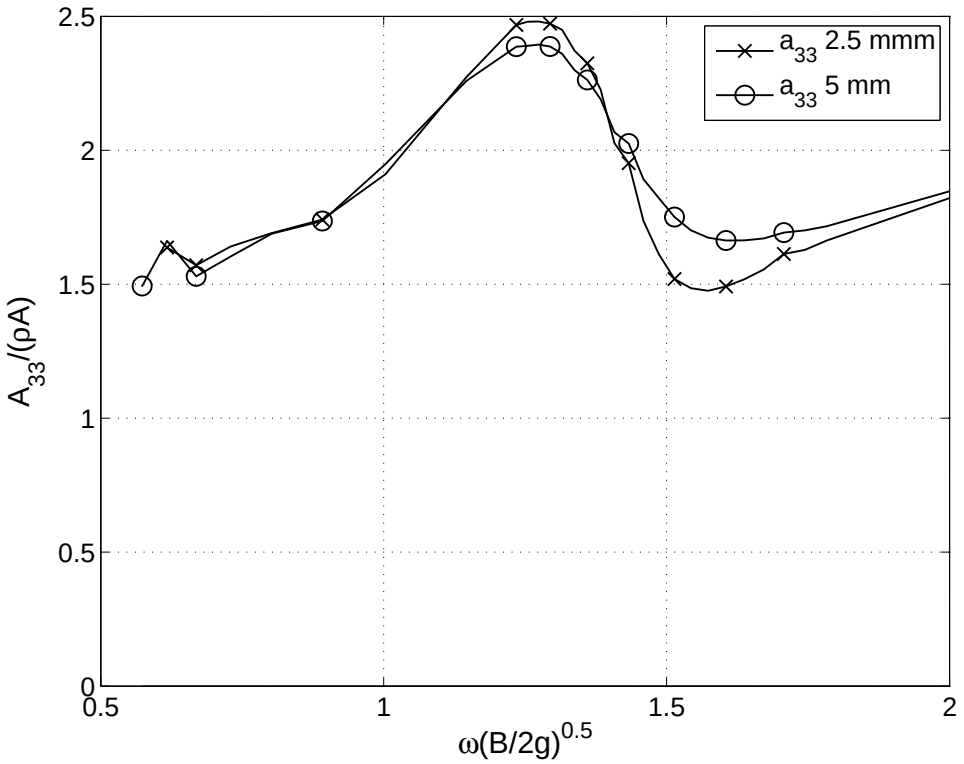

(a) Added mass a_{33}, $b = 0.01m$ forcing amplitude 2.5 and 5 *mm*.

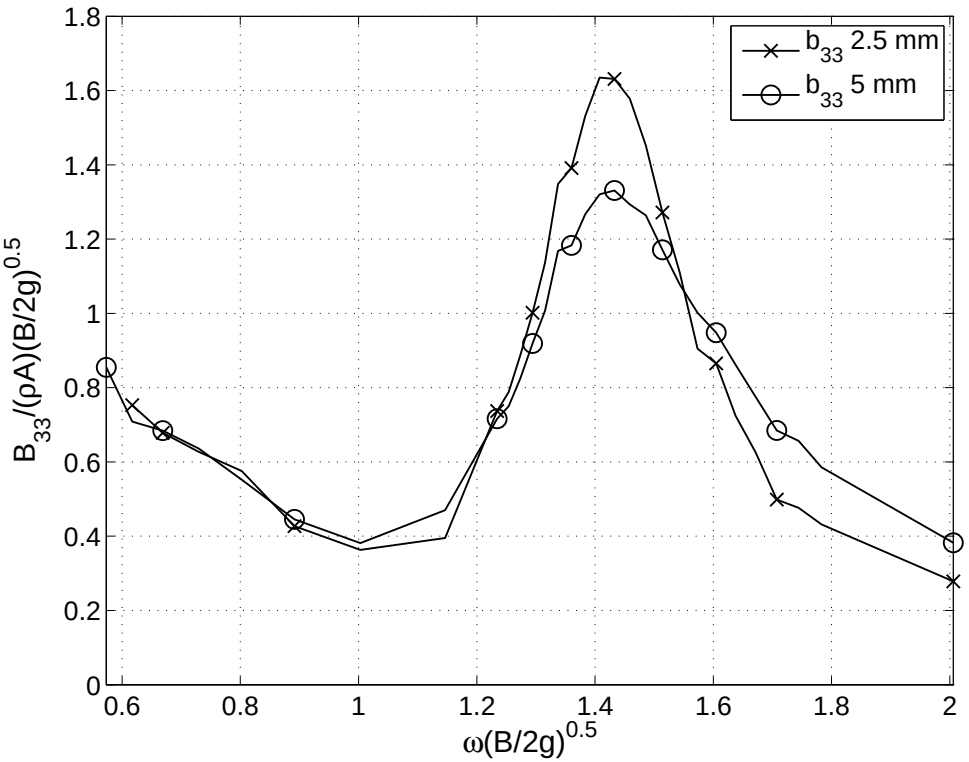

(b) Damping b_{33}, $b = 0.01$ forcing amplitude 2.5 and 5 *mm*.

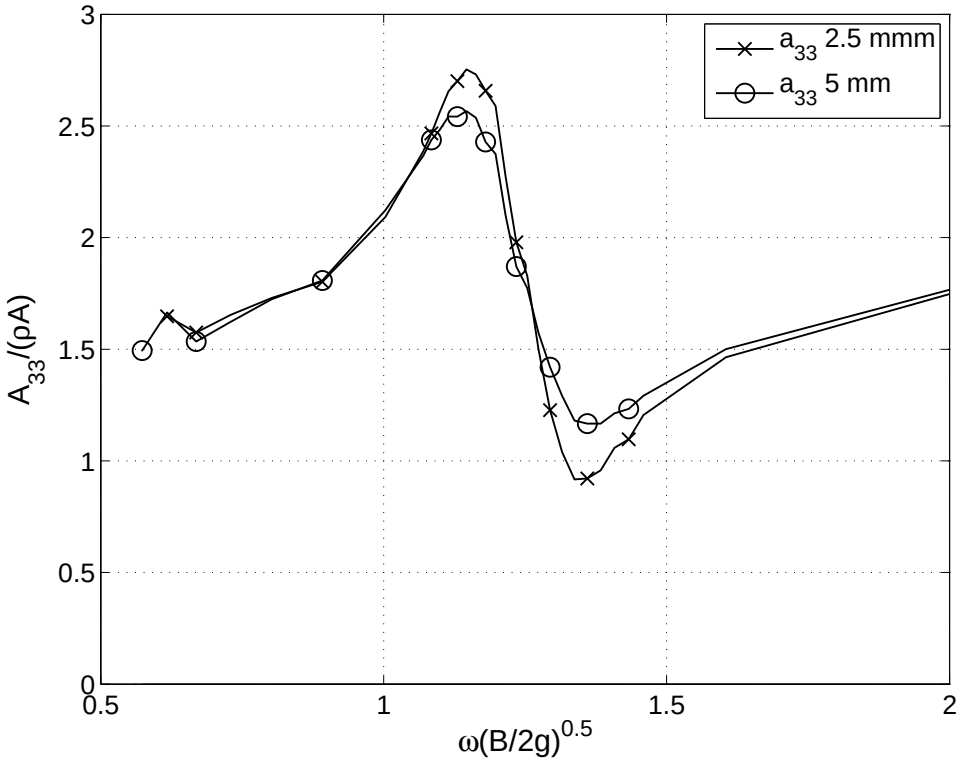

(a) Added mass a_{33}, $b = 0.02m$ forcing amplitude 2.5 and 5 *mm*.

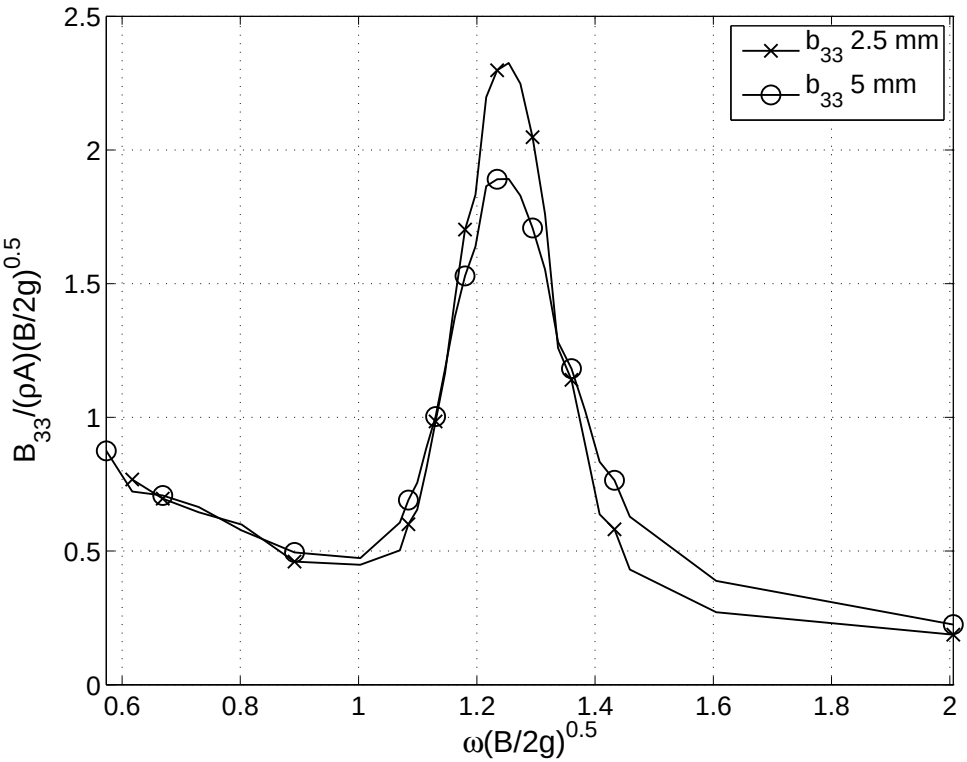

(b) Damping b_{33}, $b = 0.02$ forcing amplitude 2.5 and 5 *mm*.

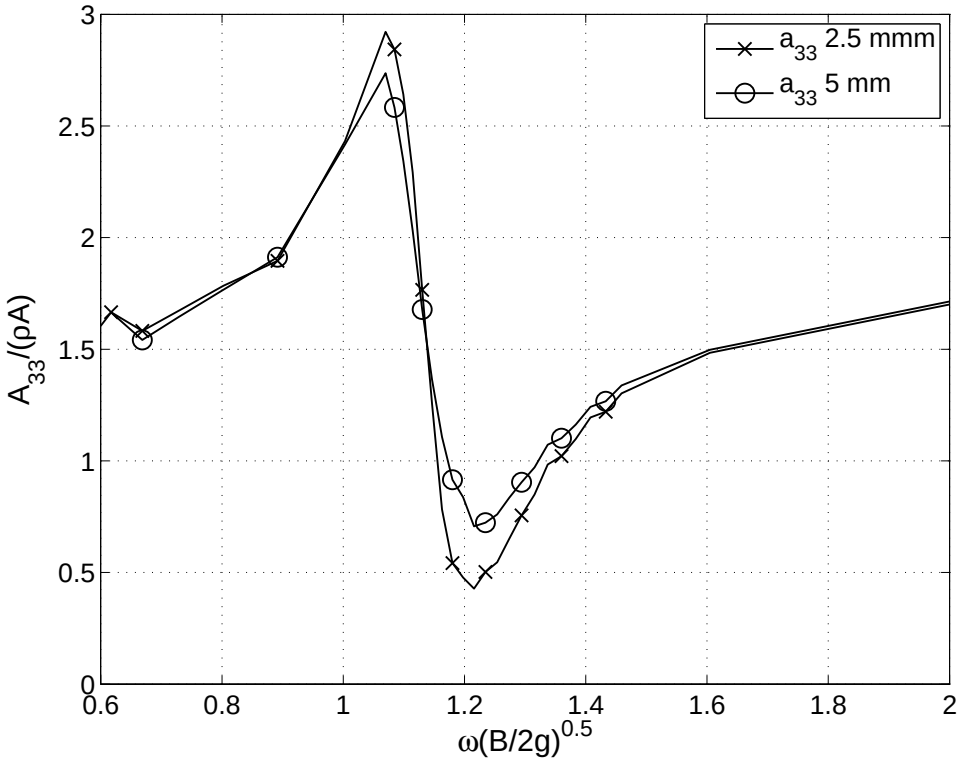

(a) Added mass a_{33}, $b = 0.03m$ forcing amplitude 2.5 and 5 *mm*.

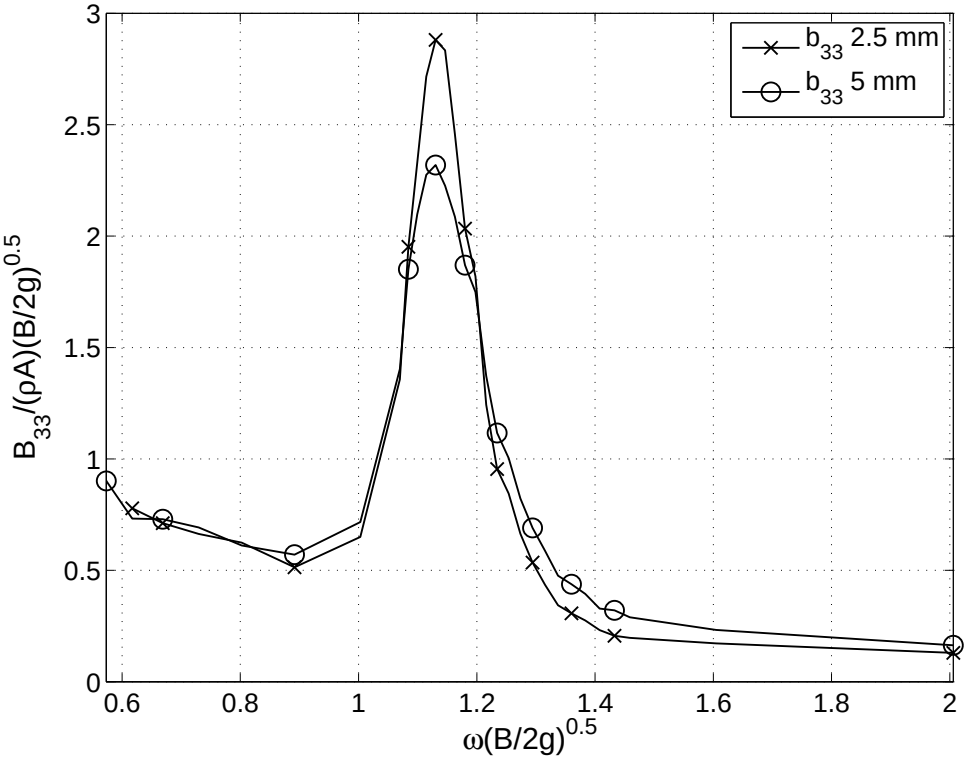

(b) Damping b_{33}, $b = 0.03$ forcing amplitude 2.5 and 5 *mm*.

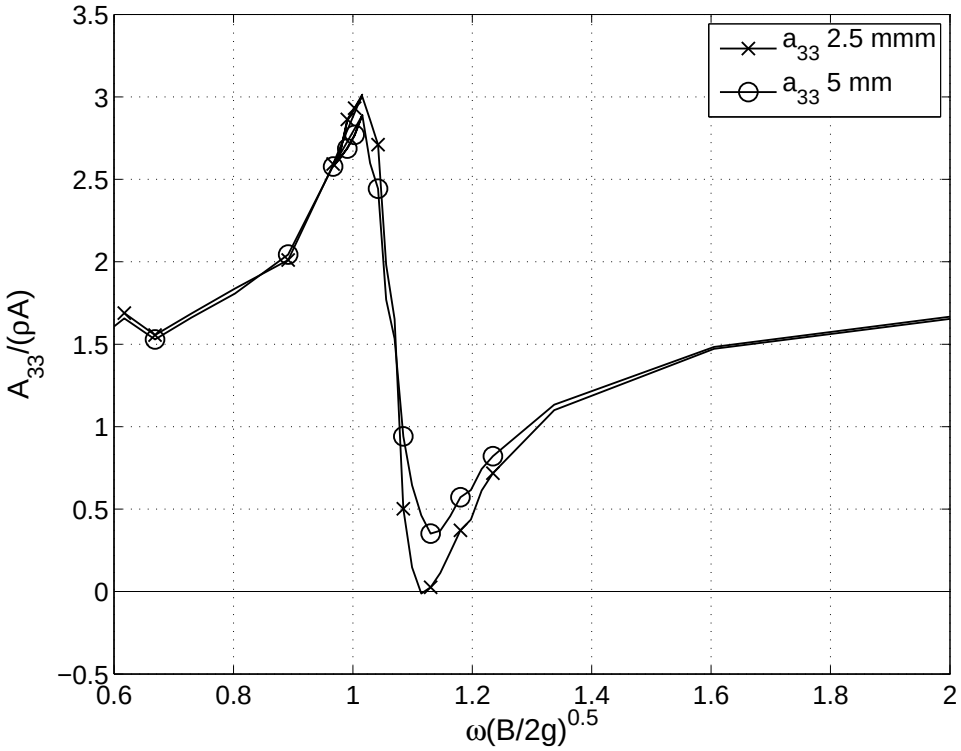

(a) Added mass a_{33}, $b = 0.04m$ forcing amplitude 2.5 and 5 *mm*.

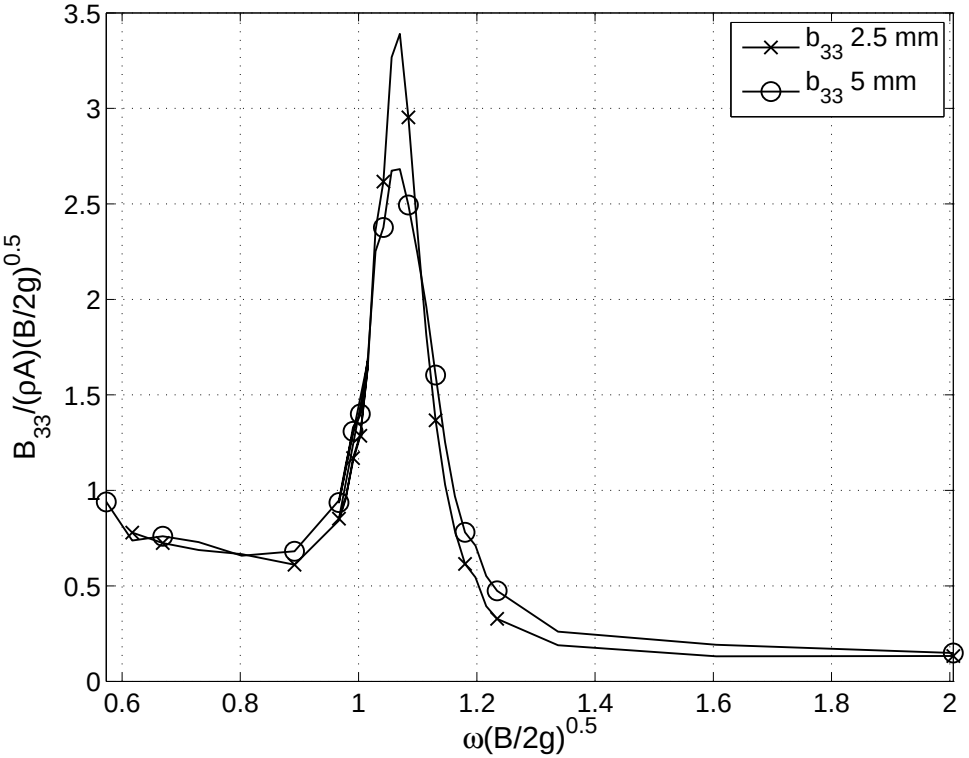

(b) Damping b_{33}, $b = 0.04$ forcing amplitude 2.5 and 5 *mm*.

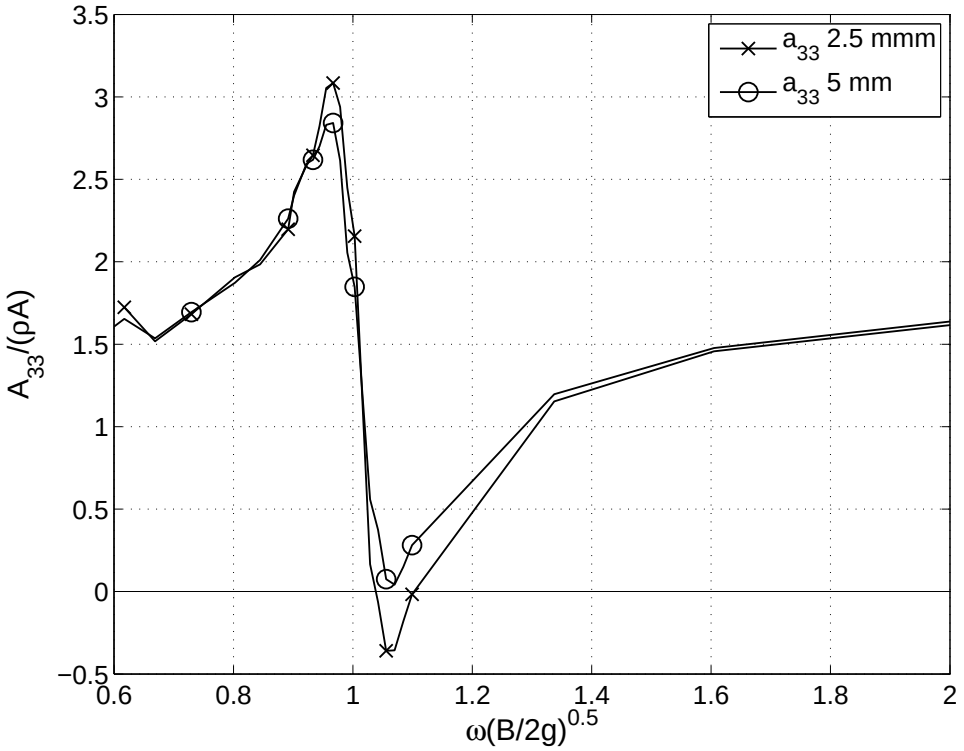

(a) Added mass a_{33}, $b = 0.05m$ forcing amplitude 2.5 and 5 *mm*.

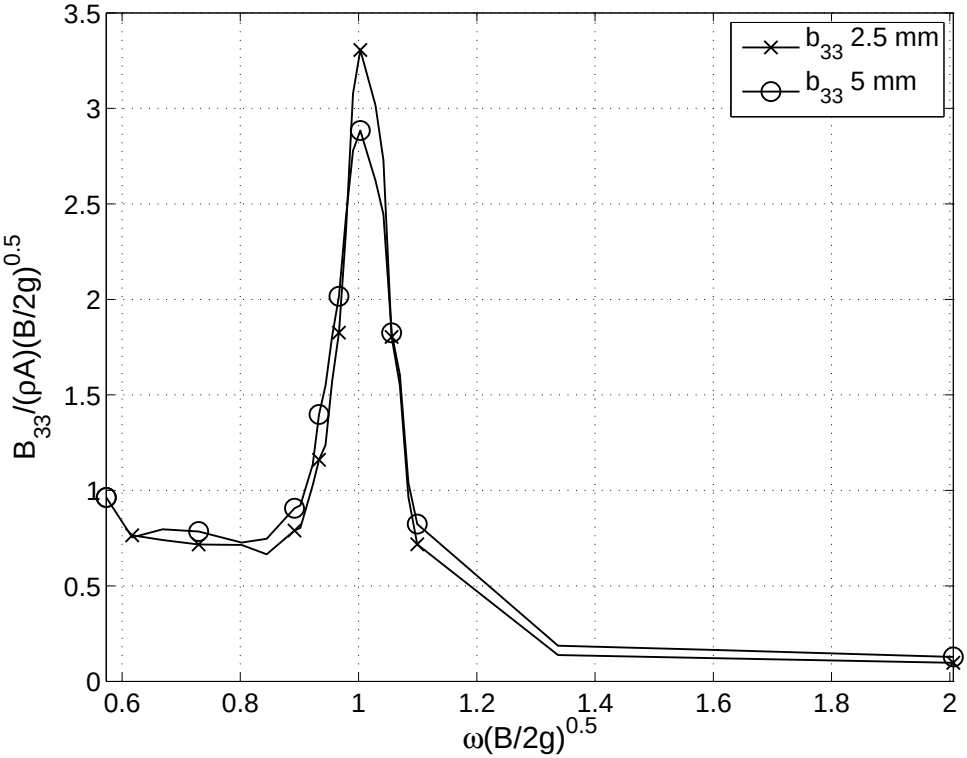

(b) Damping b_{33}, $b = 0.05$ forcing amplitude 2.5 and 5 *mm*.

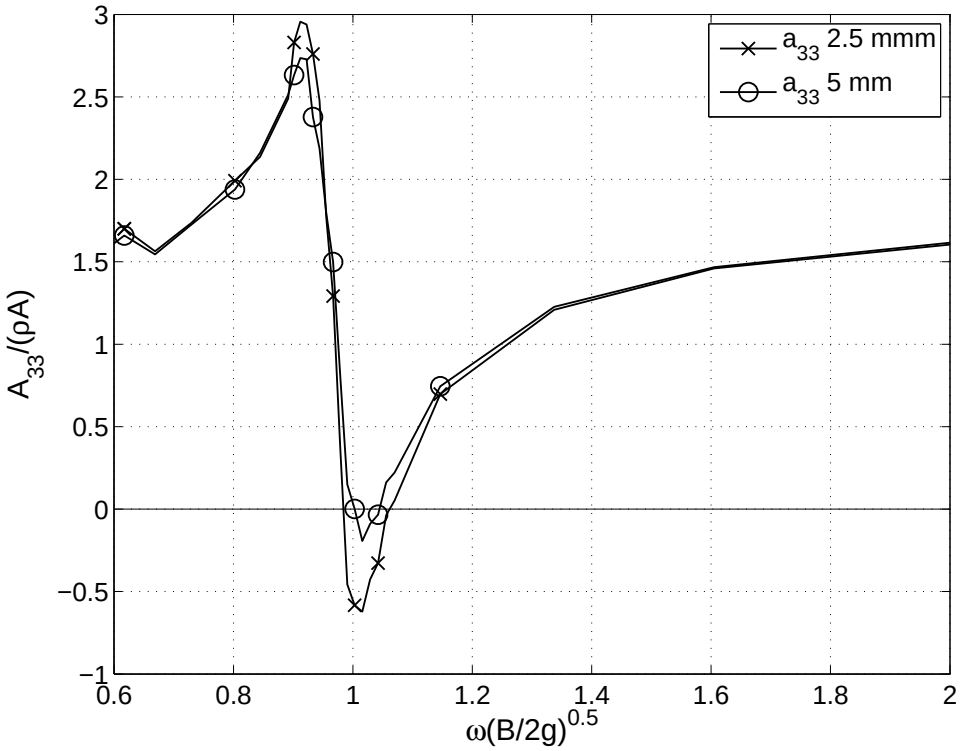

(a) Added mass a_{33}, $b = 0.06m$ forcing amplitude 2.5 and 5 *mm*.

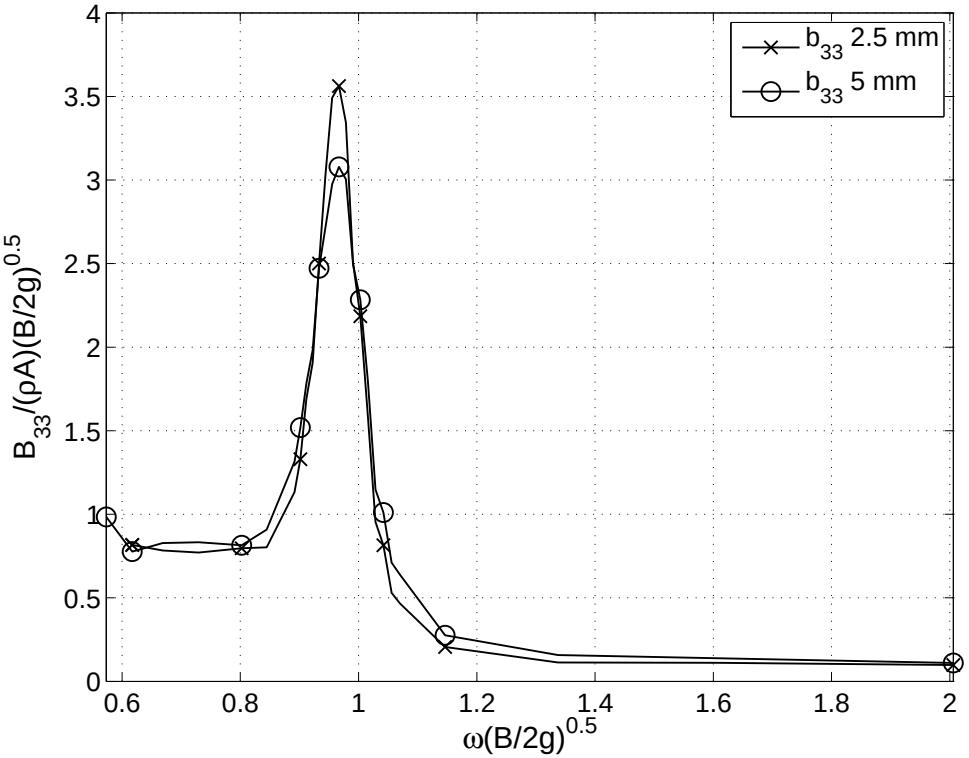

(b) Damping b_{33}, $b = 0.06$ forcing amplitude 2.5 and 5 *mm*.

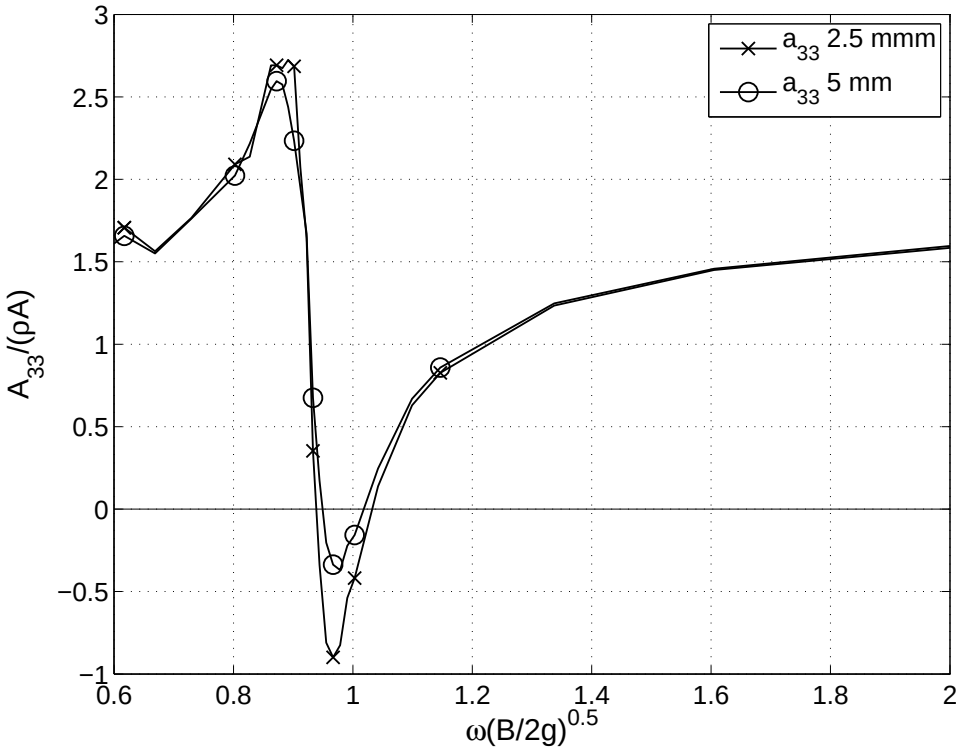

(a) Added mass a_{33}, $b = 0.07m$ forcing amplitude 2.5 and 5 *mm*.

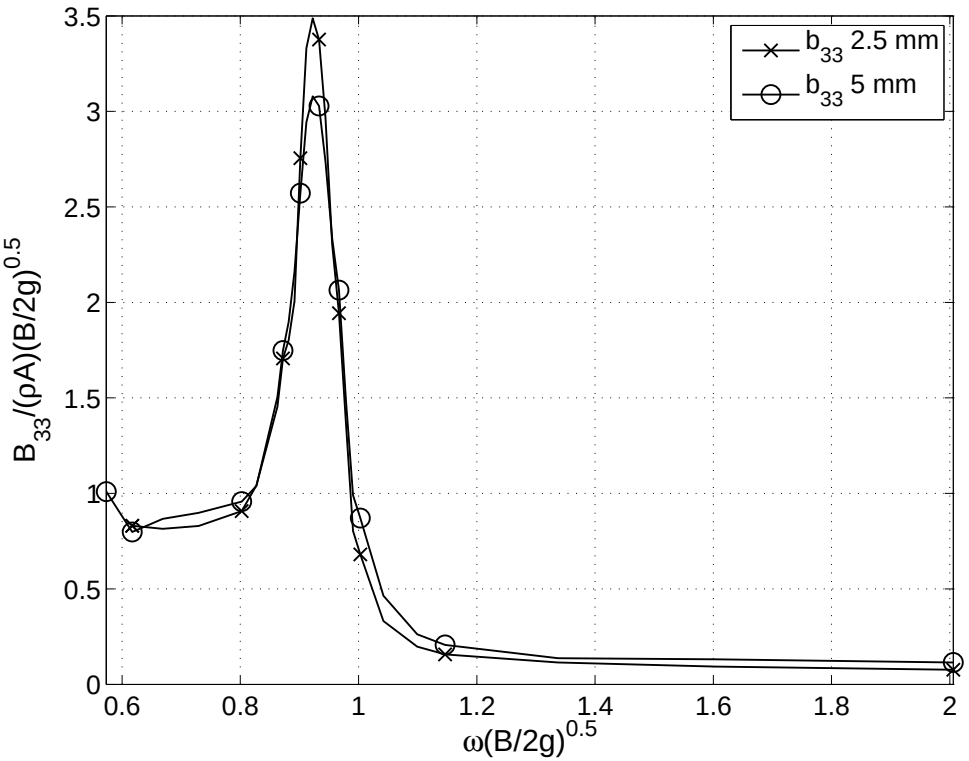

(b) Damping b_{33}, $b = 0.07$ forcing amplitude 2.5 and 5 *mm*.

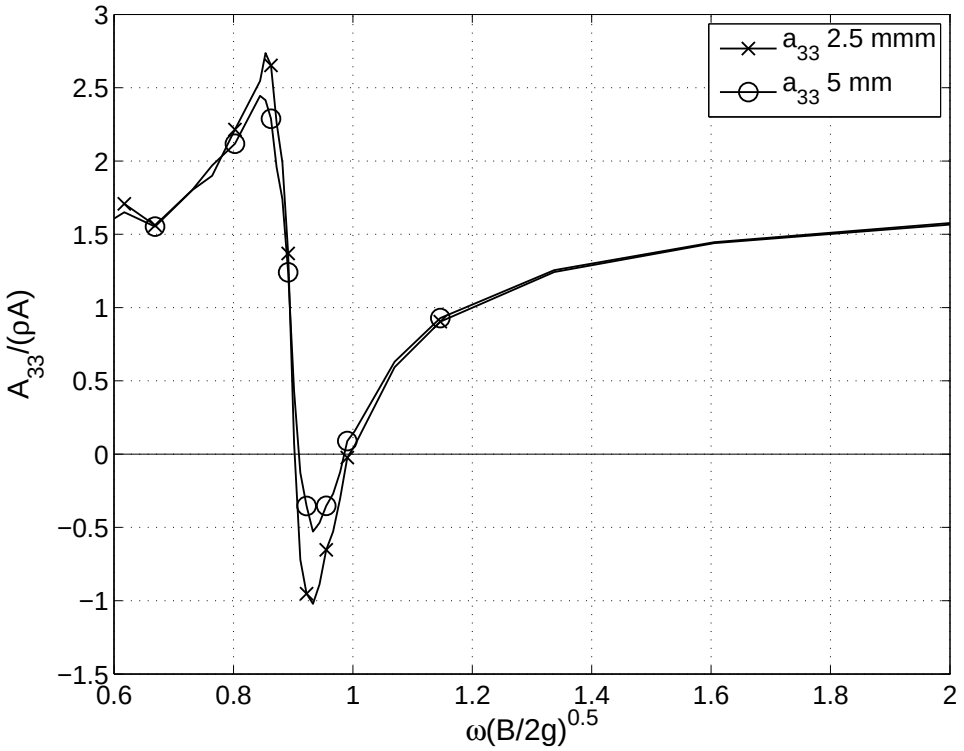

(a) Added mass a_{33}, $b = 0.08m$ forcing amplitude 2.5 and 5 *mm*.

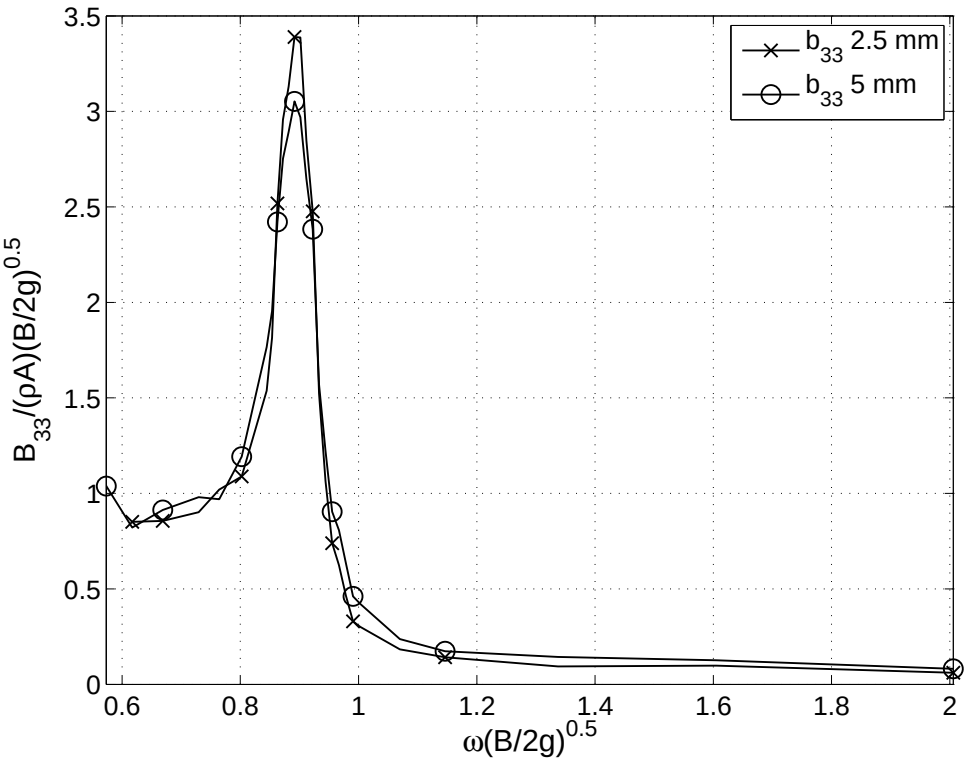

(b) Damping b_{33}, $b = 0.08$ forcing amplitude 2.5 and 5 *mm*.

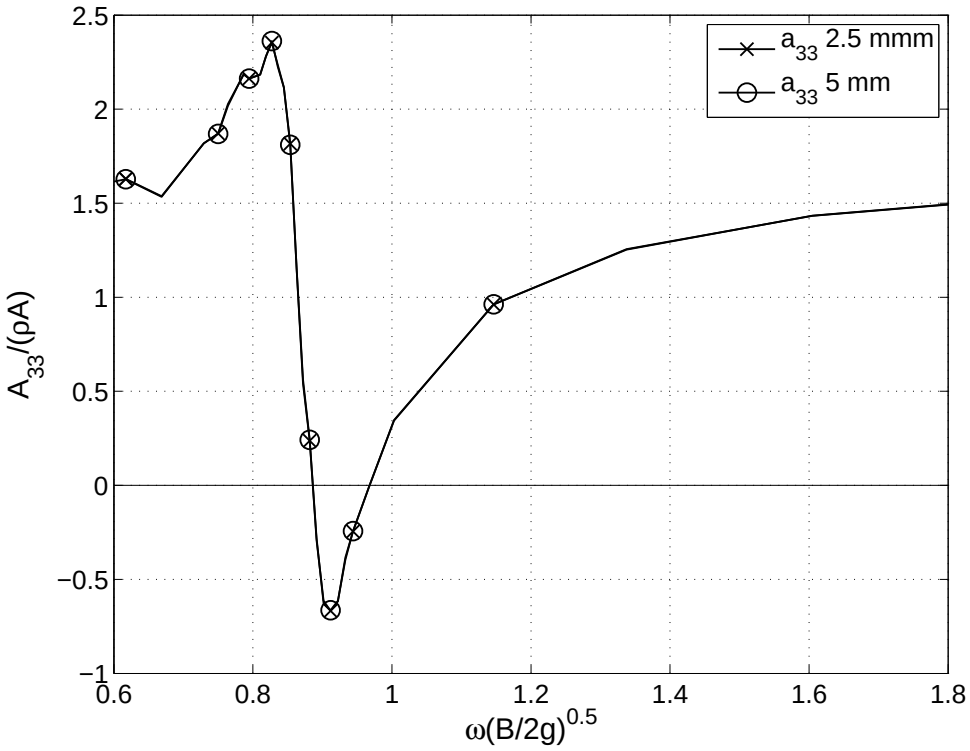

(a) Added mass a_{33}, $b = 0.09m$ forcing amplitude 2.5 and 5 *mm*.

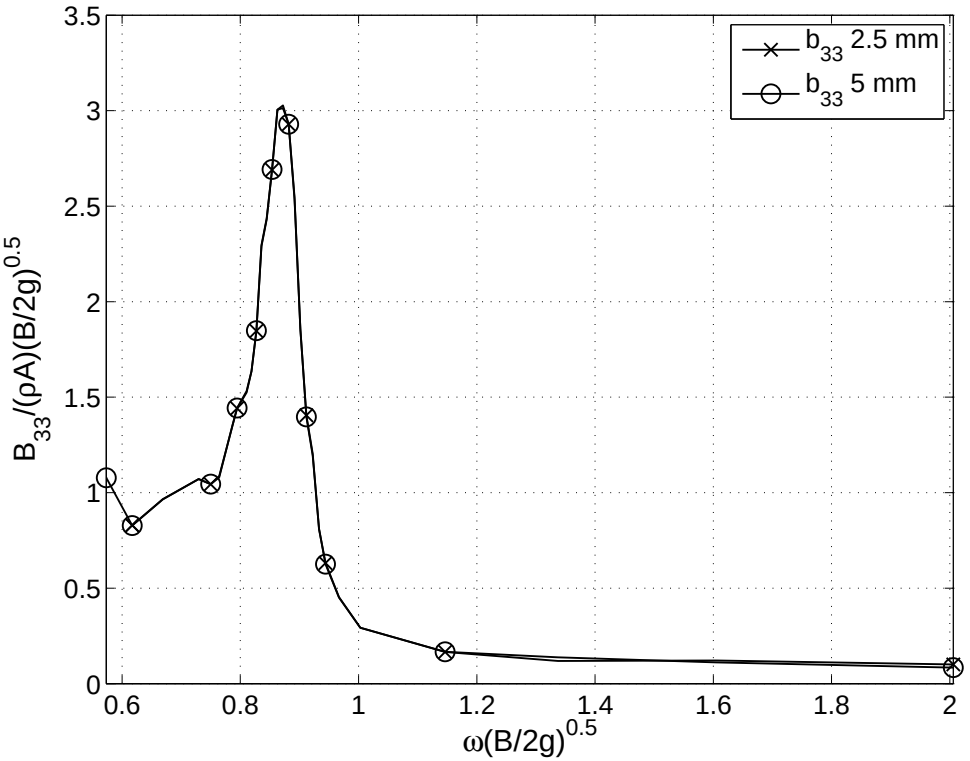

(b) Damping b_{33}, $b = 0.09$ forcing amplitude 2.5 and 5 *mm*.

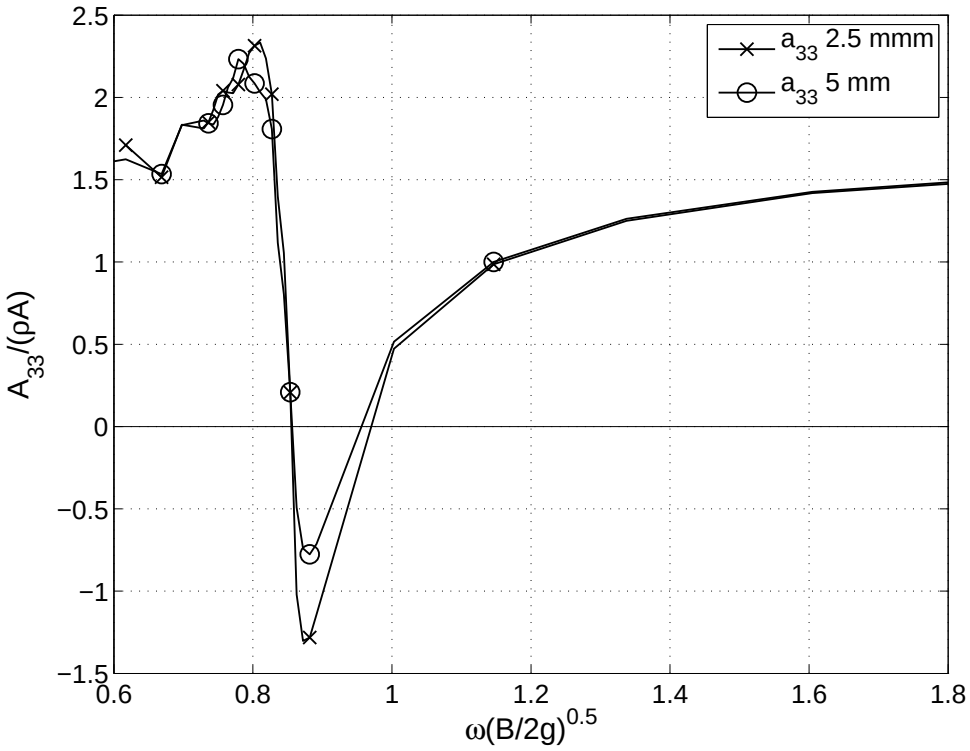

(a) Added mass a_{33}, $b = 0.10m$ forcing amplitude 2.5 and 5 *mm*.

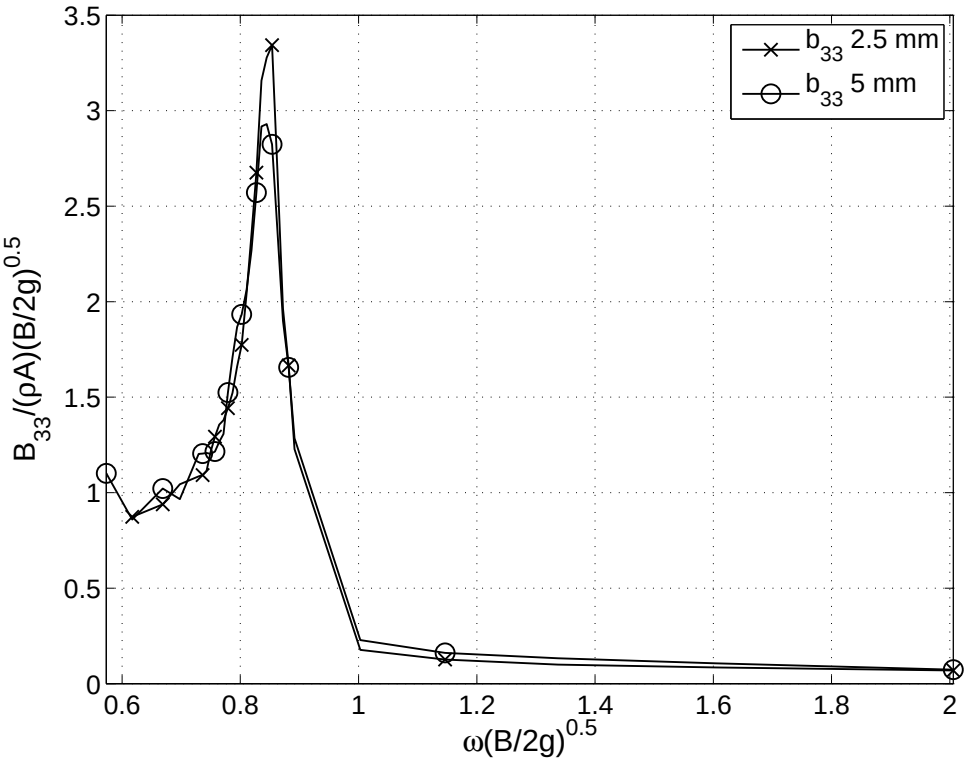

(b) Damping b_{33}, $b = 0.10$ forcing amplitude 2.5 and 5 *mm*.

Appendix B

Numerical results

Open water tests

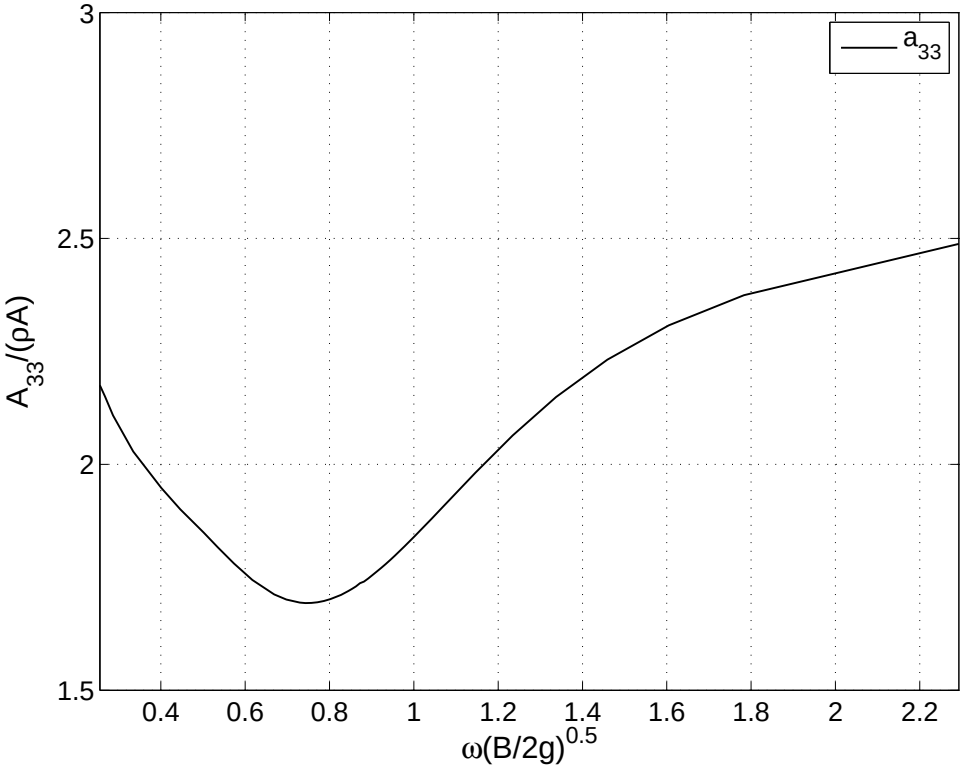

(a) Added mass a_{33}.

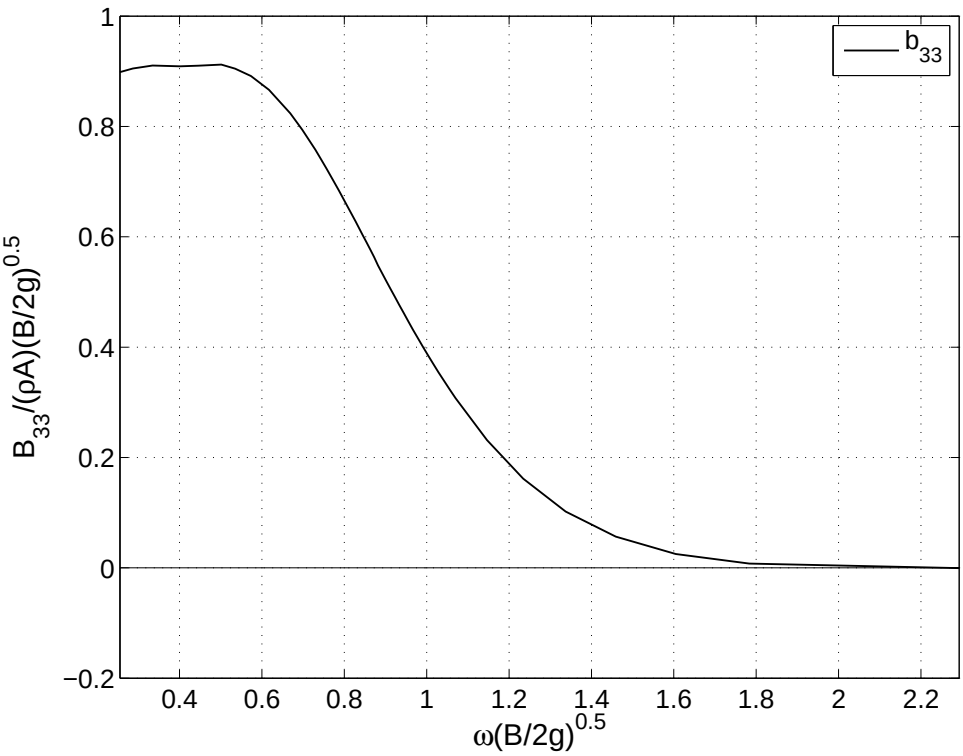

(b) Damping b_{33}.

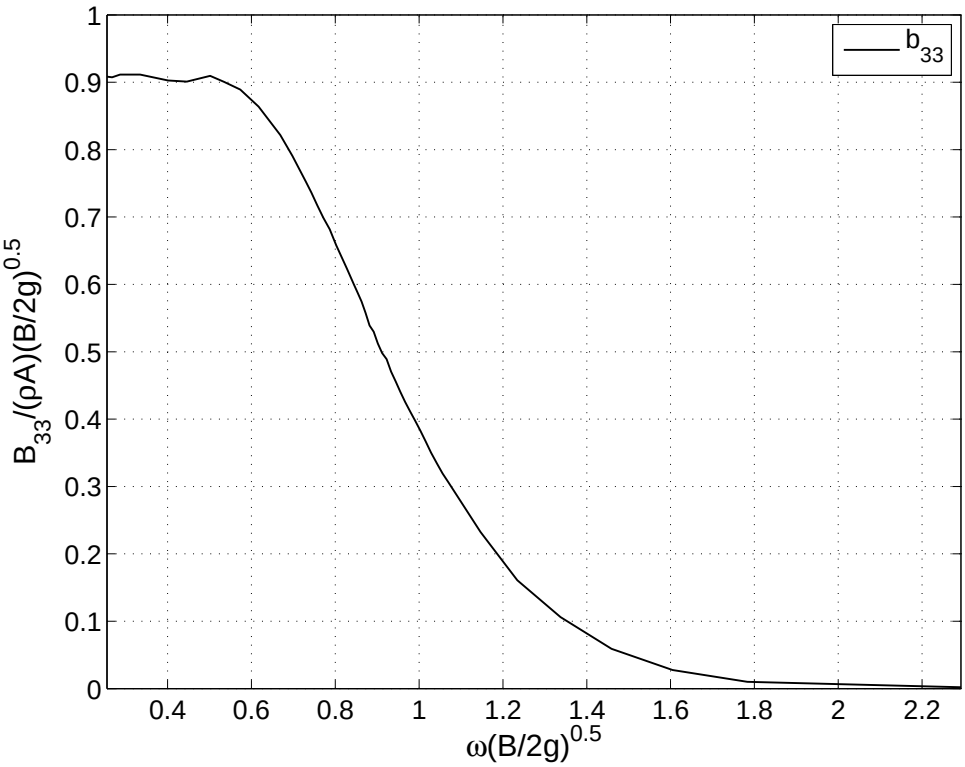

Figure B.1: Damping b_{33} from radiating waves.

Tests with two ice-floes

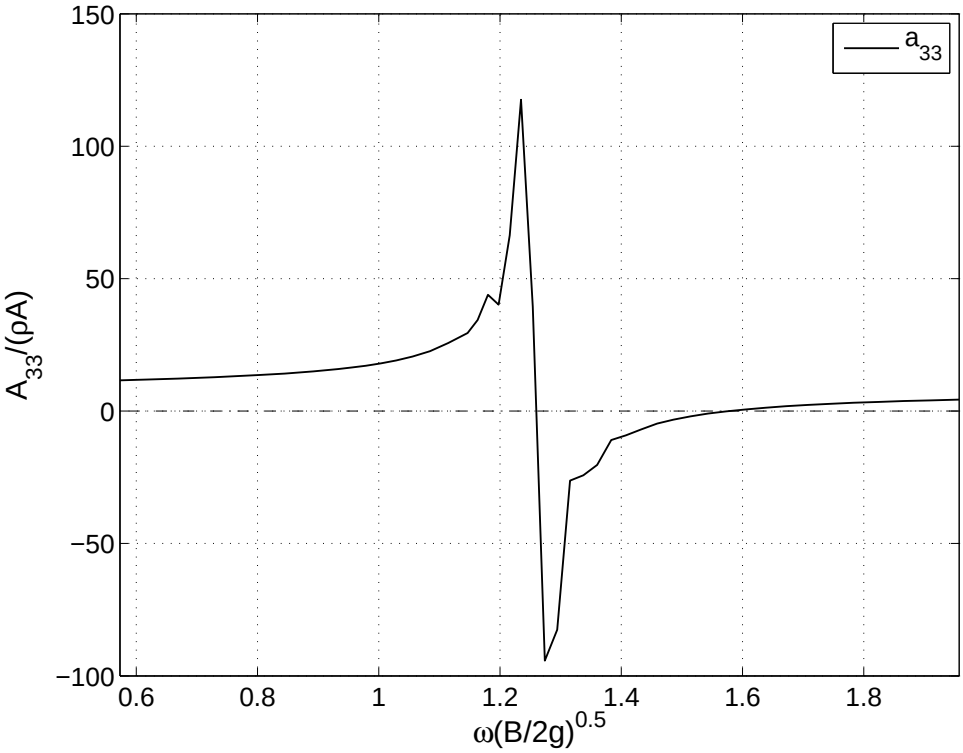

(a) Added mass a_{33}, $b = 0.01\ m$.

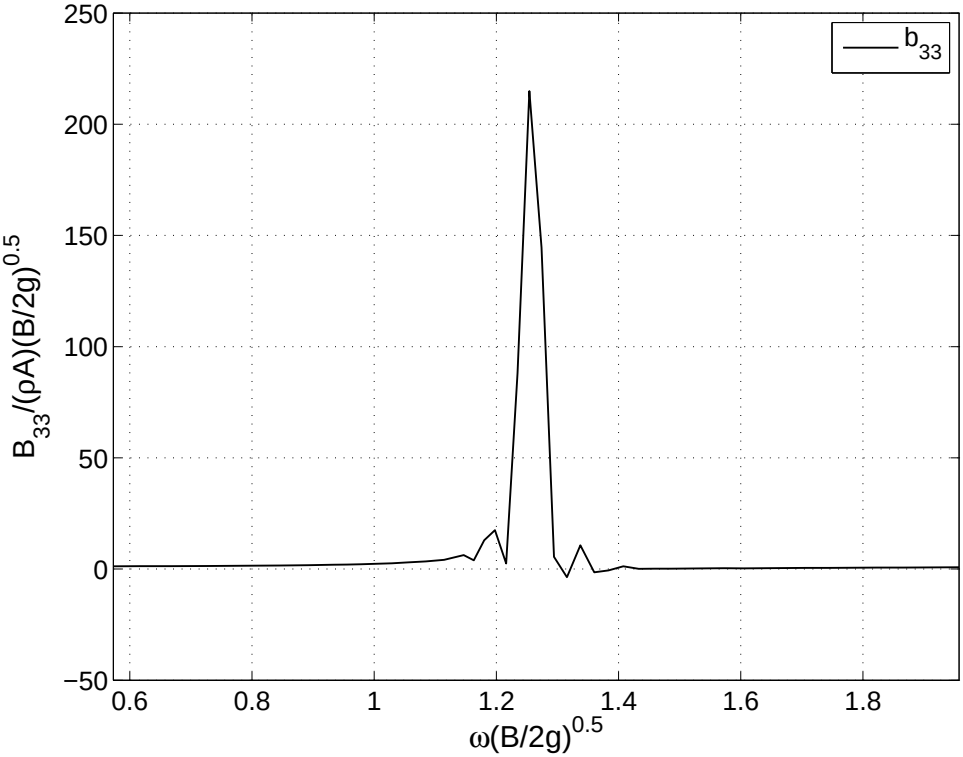

(b) Damping b_{33}, $b = 0.01\ m$.

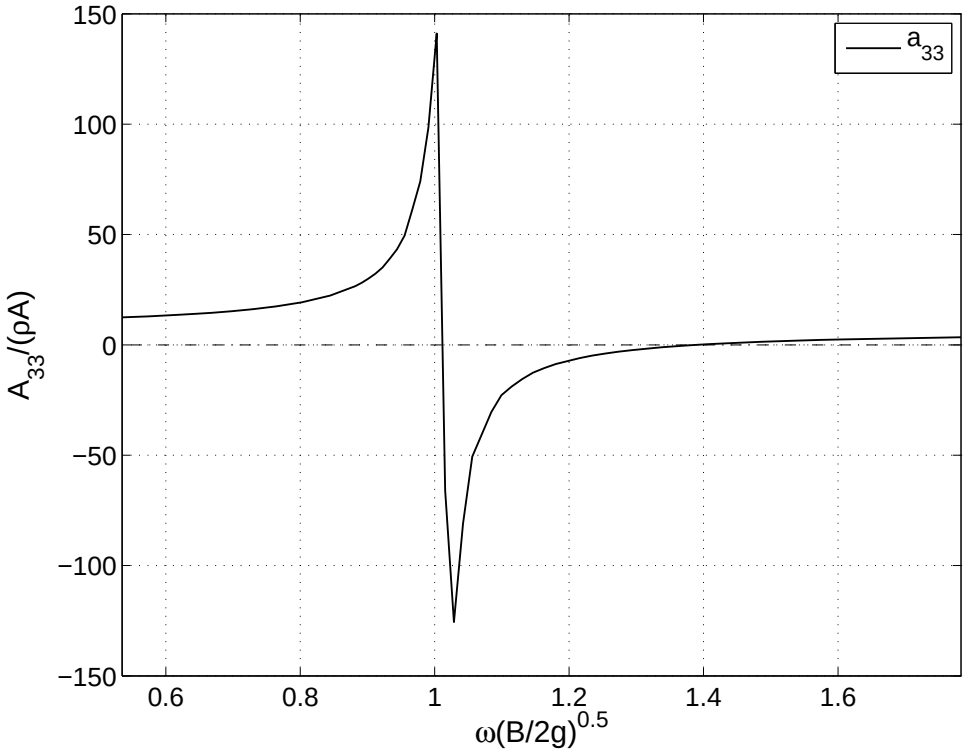

(a) Added mass a_{33}, $b = 0.02\ m$.

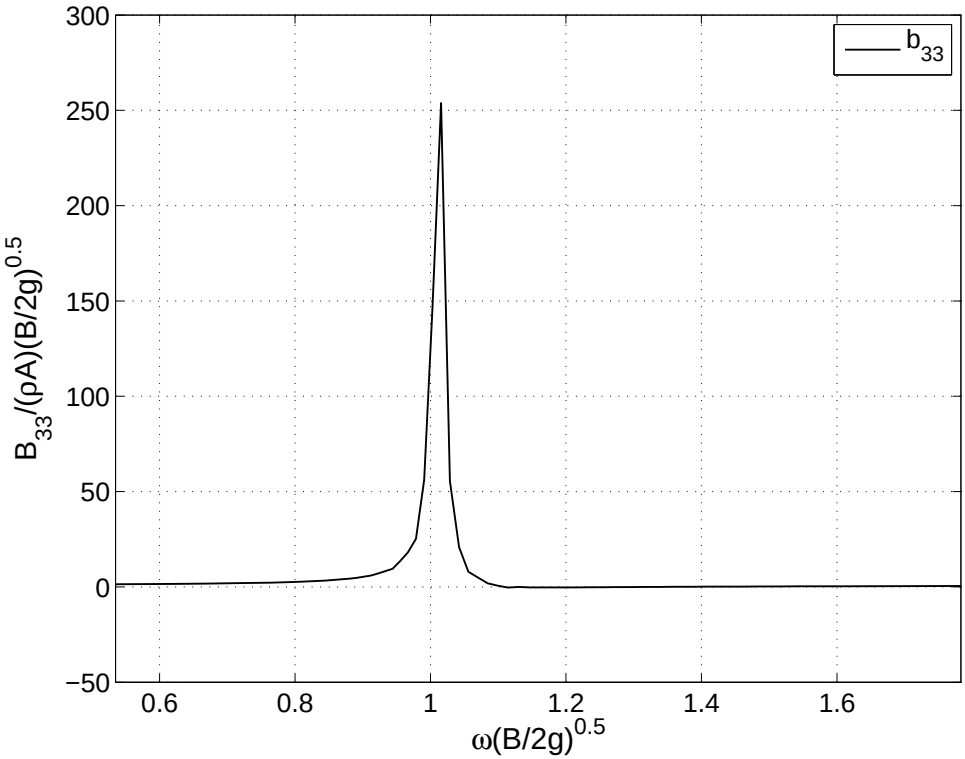

(b) Damping b_{33}, $b = 0.02\ m$.

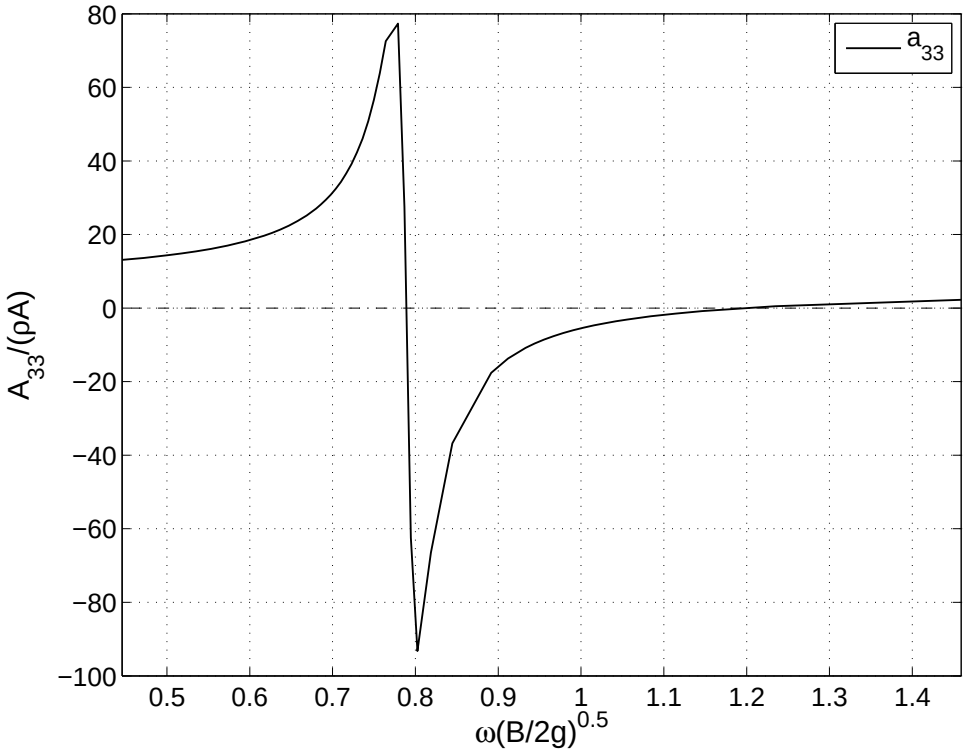

(a) Added mass a_{33}, $b = 0.04\ m$.

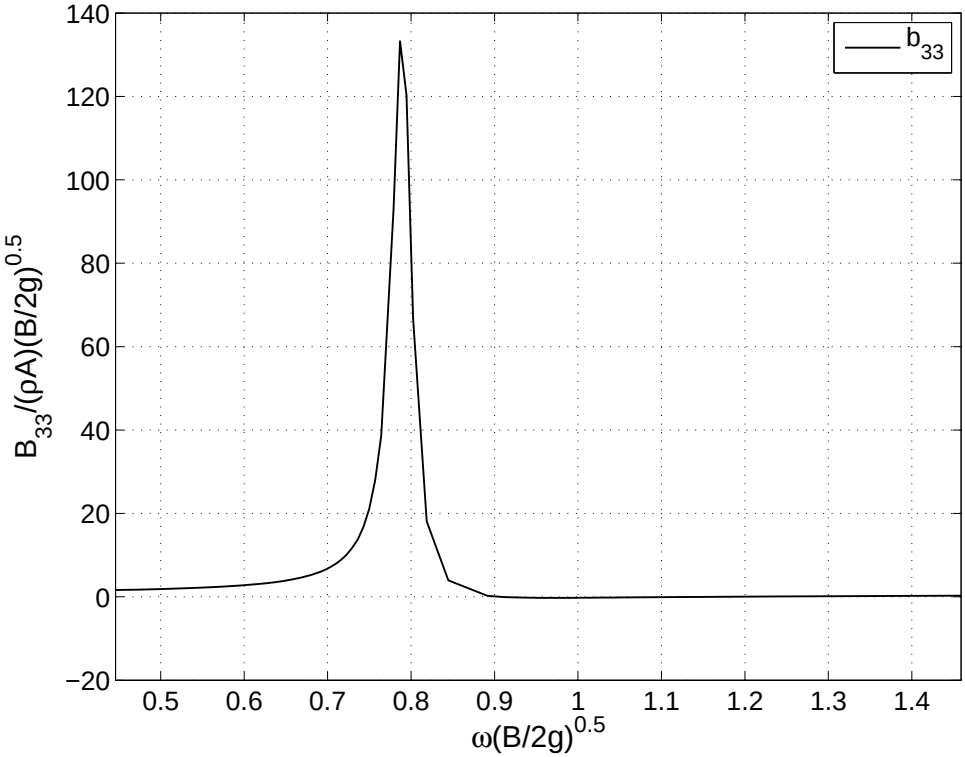

(b) Damping b_{33}, $b = 0.04\ m$.

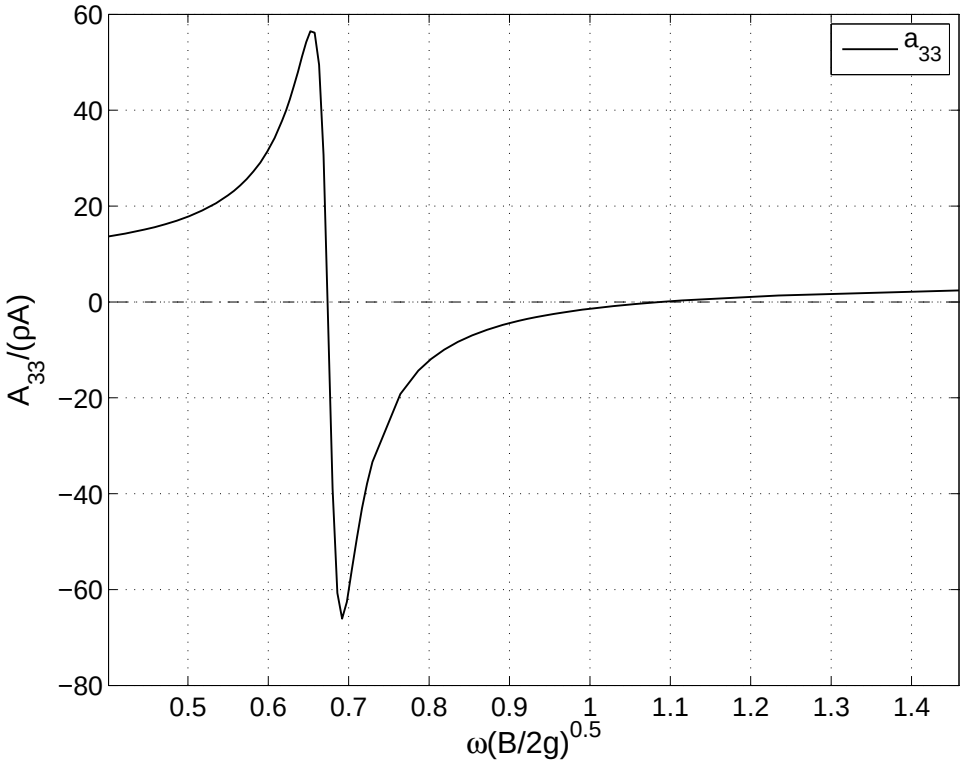

(a) Added mass a_{33}, $b = 0.06\ m$.

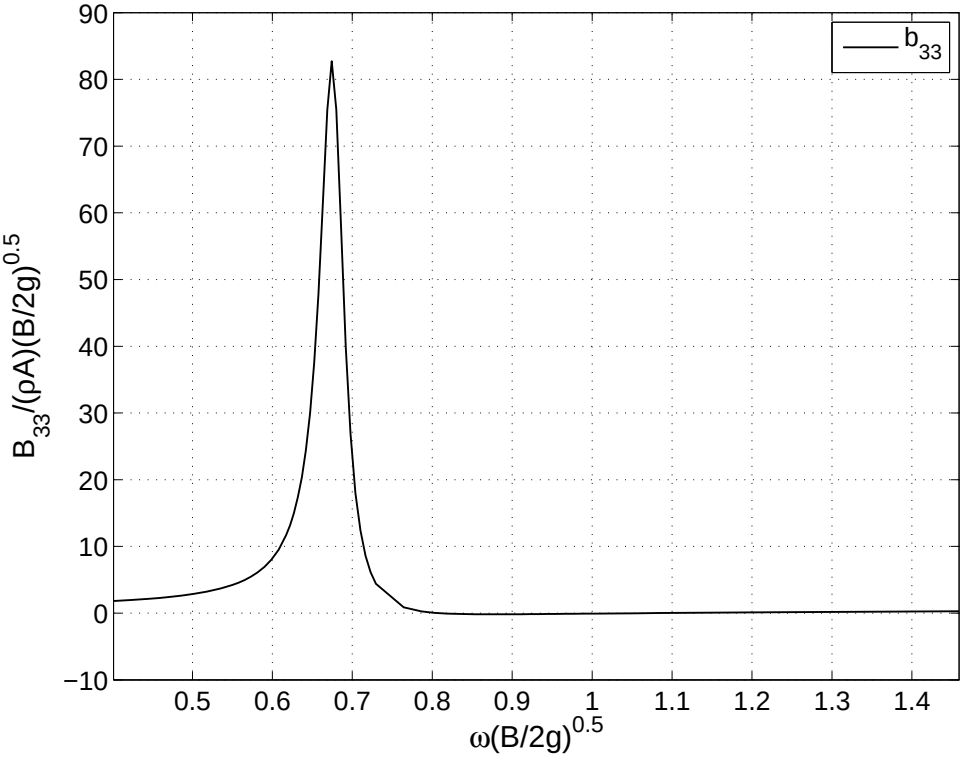

(b) Damping b_{33}, $b = 0.06\ m$.

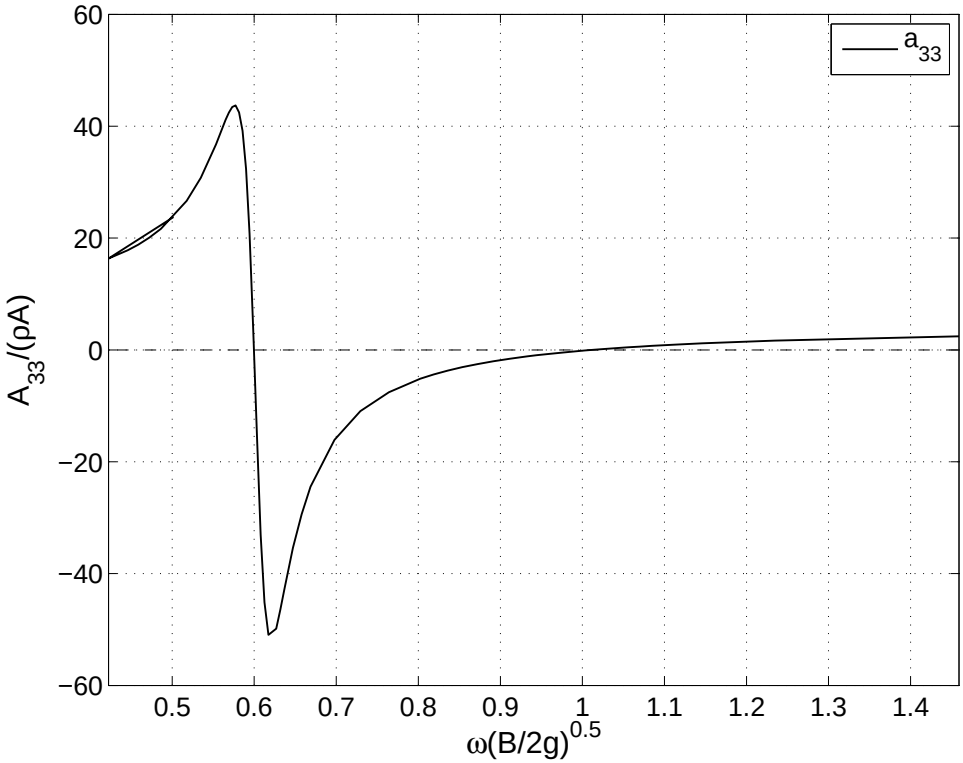

(a) Added mass a_{33}, $b = 0.08\ m$.

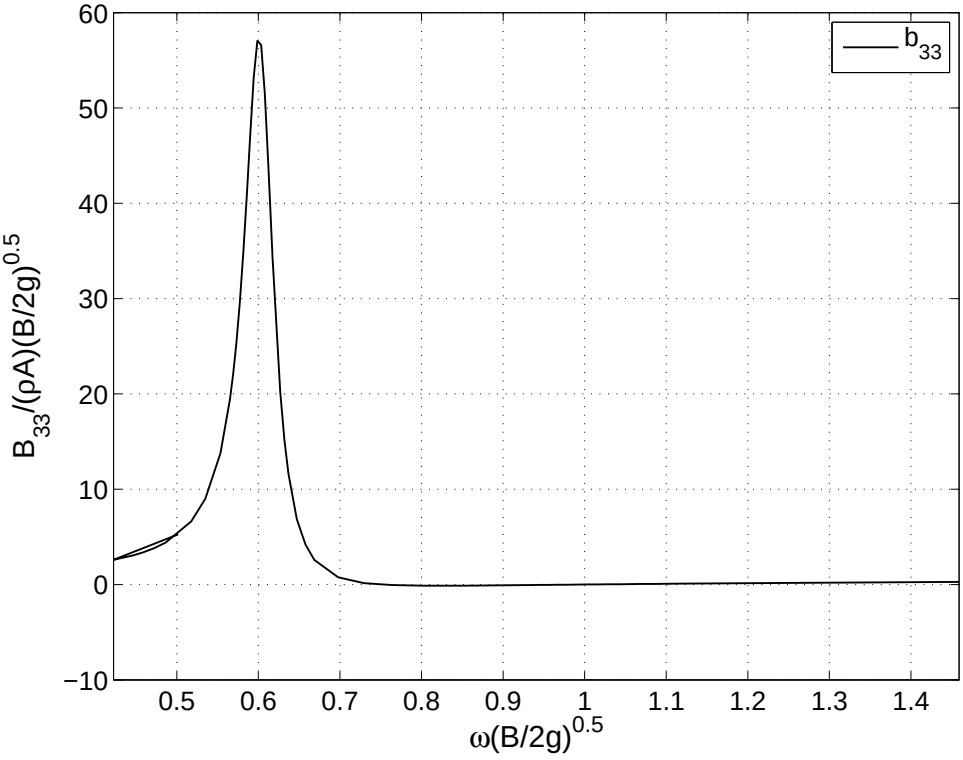

(b) Damping b_{33}, $b = 0.08\ m$.

Tests with one ice-floe

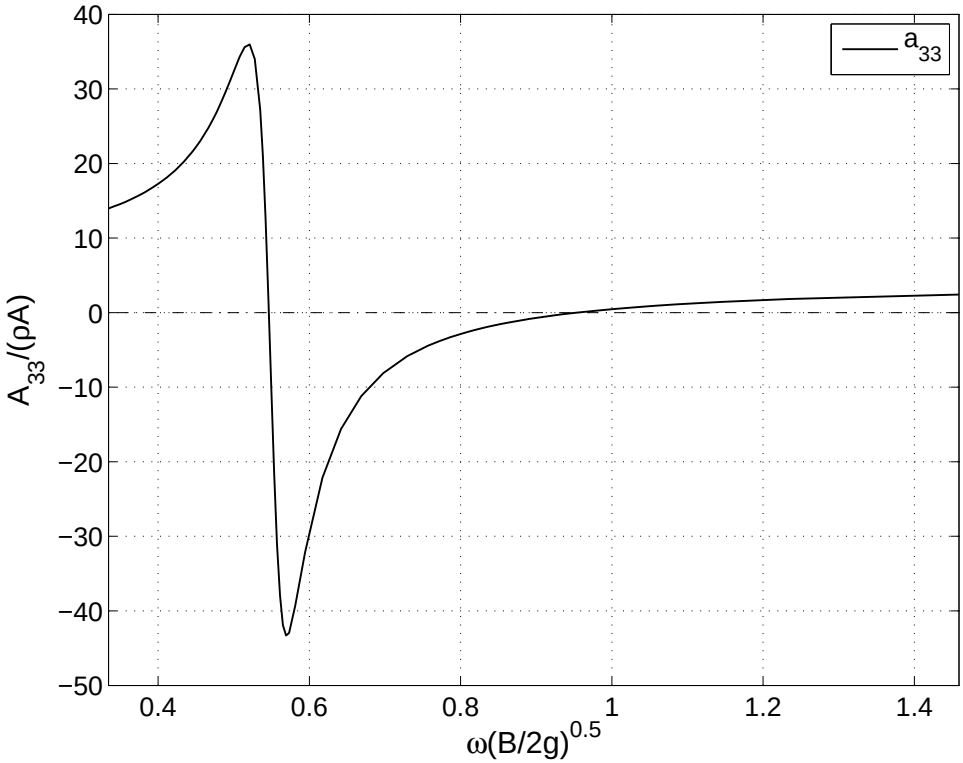

(a) Added mass a_{33}, $b = 0.10\ m$.

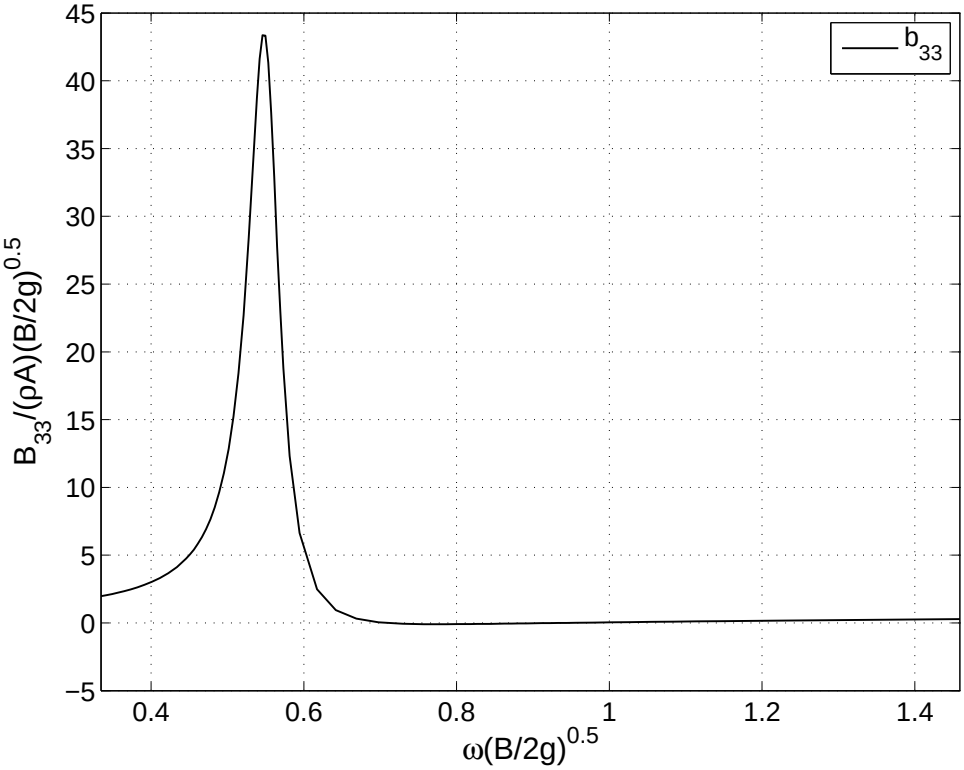

(b) Damping b_{33}, $b = 0.10\ m$.

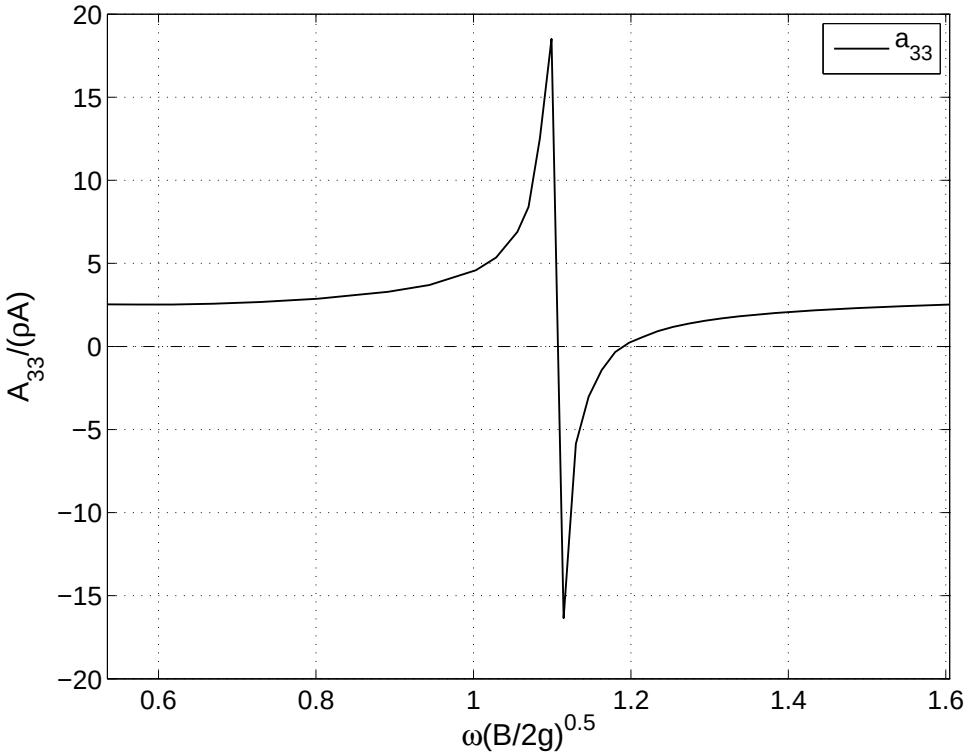

(a) Added mass a_{33}, $b = 0.04\ m$.

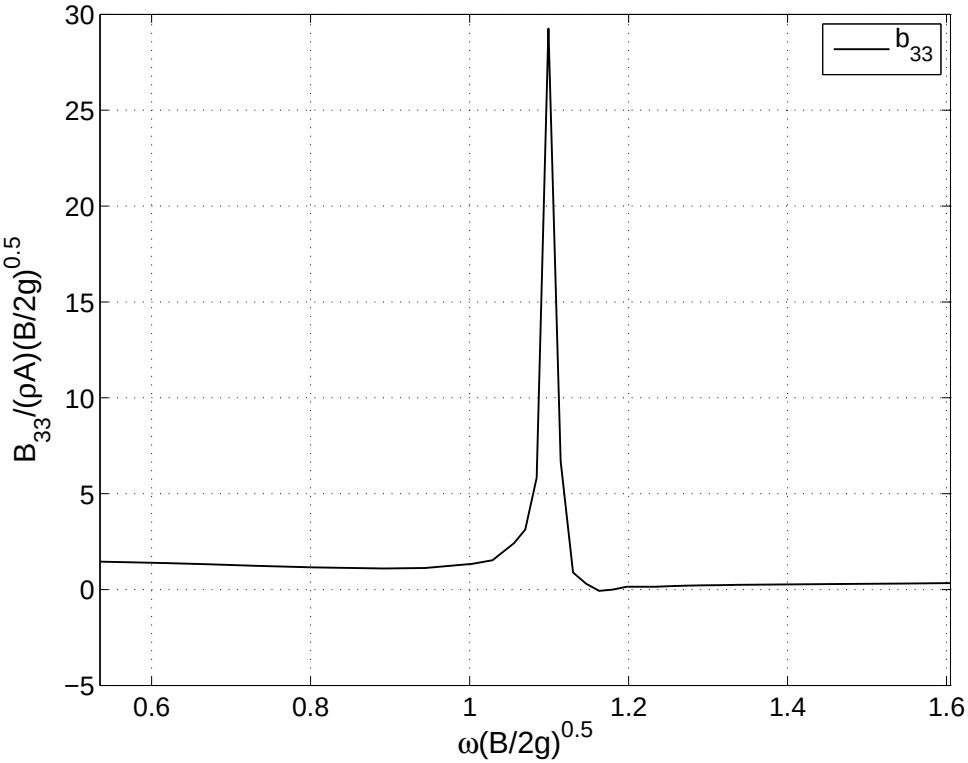

(b) Damping b_{33}, $b = 0.04\ m$.

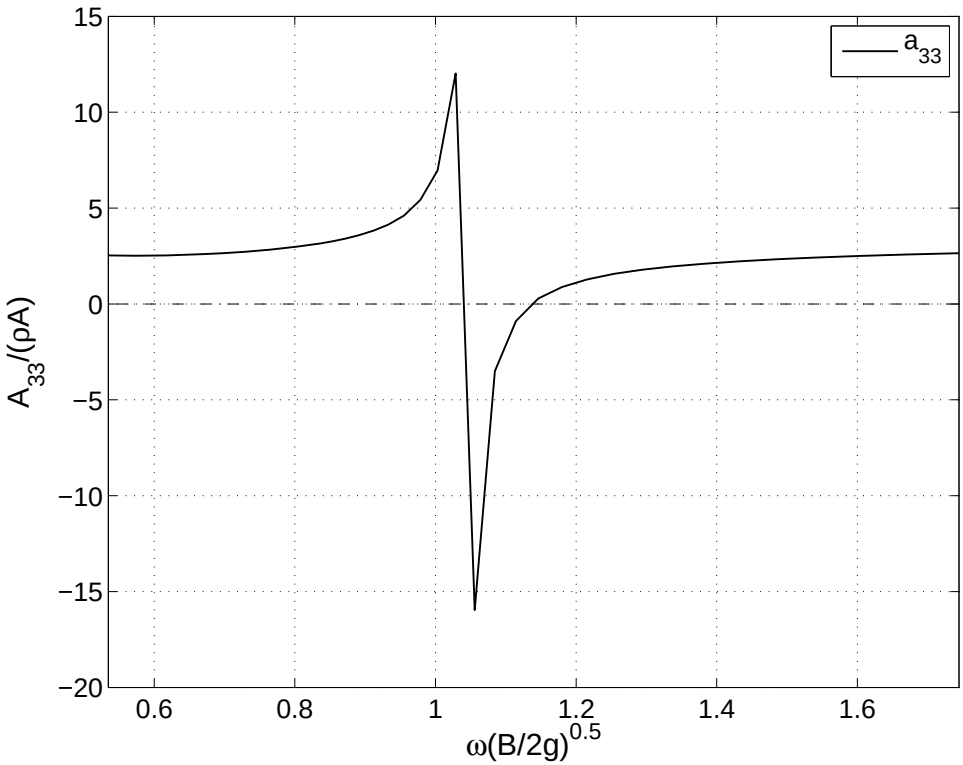

(a) Added mass a_{33}, $b = 0.05\ m$.

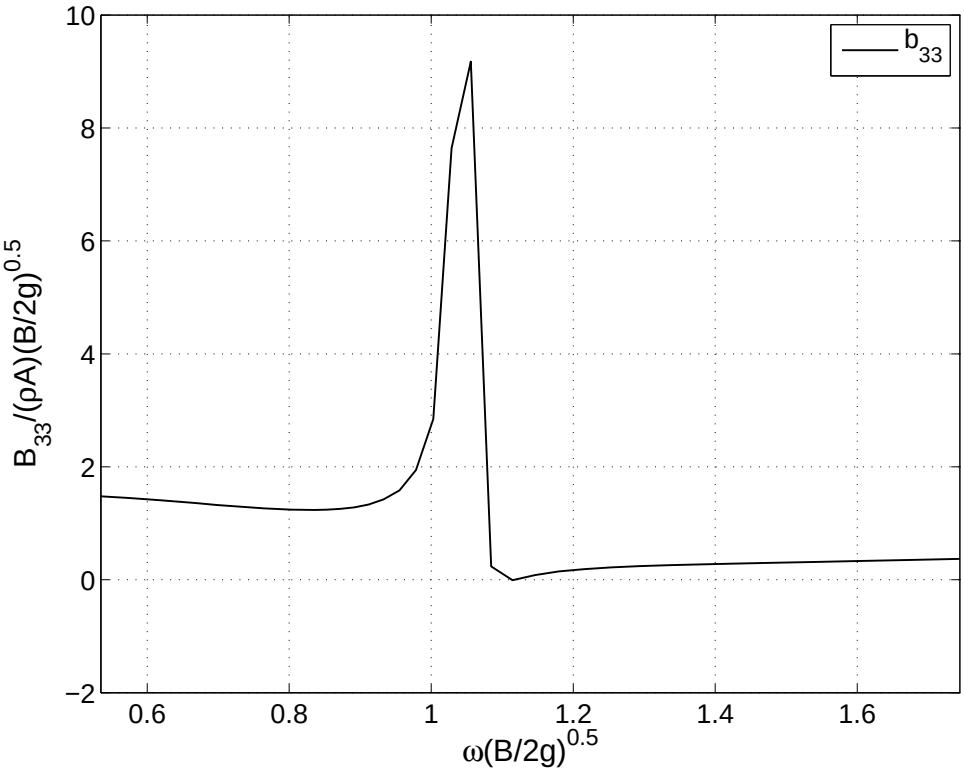

(b) Damping b_{33}, $b = 0.05\ m$.

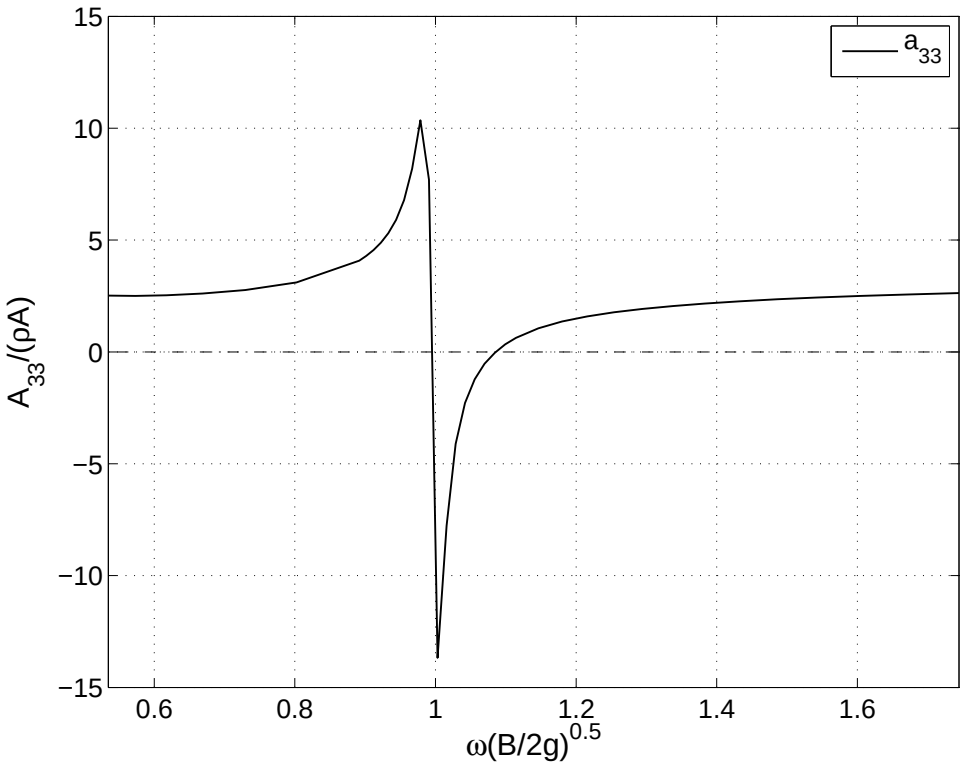

(a) Added mass a_{33}, $b = 0.06\ m$.

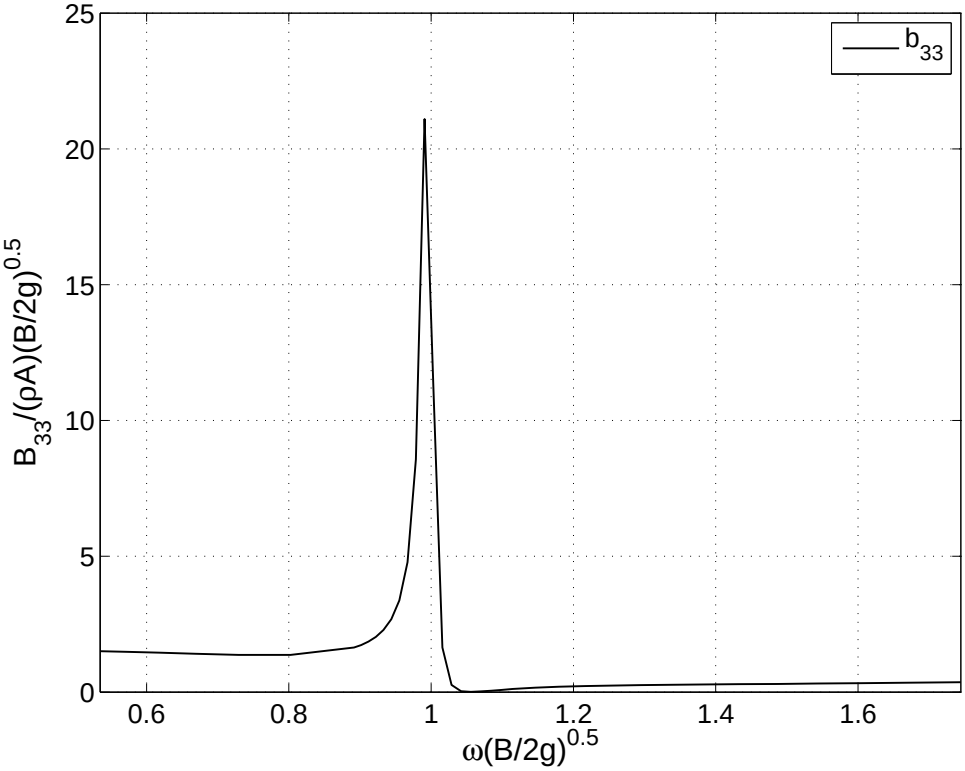

(b) Damping b_{33}, $b = 0.06\ m$.

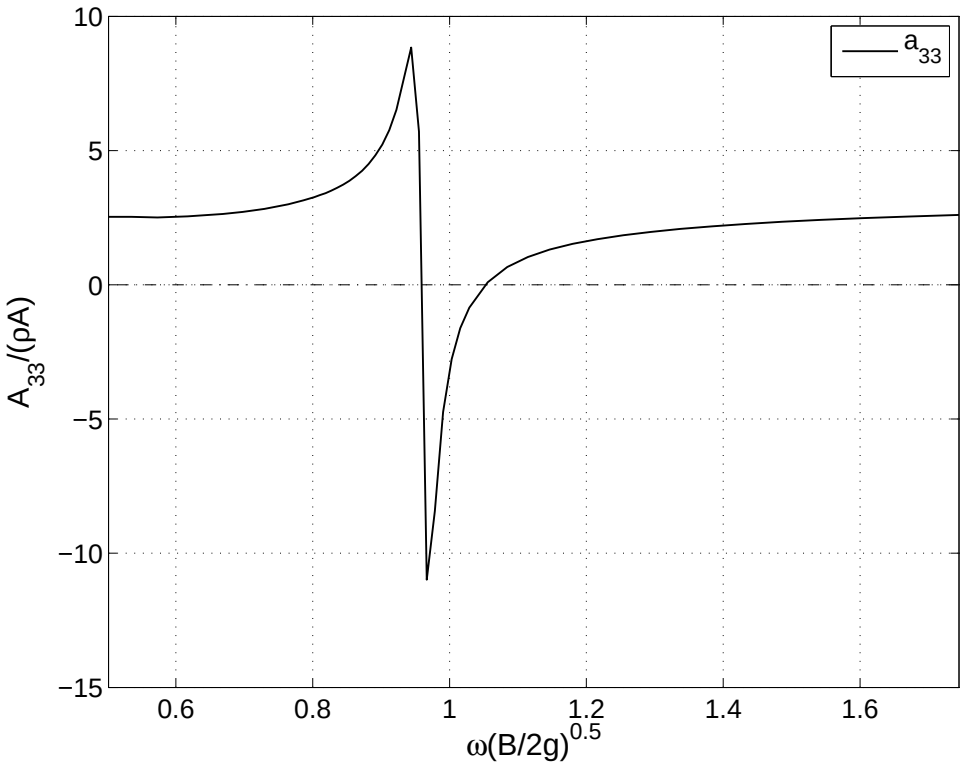

(a) Added mass a_{33}, $b = 0.07\ m$.

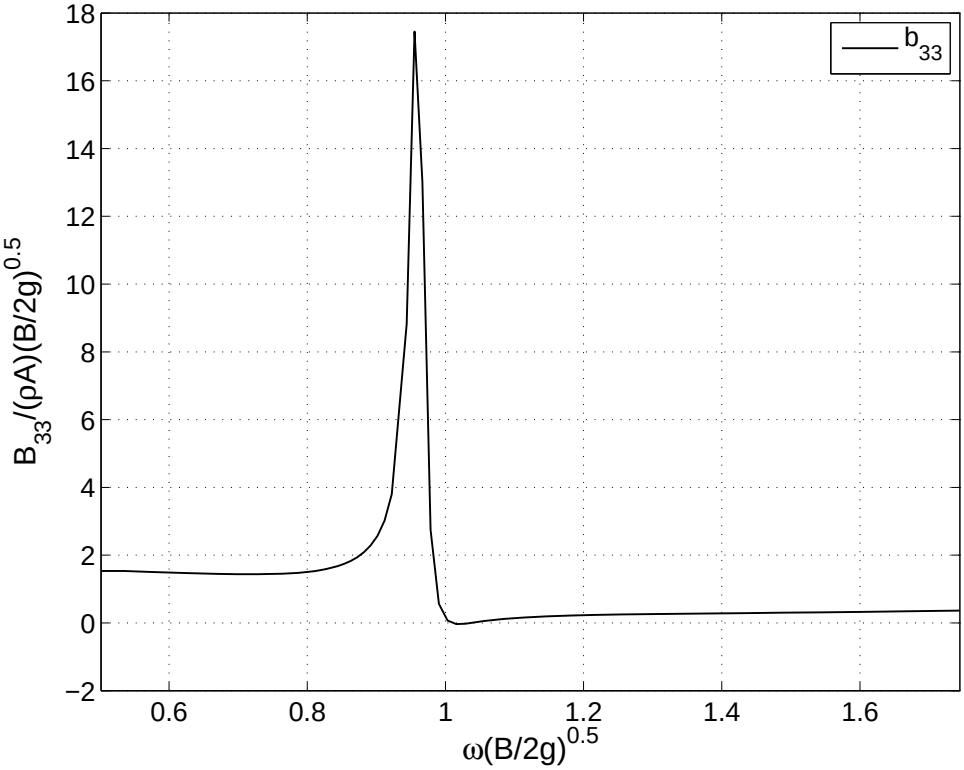

(b) Damping b_{33}, $b = 0.07\ m$.

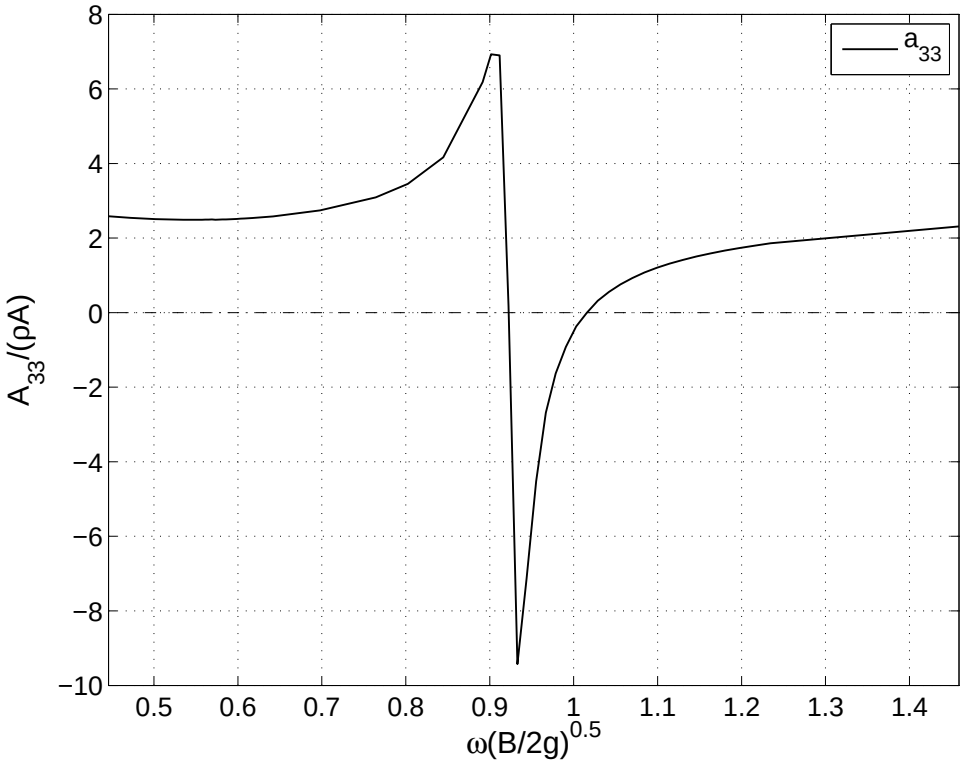

(a) Added mass a_{33}, $b = 0.08\ m$.

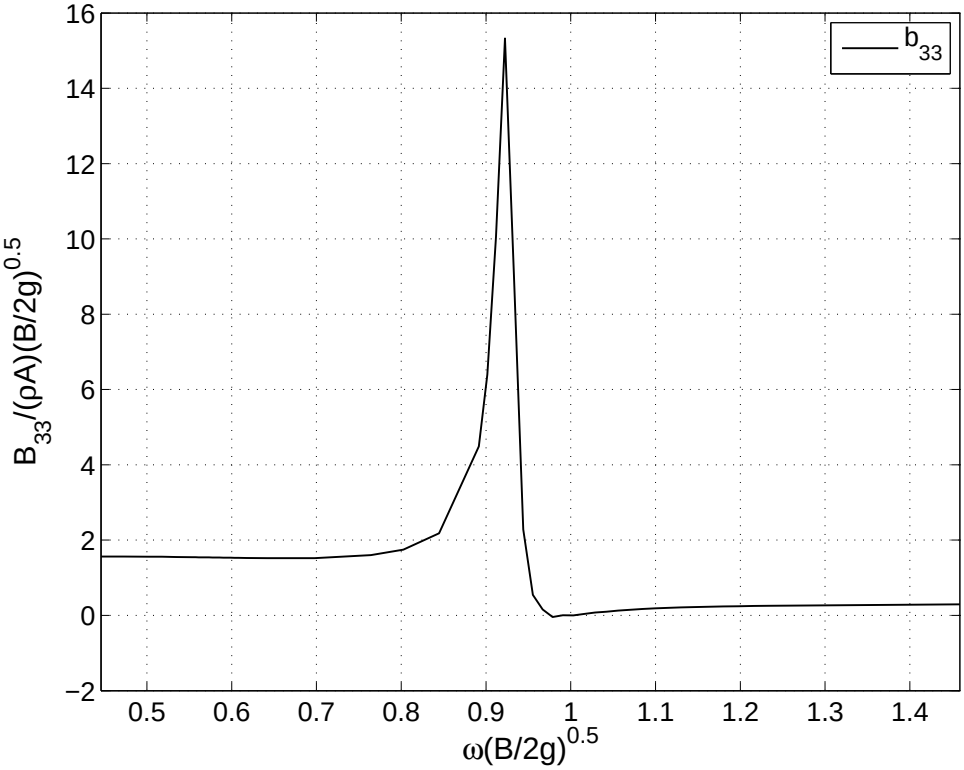

(b) Damping b_{33}, $b = 0.08\ m$.

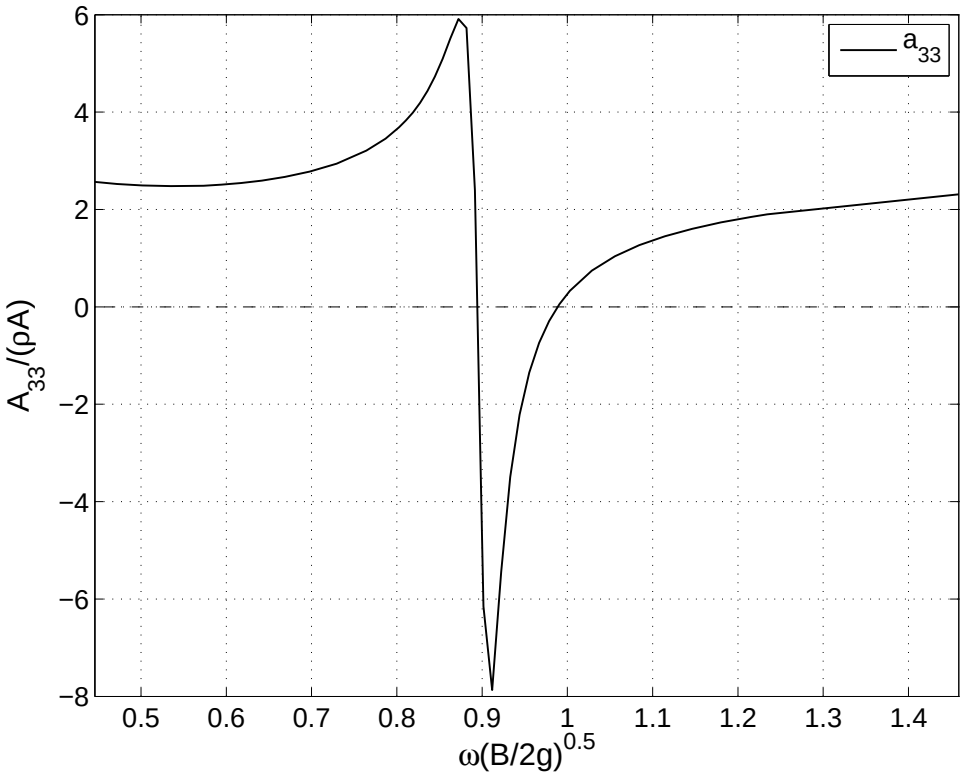

(a) Added mass a_{33}, $b = 0.09\ m$.

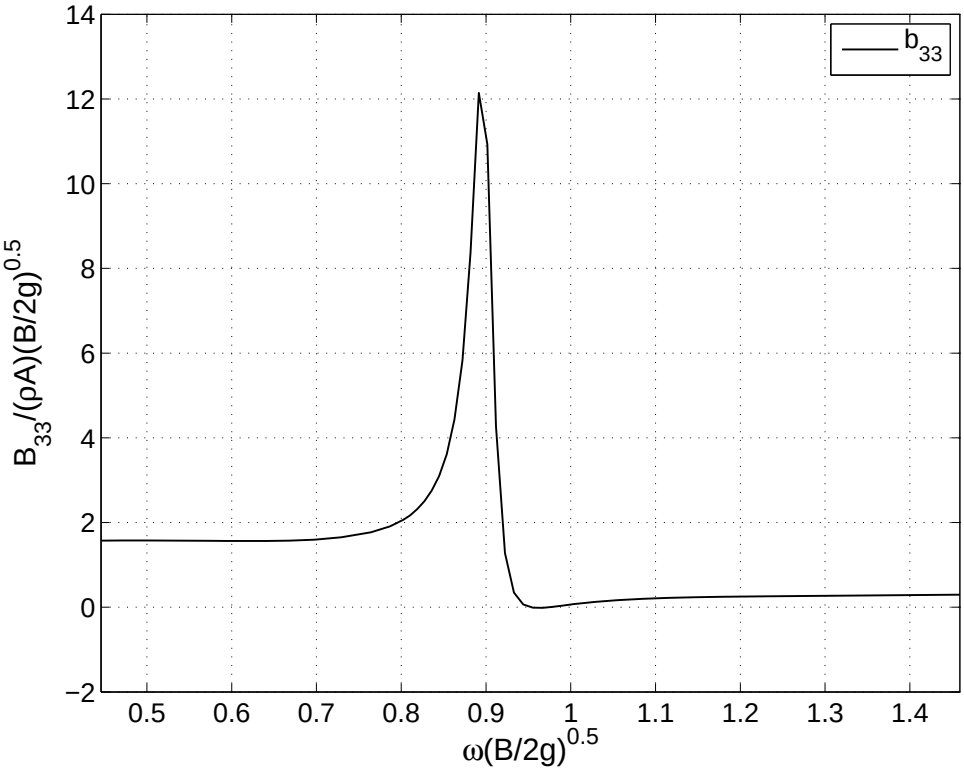

(b) Damping b_{33}, $b = 0.09\ m$.

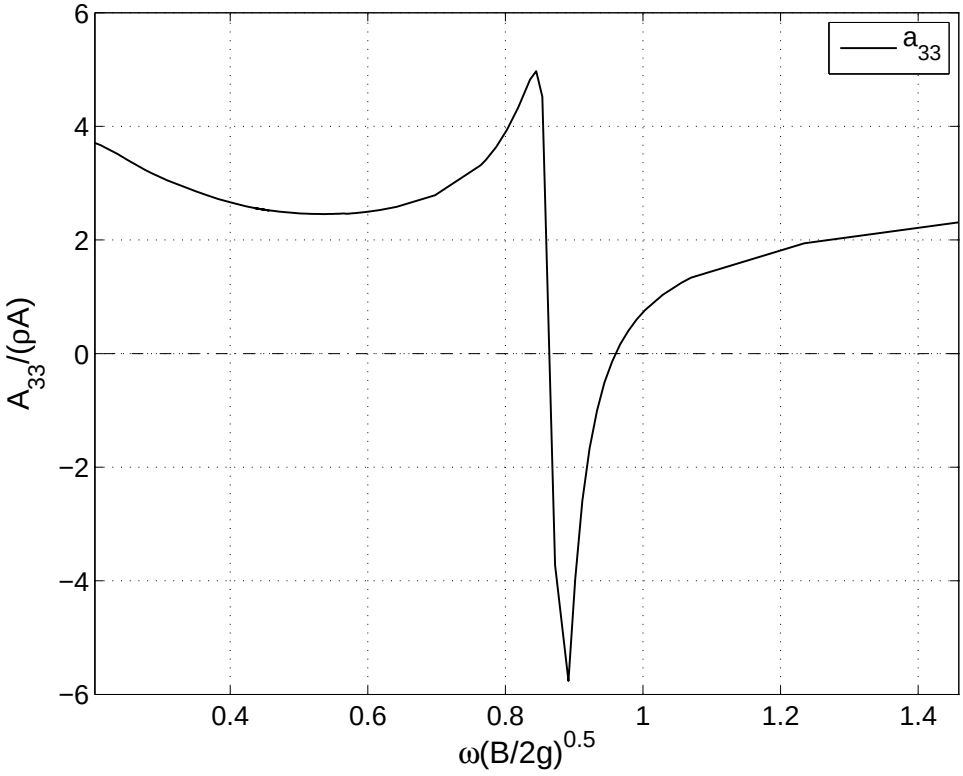

(a) Added mass a_{33}, $b = 0.10\ m$.

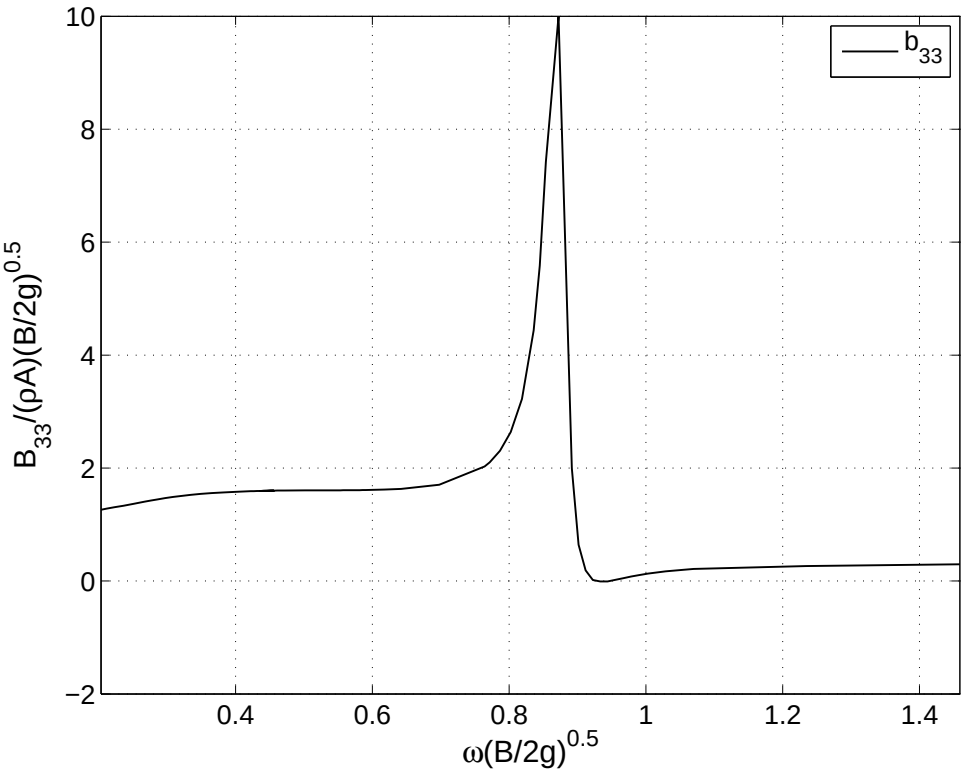

(b) Damping b_{33}, $b = 0.10\ m$.

Appendix C

Attached CD

The attached CD contains a folder with the matlab files used to do the calculations. If there is questions about the matlab files or data files is wanter the author may be contacted. In addition Trygve Kristiansen has back up of all data files.

Folder	Matlab
Filename	Description
CreateInp.m	Make input files for numerical wave tank
common.m	Read datafile from numerical calculation. Used by A33andB33.m, plotzeta.m analy
analyzeRuns.m	Plot time series from numerical wave tank
plotzeta.m	Plot the numerical calculation time step by time step (by Trygve Kristiansen)
konvergens.m	Plot convergency test for the numerical wave tank
FindCD.m	Calculate the drag coefficient C_D
uncertainty.m	Calculate the standard deviation in the experiments
createActuatorfile.m	Create the test program for the actuator in the experiemnts (by Trygve Kristiansen)
splitCatmanfiles.m	Split logging data from experiments into one file for each tested frequency (by Tryg
analyzeExperiments.m	Plot measured time series from experiments (by MARINTEK)
bpass.m	Band pass filter (by Trygve Kristiansen)
findK.m	Find wave number k (by Trygve Kristiansen)
ShallowWater.m	Plot wavelengths divided by 4 to find shallow water waves
findA33andB33	Calculate added mass and damping from experiments